COCAINE-INDUCED LIPIDOMIC ALTERATIONS FOR THE STUDY OF ADDICTIVE BEHAVIORS

by

SUMITRA PATI

(Under the Direction of Brian S. Cummings)

ABSTRACT

Although the neurochemical and neurobiological effects of various drugs of abuse are well-characterized, there is little information regarding the role of complex lipid remodeling within the context of addiction. The series of studies presented herein addressed these gaps in knowledge by testing the hypothesis that cocaine induces lipid alterations that may serve as indicators of addictive behaviors. Firstly, we demonstrated the effects of dietary fat intake and aging on the blood lipidome. These findings occurred in a stimuli-independent manner across several models, and emphasized the need to consider these factors in experiments prior to assessing the effect of any stimuli on lipidomic changes in the blood. Untargeted lipidomics revealed blood lipid remodeling of phospholipids, glycerolipids, and fatty acyls using both preclinical and clinical models of cocaine exposure. Cocaine exposure demonstrated region-specific changes in the rat brain lipidome that suggest that addictive behaviors, i.e. sensitization, extinction, and reinstatement, can induce widespread lipid alterations. Blood lipid changes could also be correlated to behavioral sensitization to cocaine in both rats and human models of exposure. Cocaine differentially regulated genes involved in fatty acid

metabolism and mitochondrial biogenesis region-specifically in the brain. These effects indicate a potential role for cocaine in the maintenance of CNS energetics and lipid regulation. In summary, the data presented here demonstrated comprehensive lipidomic assessment of cocaine-induced lipid remodeling in blood and brain profiles. These findings provide a platform for discerning how changes in the lipidome may mediate some of the molecular adaptions of the brain in response to drugs of abuse.

INDEX WORDS: lipids, lipidomics, addiction, cocaine, blood, brain

COCAINE-INDUCED LIPIDOMIC ALTERATIONS FOR THE STUDY OF ADDICTIVE BEHAVIORS

by

SUMITRA PATI

B.S., College of Charleston, 2011

M.S., Claflin University, 2013

A Dissertation Submitted to the Graduate Faculty of The University of Georgia in Partial Fulfillment of the Requirements for the Degree

DOCTOR OF PHILOSOPHY

ATHENS, GEORGIA

2017

COCAINE-INDUCED LIPIDOMIC ALTERATIONS FOR THE STUDY OF ADDICTIVE BEHAVIORS

by

SUMITRA PATI

Major Professor: Brian S. Cummings

Committee: Michael Bartlett
James Franklin
Kun Lu
John J. Wagner

Electronic Version Approved:

Suzanne Barbour
Dean of the Graduate School
The University of Georgia
December 2017

DEDICATION

To my husband, *David*

For your everlasting support, encouragement, and capacity to make the good times better and the hard times easier

To *Tony and Cleo,* for your companionship and continuous ability to make me smile

ACKNOWLEDGEMENTS

I would like to express my sincerest appreciation to all the people whose personal and professional contributions have made this work possible. First and foremost, I would like to express my deepest gratitude to my academic advisor, Professor Brian S. Cummings, for his continuous mentorship. He provided me with a rewarding graduate school experience by granting me intellectual freedom in my work, engaging me in new ideas, and demanding a high quality of work in all my endeavors. I would not be where I am today without his valuable training and support. I would also like to thank my committee members, Dr. Michael Bartlett, Dr. James Franklin, Dr. Kun Lu, and Dr. John Wagner for their scientific insight and advice throughout. I am especially grateful to Professor John Wagner for his guidance and immensely helpful discussions. My fellow lab mates and colleagues, Dr. Natalie Scholpa, Wided Missaoui, and Ramya Kolli, deserve recognition for their advice, friendship, and training over the years. I want to thank all my family and friends for their ceaseless encouragement and love throughout this process. I am wholeheartedly indebted to my mother and sister, who deserve endless thanks for their support, inspiration, and perspective. I am particularly grateful for the constant companionship of Tony and Cleo, who always remind me to embrace joy. Finally, my wonderful husband, David, deserves thanks for his unequivocal love and support throughout, and without whom this work could never have been accomplished.

TABLE OF CONTENTS

Page

LIST OF TABLES

Page

LIST OF FIGURES

Page

CHAPTER 1

INTRODUCTION

1. Lipid Physiology

Biological Roles of Lipids

Lipids are essential molecules that play major roles in cellular structure, membrane dynamics, signaling, and energy storage. They are a diverse group of hydrophobic or amphipathic molecules that are soluble in nonpolar solvents [1], which can be grouped into eight categories: fatty acids, glycerolipids, glycerophospholipids, sphingolipids, sterol lipids, prenol lipids, saccharolipids and polyketides (**Figure 1.1**) [2]. The amphipathic property of lipids allows them to form bilayers to function as protective barriers around cells and organelles [3]. For this reason, lipids comprise the major component of cellular membranes. They facilitate budding, tubulation, fission and fusion, all of which are imperative processes for cell division, biological reproduction and intracellular membrane trafficking [4]. Lipid metabolites derived from degradation participate as important primary and secondary messengers in signal transduction and molecular recognition processes [4]. Finally, the relatively reduced and anhydrous nature of lipids allows them to serve as reservoirs of metabolic energy. This primarily occurs in the form of triacylglycerol (TAG) esters for the storage of caloric reserves and components for membrane biogenesis.

Synthesis and Structural Diversity

The functional diversity of lipids is reflected by their immense structural variability and the generation of thousands of different lipid species relies on a substantial investment in resources by eukaryotic cells [5]. The majority of membrane lipid synthesis occurs in the endoplasmic reticulum (ER), although, some lipids are generated in the other organelles including the mitochondria and peroxisomes. Lipids are transported to their target destinations following synthesis, via vesicles or carrier proteins.

The fatty acid lipid class consists of fatty alcohols and simple acyl structures that make up neutral and polar lipids that can function as secondary messenger molecules, be used for energy storage, and cellular metabolism. The synthesis of fatty acids (FA) is carried out by the fatty acid synthase (FAS) enzyme complex, which is comprised of acetyltransferase, malonyl/acetyl-(or palmitoyl) transacylase, ketoacyl synthase (KAS), ketoacyl reductase, dehydratase, enoyl reductase, acyl carrier protein (ACP), and thioesterase [6]. The condensation of two carbon units from malonyl-ACP forms saturated acyl chains and elongation occurs through the formation of ACP ester bond linkages. Although the mechanism of *de novo* FA synthesis is well conserved across biological systems, there is variation in the subcellular localization and organization of the FAS complexes. Glycerolipids are glycerol-containing lipids such as TAG that are essential for energy metabolism and cellular signaling. TAG formation occurs through two mechanisms: (i) the acylation of diacylglycerol (DAG) with acyl-coA at the *sn*-3 position or (ii) an acyl-CoA-independent phospholipid:diacylglycerol acyltransferase (PDAT) [7] [8]. DAG is an essential intermediate in TAG synthesis, which enters the biosynthetic pathway through the degradation of glycerophospholipids

(PLs) by phospholipases, or through the dephosphorylation of phosphatidic acid. DAGs are also precursors for phosphatidylcholine (PC) and phosphatidylethanolamine (PE) synthesis. PLs are amphipathic molecules that are fundamental for many cellular functions including maintenance of the membrane architecture. Glycerol-3-phosphate is the main precursor for PL biosynthesis via the Kennedy pathway [9].

Although the functional importance of lipids is well understood, the full significance of their biological complexity is not fully described. Recent advances in analytical methodology provide greater tools to characterize global lipid changes with systems-scale lipidomics to characterize the wide range of lipids and their various roles in physiology.

2. Lipid Signaling in Disease

It is widely recognized that perturbations in intracellular lipid metabolism contribute to a plethora of diseases. A vast number of studies have emerged since the 1980s implicating lipids with disease progression and as markers (**Table 1.1**) of inflammation, cancer, cardiac and metabolic disorders, and neurodegenerative diseases. Specifically, the discovery that phosphatidylinositol-4,5-bisphosphate could by hydrolyzed by phospholipase C to DAG and inositol-1,4,5-tris-phosphate greatly bolstered lipid research. The finding that these products function as secondary messengers to activate protein kinase C, along with the identification of inositol and phosphoinositide kinases, brought attention to the significance of phosphoinositide signaling. Furthermore, the link between lipid signaling and these various diseases demonstrates the diversity of lipid

function that reaches far beyond the maintenance of cellular structure and energy storage [10].

Inflammation and Cancer

Bioactive lipid mediators such as eicosanoids and free fatty acids are well documented for their role in modulating inflammatory responses [11, 12]. These mediators are generated from arachidonic acid (AA) and related polyunsaturated fatty acids (PUFA) upon enzymatic release from membrane phospholipids [13]. PUFAs are essential for many biological functions that are enabled by lipid mediators (i.e. prostaglandins, leukotrienes, and lipoxins), which perform as endogenous regulators of inflammation [14]. PUFAs exert anti-inflammatory effects [11], although they can undergo lipid peroxidation during inflammation-induced oxidative stress resulting in the production of isoprostanes and hydroxy fatty acids [15]. Of these PUFA-derived mediators, AA is the most common precursor that forms from the phospholipase A_2 (PLA_2)-mediated cleavage of membrane phospholipids. Following release, AA can be metabolized by cyclooxygenases (COX), lipoxygenases (LOX), or cytochrome P450 monooxygenases (CYP) [16]. Downstream products such as AA-derived lipoxins and docosahexaenoic acid (DHA)- and eicosapentaenoic acid (EPA)-derived resolvins have anti-inflammatory properties [17]. For example, they are able to regulate homeostasis during infection by signaling the phagocytosis of apoptotic immune and epithelial cells [15]. Interestingly, saturated fatty acids are not known to be involved in protective mechanisms and can amplify the proinflammatory action of lipopolysaccharides [11].

Several lipid classes are responsible for generating intra- and extracellular lipid signals that participate in cancer metastasis and tumor growth, reviewed in detail elsewhere [18]. Studies indicate that sphingolipids and their metabolites can serve as modulators of cell survival, growth migration, and angiogenesis [18]. For example, increases in ceramide levels are correlated to cellular stress such as DNA damage and suggest a role in the progression of cancer [18]. Dysregulated PL metabolism is also observed in cancer cells including elevated levels of intermediates in phosphatidylcholine (PC) synthesis and other choline-containing PLs [19, 20]. As such, these lipids have been explored as targets for anti-cancer therapies [21-23] and evaluated as prognostic biomarkers [24, 25]. The PC intermediate glycerophosphocholine, is a precursor for signaling molecules such as phosphatidic acid (PA), which is shown to be involved in the development of anti-cancer drug resistance to rapamycin [26]. Another PL implicated in cancer is lysophosphatidic acid (LPA), a bioactive signaling lipid formed by the metabolism of PA via phospholipases A_1-A_2 [27]. LPA is responsible for broad cellular responses such as proliferation, survival, and migration, and increased LPA levels have been implicated in several types of cancer [28, 29].

Metabolic Syndrome

Although lipid signaling is involved in the physiopathology of inflammation and cancer, it is best known for its central contribution to metabolic syndromes [18]. As discussed above, many lipid-derived signals function as mediators of inflammatory response. Inflammation has become known to be one of the classical features of metabolic

disorders such as obesity and type 2 diabetes [30]. Lipids are essential contributors to our energy supply. In fact, studies demonstrate that lipid oxidation contributes up to 80% of energy during muscular exercise [31]. It is only when dietary lipid intake surpasses energy expenditure that TAG lipid storage takes place in adipose tissue resulting in excess body weight and obesity. Additionally, this oversupply in energy-rich intake is one of the key components to the development of metabolic syndrome [18].

The fatty acid (FA) composition of ingested fats can generally dictate lipid substrate utilization for energy [11]. FAs have a wide range of metabolic functions that can serve as signaling molecules, which are linked to various health problems related to obesity [32]. Intriguingly, human plasma levels of free fatty acids (FFA) are elevated in obese persons and this has been attributed to heightened release from adipose tissue [33]. Long-term elevation of plasma FFA levels can prompt the inhibition of insulin-induced anti-lipolysis, thereby contributing to the development of insulin resistance and type 2 diabetes [11, 34]. Further, FFA availability can be sensed by peroxisome proliferator-activated receptors (PPAR), i.e. nuclear receptors that coordinate FA storage, degradation, and adipocyte differentiation. Adipocyte lipid responses are also controlled by chaperone proteins like fatty acid binding proteins (FABPs).

Cellular stress is another phenomenon that occurs in response to lipid accumulation and makes up a prominent component of metabolic disorders. This is primarily due to saturated FA and sterol buildup, which can lead to stress-induced damage to the ER and mitochondria [35-37]. Such damage creates widespread effects including mitochondrial dysfunction and oxidative stress, which are key features underlying obesity, type 2 diabetes, and insulin resistance [38-40].

The association between sterol lipids, e.g. cholesterol, and cardiovascular disease is one of most widely studied fields in lipid research. Briefly, cholesterol levels exist in high abundance within plasma and can be detected by their association with low- and high-density lipoproteins. Plasma cholesterol levels are clinically used for their strong correlation with a person's risk for cardiovascular events. Specifically, high levels of low-density associated cholesterol indicate heightened risk for coronary artery disease and stroke. Thus, the maintenance of physiological cholesterol levels has been targeted for their therapeutic potential with pharmacological inhibitors.

Thus, lipids are associated with the induction of cellular effects via inflammatory and independent processes that may offer important insight into the onset and progression in inflammatory, metastatic, and metabolic diseases.

Neurological Disorders

The highest lipid concentrations are found in adipose tissue and within the central nervous system (CNS), suggesting an essential role for lipid metabolism within these regions. One of the most abundant lipid classes within the brain that has been implicated in various CNS disorders are sphingolipids. A prime example is free sphingoid base sphingosine-1-phosphate (S1P). This lipid has vast messenger functions that include immune cell trafficking, vascular maintenance, and cell-to-cell communication [41]. Glycerophospholipids (PLs) are also present in relatively high concentrations and make up ~25% of the dry weight in an adult brain [42]. PLs are found in myelin and neural membranes, along with cholesterol and glycolipids, with the major groups being ethanolamine plasmalogen and phosphatidylcholine (PC) [42]. Some of the integral functions of CNS lipids include their ability to participate in

signaling and as modulators of synaptic transmission, which possess broad implications for many clinical neurological disorders including stroke and CNS traumas [43], neurodegenerative diseases [44], mental disorders, and addiction (**Table 1.2**) [45].

Stroke and Brain Injury

Cerebral ischemia or stroke refers to the interruption or obstruction of brain blood flow. This is a leading cause of death [46] and it is thought to occur due to multiple processes. A major contributor to this neuropathology is atherosclerosis, which forms by the accumulation of mainly low-density lipoprotein (LDL)-derived lipids and apoB-100 in the walls of midsized arteries [47]. LDL is a carrier of circulating cholesterol comprised by a core of cholesteryl esters and triacylglycerols and surface film of phosphatidylcholine (PC), sphingomyelin (SM) and unesterified cholesterol [47]. A link between atherosclerosis and ceramide lipids has been suggested through elevated LDL-induced sphingomyelinase activity. Specifically, the release of ceramide is thought to correlate to LDL aggregation during the early stages of atherosclerosis [48].

Increased levels of lipoprotein-PLA2 (Lp-PLA_2), also known as platelet activating factor (PAF) acetylhydrolase, are also associated with coronary heart disease, stroke, and dementia [49, 50]. Lp-PLA_2 can hydrolyze LDL-derived PC to produce oxidized fatty acids and lyso-PC lipids that are associated with endothelial function [47]. Studies indicate that the loss of PC via oxidation, phospholipase-mediated degradation, or synthesis inhibition may contribute to stroke injury [51]. Interestingly, CDP-choline treatment attenuated these effects within stroke injury models. CDP-choline is the rate-limiting intermediate in PC biosynthesis and has undergone clinical trials, reviewed in

detail [52], for its therapeutic potential in several CNS disorders including cerebral ischemia, traumatic brain injury (TBI) hypoxia, learning and memory disorders, and drug addiction. Another key player in brain injury can be attributed to oxidative stress, which the brain is susceptible to given its high energetic demand for oxygen coupled with the great abundance of polyunsaturated fatty acids (PUFA) [47]. This combination heightens the occurrence of lipid peroxidation to PUFAs and is not easily reversed due to the limited number of antioxidant defenses in the CNS [47]

Neurodegenerative Disorders

Emerging evidence demonstrates the importance of cholesterol in the onset and progression of Alzheimer's disease (AD), a brain disorder that progressively affects memory and cognition [47]. One of the key studies to provide a role of cholesterol in AD pathogenesis identified the gene encoding the variant for the APOE ε4 allele [53]. Moses, *et al*. established a role for PL metabolism in AD by linking Group IIA PLA_2 as an inflammatory factor. Specifically, the brains of AD patients showed upregulated Group IIA PLA_2 expression as well as a correlation between hippocampal Group IIA PLA_2 with Aß plaque formation [54]. Another study suggested that $sPLA_2$ may contribute to AD-related lipid peroxidation from oxidative damage through the release of arachidonic acid [55]. Moreover, the association between PLs and AD was shown in a recent study that identified ten phospholipids in human plasma and cerebrospinal fluid that can serve as biomarkers for the onset of amnestic mild cognitive impairment or AD [56]. Lipid peroxidation also plays a large role in Parkinson's disease (PD), a disorder characterized by the degeneration of dopaminergic neurons of the substantia nigra that causes tremors, rigidity, and uncontrollable movement [47]. Markers of lipid peroxidation

were elevated in PD [57] and are thought to result from phospholipase activation. This hypothesis is supported by a study showing the resistance of $cPLA_2$-deficient mice to 1-methyl-4-phenyl-1,2,3,6-tetrohydropyridine (MPTP)-induced neurotoxicity [58].

The endocannabinoid (EC) system is known to have a neuroprotective role in neurodegenerative diseases and CNS injury, which Pacher, *et al*. has reviewed in detail [59]. ECs are constituted of amides, esters, and ethers of long chain PUFA. Two of the extensively investigated ECs are: N-arachidonoylethanolamine (AEA, anandamide) and 2-arachidonylglycerol (2-AG). Both of these lipids function as cell signaling activators [60]. Hypoactivity of the EC system is thought to underlie abnormalities in neurotransmission in Huntington's disease (HD), which is a rare genetic disorder that affects coordination and cognition [60]. Maccarrone, *et al*. demonstrated that inhibition of fatty acid amide hydrolase and monoacylglycerol lipase counteracts HD-related neurodeficits in correlation with increased EC levels [60]. Disorders in lipid metabolism, specifically deficiencies in acidic sphingomyelinase (ASMase), can also result in the development of genetic pediatric neurodegenerative conditions such as Niemann-Pick Diseases (NPD) [61]. Additionally, mental illnesses such as schizophrenia are also linked to dysregulated PL metabolism. These abnormalities are hypothesized to occur through increased PLA_2 activity and increased PL hydrolysis with uncharacteristic decreases in PUFA incorporation into PLs [62].

Drugs of Abuse

Recent advances in addiction research have increased the attention to the interaction between drugs of abuse and lipids in the brain. The focus of such research revolves around the many functions of CNS lipids, including their utility as neuromodulators, role

in synaptic plasticity following exposure to drugs of abuse, and membrane subdomain interactions with signal transduction pathways [63]. While it is unknown whether lipids mediate, counteract, or actively participate in the effects of reinforcing drugs on synaptic plasticity, these functions are hypothesized to be integral to the synaptic changes underlying drug addiction [63]. It is also likely that the well characterized motivational neurocircuitry of dopaminergic (DA) transmission represents a small piece of the interplay of multiple circuits and cellular events in addiction [45, 63].

The involvement of lipid signaling in the development and maintenance of addiction can be attributed to several mechanisms including alterations in the metabolic and signaling pathways of cannabinoids (CB), prostaglandins (PG), and sex steroids. For example, treatment with selective cannabinoid type 2 receptors (CB2) antagonists suggest roles for CB2 in addiction [64]. Further, activation of the CB2 receptor decreases in cocaine-induced reinstatement rather than reward itself [64]. Signaling lipid molecules like ECs exhibit wide behavioral effects by influencing reward and motivation, euphoria, and memory [65, 66]. Evidence also shows that ECs are responsible for modulating synaptic transmission and mediating synaptic plasticity in regions involved in drug reward and reinforcement, reviewed in detail elsewhere [67]. Alcohol exposure can stimulate PG release and metabolism [68]. Interestingly, studies show that estrogen receptors can influence the reward circuitry for stimulants such as cocaine and amphetamine [45]. Moreover, there is significant crosstalk between these lipid signaling networks that appear to function both independently and synergistically.

The link between lipids and addiction is not limited to a handful of classes. Several other types of lipids have emerged as modulators of synaptic function, including

PLs, fatty acids, platelet activating factors (PAF), and S1P [63]. One study suggested an association between cocaine and increases in brain PL precursors that may mediate some of the cocaine-induced effects of DA receptor stimulation [69]. Additionally, pathways that stimulate the release of AA, such as activators of PLA_2, demonstrated inhibitory effects on DA uptake. Dietary deficiency in α-linolenic acid, the precursor of long-chain n–3 polyunsaturated fatty acids (PUFA), altered dopaminergic neurotransmission [70, 71]. Huston, et al. also suggested a role for the acid sphingomyelinase (ASM)-ceramide pathway in the brain in the involvement of the learning of extinction behavior [72]. The products of PC-containing PL metabolism via $cPLA_2$, AA and lyso-PAF, can act as a retrograde messenger of long-term potentiation (LTP) within the hippocampus [73]. Lastly, the habits and metabolic effects of individuals exposed to drugs of abuse can bring about changes in substrates for neuronal membrane lipid biogenesis and cholesterol metabolism [63].

3. Summary

The studies described above have identified many messengers related to lipid signaling that have immense implications for clinical applications. However, given the sheer number and diversity of lipids, these findings are likely just the surface of understanding lipid pathophysiology. Recent advances in the development of methods for lipid analysis have made it possible to better characterize the perturbations in lipid metabolism that occur in various diseases. With the potential of lipids to serve as indices of peripheral tissue status, identifying lipid alterations in metabolic and neurological disorders has become of particular interest. Many studies have focused on identifying the neurochemical and neurobiological effects of various drugs of abuse, but recent work

shows a growing body of literature interested in the effects of cocaine use on lipid remodeling. It has become essential to investigate and validate how lipid remodeling occurs in both preclinical and clinical models of addiction. Further, there are gaps in knowledge regarding the link between complex lipid remodeling and their role in addictive behaviors. Such lipidomic research may reveal novel signaling mechanisms or targets for the detection and treatment of addiction.

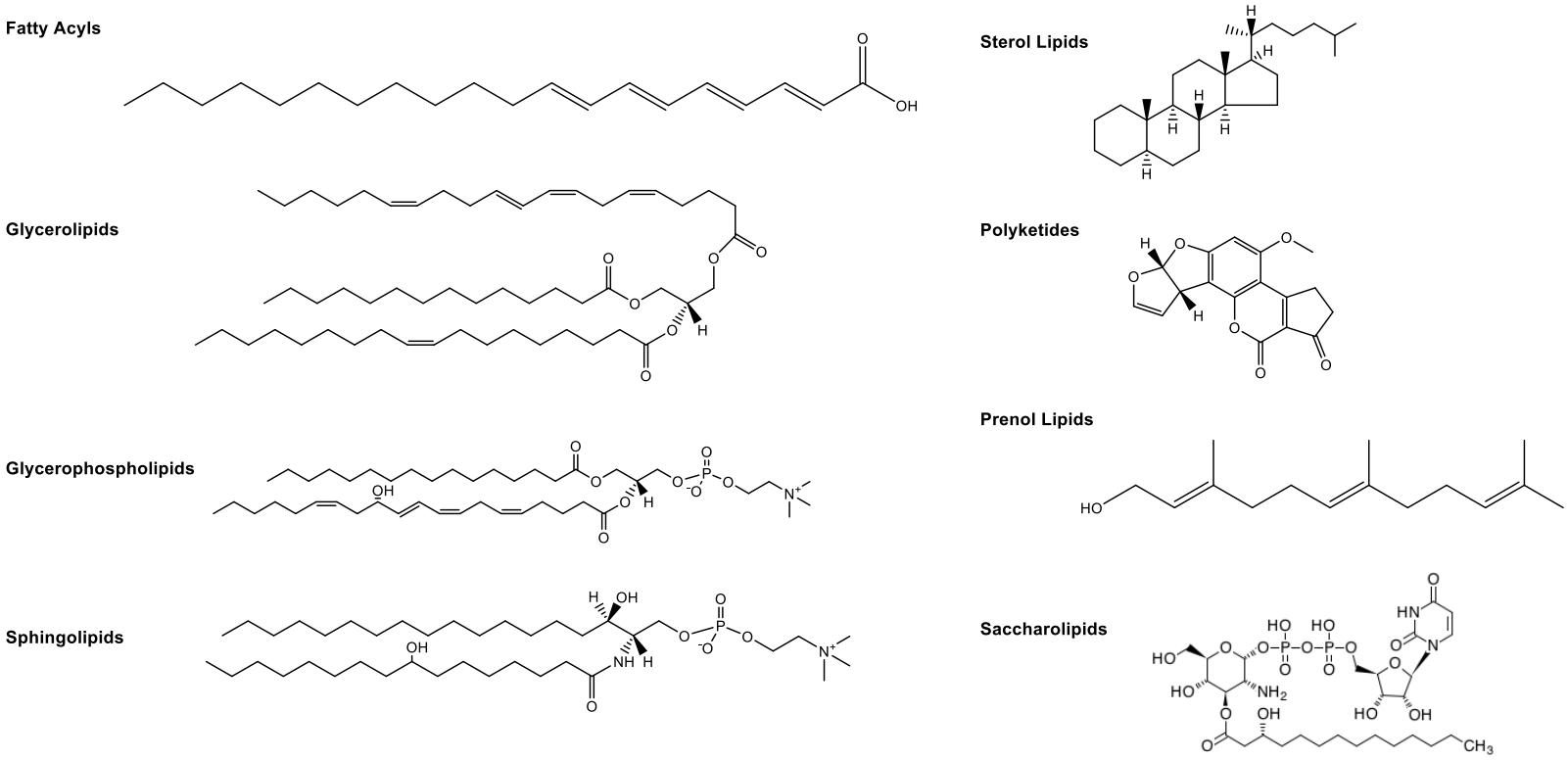

Figure 1.1. Structures of lipid classes. All structures were generated with ChemDraw Professional 15.1 (Cambridge Scientific. Inc.)

Table 1.1. Lipid markers in disease. Modified and adapted from Hu, Chunxiu, *et al*. [74].

Disease Model	Lipid Signals	Reference
Obesity	– Long-chain TGs – Cer – LysoPC – Ether PLs	[75, 76]
Diabetes	– CL	[77]
Cardiovascular Disease	– Cho esters – Long-chain TGs	[78]
	Cancer	
Pancreatic	– PI – Acyl-, alkyl- and alkenyl-LPA	[79]
Ovarian	– LysoPI – SphingosylPC	[80]
Breast	– Choline PLs	[81]
Rheumatoid Arthritis	– PC – LysoPC	[82]
Chronic Glomerulonephritis	– PI – PS	[83]
Mitochondrial Dysfunction	– CL	[84]
Epithelial Barrier Dysfunction	– n-3 PUFAs	[85]
Barth Syndrome	– MonolysoCL – CL	[86]
Fabry Disease	– SM (22:0) – GlucosylCer (22:0) – Cer trihexoside (24:1) – LactosylCer (24:1)	[87]
Gaucher Disease	– Cer monohexoside	[88]
Statin-Induced Myopathy	– PE (36:1) – PE (40:4) – TG (54:2), (54:3), (56:5) – SM (d:18/22:0), – PC (O-38:5), (O-34:3) – Cho Esters (18:0), (18:2)	[89]

Abbreviations: Triacylglyceride, TG; Phospholipid, PL; Cholesterol, Cho; Cardiolipin, CL; Ceramide, Cer; Sphingomyelin, SM; Phosphatidic acid, PA; Phosphatidylcholine, PC; Phosphatidylethanolamine, PE; Phosphatidylinositol, PI; Phosphatidylserine, PS; Polyunsaturated fatty acid, PUFA.

Table 1.2. Lipid signaling in neurological disorders. Modified and adapted from R.M. Adibhatla, *et al*. [44]

Neurological Disease	Mechanism of Lipid Regulation	Reference
Addiction	– Treatment with CDP-choline ↓ drug craving – ↓ PUFA levels as predictors of relapse – Dietary PUFAs influence dopamine levels – Role for ASMase-ceramide pathway in extinction behavior – ↑ Brain PL precursors associated with dependence – ↓ Activity of PL metabolic enzymes – Stimulated release of AA, i.e. activators of PLA_2, inhibited DA uptake – AA and lyso-PAF are retrograde messengers of LTP in hippocampus	[69] [72] [73] [90, 91] [72] [69]
Alzheimer's Disease	– Sulfatide – PLs predictive of amnestic mild cognitive impairment or AD onset – Altered Cho and lipid homeostasis – ↓ DHA levels – PLA_2 upregulation and ↑$sPLA_2$-IIA expression – ↑ Lipid peroxidation	[92] [93, 94] [56] [55] [54, 58] [95]
Amyotrophic Lateral Sclerosis	– Lipid peroxidation	[96]
Bipolar Disorder & Epilepsy	– ↓ DHA levels	[95]
Huntington Disease	– Inhibition of FAAH, MAGL, EMT provided symptomatic relief	[60, 97]
Multiple Sclerosis	– Lipid peroxidation products from ROS – $cPLA_2$ highly expressed – ↑ $sPLA_2$ levels prior to onset of symptoms – ↓ DHA levels – $sPLA_2$ inhibition blocks inflammation	[58, 95] [98]

Niemann-Pick Disease	– A-SMase activity leads to accumulation of lysosomal SM – Excessive accumulation of Cho and SL	[99, 100]
Parkinson's Disease	– Protective effects from knockout of $cPLA_2$ – PUFAs promote α-synuclein aggregation – PLA_2 inhibition therapy	[58, 101]
Schizophrenia	– Altered lipid metabolism correlates to defects in neurological development	[62, 102]
Stroke	– ↑ $sPLA_2$ – Protective effects from knockout of $cPLA_2$ – ↓ DHA levels	[95] [103] [104]

Abbreviations: Polyunsaturated fatty acid, PUFA; Phospholipid, PL; Acid sphingomyelinase, ASMase; Arachidonic Acid, AA; lyso-platelet activating factor, lyso-PAF; Dopamine, DA; long-term potentiation, LTP; Cholesterol, Cho; Docosahexaenoic acid, DHA; Fatty acid amide hydrolase, FAAH; Monoacylglycerol lipase, MAGL; Endocannabinoid membrane transporter, EMT; Reactive oxygen species, ROS; Sphingolipid, SL; Sphingomyelin, SM.

References

[1] M.I. Gurr, A.T. James, Lipids: what they are and how the biochemist deals with them, in: M.I. Gurr, A.T. James (Eds.) Lipid Biochemistry: An Introduction, Springer Netherlands, Dordrecht, 1980, pp. 1-17.

[2] E. Fahy, S. Subramaniam, R.C. Murphy, M. Nishijima, C.R. Raetz, T. Shimizu, F. Spener, G. van Meer, M.J. Wakelam, E.A. Dennis, Update of the LIPID MAPS comprehensive classification system for lipids, J Lipid Res, 50 Suppl (2009) S9-14.

[3] D.A. Brown, E. London, Structure and Origin of Ordered Lipid Domains in Biological Membranes, The Journal of Membrane Biology, 164 (1998) 103-114.

[4] G. van Meer, D.R. Voelker, G.W. Feigenson, Membrane lipids: where they are and how they behave, Nature reviews. Molecular cell biology, 9 (2008) 112-124.

[5] M. Sud, E. Fahy, D. Cotter, A. Brown, E.A. Dennis, C.K. Glass, A.H. Merrill, Jr., R.C. Murphy, C.R. Raetz, D.W. Russell, S. Subramaniam, LMSD: LIPID MAPS structure database, Nucleic acids research, 35 (2007) D527-532.

[6] E. Schweizer, J. Hofmann, Microbial type I fatty acid synthases (FAS): major players in a network of cellular FAS systems, Microbiology and molecular biology reviews, 68 (2004) 501-517.

[7] A. Dahlqvist, U. Ståhl, M. Lenman, A. Banas, M. Lee, L. Sandager, H. Ronne, S. Stymne, Phospholipid: diacylglycerol acyltransferase: an enzyme that catalyzes the acyl-CoA-independent formation of triacylglycerol in yeast and plants, Proceedings of the National Academy of Sciences, 97 (2000) 6487-6492.

[8] U. Ståhl, A.S. Carlsson, M. Lenman, A. Dahlqvist, B. Huang, W. Banaś, A. Banaś, S. Stymne, Cloning and Functional Characterization of a Phospholipid:Diacylglycerol Acyltransferase from Arabidopsis, Plant Physiology, 135 (2004) 1324-1335.

[9] E.P. Kennedy, Biosynthesis of complex lipids, in: Federation proceedings, vol. 20, 1961, pp. 934.

[10] O. Quehenberger, A.M. Armando, A.H. Brown, S.B. Milne, D.S. Myers, A.H. Merrill, S. Bandyopadhyay, K.N. Jones, S. Kelly, R.L. Shaner, Lipidomics reveals a remarkable diversity of lipids in human plasma, Journal of lipid research, 51 (2010) 3299-3305.

[11] O. Quehenberger, E.A. Dennis, The human plasma lipidome, The New England journal of medicine, 365 (2011) 1812-1823.

[12] C.N. Serhan, N. Chiang, T.E. Van Dyke, Resolving inflammation: dual anti-inflammatory and pro-resolution lipid mediators, Nature reviews. Immunology, 8 (2008) 349-361.

[13] M.W. Buczynski, D.S. Dumlao, E.A. Dennis, Thematic Review Series: Proteomics. An integrated omics analysis of eicosanoid biology, Journal of lipid research, 50 (2009) 1015-1038.

[14] M.J. Stables, D.W. Gilroy, Old and new generation lipid mediators in acute inflammation and resolution, Progress in lipid research, 50 (2011) 35-51.

[15] Vincent C. Tam, O. Quehenberger, Christine M. Oshansky, R. Suen, Aaron M. Armando, Piper M. Treuting, Paul G. Thomas, Edward A. Dennis, A. Aderem, Lipidomic Profiling of Influenza Infection Identifies Mediators that Induce and Resolve Inflammation, Cell, 154 (2013) 213-227.

[16] M. Arita, Mediator lipidomics in acute inflammation and resolution, The Journal of Biochemistry, 152 (2012) 313-319.
[17] C.N. Serhan, C.B. Clish, J. Brannon, S.P. Colgan, N. Chiang, K. Gronert, Novel functional sets of lipid-derived mediators with antiinflammatory actions generated from omega-3 fatty acids via cyclooxygenase 2–nonsteroidal antiinflammatory drugs and transcellular processing, Journal of Experimental Medicine, 192 (2000) 1197-1204.
[18] M.P. Wymann, R. Schneiter, Lipid signalling in disease, Nature reviews. Molecular cell biology, 9 (2008) 162.
[19] W. Negendank, Studies of human tumors by MRS: a review, NMR in Biomedicine, 5 (1992) 303-324.
[20] E. Ackerstaff, K. Glunde, Z.M. Bhujwalla, Choline phospholipid metabolism: a target in cancer cells?, Journal of cellular biochemistry, 90 (2003) 525-533.
[21] K. Nakagami, T. Uchida, S. Ohwada, Y. Koibuchi, Y. Suda, T. Sekine, Y. Morishita, Increased choline kinase activity and elevated phosphocholine levels in human colon cancer, Cancer Science, 90 (1999) 419-424.
[22] A.R. de Molina, R. Gutierrez, M.A. Ramos, J.M. Silva, J. Silva, F. Bonilla, J.J. Sanchez, J.C. Lacal, Increased choline kinase activity in human breast carcinomas: clinical evidence for a potential novel antitumor strategy, Oncogene, 21 (2002) 4317.
[23] E. Iorio, A. Ricci, M. Bagnoli, M.E. Pisanu, G. Castellano, M. Di Vito, E. Venturini, K. Glunde, Z.M. Bhujwalla, D. Mezzanzanica, Activation of phosphatidylcholine cycle enzymes in human epithelial ovarian cancer cells, Cancer research, 70 (2010) 2126-2135.

[24] A.R. de Molina, J. Sarmentero-Estrada, C. Belda-Iniesta, M. Tarón, V.R. de Molina, P. Cejas, M. Skrzypski, D. Gallego-Ortega, J. de Castro, E. Casado, Expression of choline kinase alpha to predict outcome in patients with early-stage non-small-cell lung cancer: a retrospective study, The lancet oncology, 8 (2007) 889-897.

[25] N. Jagannathan, M. Kumar, V. Seenu, O. Coshic, S. Dwivedi, P. Julka, A. Srivastava, G. Rath, Evaluation of total choline from in-vivo volume localized proton MR spectroscopy and its response to neoadjuvant chemotherapy in locally advanced breast cancer, British journal of cancer, 84 (2001) 1016.

[26] D.A. Foster, Phosphatidic acid signaling to mTOR: signals for the survival of human cancer cells, Biochimica et Biophysica Acta (BBA)-Molecular and Cell Biology of Lipids, 1791 (2009) 949-955.

[27] A. Tokumura, E. Majima, Y. Kariya, K. Tominaga, K. Kogure, K. Yasuda, K. Fukuzawa, Identification of human plasma lysophospholipase D, a lysophosphatidic acid-producing enzyme, as autotaxin, a multifunctional phosphodiesterase, Journal of Biological Chemistry, 277 (2002) 39436-39442.

[28] W.H. Moolenaar, L.A. van Meeteren, B.N. Giepmans, The ins and outs of lysophosphatidic acid signaling, Bioessays, 26 (2004) 870-881.

[29] G.B. Mills, W.H. Moolenaar, The emerging role of lysophosphatidic acid in cancer, Nature reviews. Cancer, 3 (2003) 582.

[30] G.S. Hotamisligil, Inflammation and metabolic disorders, Nature, 444 (2006) 860.

[31] F. Pirnay, M. Lacroix, F. Mosora, A. Luyckx, P. Lefebvre, Effect of glucose ingestion on energy substrate utilization during prolonged muscular exercise, European journal of applied physiology and occupational physiology, 36 (1977) 247-254.

[32] A. Santomauro, G. Boden, M. Silva, D.M. Rocha, R.F. Santos, M. Ursich, P.G. Strassmann, B.L. Wajchenberg, Overnight lowering of free fatty acids with Acipimox improves insulin resistance and glucose tolerance in obese diabetic and nondiabetic subjects, Diabetes, 48 (1999) 1836-1841.

[33] G.M. Reaven, C. Hollenbeck, C.-Y. Jeng, M.S. Wu, Y.-D.I. Chen, Measurement of plasma glucose, free fatty acid, lactate, and insulin for 24 h in patients with NIDDM, Diabetes, 37 (1988) 1020-1024.

[34] G. Boden, Fatty acid—induced inflammation and insulin resistance in skeletal muscle and liver, Current diabetes reports, 6 (2006) 177-181.

[35] Y. Wei, D. Wang, F. Topczewski, M.J. Pagliassotti, Saturated fatty acids induce endoplasmic reticulum stress and apoptosis independently of ceramide in liver cells, American Journal of Physiology-Endocrinology and Metabolism, 291 (2006) E275-E281.

[36] Y. Li, M. Ge, L. Ciani, G. Kuriakose, E.J. Westover, M. Dura, D.F. Covey, J.H. Freed, F.R. Maxfield, J. Lytton, Enrichment of Endoplasmic Reticulum with Cholesterol Inhibits Sarcoplasmic-Endoplasmic Reticulum Calcium ATPase-2b Activity in Parallel with Increased Order of Membrane Lipids IMPLICATIONS FOR DEPLETION OF ENDOPLASMIC RETICULUM CALCIUM STORES AND APOPTOSIS IN CHOLESTEROL-LOADED MACROPHAGES, Journal of Biological Chemistry, 279 (2004) 37030-37039.

[37] B. Feng, P.M. Yao, Y. Li, C.M. Devlin, D. Zhang, H.P. Harding, M. Sweeney, J.X. Rong, G. Kuriakose, E.A. Fisher, The endoplasmic reticulum is the site of cholesterol-induced cytotoxicity in macrophages, Nature cell biology, 5 (2003) 781.

[38] S. Furukawa, T. Fujita, M. Shimabukuro, M. Iwaki, Y. Yamada, Y. Nakajima, O. Nakayama, M. Makishima, M. Matsuda, I. Shimomura, Increased oxidative stress in obesity and its impact on metabolic syndrome, The Journal of clinical investigation, 114 (2017) 1752-1761.

[39] N.E. Houstis, Reactive oxygen species play a causal role in multiple forms of insulin resistance, in, Massachusetts Institute of Technology, 2007.

[40] B.B. Lowell, G.I. Shulman, Mitochondrial dysfunction and type 2 diabetes, Science, 307 (2005) 384-387.

[41] M.-J. Lee, J.R. Van Brocklyn, S. Thangada, C.H. Liu, A.R. Hand, R. Menzeleev, S. Spiegel, T. Hla, Sphingosine-1-phosphate as a ligand for the G protein-coupled receptor EDG-1, Science, 279 (1998) 1552-1555.

[42] A.A. Farooqui, L.A. Horrocks, T. Farooqui, Glycerophospholipids in brain: their metabolism, incorporation into membranes, functions, and involvement in neurological disorders, Chemistry and physics of lipids, 106 (2000) 1-29.

[43] R.M. Adibhatla, R. Dempsey, J.F. Hatcher, Integration of Cytokine Biology and Lipid Metabolism in Stroke**, Frontiers in bioscience : a journal and virtual library, 13 1250-1270.

[44] R.M. Adibhatla, J.F. Hatcher, Role of Lipids in Brain Injury and Diseases, Future lipidology, 2 (2007) 403-422.

[45] E. Leishman, K.J. Kokesh, H.B. Bradshaw, Lipids and addiction: how sex steroids, prostaglandins, and cannabinoids interact with drugs of abuse, Annals of the New York Academy of Sciences, 1282 (2013) 25-38.

[46] A.R. Young, C. Ali, A. Duretete, D. Vivien, Neuroprotection and stroke: time for a compromise, J Neurochem, 103 (2007) 1302-1309.

[47] R.M. Adibhatla, J.F. Hatcher, Altered Lipid Metabolism in Brain Injury and Disorders, Sub-cellular biochemistry, 49 (2008) 241-268.

[48] P.K. Kinnunen, J.M. Holopainen, Sphingomyelinase activity of LDL: a link between atherosclerosis, ceramide, and apoptosis?, Trends in cardiovascular medicine, 12 (2002) 37-42.

[49] S. Lavi, J.P. McConnell, C.S. Rihal, A. Prasad, V. Mathew, L.O. Lerman, A. Lerman, Local production of lipoprotein-associated phospholipase A2 and lysophosphatidylcholine in the coronary circulation: association with early coronary atherosclerosis and endothelial dysfunction in humans, Circulation, 115 (2007) 2715-2721.

[50] H.H. Oei, I.M. van der Meer, A. Hofman, P.J. Koudstaal, T. Stijnen, M.M. Breteler, J.C. Witteman, Lipoprotein-associated phospholipase A2 activity is associated with risk of coronary heart disease and ischemic stroke: the Rotterdam Study, Circulation, 111 (2005) 570-575.

[51] R.M. Adibhatla, J.F. Hatcher, Cytidine 5′-Diphosphocholine (CDP-Choline) in Stroke and Other CNS Disorders, Neurochem Res, 30 (2005) 15-23.

[52] R.M. Adibhatla, J. Hatcher, Cytidine 5′-diphosphocholine (CDP-choline) in stroke and other CNS disorders, Neurochemical research, 30 (2005) 15-23.

[53] L. Puglielli, Aging of the brain, neurotrophin signaling, and Alzheimer's disease: is IGF1-R the common culprit?, Neurobiology of aging, 29 (2008) 795-811.

[54] G.S.D. Moses, M.D. Jensen, L.F. Lue, D.G. Walker, A.Y. Sun, A. Simonyi, G.Y. Sun, Secretory PLA(2)-IIA: a new inflammatory factor for Alzheimer's disease, Journal of Neuroinflammation, 3 (2006) 28.

[55] T.I. Williams, B.C. Lynn, W.R. Markesbery, M.A. Lovell, Increased levels of 4-hydroxynonenal and acrolein, neurotoxic markers of lipid peroxidation, in the brain in Mild Cognitive Impairment and early Alzheimer's disease, Neurobiology of aging, 27 (2006) 1094-1099.

[56] M. Mapstone, A.K. Cheema, M.S. Fiandaca, X. Zhong, T.R. Mhyre, L.H. MacArthur, W.J. Hall, S.G. Fisher, D.R. Peterson, J.M. Haley, M.D. Nazar, S.A. Rich, D.J. Berlau, C.B. Peltz, M.T. Tan, C.H. Kawas, H.J. Federoff, Plasma phospholipids identify antecedent memory impairment in older adults, Nat Med, 20 (2014) 415-418.

[57] E. Mariani, M.C. Polidori, A. Cherubini, P. Mecocci, Oxidative stress in brain aging, neurodegenerative and vascular diseases: an overview, Journal of chromatography. B, Analytical technologies in the biomedical and life sciences, 827 (2005) 65-75.

[58] A.A. Farooqui, W.Y. Ong, L.A. Horrocks, Inhibitors of brain phospholipase A2 activity: their neuropharmacological effects and therapeutic importance for the treatment of neurologic disorders, Pharmacological reviews, 58 (2006) 591-620.

[59] P. Pacher, S. BÁTkai, G. Kunos, The Endocannabinoid System as an Emerging Target of Pharmacotherapy, Pharmacological reviews, 58 (2006) 389-462.

[60] M. Maccarrone, N. Battista, D. Centonze, The endocannabinoid pathway in Huntington's disease: a comparison with other neurodegenerative diseases, Progress in neurobiology, 81 (2007) 349-379.

[61] E.H. Schuchman, The pathogenesis and treatment of acid sphingomyelinase-deficient Niemann-Pick disease, Journal of inherited metabolic disease, 30 (2007) 654-663.
[62] G.E. Berger, S. Smesny, G.P. Amminger, Bioactive lipids in schizophrenia, International review of psychiatry (Abingdon, England), 18 (2006) 85-98.
[63] C.J. Hillard, Lipids and drugs of abuse, Life Sciences, 77 (2005) 1531-1542.
[64] P. Adamczyk, J. Miszkiel, A.C. McCreary, M. Filip, M. Papp, E. Przegaliński, The effects of cannabinoid CB1, CB2 and vanilloid TRPV1 receptor antagonists on cocaine addictive behavior in rats, Brain research, 1444 (2012) 45-54.
[65] R.S. Rapaka, D. Piomelli, S. Spiegel, N. Bazan, E.A. Dennis, Targeted lipidomics: signaling lipids and drugs of abuse, Prostaglandins & other lipid mediators, 77 (2005) 223-234.
[66] A. Serrano, L.H. Parsons, Endocannabinoid influence in drug reinforcement, dependence and addiction-related behaviors, Pharmacology & therapeutics, 132 (2011) 215-241.
[67] M. van der Stelt, V. Di Marzo, The endocannabinoid system in the basal ganglia and in the mesolimbic reward system: implications for neurological and psychiatric disorders, European Journal of Pharmacology, 480 (2003) 133-150.
[68] S.N. Pennington, C.P. Smith, The effect of ethanol on thromboxane synthesis by blood platelets, Prostaglandins and medicine, 2 (1979) 43-49.
[69] B.M. Ross, A. Moszczynska, F.J. Peretti, V. Adams, G.A. Schmunk, K.S. Kalasinsky, L. Ang, N. Mamalias, S.D. Turenne, S.J. Kish, Decreased activity of brain

phospholipid metabolic enzymes in human users of cocaine and methamphetamine, Drug and alcohol dependence, 67 (2002) 73-79.
[70] L. Zimmer, S. Delion-Vancassel, G. Durand, D. Guilloteau, S. Bodard, J.-C. Besnard, S. Chalon, Modification of dopamine neurotransmission in the nucleus accumbens of rats deficient in n–3 polyunsaturated fatty acids, Journal of Lipid Research, 41 (2000) 32-40.
[71] L. Zhang, M.E. Reith, Regulation of the functional activity of the human dopamine transporter by the arachidonic acid pathway, European journal of pharmacology, 315 (1996) 345-354.
[72] J.P. Huston, J. Kornhuber, C. Mühle, L. Japtok, M. Komorowski, C. Mattern, M. Reichel, E. Gulbins, B. Kleuser, B. Topic, A sphingolipid mechanism for behavioral extinction, Journal of neurochemistry, 137 (2016) 589-603.
[73] N.G. Bazan, Synaptic lipid signaling significance of polyunsaturated fatty acids and platelet-activating factor, Journal of lipid research, 44 (2003) 2221-2233.
[74] C. Hu, R. van der Heijden, M. Wang, J. van der Greef, T. Hankemeier, G. Xu, Analytical strategies in lipidomics and applications in disease biomarker discovery, Journal of Chromatography B, 877 (2009) 2836-2846.
[75] L. Yetukuri, M. Katajamaa, G. Medina-Gomez, T. Seppänen-Laakso, A. Vidal-Puig, M. Orešič, Bioinformatics strategies for lipidomics analysis: characterization of obesity related hepatic steatosis, BMC systems biology, 1 (2007) 12.
[76] M. Kolak, J. Westerbacka, V.R. Velagapudi, D. Wågsäter, L. Yetukuri, J. Makkonen, A. Rissanen, A.-M. Häkkinen, M. Lindell, R. Bergholm, Adipose tissue

inflammation and increased ceramide content characterize subjects with high liver fat content independent of obesity, Diabetes, 56 (2007) 1960-1968.
[77] X. Han, J. Yang, K. Yang, Z. Zhao, D.R. Abendschein, R.W. Gross, Alterations in myocardial cardiolipin content and composition occur at the very earliest stages of diabetes: a shotgun lipidomics study, Biochemistry, 46 (2007) 6417-6428.
[78] J.T. Brindle, H. Antti, E. Holmes, G. Tranter, J.K. Nicholson, H.W. Bethell, S. Clarke, P.M. Schofield, E. McKilligin, D.E. Mosedale, Rapid and noninvasive diagnosis of the presence and severity of coronary heart disease using 1H-NMR-based metabonomics, Nature medicine, 8 (2002) 1439.
[79] R.D. Beger, L.K. Schnackenberg, R.D. Holland, D. Li, Y. Dragan, Metabonomic models of human pancreatic cancer using 1D proton NMR spectra of lipids in plasma, Metabolomics, 2 (2006) 125-134.
[80] Y.-j. Xiao, B. Schwartz, M. Washington, A. Kennedy, K. Webster, J. Belinson, Y. Xu, Electrospray ionization mass spectrometry analysis of lysophospholipids in human ascitic fluids: comparison of the lysophospholipid contents in malignant vs nonmalignant ascitic fluids, Analytical biochemistry, 290 (2001) 302-313.
[81] K. Natarajan, N. Mori, D. Artemov, Z.M. Bhujwalla, Exposure of human breast cancer cells to the anti-inflammatory agent indomethacin alters choline phospholipid metabolites and Nm23 expression, Neoplasia, 4 (2002) 409-416.
[82] B. Fuchs, J. Schiller, U. Wagner, H. Häntzschel, K. Arnold, The phosphatidylcholine/lysophosphatidylcholine ratio in human plasma is an indicator of the severity of rheumatoid arthritis: investigations by 31 P NMR and MALDI-TOF MS, Clinical biochemistry, 38 (2005) 925-933.

[83] L. Jia, C. Wang, S. Zhao, X. Lu, G. Xu, Metabolomic identification of potential phospholipid biomarkers for chronic glomerulonephritis by using high performance liquid chromatography–mass spectrometry, Journal of Chromatography B, 860 (2007) 134-140.

[84] X. Han, J. Yang, H. Cheng, K. Yang, D.R. Abendschein, R.W. Gross, Shotgun lipidomics identifies cardiolipin depletion in diabetic myocardium linking altered substrate utilization with mitochondrial dysfunction, Biochemistry, 44 (2005) 16684-16694.

[85] Q. Li, Q. Zhang, M. Wang, S. Zhao, G. Xu, J. Li, n-3 polyunsaturated fatty acids prevent disruption of epithelial barrier function induced by proinflammatory cytokines, Molecular immunology, 45 (2008) 1356-1365.

[86] W. Kulik, H. van Lenthe, F.S. Stet, R.H. Houtkooper, H. Kemp, J.E. Stone, C.G. Steward, R.J. Wanders, F.M. Vaz, Bloodspot assay using HPLC–tandem mass spectrometry for detection of Barth syndrome, Clinical chemistry, 54 (2008) 371-378.

[87] M. Fuller, P.C. Sharp, T. Rozaklis, P.D. Whitfield, D. Blacklock, J.J. Hopwood, P.J. Meikle, Urinary lipid profiling for the identification of Fabry hemizygotes and heterozygotes, Clinical chemistry, 51 (2005) 688-694.

[88] T. Fujiwaki, S. Yamaguchi, M. Tasaka, N. Sakura, T. Taketomi, Application of delayed extraction–matrix-assisted laser desorption ionization time-of-flight mass spectrometry for analysis of sphingolipids in pericardial fluid, peritoneal fluid and serum from Gaucher disease patients, Journal of Chromatography B, 776 (2002) 115-123.

[89] R. Laaksonen, M. Katajamaa, H. Päivä, M. Sysi-Aho, L. Saarinen, P. Junni, D. Lütjohann, J. Smet, R. Van Coster, T. Seppänen-Laakso, A systems biology strategy

reveals biological pathways and plasma biomarker candidates for potentially toxic statin-induced changes in muscle, PloS one, 1 (2006) e97.

[90] L. Buydens-Branchey, M. Branchey, Association between low plasma levels of cholesterol and relapse in cocaine addicts, Psychosomatic medicine, 65 (2003) 86-91.

[91] L. Buydens-Branchey, M. Branchey, D.L. McMakin, J.R. Hibbeln, Polyunsaturated fatty acid status and relapse vulnerability in cocaine addicts, Psychiatry research, 120 (2003) 29-35.

[92] X. Han, S. Rozen, S.H. Boyle, C. Hellegers, H. Cheng, J.R. Burke, K.A. Welsh-Bohmer, P.M. Doraiswamy, R. Kaddurah-Daouk, Metabolomics in early Alzheimer's disease: identification of altered plasma sphingolipidome using shotgun lipidomics, PloS one, 6 (2011) e21643.

[93] B. Wolozin, Cholesterol, statins and dementia, Current opinion in lipidology, 15 (2004) 667-672.

[94] R.M. Lane, M.R. Farlow, Lipid homeostasis and apolipoprotein E in the development and progression of Alzheimer's disease, J Lipid Res, 46 (2005) 949-968.

[95] A.A. Farooqui, L.A. Horrocks, T. Farooqui, Modulation of inflammation in brain: a matter of fat, J Neurochem, 101 (2007) 577-599.

[96] E.P. Simpson, Y.K. Henry, J.S. Henkel, R.G. Smith, S.H. Appel, Increased lipid peroxidation in sera of ALS patients: a potential biomarker of disease burden, Neurology, 62 (2004) 1758-1765.

[97] N. Battista, F. Fezza, A. Finazzi-Agro, M. Maccarrone, The endocannabinoid system in neurodegeneration, The Italian journal of biochemistry, 55 (2006) 283-289.

[98] T.J. Cunningham, L. Yao, M. Oetinger, L. Cort, E.P. Blankenhorn, J.I. Greenstein, Secreted phospholipase A2 activity in experimental autoimmune encephalomyelitis and multiple sclerosis, Journal of Neuroinflammation, 3 (2006) 26.

[99] S. Mukherjee, F.R. Maxfield, Lipid and cholesterol trafficking in NPC, Biochimica et biophysica acta, 1685 (2004) 28-37.

[100] A.H. Futerman, G. van Meer, The cell biology of lysosomal storage disorders, Nat Rev Mol Cell Biol, 5 (2004) 554-565.

[101] K. Welch, J. Yuan, Alpha-synuclein oligomerization: a role for lipids?, Trends in neurosciences, 26 (2003) 517-519.

[102] D. Horrobin, The lipid hypothesis of schizophrenia, New Comprehensive Biochemistry, 35 (2002) 39-52.

[103] R. Muralikrishna Adibhatla, J.F. Hatcher, Phospholipase A2, reactive oxygen species, and lipid peroxidation in cerebral ischemia, Free radical biology & medicine, 40 (2006) 376-387.

[104] T.N. Lin, Q. Wang, A. Simonyi, J.J. Chen, W.M. Cheung, Y. Y He, J. Xu, A.Y. Sun, C.Y. Hsu, G.Y. Sun, Induction of secretory phospholipase A2 in reactive astrocytes in response to transient focal cerebral ischemia in the rat brain, Journal of neurochemistry, 90 (2004) 637-645.

CHAPTER 2

EXTRACTION, CHROMATOGRAPHIC AND MASS SPECTROMETRIC METHODS FOR LIPID ANALYSIS[1]

[1] Sumitra Pati, Ben Nie, Robert D. Arnold and Brian S. Cummings. (2016) *Biomedical Chromatography.* Reprinted with permission from publisher.

Abstract

Lipids make up a diverse subset of biomolecules that are responsible for mediating a variety of structural and functional properties as well as modulating cellular functions such as trafficking, regulation of membrane proteins and subcellular compartmentalization. In particular, phospholipids are the main constituents of biological membranes and play major roles in cellular processes like transmembrane signaling and structural dynamics. The chemical and structural variety of lipids makes analysis using a single experimental approach quite challenging. Research in the field relies on the use of multiple techniques to detect and quantify components of cellular lipidomes as well as determine structural features and cellular organization. Understanding these features can allow researchers to elucidate the biochemical mechanisms by which lipid-lipid and/or lipid-protein interactions take place within the conditions of study. Herein, we provide an overview of essential methods for the examination of lipids, including extraction methods, chromatographic techniques and approaches for mass spectrometric analysis.

Abbreviations/Acronyms: phospholipids (PLs), phosphatidylcholines (PC), phosphatidylethanolamines (PE), phosphatidylinositols (PI), phosphatidylserines (PS), phosphatidylglycerols (PG), phosphatidic acids (PA), organic solvent extraction (OSE), solid-phase extraction (SPE), methyl tert-butyl ether (MTBE), SPE liquid chromatography (SPC-LC), high-performance liquid chromatography (HPLC), high-performance thin-layer chromatography (HP-TLC), thin-layer chromatography (TLC), two-dimensional TLC (2D-TLC), gas chromatography (GC), flame ionization detectors (FID), normal phase liquid chromatography (NP-LC), reversed-phase liquid

chromatography (RP-LC), hydrophilic interaction liquid chromatography (HILIC), refractive index detection (RID), evaporative light-scattering detection (ELSD), evaporative laser light scattering detector (ELLSD), electrochemical detection (ECD), suppressed conductivity detection (SCD), charged aerosol detection (CAD), infrared (IR), tandem mass spectrometry (MS/MS), multiple reaction monitoring (MRM), electron ionization (EI), field ionization (FI), time-of-flight (TOF), fast atom bombardment (FAB), electrospray ionization (ESI), rapid evaporative ionization mass spectrometry (REIMS), chemical ionization (CI), atmospheric pressure chemical ionization (APCI), matrix-assisted laser desorption/ionization (MALDI), atmospheric pressure ionization (API), atmospheric pressure photoionization (APPI), mass spectrometric imaging (MSI), secondary ion mass spectrometry (SIMS), desorption electrospray ionization (DESI).

1. Introduction

Lipids make up a diverse subset of biomolecules that can be grouped into the following categories: fatty acids, glycerolipids, glycerophospholipids, sphingolipids, sterol lipids, prenol lipids, saccharolipids and polyketides [1]. They are responsible for mediating a variety of structural and functional properties, and reside predominantly in cell membranes as the primary constituents of the bilayer. Lipid bilayers also house various embedded proteins that contribute to the cell membrane functionality. Lipids are not only essential for cellular architecture, but are involved in processes that modulate cellular function such as trafficking, regulation of membrane proteins and subcellular compartmentalization. Of the categories mentioned above, phospholipids (PLs) are one of the most abundant constituents of biological membranes and play important roles in cellular processes like transmembrane signaling and structural dynamics. The major PL

classes (**Figure 2.1**) are: (1) phosphatidylcholines (PC), (2) phosphatidylethanolamines (PE), (3) phosphatidylinositols (PI), (4) phosphatidylserines (PS), (5) phosphatidylglycerols (PG), and (6) phosphatidic acids (PA). Of these, (1)-(5) are predominantly found in the membranes of mammalian cells. These can often exist as phospholipid variants, with a diverse array of alkyl chains, such as sphingolipids, plasmalogens, glycerol diesters, and poly-phosphorylated species. PLs are amphipathic molecules that can be distinguished by two hydrophobic fatty acyl molecules esterified at the *sn*-1 and *sn*-2 positions of glycerol and a polar head group linked by a phosphate residue at the *sn*-3 position. PL classes differ in terms of size, shape, charge and chemical composition, which give rise to an asymmetric distribution within the membrane. The chemical and physical properties of membranes are greatly determined by the PL composition. PLs can also stabilize membrane-bound proteins and serve as cofactors for enzymatic reactions. The generation of first and second messengers e.g. inositol trisphosphate, phosphatidylinositol 4,5-bisphosphate, platelet-activating factor are responsible for regulating PL metabolism, secretion, cellular architecture and membrane fusion. Although the structural building blocks for lipid molecules are not very complex, they have the potential to generate almost 100,000 different molecular species [2, 3]. This lipid diversity is regulated and synthesized by a considerable part of the genome, and the role of this compositional complexity remains broadly defined.

The complete profile of lipid species present in a cell, organelle or tissue refers to the *lipidome*, whereas the study of lipid profiles within biological systems can be referred to as lipidomics [4]. Lipidomics seeks to identify lipid alterations within a target system, characterize molecular species and determine the roles of genes and proteins

involved in lipid metabolism and lipid-mediated signaling [4, 5]. Identifying the biological significance of lipid alterations can provide insight into processes that regulate cellular homeostasis in health and disease states. Although lipids stand out among cellular metabolites in the sheer number of unique species, this class of biomolecules remained in the shadow of the ongoing 'omics' revolution for a long time. The chemical and structural variety of lipids makes analysis using a single experimental approach quite challenging [5, 6]. Research in the field relies on the use of multiple techniques to detect and quantify components of cellular lipidomes as well as determine structural features and cellular organization. Understanding these features can allow researchers to elucidate the biochemical mechanisms by which lipid-lipid, lipid-protein interactions take place within the conditions of the study. Lipidomics studies, both untargeted and targeted, use similar experimental protocols that have been heavily bolstered by recent developments in modern mass spectrometry (MS) -based analytical platforms (**Figure 2.2**). Lipidomics is a rapidly expanding field of research, which has emerged as a valuable approach to understanding lipid biology in the biosciences.

Herein, we will provide an overview of essential methods for the analysis of lipids, including extraction methods, chromatographic techniques and approaches for mass spectrometric analysis.

2. Extraction Techniques

The complexity of biological samples, such as tissues, cells and body fluids, often requires optimization of techniques for sample preparation. For the extraction and analysis of lipids, there are two major challenges to overcome, which are extraction

efficiency and complete removal of non-lipid contents. By optimizing sample preparation, it is possible to increase throughput and analyses reproducibility. This section will discuss organic solvent extraction (OSE) and solid-phase extraction (SPE), which have been used extensively for lipid sample preparation. **Figure 2.3** provides a summary of these extraction techniques.

Organic solvent extraction

Proper organic solvent extraction relies heavily on selection of lipid-soluble solvents. For polar lipids containing both hydrophilic and hydrophobic groups, appropriate organic solvents include chloroform and methanol. Alkane solvents are well-suited for extraction of nonpolar lipids lacking hydrophilic groups, such as triacyglycerols and sterols. Lipid solubility can be quantified directly using pure lipid standards, however, predicting or measuring extraction efficiencies is often a challenge when extracting lipids from biological samples. This is due mainly to the strong interactions between lipids and cell biopolymers such as proteins and polysaccharides. Extraction solvents should be selected carefully in order to disrupt these molecular associations, with a balance of both polar and nonpolar characteristics. Polar solvents such as methanol have high dielectric constants that are able to access regions of ion-dipole interactions and hydrogen bonds, and can interrupt such associations.

The Folch method, published in 1957, is the most commonly used lipid extraction technique [7]. It uses a mixture of chloroform and methanol in a 2:1 ratio, which can simultaneously overcome both hydrophobic and polar interactions between lipids and biopolymers. A wash step is incorporated following extraction, to remove non-lipid

components using small volumes of water. It is critical that the ratio of chloroform:methanol:water is maintained at 8:4:3 to prevent the loss of polar lipids as a result of excess water. This method yields higher lipid extraction efficiency than any other single solvent method.

The Bligh and Dyer method was introduced as a variation of the Folch method [8], which incorporated water present within samples into the solvent system and made the extraction procedure convenient and economical. Generally, the Folch method is used for the extraction of lipids from solid tissue whereas the Bligh-Dyer method is advantageous for biological fluids [9].

Charged, polar lipids such as glycerophospholipids are able to bind to various biopolymers through ionic interactions that cannot by easily disrupted by polar organic solvents. In such cases, pH adjustments to the aqueous medium prior to extraction can be beneficial for achieving quantitative extraction. Acidification is an effective way to increase extraction efficiency. The addition of acid can convert negatively charged ionized molecules (lipids or biopolymers) to non-ionized forms, interrupting ionic interactions along with increasing lipid hydrophobicity. This was demonstrated in a study where the extraction of polar lipids from *M. thermoautotrophicum* cells was six times greater by replacing the water in Bligh-Dyer solvent system with 5% trichloroacetic acid [10]. We also determined that acidified extraction is not only beneficial for maximal recovery, but can also increase the ionization efficiency of lipids in mass spectrometric analysis (**Figure 2.4**). However, acidification of extraction procedures must be used cautiously, where the pH range is maintained at 2-4. Ester bonds are vulnerable to acid, and hydrolysis can take place after long exposures to concentrated acid, resulting in the

loss of lipids. To overcome this phenomenon, Nishihara *et al*. used 5% trichloroacetic acid in the place of hydrochloric acid (2 M) [10].

Temperature is another feature that should be controlled. Low temperatures are essential for large sample sizes undergoing acidified extraction and quantitation. Our laboratory, along with many others, showed that reduced temperatures reduce degradation and improve lipid stability (**Figure 2.5**). The control of both pH and temperature can prevent the occurrence or reduce the rate of hydrolysis. It is important to note that acidified extraction methods are not suitable for the long-term storage of samples, thus requiring analysis immediately following extraction.

A liquid-liquid extraction method utilizing methyl tert-butyl ether (MTBE)/methanol was developed recently and simplified the handling of samples in comparison to the Folch and Bligh-Dyer methods [11]. In this method, the low density of MTBE causes the lipid-containing organic phase to form the upper layer during liquid-phase extraction. In the Folch and Bligh-Dyer methods, the lipid-containing phase forms the lower layer due to the high density of chloroform, which can make lipid layer collection difficult. Also, non-extractable matrices such as denatured proteins can be removed by centrifugation easily since they form a dense pellet at the bottom of the extraction tube instead of in between the upper and lower phases as observed with the Folch and Bligh-Dyer methods. This suggests that the MTBE method yields similar or better recoveries of most major lipid classes compared to Folch or Bligh-Dyer. It can also be used for the simultaneous extraction of lipids and metabolites for metabolic profiling and lipidomic analysis. MTBE extractions can be performed on limited amounts of tissue samples (i.e. 2.5 mg) and is suitable for the handling of clinical specimens [12].

Organic solvent extraction, such as chloroform and methanol, has been used widely for lipid research and while there are various advantages, limitations persist. Some of these include labor-intensive and time-consuming procedures such as multiple extractions per sample for optimal recovery. Extraction efficiencies can be inconsistent, especially in the presence of emulsifiers, a common occurrence in complex biological samples. Emulsions can result in the partial or complete loss of complex glycolipids and polar prostaglandins in the aqueous layers [12]. Further, the need for high volumes of toxic, organic solvents requires researchers to utilize extra preparative measures for safety.

It's important to point out that methanol, mentioned in the methods above, does not typically serve as an extraction reagent for lipids since it is miscible with water. Rather, it is used as a reagent that disrupts the interaction between lipids and biopolymers. Similar solvents would be ethanol, 1-propanol, 2-propanol, and n-butanol. While ethanol may offer a similar disruption effect as methanol, 1- and 2-propanol may be weaker due to the larger hydrophobic moiety. N-butanol is the weakest in disruption among these four solvents, but it is only partially miscible with water, and sometimes can be used to extract lipids without the aid of other organic solvents. Altering solvents with the goals of providing a cleaner matrix is usually more applicable when the analyte is fully understood. In this case, the solvents can be chosen accordingly to inhibit the extraction of undesirable lipids and non-lipid content. However, this is not always the case in most lipid research, especially in lipidomics where hundreds, if not thousands, of lipids are extracted at once. Generally, a recommended approach would be to extract

total lipids as much as possible, then further clean the sample using SPE if necessary. In such a scenario, methanol is usually the best choice.

Solid-phase extraction

Solid-phase extraction (SPE) was first introduced in the mid-1970s as a method for quick and efficient sample preparation for lipid analysis [13]. This technique uses principles similar to those in liquid chromatography where lipids in hydrophilic media are retained on the SPE column, while the non-lipid impurities are allowed to pass through. Lipids are then eluted and collected using organic solvents with lower polarities. SPE is a useful method for the isolation and purification of targeted lipids along with the enrichment of minor lipid species. The cartridges come in a variety of formats for the handling of different lipids, matrices, volumes and sample concentrations. Some of these include the syringe barrel, large volume capacity barrel, 96-well format and pipette tip format. SPE cartridges, like columns used in HPLC, can be classified by reversed-phase, normal phase and ion exchange. SPE is powerful for a broad range of applications and when combined with a variety of elution procedures, is useful for total lipid purification as well as class separation.

With reversed-phase SPE (C_{18}) cartridges, crude lipid extracts obtained from the Folch or Bligh-Dyer method can be diluted with water/methanol, and then loaded on the activated SPE cartridge. As the polarity of the solvent is increased, lipids remain bound to the column through hydrophobic interactions while water-soluble impurities can pass through. The remaining lipids can be collected by elution using chloroform:methanol (1:2, v/v). Alternatively, a two-step elution can permit two fractions to be collected. This

would require the first elution to be performed with methanol:water (12:1, v/v), and the second elution using chloroform:methanol (1:2, v/v). In doing so, the first fraction contains gangliosides, phosphatidylserine, phosphatidylinositol, phosphatidic acid, and sulfatides, while the second fraction contains all phospholipids, cerebrosides and cholesterol [14].

Normal-phase SPE bind lipids via polar interactions, such as hydrogen-bonding and ion-dipole forces, and can used to separate polar lipids from nonpolar lipids that lack polar functional groups. The cartridges available for normal-phase SPE include amino- (NH_2), cyano- (CN), and silica (Si) phases. Kaluzny *et al.* [15] demonstrated that aminopropyl (NH_2) Normal-phase SPE can serve as an effective technique to separate different lipid classes including cholesterol, cholesteryl esters, triglycerides, diglycerides, monoglycerides, fatty acids and phospholipids. For example, Kaluzny et al., reported the performance of three NH_2-SPE cartridges loaded with crude lipid extracts. The first elution was performed with chloroform:isopropanol (2:1, v/v), ethanol:acetic acid (98:2, v/v), and methanol and sequentially produced three fractions. The first contained cholesterol, cholesteryl esters, tryglycerides, diglycerides and monoglycerides, which were then loaded onto a second cartridge. The second and third fractions contained fatty acids and phospholipids, respectively. Additional elution steps were carried out sequentially with hexane (100), hexane:dichloromethane:ethanol (89:10:1, v/v), hexane:ethyl acetate (95:5, v/v), hexane:ethyl acetate (85:15, v/v), and chloroform:methanol (2:1, v/v). This yielded five fractions that include 1) cholesterol esters, and later fractions with 3) 90% of cholesterol, 4) diglycerides, and 5) monoglycerides. A third cartridge was then able to separate the second fraction (2) into

triglycerides and 10% of cholesterol. A modified procedure was also developed for separating chlorinated fatty acid methyl esters from the unchlorinated counterparts [16]. Ion-exchange SPE, another useful technique for the isolation and separation of lipid species, can be classified into weak or strong cation and anion exchangers. Strong cation exchangers contain negatively charged benzenesulfonic acids or propylsulfonic acids, while weak cation exchangers have carboxylic acids that are charged at high pH ranges and neutral at low pH ranges. Strong anion exchangers possess positively charged quaternary amines, while weak anion exchangers have primary, secondary, or tertiary amines that are positively charged at low pH but neutral at high pH. An earlier method used silver ion-exchangers that have silica-based benzenesulfonic acid SPE cartridges, which can be loaded with a solution of silver nitrate in acetonitrile:water (10:1, v/v) for conversion to the ionic form of silver. The elution scheme for isolating fractions from these ion-exchange cartridges uses varying ratios of dichloromethane, acetone, and acetonitrile to separate saturated monoenes, dienes, trienes, tetraenes, pentaenes, hexaenes-fatty acid methyl ester derivatives [17]. A similar study was performed to achieve separation of saturated, unsaturated and trans-unsaturated fatty acids [18]. Ion-exchange SPE cartridges are used widely by researchers for the removal of lipids from analytes of interest [19, 20]. Method development can be optimized easily for separating positively or negatively charged lipids, and is especially appropriate for phospholipids. Anionic phospholipids such as phosphatidic acid and phosphatidylserine are negatively charged at high pH ranges, permitting them to be retained on strong anion-exchange SPE cartridges, allowing cationic phospholipids (neutral at high pH ranges) to pass through. Eluting solvent pH is easily adjusted to < 3, where anionic

phospholipids are neutral and can be easily collected from the SPE cartridge. Similar procedures can be performed for cationic phospholipids using strong cation exchange SPE. Zwitterionic phospholipids are negatively charged at high pH and positively charged at low pH, which makes them good candidates for either strong anion/cation exchange SPE with pH adjustments. Mixed mode ion-exchange SPE is a combination of reversed-phase and ion-exchange modes and provides an additional dimension of separation for charged and neutral lipids using proper strengths of organic solvents.

SPE is not only an effective tool for analysis of crude lipid extracts, but can be applied directly to some biofluid samples such as serum, urine and cerebrospinal fluid. It is important to note that acidification is an essential step prior to sample loading onto SPE cartridges in order to increase lipid retention. Further, low loading and reduced flow rates should be employed for maximal retention. On-line SPE liquid chromatography (SPC-LC) is the preferred method when compared to manual SPE (off-line). It is highly reproducible, less time-consuming and labor intensive, and reduces the potential of exposure to potentially hazardous biological samples. Although on-line SPE has several advantages including high-throughput features for large sample sizes, clinical research, and diagnostics, it has higher instrumentation costs [21].

Chromatographic Methods

One method employed for many lipidomic studies involves the direct infusion of whole lipid extracts into ESI sources. [22-27]. This is referred to as a “shotgun” approach [28] and involves no chromatographic separation of lipid classes prior to infusion. This platform permits analysis of the lipidome directly from crude lipid extracts where lipids

undergo intrasource separation and can be analyzed using precursor ion and neutral loss scans to identify key lipid fragments. While shotgun lipidomics is simple, high-throughput and quick, requiring short data acquisition times, a significant disadvantage of this approach is that many compounds, such as major phospholipid molecular species and their counter-ions, can compete for ionization upon simultaneous infusion into the ESI source and result in ion suppression [29, 30]. As a result of this competition, ion-suppression can interfere with the detection of minor species within a sample matrix. Detection and sensitivity can also be limited by the presence of isobaric species [31]. Introducing a preliminary separation step prior to infusion, such as high performance liquid chromatography (HPLC), high-performance thin-layer chromatography (HP-TLC) or gas chromatography (GC), can minimize suppression, allowing compounds to be resolved sequentially with greater ionization yields and increased sensitivity [29, 30, 32, 33].

Gas chromatography (GC) can be used for phospholipid analysis, however this is not an optimal choice given that separation is dependent on analyte volatility; [34, 35]. For this technique, phospholipids can be hydrolyzed to diacyglycerols with phospholipase C and derivatized for GC analysis [36]. A further drawback is that these analyses require high column temperatures that can result in sample degradation, compromised sensitivity and data quality. Capillary columns are commonly used and provide chromatographic resolution as well as reproducible retention times [37]. Although there is a wide range of stationary phases available for GC, methyl-phenyl columns are typically used, and flame ionization detectors (FID) serve as the most common detection method [37].

Thin-layer chromatography (TLC) was the earliest and widely established chromatographic method used for lipid assessment that continues to be employed today [38-40]. Recent advancements in the application of TLC and HP-TLC have resulted in greater separation efficiencies during lipid analysis [41]. TLC has proven to be a highly effective and versatile technique for phospholipid separation [40]. The majority of TLC-based phospholipid separations are performed using a silica gel stationary phase, in conjunction with organic solvents such as chloroform, methanol, water and modifiers as the mobile phase [42]. Separation takes place on layers of silica gel adsorbent on glass plates where lipid samples are applied as discrete spots. Lipid samples travel in the mobile phase at different rates based on their affinity for the silica adsorbent. One-dimensional TLC is useful for simple mixtures, while two-dimensional TLC (2D-TLC) yields better resolution for complex lipid mixtures. HP-TLC is commonly coupled with densitometric quantification and various detection reagents can be used to identify resolved lipid classes [43-47]. TLC and HP-TLC are advantageous because of simplicity, high resolving power, and affordability, but are limited by low resolution, sensitivity and lipid recovery [41, 48]. Although TLC is a quick method with no sample carryover as each analyte has a new stationary phase, liquid chromatography typically gives better separation [40] and may be coupled to a variety of detectors.

High-performance liquid chromatography (HPLC), in comparison to other chromatographic methods, is the most popular method and has very broad applications in lipid analysis. This is possibly due to the ability to utilize multiple HPLC methodologies for isolation and analysis of phospholipids. Partition chromatography is defined by two polarity modes: normal phase liquid chromatography (NP-LC) and

reversed-phase liquid chromatography (RP-LC) [41]. Generally, NP-LC separates lipid classes, while RP-LC separates based on fatty-acyl composition [49]. For this reason, NP-LC is useful for separating phospholipids with differing head groups, while RP-LC can separate phospholipids of the same class. Both normal-phase and reversed-phase based separation methods have been used for the separation of lipid classes; however, complete class separation has not been shown [50, 51]. While the mobile phases selected for HPLC vary depending on the column of choice, typical solvents used for chromatographic elution include alcohols, such as methanol and 2-propanol, acetonitrile, hexane, chloroform and/or water [52]. For subsequent mass spectrometric analyses, acetic or formic acid are added along with an amino-base (ammonia, methylamine, diisopropylamine and piperidine) in order to facilitate ion-pairing in both negative and positive ionization modes [29].

Normal phase (NP) methods are used in HPLC to accomplish initial separation of phospholipid classes through either gradient or isocratic elution [53-56]. In normal phase chromatography, phospholipids elute in order from the most hydrophobic to the most hydrophilic using a polar stationary phase and a less polar mobile phase [54]. Elution patterns are based largely on the polar properties of the phospholipid head group. During instances where head groups possess the similar polarities, separation is accomplished based on differences in their backbone. Commonly used normal phase stationary phases include silica, alumina and cyano columns [57, 58]. Silica is the most common of the non-bonded phases and yields greater selectivity; however, this method can be limited by retention time reproducibility across runs due to water adsorption [57, 58]. Alumina is not as common because of its low theoretical plate number, as well as

retention time variability and poor sample recovery. Cyano stationary phases are quite stable and can also be used for phospholipid analysis. Selection of solvents for normal phase chromatography requires consideration of several factors, including solvent strength, localization, basicity and cutoffs for UV detection [57, 58]. Disadvantages to using normal phases include lengthy elution and equilibration times resulting in low-throughput. Chloroform and hexane are commonly used mobile phases, both of which introduce ionization challenges when coupled with MS [59]. A more recently identified approach that can be used to retain amphiphilic compounds such as phospholipids is hydrophilic interaction liquid chromatography (HILIC) [60, 61]. This technique is a combination of a polar stationary phase with a highly organic mobile phase that increases the retention of solutes as the percentage of organic solvent is increased [60]. Although HILIC is a variant of normal phase chromatography, reversed-phase solvent systems are frequently used to avoid the issues commonly encountered with conventional normal phase methods. Some of the advantages HILIC presents are lower back pressures and higher sensitivity when coupled with ESI-MS.

Reversed-phase (RP) chromatography uses a non-polar stationary phase and a polar mobile phase and is based on lipophilicity, where lipids within the same class separate according to carbon chain length and quantity of double bonds [62, 63]. $C_{18,}$ $C_{8,}$ and octadecylsilyl reversed-phase columns have been employed using eluting solvents such as methanol, isopropanol, acetonitrile, hexane and chloroform [29, 64, 65]. When using these columns, hydrophobic C_{18} groups interact with the hydrophobic fatty acid chains of phospholipids [66]. As a result, phospholipids with longer fatty acid chains possess greater solute hydrophobicity, and retention times are decreased as the

number of double bonds on fatty acid chains is increased [66]. Resolution following separation and speed optimization can be implemented with higher column temperatures with or without gradients, along with column particle sizes less than 2 µm [65]. A disadvantage to using reversed-phase conditions is that hydrophilic compounds are often not as well-retained as observed in NP-LC [57, 58]. As an alternative, two-dimensional liquid chromatography (2D-LC), made up by a combination of separation systems i.e. NP-RP-LC, can offer increased chromatographic selectivity as well as optimize lipid separation.

Detectors

The most common chromatographic detection methods include refractive index detection (RID), evaporative light-scattering detection (ELSD), electrochemical detection (ECD), suppressed conductivity detection (SCD) and charged aerosol detection (CAD) [41]. ELSD utilizes a universal detector that responds to any analyte different from the mobile phase through continuous monitoring, resulting in minimal background signal. ELSD is compatible with a broad range of solvents as well as gradient elution, although isocratic elution, a feature not permitted by RID, is optimal. Furthermore, unlike ultra-violet (UV) detection, the output signal from ELSD is independent of acyl chain length and degree of saturation [41]. UV detectors are used very frequently for HPLC, as they are relatively inexpensive and easily accessible. These detectors are sensitive, selective, and are optimal for natural lipids containing conjugated double bonds. While UV detection is widely used for phospholipid analysis [67], fluorescence-based detection is not, since only a few rare lipids possess natural fluorescence. Fluorescence

can be useful, however, for analysis of fatty acids following conversion to suitable derivatives. Similarly, infrared (IR) detectors are limited to nonpolar lipids with a narrow window for absorbance detection [68]. Recently, detectors with laser light sources have emerged and exceeded the capabilities of previous technologies. One example is the evaporative laser light scattering detector (ELLSD), which has outperformed ELSD in terms of sensitivity, stability and reproducibility [41]. CAD, developed only in 2004, has also demonstrated greater sensitivity than ELSD with a broader dynamic range [69, 70]. Normal phase chromatography is often coupled to ELSD [71] or UV detection [72]. These detectors are restricted by the lack of selectivity and choice of mobile phase, making MS the preferred detector for lipidomic studies [73, 74].

3. Mass Spectrometry

During MS analysis lipid samples undergo ionization and vaporization upon entering the mass spectrometer, and are sorted by mass to charge ratio (*m/z)* within the mass analyzer [75]. Introduction of crude lipid extracts with no prior separation via direct infusion is called shotgun lipidomics [6, 24, 76]. The shotgun approach, discussed in detail above, is a rapid and effective way to assess lipid profiles. Although an informative and high throughput approach, shotgun analyses can often be complicated by ion suppression [77], as well as inherent bias towards more abundant and easily ionized lipids [75, 78]. The alternative to the shotgun method is incorporation of a chromatographic separation prior to MS analysis, resulting in reduced ion suppression and greater sensitivity [79]. However, ionization conditions and column memory effect, the carryover of sample constituents across analysis, can pose significant challenges.

Major lipidomic approaches are either the targeted study of individual lipid classes or their subclasses [78, 80], or global, broad spectrum profiling of crude lipid extracts. Unfortunately, global lipidomics often results in complex spectra containing numerous isobaric species, and targeted approaches often encounter low abundances of desired lipid classes. Chromatography can address both of these issues by separating target analytes from complex matrices [81].

Crude lipid extracts can also be used for direct identification of lipids based on mass via high-resolution mass spectrometers such as the Fourier transform ion cyclotron resonance and FT-Orbitrap. [6, 82]. This is known as top-down lipidomics and these instruments facilitate rapid scanning and high mass accuracy [24, 75]. The top-down approach is primarily used for determining alterations in lipid patterns. For the majority of lipid studies, however, tandem mass spectrometry (MS/MS) is the dominant method [6]. The application of tandem MS experiments is referred to as bottom-up lipidomics, where various scanning options (precursor ion scan, product ion scan, neutral loss scan) are used to generate specific fragment ions [6, 83]. Selected reaction monitoring or multiple reaction monitoring (MRM) can be used to maximize sensitivity for specific precursors or fragment mass pairs [75]. There have been newer developments using nanospray technologies, which have increased the sensitivity of lipid analysis as well as sample throughput using chip-based nanospray array devices [84]. For example, nano-electropray sources [85-87] are able to allow analysis of picomolar or sub-picomolar levels of lipids [88].

Over the past 40 years, GC-MS coupled with electron ionization (EI) has served as a basis for lipid identification and quantification. Although widely used, limitations

with this method persist [89]. Throughout the mid-1970s, field ionization (FI) was employed; however, lower and less stable ion currents made this method unpopular [90]. Recently, FI has been used in conjunction with orthogonal acceleration time-of-flight (TOF) MS. This combination has overcome some of the previous challenges posed by FI [91]. Another earlier method used for the analysis of complex, high molecular weight lipids was fast atom bombardment (FAB) MS. It is important to note that findings from studies conducted using FAB, coupled with tandem MS, have laid the foundation for our understanding of the fragmentation of lipid ionization [92]. However, the drawbacks of FAB, including low sensitivity, matrix ions and source fragmentation, greatly limited analysis and quantitation [81]. The introduction of electrospray ionization (ESI) MS applied to the analysis of glycerophospholipids addressed many of these limitations, including increasing sensitivity by two orders of magnitude, thereby permitting the detection of more than 50 phospholipid species [93-95]. ESI allows two approaches for lipidomic studies: shotgun lipidomics or chromatography-coupled MS for phospholipid identification and quantitation. While both approaches possess their strengths, the combination of the two can be the most effective [31, 81].

Techniques based on ambient ionization, such as desorption electrospray ionization (DESI), have recently emerged and been applied to lipid analysis [96, 97]. DESI offers direct sampling from biological tissues and does not require high-vacuum conditions [98]. Rapid evaporative ionization mass spectrometry (REIMS) represents another method for lipid analysis, in which ions are formed from the rapid thermal evaporation of biological tissue from a surgical electrode and then extracted into the MS [99]. The use of tandem MS techniques, such as parent ion and neutral loss scanning

[100, 101], in combination with ESI and MALDI, has been essential in advancing the field of lipidomics [81]. Tandem MS with CID is an excellent tool for elucidating lipid structures, as well as enhancing analytical sensitivity in both global and targeted lipidomics [81].

Ionization methods

The distinction between “hard” and “soft” ionization MS methods is heavily dependent of the properties of the analyte of interest [102]. Most modern ionization methods are considered to be soft ionization when compared to EI [103]. EI makes use of fast electrons in order to ionize the analyte molecules in the gas phase by the removal of one electron. This method has been used exclusively for decades, mainly because of its suitability for the investigation of small and/or volatile compounds [104]. However, EI is not very effective for analyzing larger molecules with low volatilities. While detection of phospholipid molecular ions is possible using EI, the abundance of fragment ions makes it difficult to analyze complex mixtures [105]. For this reason, EI-MS is now used for assessing free fatty acids in lipid samples. Chemical ionization (CI) is another ionization method used frequently for lipid analyses, and can be used alone or in combination with atmospheric pressure (APCI) [102, 106].

The advent of soft-ionization methods should be considered a milestone in the history of modern mass spectrometry as it enabled analyses of molecules refractive to EI. These methods include electrospray ionization (ESI) and matrix-assisted laser desorption and ionization (MALDI). ESI and MALDI are the most popular ion sources for lipidomics studies and are commercially available in the majority of MS devices [102]. It

is important to note that they are often regarded as competitive methods; however, they should be considered complementary [102].

Electrospray Ionization (ESI)

The most widely used atmospheric pressure ionization (API) modes are electrospray ionization (ESI) and atmospheric pressure chemical ionization (APCI) [51, 106]. ESI is an appropriate technique for polar compounds including phospholipids [107-111], while APCI is better suited for less polar molecules [112-115]. The soft-ionization of ESI is quite effective for polar lipids since they are readily ionized in both negative and positive ion modes, i.e. protonation $[M+H]^+$ or deprotonation $[M-H]^-$, resulting in a single intact ion [81]. ESI-MS performed on samples containing phospholipids generate unique fragment ions, indicating a loss of the polar head group, which can be diagnostic for the presence of individual classes. For example, *m/z 184* is indicative of choline-containing phospholipids and can be detected during product ion analysis of protonated choline-containing phospholipid molecular species. Table 1 provides a summary of unique fragments including adducts, in both positive and negative ion mode, which can be used for phospholipid identification. While saturated and monounsaturated fatty acids ionize well in the negative ion mode, it can be difficult to detect fragment ions. Our approach for detection and MS/MS quantification is to utilize precursor ion scanning as the product ion.

Another method for lipid analysis is atmospheric pressure photoionization (APPI), which can extend the range of ionizable compounds. [116-118]. ESI, APCI and APPI were recently compared [119] with regard to their quantitative accuracy and sensitivity

for neutral lipids such as fatty acids, diacylgycerols and triacylglycerols. The results proved LC-APPIMS to be useful for quantitative analysis, and ESI and APCI more effective for the analysis of polar lipids, with ESI excelling in reproducibility [119]. Analysis using APPI and ESI coupled with HPLC, can be particularly useful for determining information about the polar range of lipids present within complex samples [119].

MALDI

Following lipid studies using ESI-MS, there were initial reports using matrix-assisted laser desorption/ionization (MALDI) of glycerophospholipid and sphingolipid species [120-122]. Given that MALDI is a soft-ionization technique, it yields quasi-molecular ions, instead of radical cations, from abstraction of an electron from the analyte of interest [123]. While APCI [106] and ESI [124] are commonly used and often preferred for lipidomics studies [125], MALDI-MS has proven to be an effective method and is gaining popularity [126, 127]. This is partly due to the growing interest in MALDI-MS imaging for lipid studies [128]. The MALDI-MS approach relies on the utilization of a matrix that initially absorbs the energy of the laser and mediates the generation of ions [102], where the suitability of a certain compound as a matrix is determined by the type of laser and its emission wavelength [102]. Factors that constitute a good MALDI matrix include excellent signal-to-noise (S/N) ratio for the peaks of the analyte of interest, high absorbance at the laser emission wavelength, low background to avoid interferences between the matrix and the analyte ions, specificity for a single analyte adduct, and low tendency for cluster formation [102, 129]. Some advantages of MALDI are that

measurements are high throughput, time-efficient, relatively inexpensive and require simpler sample purification due to high tolerance for salts and impurities. Separation by ion mobility has also been used along with MALDI-MS to fractionate lipids [130-132].

The phosphatidylcholine (PC) class of phospholipids has been studied most frequently using MALDI-MS. This is primarily because PCs are the most abundant constituents of eukaryotic cellular membranes and are commercially available with a wide range of fatty acid residues and ether derivatives. Additionally, PCs can be easily detected in positive ion mode by their quaternary ammonia group with a permanent positive charge [102]. Unlike ESI, MALDI analysis of phospholipids can result in positive ions for all subclasses, permitting a broader range of detection per acquisition [32, 133]. Phosphatidylinositol (PI), phosphatidylserine (PS) and phosphatidic acid (PA) are inherently less abundant and have high negative charge densities, thus are not easily detected [134]. It was recently demonstrated that performing a preliminary PC removal step through binding with a small column filled with a silica gel cation exchanger (SCX), allows easy monitoring and quantification of other phospholipids such as PI [135, 136]. See Gellerman et al. 2006 for a review on the detection limitations of various phospholipid classes,. Detection limitations are particularly important for direct infusion lipid studies using crude lipid extracts from biological samples. In such samples, phospholipids containing quaternary ammonia groups like PCs tend to suppress other classes [32]. Various lipid classes have also been shown to influence the relative intensities of others when recorded at varying analyte concentrations [102]. The use of an acidic add-on, such as DHB, or an alkaline add-on, such as 9-AA, is recommended for acquiring spectra in the positive or negative mode, respectively [102].

Mass Spectrometric Imaging

Two-dimensional (2D) MS-based imaging [137-140] has proven to be a powerful technique for investigating spatial distribution of lipid within substructures of tissues, in which an analyte's properties are presented as a function of its spatial distribution within the x-y plane. This is an advantageous approach because it does not rely on tedious histochemical labeling protocols [141, 142]. Structure-specific lipid analysis is an especially striking feature of mass spectrometric imaging (MSI), given that lipid analysis is typically performed following extraction protocols that remove information about tissue location [143].

Based on the 2D data obtained, three-dimensional (3D) images can also be recapitulated [144]. MALDI-MS is well-established and has become a popular technique to employ for imaging. The advent of MALDI imaging observed a paradigm shift from earlier methods with the ability to analyze secondary ions from biological tissue slices [143, 145]. This method is employed by fixing tissue slices onto MALDI targets, which are then covered by a matrix so that spectral intensities can be used to create an image. The site of the laser spot results in the formation of both positive and negative ions as the biomolecules and neutral matrix analytes are lifted from the underlying tissue. Phospholipids tend to generate an abundant number of negative ions during MALDI-MSI due to the phosphodiester moiety that can exist as a very stable gas phase anion [143], and is utilized more so for the observation of acidic phospholipids such as PI, PA, PG and PS [143]. The resulting mass spectra translate to image pixels based on specific x-y coordinates. Contributors to pixel size are altered by the size of MALDI matrix crystals as well as the laser spot itself [143]. Information regarding x-y

coordinates, *m/z* ratios and ion intensity can be obtained from the acquired mass spectra. Thin tissue sections (15 μm) are usually used, resulting in a lateral resolution of 25–100 μm [143]. For concentration quantitation, certain lipid classes can be detected, although quaternary ammonia group compounds are often overestimated in the positive ion mode. This can make absolute lipid quantitation cumbersome [143]. The presence of matrix compounds and prior chromatographic separation can be incorporated to overcome such issues. **Figure 2.6** shows an example of MS-based imaging using MALDI-FTICR-MS investigating the phospholipid distribution within substructures such as the hippocampus and cerebellum, of sagittal brain slices from cocaine- and saline-treated rats. This technique can provide essential information regarding the localization of lipid changes within specific regions of whole tissue, such as the brain

In addition to MALDI, secondary ion mass spectrometry (SIMS) has been used widely for molecular imaging. SIMS involves the use of ion beams that are focused upon inorganic surfaces, which result in the emission of secondary ions that can be analyzed for mass [143]. Both MALDI and SIMS are carried out under a vacuum. DESI is a newer, user-friendly method, based on ambient ionization that requires minimal sample preparation and simple analysis [146-148]. Using DESI-MS imaging, a recent study was able to assemble a 3D molecular reconstruction of a mouse brain [149].

Challenges in Lipid Research

As discussed earlier, complete lipid extraction and resolved chromatographic separation pose difficult challenges for researchers. Another aspect of lipid research that can be difficult in lipid analysis is the validation of structurally characterized molecular species.

There are many mass spectrometric platforms used with various ionization techniques; however, the extent of crossover in terms of detection, sensitivity, and feature identification is quite limited. **Figure 2.7** demonstrates such variability, in positive ion mode analysis, across three different platforms of ESI-MS: iontrap, TOF, and triple-quadrupole MS. Databases for identification of lipid feature assignment are also limited since they are platform specific and are primarily suited for LC-MS lipid analysis rather than direct infusion data. In recent years, there has been an increasing number of research consortia along with individual laboratories that are focusing their efforts toward standardizing experimental protocols and establishing lipid networks [150]. The advent of newer bioinformatics tools, protocols and instrumentation provide advanced lipidomics approaches for users to perform comprehensive analysis [151].

4. Conclusion

The development of chromatographic techniques, novel ionization methods and fragmentation strategies have greatly advanced the field of lipidomics, making it now possible to acquire the entire lipidome of cells or individual organelles. These advances have led to the development of sophisticated bioinformatics approaches for automated analyses of complex datasets. There are a growing number of programs and/or software packages that can be used for robust data-processing of -omic data, which can be used for spectral filtering, peak detection, alignment, normalization, multivariate analysis, along with mechanistic relevance through metabolic pathway analyses. The available software packages and programs were developed to be dependent on queries of ion masses and elution times, and can be used for both shotgun and

chromatography-coupled lipidomics. Examples of such software include LIMSA, LipidXplorer, MetaboAnalyst, XCMS, and MZMine [152-156]. The use of such analyses can provide essential information for identifying targets for biomarker development along with the mechanistic roles of lipid mediation/association in disease states and progression. Furthermore, findings from lipidomic studies can be integrated with genomic and proteomic data to provide a better understanding of the role lipids play in various biological and disease processes.

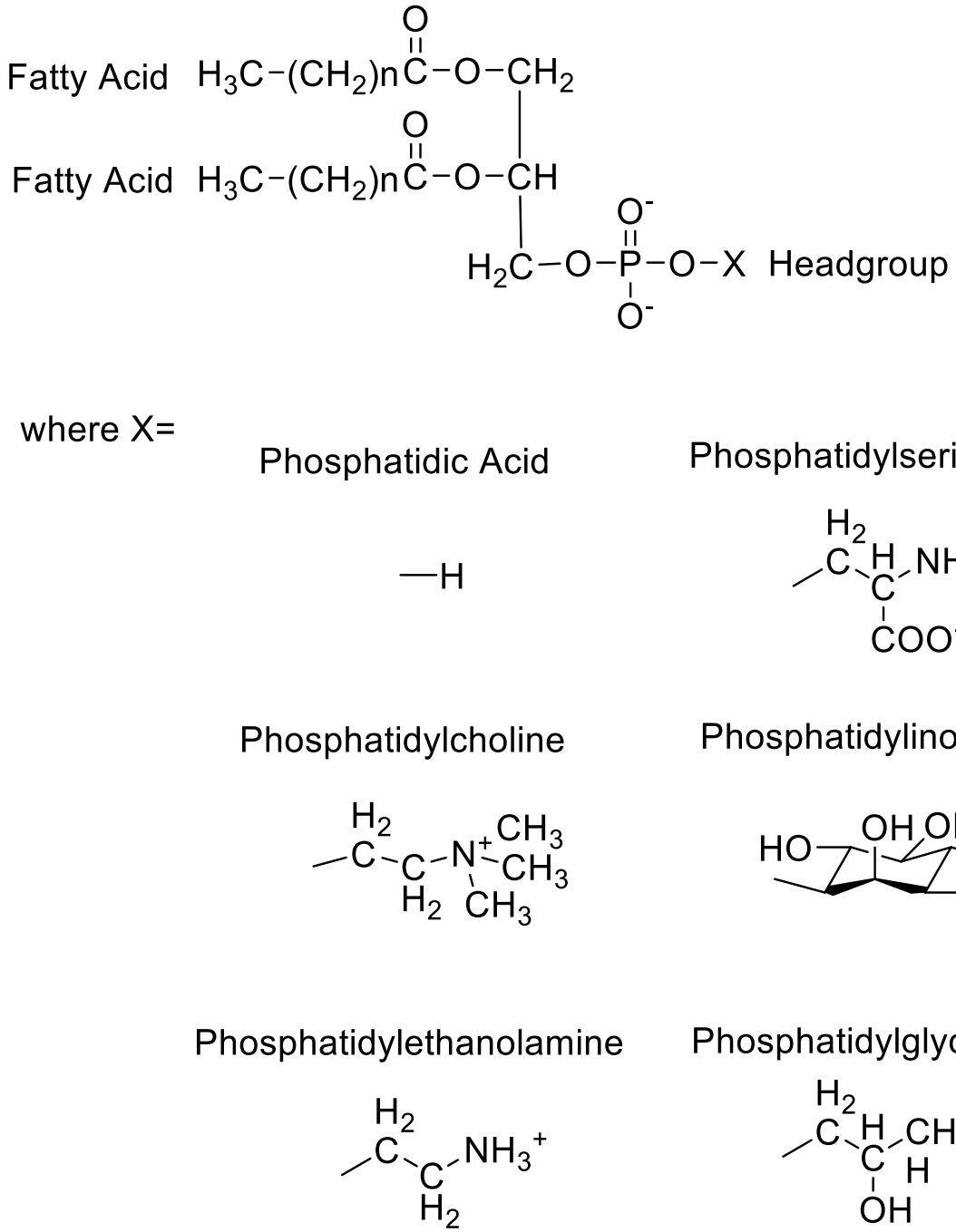

Figure 2.1. Structures of phospholipid classes. All structures were generated with ChemDraw Professional 15.1 (Cambridge Scientific. Inc.)

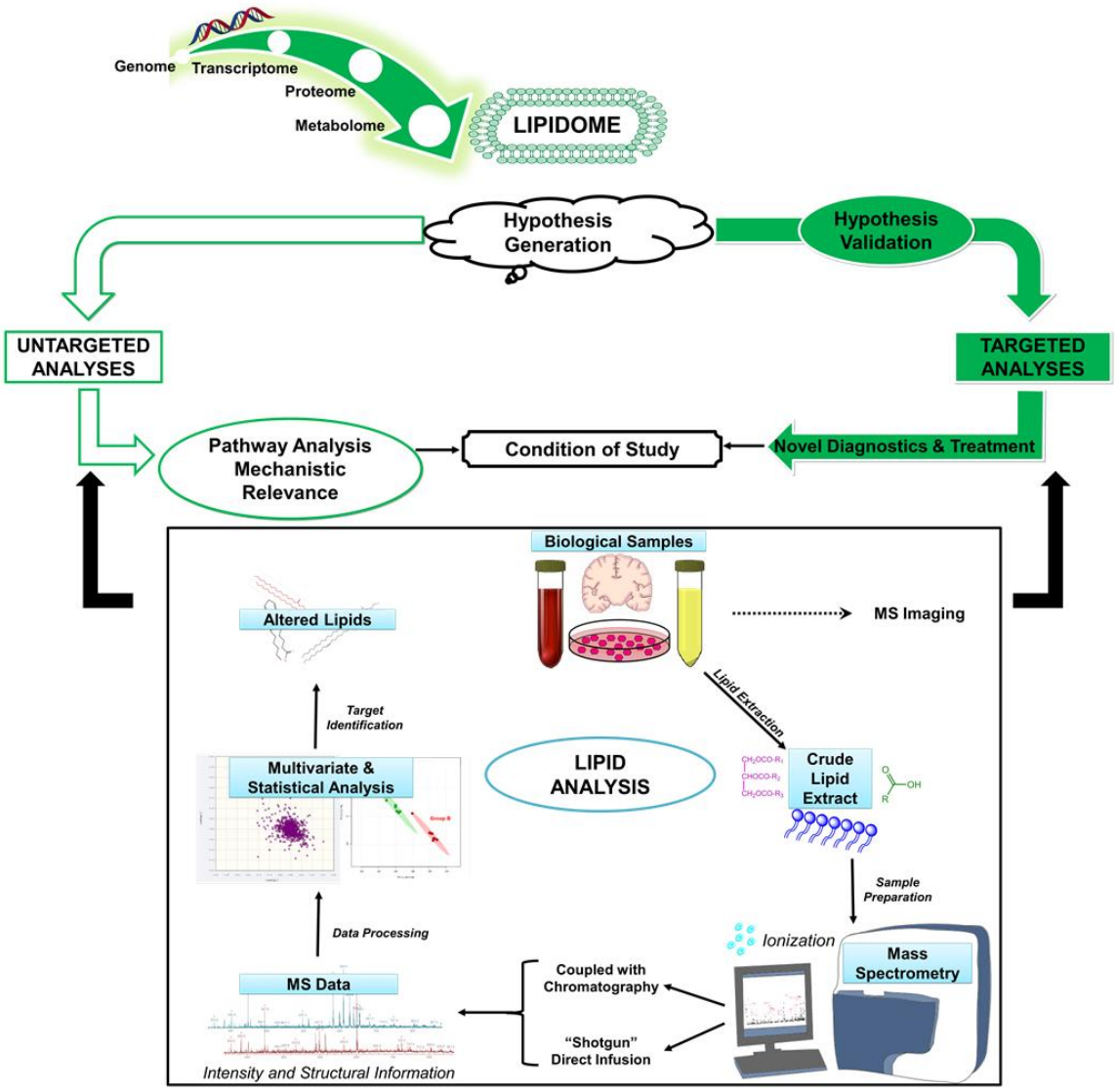

Figure 2.2. Lipidomic workflow.

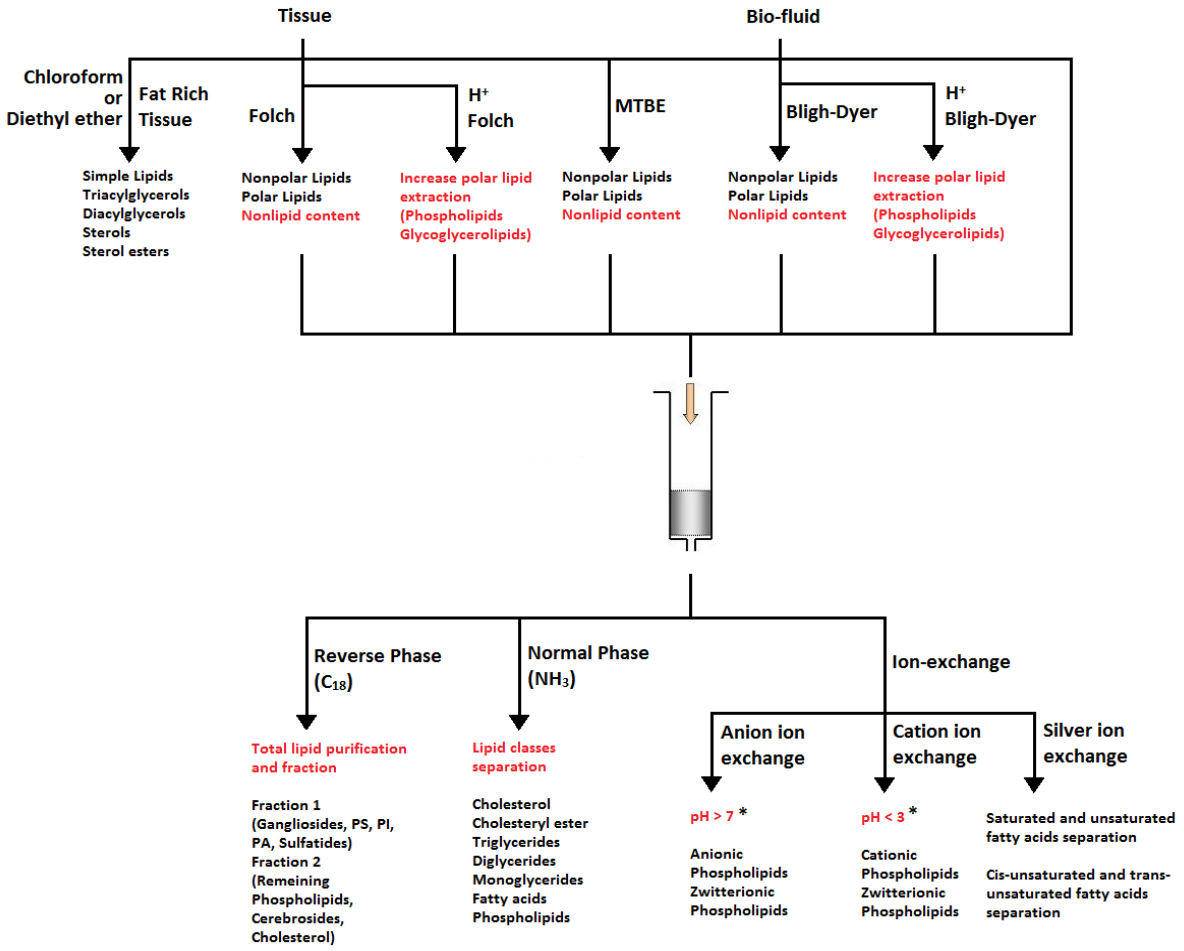

Figure 2.3. Overall applications of extraction techniques on lipids research. *pH values are approximated, pH adjustment depends on analytes

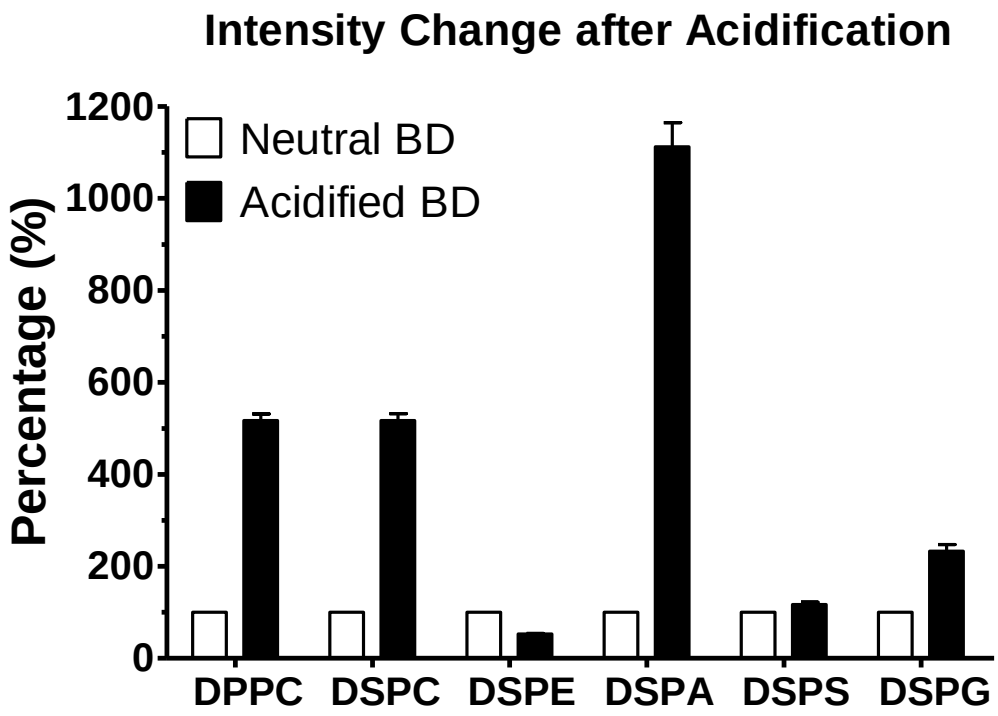

Figure 2.4. Effect of acidification on the signal intensity of DPPC, DSPC, DSPE, DSPA, DSPS, and DSPG after acidified Bligh-Dyer (BD) extraction. 6 different phospholipids were prepared, extracted using neutral or acidified BD extraction, then analyzed using ESI-MS. The intensity changes after acidification were shown via comparing to control. The conventional BD extraction was set as control and made 100%. Data presented as mean ± SEM (n=3).

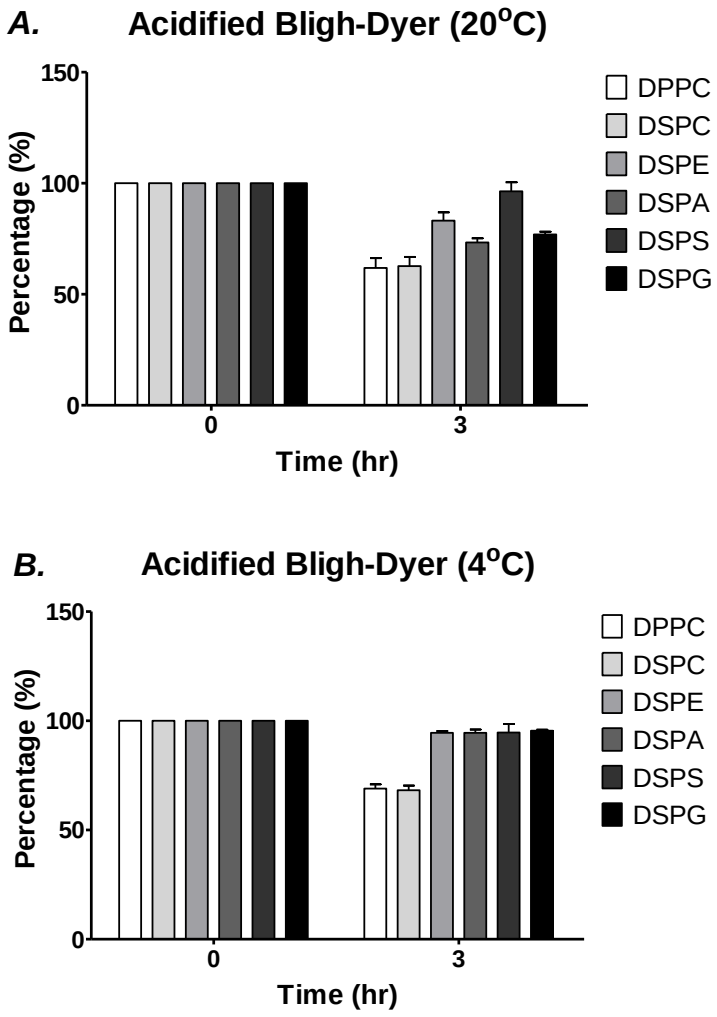

Figure 2.5. Effect of acidification on stability of phospholipids after acidified Bligh-Dyer (BD) extraction. 6 different phospholipids were prepared, extracted using neutral or acidified BD extraction. The extracts were allowed to incubate at either 20ºC or 4ºC for 0 or 20 hr prior to analysis using ESI-MS. With acidified BD extraction, a varying extent of degradation was observed with all phospholipids except DSPS at 20ºC (A). At 4ºC (B), only PCs shows significant degradation. No significant degradation was observed in samples extracted using conventional BD extraction. The time point of 0 hr was set as a control with the value being set at 100%. Data are presented as mean ± SEM (n=3).

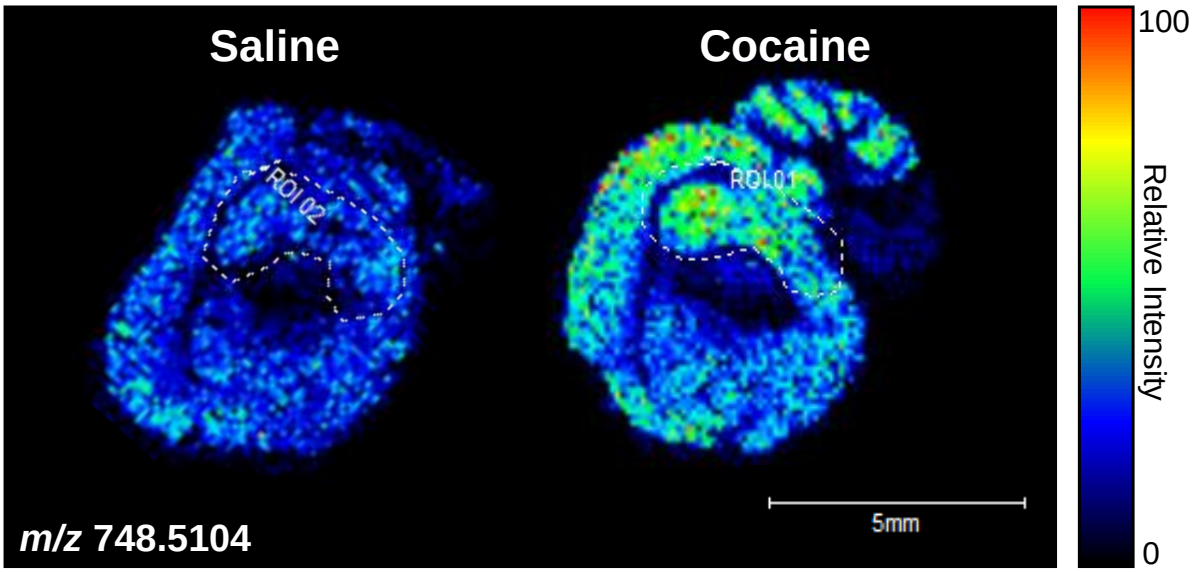

Figure 2.6. MALDI-FTICR-MS relative expression and distribution of phospholipid species (*m/z* 748.5104). MALDI-FTICR-MS was performed on adult mouse sagittal brain sections acquired in the negative ion mode. *Left panel*: saline-treated; *Right panel*: cocaine-treated. The color scale to the right of the panel represents the relative intensity normalized to total ion count (TIC). Scale bar: 5 mm.

Figure 7.

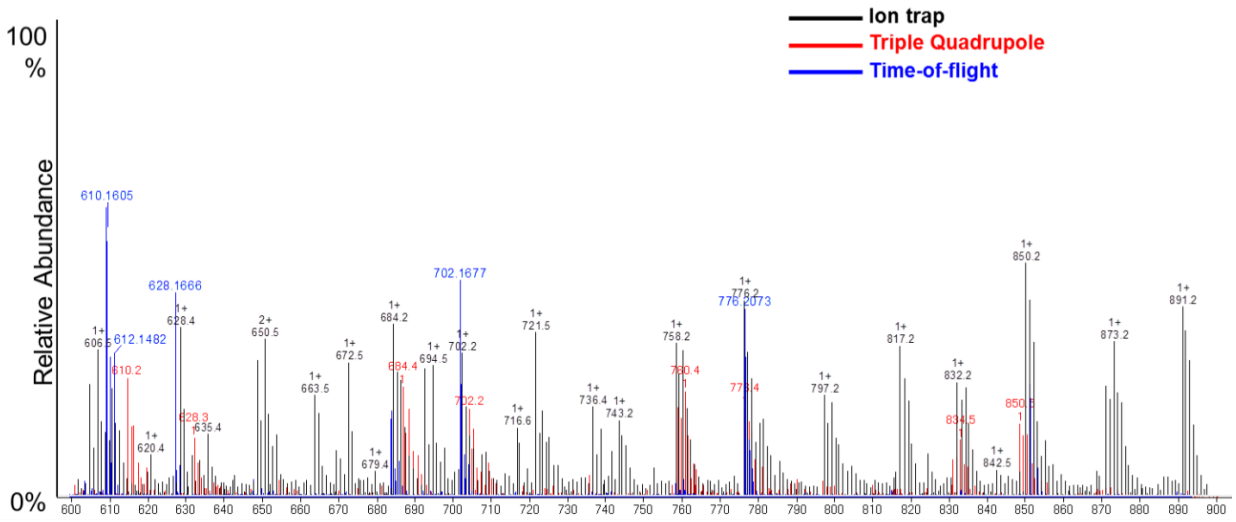

Figure 2.7. Comparison of different MS platforms with ESI-MS. The following platforms were used: Trap XCT ion-trap (Agilent Technologies, Santa Clara, CA), LCT Premier TOF (Waters, MA), and triple-quadrupole (Agilent 6460 LC-MS QQQ System). ESI-MS was performed as described previously [157-159] with a nitrogen drying gas flow-rate of 8 L/min at 350ºC and a nebulizer pressure of 30 psi. The scanning range was from 600 to 900 *m/z* on 5 µL of the sample scanned in positive ion mode for 2.5 min with a mobile phase of acetonitrile: methanol: water (2:3:1) in 0.1% ammonium formate.

Table 2.1. Headgroup fragments for phospholipid fragments.

	Characteristic Headgroup Fragments *(m/z)*	
Class	**Positive Ion Mode (ESI+)**	**Negative Ion Mode (ESI-)**
PA	---	---
PC	184 60	224
PE	141	196
PG	---	227
PI	---	223 241 259 297 315
PS	87	185

Abbreviations/Acronyms: electrospray ionization (ESI), phosphatidic acids (PA), phosphatidylcholines (PC), phosphatidylethanolamines (PE), phosphatidylglycerols (PG), phosphatidylinositols (PI), phosphatidylserines (PS),

References

[1] E. Fahy, S. Subramaniam, R.C. Murphy, M. Nishijima, C.R. Raetz, T. Shimizu, F. Spener, G. van Meer, M.J. Wakelam, E.A. Dennis, Update of the LIPID MAPS comprehensive classification system for lipids, Journal of lipid research, 50 (2009) S9-S14.

[2] G. van Meer, Cellular lipidomics, The EMBO journal, 24 (2005) 3159-3165.

[3] L. Yetukuri, K. Ekroos, A. Vidal-Puig, M. Orešič, Informatics and computational strategies for the study of lipids, Molecular BioSystems, 4 (2008) 121-127.

[4] R.W. Gross, X. Han, Lipidomics at the interface of structure and function in systems biology, Chemistry & biology, 18 (2011) 284-291.

[5] M.R. Wenk, Lipidomics: new tools and applications, Cell, 143 (2010) 888-895.

[6] A. Shevchenko, K. Simons, Lipidomics: coming to grips with lipid diversity, Nature Reviews Molecular Cell Biology, 11 (2010) 593-598.

[7] J. Folch, M. Lees, G. Sloane-Stanley, A simple method for the isolation and purification of total lipids from animal tissues, J biol chem, 226 (1957) 497-509.

[8] E.G. Bligh, W.J. Dyer, A rapid method of total lipid extraction and purification, Canadian journal of biochemistry and physiology, 37 (1959) 911-917.

[9] J. Schiller, R. Süß, J. Arnhold, B. Fuchs, J. Lessig, M. Müller, M. Petković, H. Spalteholz, O. Zschörnig, K. Arnold, Matrix-assisted laser desorption and ionization time-of-flight (MALDI-TOF) mass spectrometry in lipid and phospholipid research, Progress in lipid research, 43 (2004) 449-488.

[10] M. Nishihara, K. Yosuke, Extraction and composition of polar lipids from the archaebacterium, Methanobacterium thermoautotrophicum: effective extraction of tetraether lipids by an acidified solvent, Journal of Biochemistry, 101 (1987) 997-1005.
[11] V. Matyash, G. Liebisch, T.V. Kurzchalia, A. Shevchenko, D. Schwudke, Lipid extraction by methyl-tert-butyl ether for high-throughput lipidomics, Journal of lipid research, 49 (2008) 1137-1146.
[12] S. Chen, M. Hoene, J. Li, Y. Li, X. Zhao, H.-U. Häring, E.D. Schleicher, C. Weigert, G. Xu, R. Lehmann, Simultaneous extraction of metabolome and lipidome with methyl tert-butyl ether from a single small tissue sample for ultra-high performance liquid chromatography/mass spectrometry, Journal of Chromatography A, 1298 (2013) 9-16.
[13] E.M. Thurman, M.S. Mills, Solid-phase extraction: principles and practice, Wiley New York, 1998.
[14] T. Kyrklund, Two procedures to remove polar contaminants from a crude brain lipid extract by using prepacked reversed-phase columns, Lipids, 22 (1987) 274-277.
[15] M. Kaluzny, L. Duncan, M. Merritt, D. Epps, Rapid separation of lipid classes in high yield and purity using bonded phase columns, Journal of Lipid Research, 26 (1985) 135-140.
[16] G. Åkesson-Nilsson, Isolation of chlorinated fatty acid methyl esters derived from cell-culture medium and from fish lipids by using an aminopropyl solid-phase extraction column, Journal of Chromatography A, 996 (2003) 173-180.
[17] W.W. Christie, Silver ion chromatography using solid-phase extraction columns packed with a bonded-sulfonic acid phase, Journal of lipid research, 30 (1989) 1471-1473.

[18] H. Goto, N. Shionoya, M. Sugie, M. Tominaga, O. Shimelis, M. Taniguchi, T. Igarashi, Y. Hirata, Novel pre-fractionation method of trans fatty acids by gas chromatography with silver-Ion cartridge column, Journal of oleo science, 61 (2012) 49-56.

[19] S.H. Yoon, M.-S. Kim, S.H. Kim, H.M. Park, H. Pyo, Y.M. Lee, K.-T. Lee, J. Hong, Effective application of freezing lipid precipitation and SCX-SPE for determination of pyrrolizidine alkaloids in high lipid foodstuffs by LC-ESI-MS/MS, Journal of Chromatography B, 992 (2015) 56-66.

[20] J.X. Shen, R.J. Motyka, J.P. Roach, R.N. Hayes, Minimization of ion suppression in LC–MS/MS analysis through the application of strong cation exchange solid-phase extraction (SCX-SPE), Journal of pharmaceutical and biomedical analysis, 37 (2005) 359-367.

[21] W.H. de Jong, K.S. Graham, J.C. van der Molen, T.P. Links, M.R. Morris, H.A. Ross, E.G. de Vries, I.P. Kema, Plasma free metanephrine measurement using automated online solid-phase extraction HPLC–tandem mass spectrometry, Clinical chemistry, 53 (2007) 1684-1693.

[22] X. Han, R.W. Gross, Shotgun lipidomics: multidimensional MS analysis of cellular lipidomes, Expert Review of Proteomics, 2 (2005) 253-264.

[23] X. Han, K. Yang, J. Yang, H. Cheng, R.W. Gross, Shotgun lipidomics of cardiolipin molecular species in lipid extracts of biological samples, Journal of Lipid Research, 47 (2006) 864-879.

[24] X. Han, J. Yang, H. Cheng, K. Yang, D.R. Abendschein, R.W. Gross, Shotgun Lipidomics Identifies Cardiolipin Depletion in Diabetic Myocardium Linking Altered

Substrate Utilization with Mitochondrial Dysfunction†, Biochemistry, 44 (2005) 16684-16694.

[25] F.-F. Hsu, A. Bohrer, J. Turk, Formation of lithiated adducts of glycerophosphocholine lipids facilitates their identification by electrospray ionization tandem mass spectrometry, J Am Soc Mass Spectrom, 9 (1998) 516-526.

[26] D. Schwudke, J. Oegema, L. Burton, E. Entchev, J.T. Hannich, C.S. Ejsing, T. Kurzchalia, A. Shevchenko, Lipid Profiling by Multiple Precursor and Neutral Loss Scanning Driven by the Data-Dependent Acquisition, Analytical Chemistry, 78 (2006) 585-595.

[27] A. Koulman, B.A. Tapper, K. Fraser, M. Cao, G.A. Lane, S. Rasmussen, High-throughput direct-infusion ion trap mass spectrometry: a new method for metabolomics, Rapid Communications in Mass Spectrometry, 21 (2007) 421-428.

[28] X. Han, R.W. Gross, Shotgun lipidomics: electrospray ionization mass spectrometric analysis and quantitation of cellular lipidomes directly from crude extracts of biological samples, Mass spectrometry reviews, 24 (2005) 367-412.

[29] C. Wolf, P.J. Quinn, Lipidomics: Practical aspects and applications, Progress in Lipid Research, 47 (2008) 15-36.

[30] L.D. Roberts, G. McCombie, C.M. Titman, J.L. Griffin, A matter of fat: An introduction to lipidomic profiling methods, Journal of Chromatography B, 871 (2008) 174-181.

[31] P.T. Ivanova, S.B. Milne, D.S. Myers, H.A. Brown, Lipidomics: a mass spectrometry based systems level analysis of cellular lipids, Current Opinion in Chemical Biology, 13 (2009) 526-531.

[32] M. Petković, J. Schiller, M. Müller, S. Benard, S. Reichl, K. Arnold, J. Arnhold, Detection of Individual Phospholipids in Lipid Mixtures by Matrix-Assisted Laser Desorption/Ionization Time-of-Flight Mass Spectrometry: Phosphatidylcholine Prevents the Detection of Further Species, Analytical Biochemistry, 289 (2001) 202-216.

[33] M.R. Wenk, L. Lucast, G. Di Paolo, A.J. Romanelli, S.F. Suchy, R.L. Nussbaum, G.W. Cline, G.I. Shulman, W. McMurray, P. De Camilli, Phosphoinositide profiling in complex lipid mixtures using electrospray ionization mass spectrometry, Nat Biotech, 21 (2003) 813-817.

[34] P.H. Axelsen, R.C. Murphy, Quantitative analysis of phospholipids containing arachidonate and docosahexaenoate chains in microdissected regions of mouse brain, Journal of Lipid Research, 51 (2010) 660-671.

[35] J.S. Buyer, M. Sasser, High throughput phospholipid fatty acid analysis of soils, Applied Soil Ecology, 61 (2012) 127-130.

[36] K.-Y. Tserng, R. Griffin, Quantitation and molecular species determination of diacylglycerols, phosphatidylcholines, ceramides, and sphingomyelins with gas chromatography, Analytical Biochemistry, 323 (2003) 84-93.

[37] W.B. Dunn, D. Broadhurst, P. Begley, E. Zelena, S. Francis-McIntyre, N. Anderson, M. Brown, J.D. Knowles, A. Halsall, J.N. Haselden, A.W. Nicholls, I.D. Wilson, D.B. Kell, R. Goodacre, Procedures for large-scale metabolic profiling of serum and plasma using gas chromatography and liquid chromatography coupled to mass spectrometry, Nature Protocols, 6 (2011) 1060-1083.

[38] B. Fuchs, J. Schiller, R. Suss, M. Schurenberg, D. Suckau, A direct and simple method of coupling matrix-assisted laser desorption and ionization time-of-flight mass

spectrometry (MALDI-TOF MS) to thin-layer chromatography (TLC) for the analysis of phospholipids from egg yolk, Analytical and bioanalytical chemistry, 389 (2007) 827-834.

[39] A.M. Weerheim, A.M. Kolb, A. Sturk, R. Nieuwland, Phospholipid Composition of Cell-Derived Microparticles Determined by One-Dimensional High-Performance Thin-Layer Chromatography, Analytical Biochemistry, 302 (2002) 191-198.

[40] J.C. Touchstone, Thin-layer chromatographic procedures for lipid separation, Journal of Chromatography B: Biomedical Sciences and Applications, 671 (1995) 169-195.

[41] A. Carrasco-Pancorbo, N. Navas-Iglesias, L. Cuadros-Rodríguez, From lipid analysis towards lipidomics, a new challenge for the analytical chemistry of the 21st century. Part I: Modern lipid analysis, TrAC Trends in Analytical Chemistry, 28 (2009) 263-278.

[42] D. Handloser, V. Widmer, E. Reich, Separation of Phospholipids by HPTLC – An Investigation of Important Parameters, Journal of Liquid Chromatography & Related Technologies, 31 (2008) 1857-1870.

[43] F.M. Helmy, Comparative studies of the endogenous phospholipids and their in vitro hydrolysis by endogenous phospholipases of various tissues from 7-day-old chicks: a thin layer chromatographic and densitometric analysis, Cell biochemistry and function, 22 (2004) 389-398.

[44] D. Sommerer, R. Süß, S. Hammerschmidt, H. Wirtz, K. Arnold, J. Schiller, Analysis of the phospholipid composition of bronchoalveolar lavage (BAL) fluid from man and

minipig by MALDI-TOF mass spectrometry in combination with TLC, Journal of Pharmaceutical and Biomedical Analysis, 35 (2004) 199-206.

[45] M.K. Moe, T. Anderssen, M.B. Strom, E. Jensen, Vicinal hydroxylation of unsaturated fatty acids for structural characterization of intact neutral phospholipids by negative electrospray ionization tandem quadrupole mass spectrometry, Rapid communications in mass spectrometry : RCM, 18 (2004) 2121-2130.

[46] G. Grizard, B. Sion, D. Bauchart, D. Boucher, Separation and quantification of cholesterol and major phospholipid classes in human semen by high-performance liquid chromatography and light-scattering detection, Journal of chromatography. B, Biomedical sciences and applications, 740 (2000) 101-107.

[47] J.H. Zhong, Q.Y. Guo, R.G. Ye, B. Lindholm, T. Wang, Phospholipids in dialysate and the peritoneal surface layer, Advances in peritoneal dialysis. Conference on Peritoneal Dialysis, 16 (2000) 36-41.

[48] I. Cartwright, Separation and Analysis of Phospholipids by Thin Layer Chromatography, in: J. Graham, J. Higgins (Eds.) Biomembrane Protocols, vol. 19, Humana Press, 1993, pp. 153-167.

[49] J.T. Lin, HPLC Separation of Acyl Lipid Classes, Journal of Liquid Chromatography & Related Technologies, 30 (2007) 2005-2020.

[50] J.M. Castro-Perez, J. Kamphorst, J. DeGroot, F. Lafeber, J. Goshawk, K. Yu, J.P. Shockcor, R.J. Vreeken, T. Hankemeier, Comprehensive LC−MSE Lipidomic Analysis using a Shotgun Approach and Its Application to Biomarker Detection and Identification in Osteoarthritis Patients, Journal of Proteome Research, 9 (2010) 2377-2389.

[51] B.L. Peterson, B.S. Cummings, A review of chromatographic methods for the assessment of phospholipids in biological samples, Biomedical Chromatography, 20 (2006) 227-243.
[52] S. Uran, Å. Larsen, P.B. Jacobsen, T. Skotland, Analysis of phospholipid species in human blood using normal-phase liquid chromatography coupled with electrospray ionization ion-trap tandem mass spectrometry, Journal of Chromatography B: Biomedical Sciences and Applications, 758 (2001) 265-275.
[53] R. Taguchi, J. Hayakawa, Y. Takeuchi, M. Ishida, Two-dimensional analysis of phospholipids by capillary liquid chromatography/electrospray ionization mass spectrometry, Journal of Mass Spectrometry, 35 (2000) 953-966.
[54] T. Houjou, K. Yamatani, M. Imagawa, T. Shimizu, R. Taguchi, A shotgun tandem mass spectrometric analysis of phospholipids with normal-phase and/or reverse-phase liquid chromatography/electrospray ionization mass spectrometry, Rapid Communications in Mass Spectrometry, 19 (2005) 654-666.
[55] M. Hermansson, A. Uphoff, R. Käkelä, P. Somerharju, Automated Quantitative Analysis of Complex Lipidomes by Liquid Chromatography/Mass Spectrometry, Analytical Chemistry, 77 (2005) 2166-2175.
[56] P.T. Ivanova, S.B. Milne, M.O. Byrne, Y. Xiang, H.A. Brown, Glycerophospholipid Identification and Quantitation by Electrospray Ionization Mass Spectrometry, in: H.A. Brown (Ed.) Methods in Enzymology, vol. Volume 432, Academic Press, 2007, pp. 21-57.
[57] V. Meyer, Practical high-performance liquid chromatography, Chichester ; New York : Wiley, 1998.

3rd ed., 1998.

[58] L.R. Snyder, J.J. Kirkland, J.L. Glajch, Practical HPLC method development, New York : Wiley, c1997.

2nd ed., 1997.

[59] M.A. Henderson, J.S. McIndoe, Ionic liquids enable electrospray ionisation mass spectrometry in hexane, Chemical Communications, (2006) 2872-2874.

[60] C. Zhu, A. Dane, G. Spijksma, M. Wang, J. van der Greef, G. Luo, T. Hankemeier, R.J. Vreeken, An efficient hydrophilic interaction liquid chromatography separation of 7 phospholipid classes based on a diol column, Journal of Chromatography A, 1220 (2012) 26-34.

[61] M. Schwalbe-Herrmann, J. Willmann, D. Leibfritz, Separation of phospholipid classes by hydrophilic interaction chromatography detected by electrospray ionization mass spectrometry, Journal of Chromatography A, 1217 (2010) 5179-5183.

[62] K.H. Pietiläinen, M. Sysi-Aho, A. Rissanen, T. Seppänen-Laakso, H. Yki-Järvinen, J. Kaprio, M. Orešič, Acquired Obesity Is Associated with Changes in the Serum Lipidomic Profile Independent of Genetic Effects – A Monozygotic Twin Study, PLoS ONE, 2 (2007) e218.

[63] J.S. Perona, V. Ruiz-Gutierrez, Simultaneous determination of molecular species of monoacylglycerols, diacylglycerols and triacylglycerols in human very-low-density lipoproteins by reversed-phase liquid chromatography, Journal of chromatography. B, Analytical technologies in the biomedical and life sciences, 785 (2003) 89-99.

[64] G. Medina-Gomez, S.L. Gray, L. Yetukuri, K. Shimomura, S. Virtue, M. Campbell, R.K. Curtis, M. Jimenez-Linan, M. Blount, G.S.H. Yeo, M. Lopez, T. Seppänen-Laakso,

F.M. Ashcroft, M. Orešič, A. Vidal-Puig, PPAR gamma 2 Prevents Lipotoxicity by Controlling Adipose Tissue Expandability and Peripheral Lipid Metabolism, PLoS Genet, 3 (2007) e64.

[65] P.D. Rainville, C.L. Stumpf, J.P. Shockcor, R.S. Plumb, J.K. Nicholson, Novel Application of Reversed-Phase UPLC-oaTOF-MS for Lipid Analysis in Complex Biological Mixtures: A New Tool for Lipidomics, Journal of Proteome Research, 6 (2007) 552-558.

[66] D. Zhai, P. Reilly, Effect of FA chain length on normal- and reversed-phase HPLC of phospholipids, J Amer Oil Chem Soc, 79 (2002) 1187-1190.

[67] W.W. Christie, High-performance liquid chromatography and lipids : a practical guide, Oxford [Oxfordshire] ; New York : Pergamon Press, 1987.
1st ed., 1987.

[68] R.J. Hamilton, S.F. Mitchell, P.A. Sewell, Techniques for the detection of lipids in high-performance liquid chromatography, Journal of chromatography, 395 (1987) 33-46.

[69] H.Y. Eom, S.Y. Park, M.K. Kim, J.H. Suh, H. Yeom, J.W. Min, U. Kim, J. Lee, J.R. Youm, S.B. Han, Comparison between evaporative light scattering detection and charged aerosol detection for the analysis of saikosaponins, Journal of chromatography. A, 1217 (2010) 4347-4354.

[70] R.A. Moreau, Lipid analysis via HPLC with a charged aerosol detector, Lipid Technology, 21 (2009) 191-194.

[71] E. Hvattum, S. Uran, A.G. Sandbæk, A.Å. Karlsson, T. Skotland, Quantification of phosphatidylserine, phosphatidic acid and free fatty acids in an ultrasound contrast agent by normal-phase high-performance liquid chromatography with evaporative light

scattering detection, Journal of Pharmaceutical and Biomedical Analysis, 42 (2006) 506-512.

[72] T. Saldanha, A.C.H.F. Sawaya, M.N. Eberlin, N. Bragagnolo, HPLC Separation and Determination of 12 Cholesterol Oxidation Products in Fish: Comparative Study of RI, UV, and APCI-MS Detectors, Journal of Agricultural and Food Chemistry, 54 (2006) 4107-4113.

[73] C. Wang, S. Xie, J. Yang, Q. Yang, G. Xu, Structural identification of human blood phospholipids using liquid chromatography/quadrupole-linear ion trap mass spectrometry, Analytica Chimica Acta, 525 (2004) 1-10.

[74] M. Malavolta, F. Bocci, E. Boselli, N.G. Frega, Normal phase liquid chromatography–electrospray ionization tandem mass spectrometry analysis of phospholipid molecular species in blood mononuclear cells: application to cystic fibrosis, Journal of Chromatography B, 810 (2004) 173-186.

[75] W.J. Griffiths, Y. Wang, Mass spectrometry: from proteomics to metabolomics and lipidomics, Chemical Society Reviews, 38 (2009) 1882-1896.

[76] D. Schwudke, G. Liebisch, R. Herzog, G. Schmitz, A. Shevchenko, Shotgun Lipidomics by Tandem Mass Spectrometry under Data-Dependent Acquisition Control, Methods in enzymology, 433 (2007) 175-191.

[77] S.J. Blanksby, T.W. Mitchell, Advances in mass spectrometry for lipidomics, Annual review of analytical chemistry (Palo Alto, Calif.), 3 (2010) 433-465.

[78] X. Han, K. Yang, R.W. Gross, Multi-dimensional mass spectrometry-based shotgun lipidomics and novel strategies for lipidomic analyses, Mass spectrometry reviews, 31 (2012) 134-178.

[79] R.C. Murphy, S.J. Gaskell, New applications of mass spectrometry in lipid analysis, Journal of Biological Chemistry, 286 (2011) 25427-25433.

[80] S.H. Lee, M.V. Williams, R.N. DuBois, I.A. Blair, Targeted lipidomics using electron capture atmospheric pressure chemical ionization mass spectrometry, Rapid Communications in Mass Spectrometry, 17 (2003) 2168-2176.

[81] S.J. Blanksby, T.W. Mitchell, Advances in Mass Spectrometry for Lipidomics, Annual Review of Analytical Chemistry, 3 (2010) 433-465.

[82] D. Schwudke, J.T. Hannich, V. Surendranath, V. Grimard, T. Moehring, L. Burton, T. Kurzchalia, A. Shevchenko, Top-down lipidomic screens by multivariate analysis of high-resolution survey mass spectra, Analytical chemistry, 79 (2007) 4083-4093.

[83] K. Schuhmann, R. Herzog, D. Schwudke, W. Metelmann-Strupat, S.R. Bornstein, A. Shevchenko, Bottom-up shotgun lipidomics by higher energy collisional dissociation on LTQ Orbitrap mass spectrometers, Analytical chemistry, 83 (2011) 5480-5487.

[84] C.S. Ejsing, J.L. Sampaio, V. Surendranath, E. Duchoslav, K. Ekroos, R.W. Klemm, K. Simons, A. Shevchenko, Global analysis of the yeast lipidome by quantitative shotgun mass spectrometry, Proceedings of the National Academy of Sciences, 106 (2009) 2136-2141.

[85] M.S. Wilm, M. Mann, Electrospray and Taylor-Cone theory, Dole's beam of macromolecules at last?, International Journal of Mass Spectrometry and Ion Processes, 136 (1994) 167-180.

[86] M. Wilm, M. Mann, Analytical properties of the nanoelectrospray ion source, Analytical chemistry, 68 (1996) 1-8.

[87] M. Wilm, A. Shevchenko, T. Houthaeve, S. Breit, L. Schweigerer, T. Fotsis, M. Mann, Femtomole sequencing of proteins from polyacrylamide gels by nano-electrospray mass spectrometry, (1996).

[88] B. Brügger, G. Erben, R. Sandhoff, F.T. Wieland, W.D. Lehmann, Quantitative analysis of biological membrane lipids at the low picomole level by nano-electrospray ionization tandem mass spectrometry, Proceedings of the National Academy of Sciences, 94 (1997) 2339-2344.

[89] S. Berry, Lipid Analysis: Isolation, Separation, Identification and Structural Analysis of Lipids, Nutrition Bulletin, 29 (2004) 72-73.

[90] G.W. Wood, P.Y. Lau, Analysis of intact phospholipids by field desorption mass spectrometry, Biological Mass Spectrometry, 1 (1974) 154-155.

[91] L. Hejazi, D. Ebrahimi, D.B. Hibbert, M. Guilhaus, Compatibility of electron ionization and soft ionization methods in gas chromatography/orthogonal time-of-flight mass spectrometry, Rapid Communications in Mass Spectrometry, 23 (2009) 2181-2189.

[92] N.J. Jensen, K.B. Tomer, M.L. Gross, FAB MS/MS for phosphatidylinostitol,-glycerol,-ethanolamine and other complex phospholipids, Lipids, 22 (1987) 480-489.

[93] X. Han, R.W. Gross, Electrospray ionization mass spectroscopic analysis of human erythrocyte plasma membrane phospholipids, Proceedings of the National Academy of Sciences, 91 (1994) 10635-10639.

[94] H.-Y. Kim, T.-C.L. Wang, Y.-C. Ma, Liquid chromatography/mass spectrometry of phospholipids using electrospray ionization, Analytical Chemistry, 66 (1994) 3977-3982.

[95] J.L. Kerwin, A.R. Tuininga, L. Ericsson, Identification of molecular species of glycerophospholipids and sphingomyelin using electrospray mass spectrometry, Journal of lipid research, 35 (1994) 1102-1114.

[96] R.G. Cooks, Z. Ouyang, Z. Takats, J.M. Wiseman, Ambient mass spectrometry, Science (New York, N.Y.), 311 (2006) 1566-1570.

[97] Z. Takats, J.M. Wiseman, B. Gologan, R.G. Cooks, Mass spectrometry sampling under ambient conditions with desorption electrospray ionization, Science (New York, N.Y.), 306 (2004) 471-473.

[98] J.M. Wiseman, S.M. Puolitaival, Z. Takáts, R.G. Cooks, R.M. Caprioli, Mass spectrometric profiling of intact biological tissue by using desorption electrospray ionization, Angewandte Chemie, 117 (2005) 7256-7259.

[99] K.C. Schäfer, J. Dénes, K. Albrecht, T. Szaniszló, J. Balog, R. Skoumal, M. Katona, M. Tóth, L. Balogh, Z. Takáts, In vivo, in situ tissue analysis using rapid evaporative ionization mass spectrometry, Angewandte Chemie International Edition, 48 (2009) 8240-8242.

[100] R. Yost, C. Enke, Triple quadrupole mass spectrometry for direct mixture analysis and structure elucidation, Analytical chemistry, 51 (1979) 1251-1264.

[101] R.N. Hayes, M.L. Gross, Collision-induced dissociation, Methods in enzymology, 193 (1989) 237-263.

[102] B. Fuchs, R. Süß, J. Schiller, An update of MALDI-TOF mass spectrometry in lipid research, Progress in Lipid Research, 49 (2010) 450-475.

[103] J. Chapman, Encyclopedia of analytical science, Academic, London, (1995).

[104] J.H. Gross, Mass spectrometry: a textbook, Springer Science & Business Media, 2004.
[105] R. Klein, Mass spectrometry of the phosphatidylcholines: dipalmitoyl, dioleoyl, and stearoyl-oleoyl glycerylphosphorylcholines, Journal of lipid research, 12 (1971) 123-131.
[106] W.C. Byrdwell, Atmospheric pressure chemical ionization mass spectrometry for analysis of lipids, Lipids, 36 (2001) 327-346.
[107] A.D. Postle, Phospholipid lipidomics in health and disease, European journal of lipid science and technology, 111 (2009) 2-13.
[108] H. Kim, H.K. Min, G. Kong, M.H. Moon, Quantitative analysis of phosphatidylcholines and phosphatidylethanolamines in urine of patients with breast cancer by nanoflow liquid chromatography/tandem mass spectrometry, Analytical and bioanalytical chemistry, 393 (2009) 1649-1656.
[109] H.K. Min, G. Kong, M.H. Moon, Quantitative analysis of urinary phospholipids found in patients with breast cancer by nanoflow liquid chromatography–tandem mass spectrometry: II. Negative ion mode analysis of four phospholipid classes, Analytical and bioanalytical chemistry, 396 (2010) 1273-1280.
[110] A.D. Postle, D.C. Wilton, A.N. Hunt, G.S. Attard, Probing phospholipid dynamics by electrospray ionisation mass spectrometry, Progress in Lipid Research, 46 (2007) 200-224.
[111] A.N. Hunt, A.D. Postle, Mass spectrometry determination of endonuclear phospholipid composition and dynamics, Methods, 39 (2006) 104-111.
[112] H. Farwanah, J. Wirtz, T. Kolter, K. Raith, R.H.H. Neubert, K. Sandhoff, Normal phase liquid chromatography coupled to quadrupole time of flight atmospheric pressure

chemical ionization mass spectrometry for separation, detection and mass spectrometric profiling of neutral sphingolipids and cholesterol, Journal of Chromatography B, 877 (2009) 2976-2982.
[113] Y. Xu, J.T. Brenna, Atmospheric Pressure Covalent Adduct Chemical Ionization Tandem Mass Spectrometry for Double Bond Localization in Monoene- and Diene-Containing Triacylglycerols, Analytical Chemistry, 79 (2007) 2525-2536.
[114] W.C. Byrdwell, E. Emken, Analysis of triglycerides using atmospheric pressure chemical ionization mass spectrometry, Lipids, 30 (1995) 173-175.
[115] R.C. Murphy, T.J. Leiker, R.M. Barkley, Glycerolipid and cholesterol ester analyses in biological samples by mass spectrometry, Biochimica et Biophysica Acta (BBA) - Molecular and Cell Biology of Lipids, 1811 (2011) 776-783.
[116] I. Marchi, S. Rudaz, J.-L. Veuthey, Atmospheric pressure photoionization for coupling liquid-chromatography to mass spectrometry: A review, Talanta, 78 (2009) 1-18.
[117] A. Delobel, S. Roy, D. Touboul, K. Gaudin, D.P. Germain, A. Baillet, F. Brion, P. Prognon, P. Chaminade, O. Laprévote, Atmospheric pressure photoionization coupled to porous graphitic carbon liquid chromatography for the analysis of globotriaosylceramides. Application to Fabry disease, Journal of Mass Spectrometry, 41 (2006) 50-58.
[118] A. Delobel, D. Touboul, O. Laprévote, Structural characterization of phosphatidylcholines by atmospheric pressure photoionization mass spectrometry, European Journal of Mass Spectrometry, 11 (2005) 409-417.

[119] S.-S. Cai, J.A. Syage, Comparison of Atmospheric Pressure Photoionization, Atmospheric Pressure Chemical Ionization, and Electrospray Ionization Mass Spectrometry for Analysis of Lipids, Analytical Chemistry, 78 (2006) 1191-1199.
[120] D. Harvey, Matrix-assisted laser desorption/ionization mass spectrometry of phospholipids, Journal of Mass Spectrometry, 30 (1995) 1333-1346.
[121] J.A. Marto, F.M. White, S. Seldomridge, A.G. Marshall, Structural characterization of phospholipids by matrix-assisted laser desorption/ionization Fourier transform ion cyclotron resonance mass spectrometry, Analytical chemistry, 67 (1995) 3979-3984.
[122] D.J. Harvey, Matrix-assisted laser desorption/ionization mass spectrometry of sphingo-and glycosphingo-lipids, Journal of Mass Spectrometry, 30 (1995) 1311-1324.
[123] B. Fuchs, J. Schiller, Application of MALDI-TOF mass spectrometry in lipidomics, European Journal of Lipid Science and Technology, 111 (2009) 83-98.
[124] M. Pulfer, R.C. Murphy, Electrospray mass spectrometry of phospholipids, Mass spectrometry reviews, 22 (2003) 332-364.
[125] W. Hou, H. Zhou, F. Elisma, S.A. Bennett, D. Figeys, Technological developments in lipidomics, Briefings in functional genomics & proteomics, 7 (2008) 395-409.
[126] J. Schiller, R. Suss, B. Fuchs, M. Muller, O. Zschornig, K. Arnold, MALDI-TOF MS in lipidomics, Frontiers in bioscience: a journal and virtual library, 12 (2006) 2568-2579.
[127] B. Fuchs, J. Schiller, MALDI-TOF MS analysis of lipids from cells, tissues and body fluids, in: Lipids in Health and Disease, Springer, 2008, pp. 541-565.
[128] L.A. McDonnell, R. Heeren, Imaging mass spectrometry, Mass spectrometry reviews, 26 (2007) 606-643.

[129] X. Lou, J.L. van Dongen, J.A. Vekemans, E. Meijer, Matrix suppression and analyte suppression effects of quaternary ammonium salts in matrix-assisted laser desorption/ionization time-of-flight mass spectrometry: an investigation of suppression mechanism, Rapid Communications in Mass Spectrometry, 23 (2009) 3077-3082.
[130] A.S. Woods, IR-MALDI-LDI combined with ion mobility orthogonal time-of-flight mass spectrometry, J. Proteome Res., 5 (2006) 1484-1487.
[131] S.N. Jackson, H.Y.J. Wang, A.S. Woods, Direct tissue analysis of phospholipids in rat brain using MALDI-TOFMS and MALDI-ion mobility-TOFMS, J. Am. Soc. Mass Spectrom., 16 (2005) 133-138.
[132] J.A. McLean, W.B. Ridenour, R.M. Caprioli, Profiling and imaging of tissues by imaging ion mobility-mass spectrometry, J. Mass Spectrom., 42 (2007) 1099-1105.
[133] R.M. Caprioli, T.B. Farmer, J. Gile, Molecular imaging of biological samples: localization of peptides and proteins using MALDI-TOF MS, Analytical chemistry, 69 (1997) 4751-4760.
[134] G.P. Gellermann, T.R. Appel, P. Davies, S. Diekmann, Paired helical filaments contain small amounts of cholesterol, phosphatidylcholine and sphingolipids, Biological chemistry, 387 (2006) 1267-1274.
[135] R.A. Johanson, R. Buccafusca, J.N. Quong, M.A. Shaw, G.T. Berry, Phosphatidylcholine removal from brain lipid extracts expands lipid detection and enhances phosphoinositide quantification by matrix-assisted laser desorption/ionization time-of-flight (MALDI-TOF) mass spectrometry, Analytical biochemistry, 362 (2007) 155-167.

[136] R.A. Johanson, G.T. Berry, Brain phosphoinositide extraction, fractionation, and analysis by MALDI-TOF MS, in: Lipidomics, Springer, 2009, pp. 189-200.

[137] M.L. Pacholski, N. Winograd, Imaging with mass spectrometry, Chemical reviews, 99 (1999) 2977-3006.

[138] L.A. McDonnell, R.M.A. Heeren, Imaging mass spectrometry, Mass Spectrom. Rev., 26 (2007) 606-643.

[139] E.H. Seeley, R.M. Caprioli, Imaging mass spectrometry: Towards clinical diagnostics, Proteomics. Clinical applications, 2 (2008) 1435-1443.

[140] S.G. Boxer, M.L. Kraft, P.K. Weber, Advances in imaging secondary ion mass spectrometry for biological samples, Annual review of biophysics, 38 (2009) 53-74.

[141] P. Nemes, A.A. Barton, A. Vertes, Three-dimensional imaging of metabolites in tissues under ambient conditions by laser ablation electrospray ionization mass spectrometry, Anal Chem, 81 (2009) 6668-6675.

[142] A.L. Lane, L. Nyadong, A.S. Galhena, T.L. Shearer, E.P. Stout, R.M. Parry, M. Kwasnik, M.D. Wang, M.E. Hay, F.M. Fernandez, J. Kubanek, Desorption electrospray ionization mass spectrometry reveals surface-mediated antifungal chemical defense of a tropical seaweed, Proceedings of the National Academy of Sciences of the United States of America, 106 (2009) 7314-7319.

[143] R.C. Murphy, J.A. Hankin, R.M. Barkley, Imaging of lipid species by MALDI mass spectrometry, Journal of Lipid Research, 50 (2009) S317-S322.

[144] T.K. Sinha, S. Khatib-Shahidi, T.E. Yankeelov, K. Mapara, M. Ehtesham, D.S. Cornett, B.M. Dawant, R.M. Caprioli, J.C. Gore, Integrating spatially resolved three-

dimensional MALDI IMS with in vivo magnetic resonance imaging, Nature methods, 5 (2008) 57-59.

[145] E.E. Jones, T.W. Powers, B.A. Neely, L.H. Cazares, D.A. Troyer, A.S. Parker, R.R. Drake, MALDI imaging mass spectrometry profiling of proteins and lipids in clear cell renal cell carcinoma, Proteomics, 14 (2014) 924-935.

[146] J.M. Wiseman, D.R. Ifa, Q. Song, R.G. Cooks, Tissue Imaging at Atmospheric Pressure Using Desorption Electrospray Ionization (DESI) Mass Spectrometry, Angewandte Chemie International Edition, 45 (2006) 7188-7192.

[147] R.G. Cooks, Z. Ouyang, Z. Takats, J.M. Wiseman, Detection Technologies. Ambient mass spectrometry, Science (New York, N.Y.), 311 (2006) 1566-1570.

[148] D.R. Ifa, J.M. Wiseman, Q. Song, R.G. Cooks, Development of capabilities for imaging mass spectrometry under ambient conditions with desorption electrospray ionization (DESI), International Journal of Mass Spectrometry, 259 (2007) 8-15.

[149] L.S. Eberlin, D.R. Ifa, C. Wu, R.G. Cooks, Three-Dimensional Vizualization of Mouse Brain by Lipid Analysis Using Ambient Ionization Mass Spectrometry, Angewandte Chemie International Edition, 49 (2010) 873-876.

[150] S.A. Murphy, A. Nicolaou, Lipidomics applications in health, disease and nutrition research, Molecular nutrition & food research, 57 (2013) 1336-1346.

[151] O. Quehenberger, A.M. Armando, A.H. Brown, S.B. Milne, D.S. Myers, A.H. Merrill, S. Bandyopadhyay, K.N. Jones, S. Kelly, R.L. Shaner, Lipidomics reveals a remarkable diversity of lipids in human plasma, Journal of lipid research, 51 (2010) 3299-3305.

[152] P. Haimi, A. Uphoff, M. Hermansson, P. Somerharju, Software tools for analysis of mass spectrometric lipidome data, Anal Chem, 78 (2006) 8324-8331.
[153] J. Xia, N. Psychogios, N. Young, D.S. Wishart, MetaboAnalyst: a web server for metabolomic data analysis and interpretation, Nucleic acids research, 37 (2009) W652-W660.
[154] R. Herzog, K. Schuhmann, D. Schwudke, J.L. Sampaio, S.R. Bornstein, M. Schroeder, A. Shevchenko, LipidXplorer: A Software for Consensual Cross-Platform Lipidomics, PLoS ONE, 7 (2012) e29851.
[155] R. Tautenhahn, G.J. Patti, D. Rinehart, G. Siuzdak, XCMS Online: a web-based platform to process untargeted metabolomic data, Analytical chemistry, 84 (2012) 5035-5039.
[156] M. Katajamaa, J. Miettinen, M. Orešič, MZmine: toolbox for processing and visualization of mass spectrometry based molecular profile data, Bioinformatics, 22 (2006) 634-636.
[157] G.R. Kinsey, J.L. Blum, M.D. Covington, B.S. Cummings, J. McHowat, R.G. Schnellmann, Decreased iPLA2gamma expression induces lipid peroxidation, cell death, and sensitizes cells to oxidant-induced apoptosis, J Lipid Res, (2008).
[158] L. Zhang, B.L. Peterson, B.S. Cummings, The effect of inhibition of Ca2+-independent phospholipase A2 on chemotherapeutic-induced death and phospholipid profiles in renal cells, Biochemical pharmacology, 70 (2005) 1697-1706.
[159] B. Peterson, K. Stovall, P. Monian, J.L. Franklin, B.S. Cummings, Alterations in phospholipid and fatty acid lipid profiles in primary neocortical cells during oxidant-induced cell injury, Chemico-biological interactions, 174 (2008) 163-176.

CHAPTER 3

EFFECTS OF HIGH-FAT DIET AND AGE ON THE BLOOD LIPIDOME AND CIRCULATING ENDOCANNABINOIDS OF FEMALE C57BL/6 MICE[1]

[1] Sumitra Pati, Saritha Krishna, Jung Hwa Lee, Matthew K. Ross, Claire B. de La Serre, Donald A. Harn, Jr., John J. Wagner, Nikolay M. Filipov, Brian S. Cummings. (2017) *BBA Molecular and Cell Biology of Lipids.* Reprinted with permission from publisher.

Abstract

Alterations in lipid metabolism play a significant role in the pathogenesis of obesity-associated disorders, and dysregulation of the lipidome across multiple diseases has prompted research to identify novel lipids indicative of disease progression. To address the significant gap in knowledge regarding the effect of age and diet on the blood lipidome, we used shotgun lipidomics with electrospray ionization-mass spectrometry (ESI-MS). We analyzed blood lipid profiles of female C57BL/6 mice following high-fat diet (HFD) and low-fat diet (LFD) consumption for short (6 weeks), long (22 weeks), and prolonged (36 weeks) periods. We examined endocannabinoid levels, plasma esterase activity, liver homeostasis, and indices of glucose tolerance and insulin sensitivity to compare lipid alterations with metabolic dysregulation. Multivariate analysis indicated differences in dietary blood lipid profiles with the most notable differences after 6 weeks along with robust alterations due to age. HFD altered phospholipids, fatty acyls, and glycerolipids. Endocannabinoid levels were affected in an age-dependent manner, while HFD increased plasma esterase activity at all time points, with the most pronounced effect at 6 weeks. HFD-consumption also altered liver mRNA levels of PPARα, PPARγ, and CD36. These findings indicate an interaction between dietary fat consumption and aging with widespread effects on the lipidome, which may provide a basis for identification of female-specific obesity- and age-related lipid biomarkers.

Abbreviations: 2-arachidonoylglycerol (2-AG), areas under the curve (AUC), diacylglycerol (DG), endocannabinoid (EC), electrospray ionization-mass spectrometry (ESI-MS), fatty acyl (FA), glucose tolerance (GTT), glycerolipid (GL), High-fat diet

(HFD), insulin sensitivity test (IST), low-fat diet (LFD), N-arachidonoyl ethanolamide (AEA), oleoylethanolamide (OEA), peroxisome proliferator-activated receptor (PPAR), phosphatidylcholines (PC), phosphatidylethanolamines (PE), phospholipids (PLs), principal component analysis (PCA), polyunsaturated fatty acids (PUFAs), tandem mass spectrometry (MS/MS), triacylglycerol (TG).

1. Introduction

Obesity is a growing public health concern that increases the risk of inflammatory and metabolic disorders such as type 2 diabetes, fatty liver, and pulmonary inflammation [1, 2] . The incidence of obesity has drastically increased over the past few decades. In a nationally representative survey (National Health and Nutrition Examination Survey, 2014) of adults in the US, the prevalence of obesity was 35% among men and 40% among women, where linear trends significantly increased for women between 2005 and 2014 [3]. The prolonged and excessive inflammation associated with obesity has also been associated with increases in certain cancers, cardiovascular disease, and Alzheimer's disease [4, 5]. While the mechanisms linking obesity and metabolic disorders are not fully understood, several studies suggest that alterations in lipid-mediated metabolism play a significant role [1, 2, 6]. These studies have led to the hypothesis that change in the blood lipidome can be exploited to identify lipid markers as prognostic indicators for obesity and type 2 diabetes [7].

Lipids are a diverse subset of biomolecules that are not only responsible for energy storage and structural regulation, but also participate in complex signaling networks whose disruption results in the pathogenesis of obesity and other ailments. A few studies have identified several lipid and lipoprotein abnormalities among obese

patients [8, 9]. For example, Hu, *et al*. reported decreases in HDL cholesterol along with altered triglyceride levels in nondiabetic obese patients [9]. Additionally, the role of dietary fat in obesity and influence of fatty food intake on inflammatory responses are well-established [4, 10]. Obesity-associated inflammation is not restricted to impaired lipid metabolism, but is also strongly linked with type 2 diabetes, as obesity is associated with insulin resistance, which heightens the risk for metabolic syndrome [11, 12].

The higher prevalence of type 2 diabetes among adults supports the assertion that aging is the precursor to insulin resistance [13-16]. While insulin resistance, type 2 diabetes, and metabolic syndrome have been studied within the context of age to some extent, including by us [17], the effect of age on the lipidome and/or age-obesity interactions have not received significant attention. However, two more recent studies demonstrate that age exerts appreciable, lipid species-specific effects on the brain lipidome [18] and, importantly, that age has profound effects on the female reproductive system (oocytes) lipidome [19]. These studies support the hypothesis that age-obesity interactions alter the lipidome. In comparison to the lack of knowledge on the effect of obesity and/or age on the plasma lipidome as a whole, it is known that obesity can alter the levels of select lipid species. For example, increased circulating endocannabinoids, especially 2-arachidonoylglycerol (2-AG), have been associated with obesity in both humans and laboratory animals, i.e. [20, 21]; however, it is not known how the endocannabinoid system is altered within the context of age in the face of high-fat diet consumption. The endocannabinoid (EC) system participates in the control of lipid and glucose metabolism and dysregulation of this system can occur following unbalanced

energy intake [22]. Such dysregulation often results in overactivity across various organs involved in energy homeostasis such as intra-abdominal adipose tissue [23]. Over-activation of the endocannabinoid system has been shown to promote insulin resistance [6]. Additionally, the essential role of the EC system in adipogenesis and lipogenesis has been reviewed in detail by Silvestri and Marzo, *et al* [22, 23].

In this study, we further investigated the effects of dietary fat consumption, age, and their interaction at the level of the lipidome using shotgun lipidomics with electrospray ionization-mass spectrometry (ESI-MS). Because of the paucity of data and the linear increase of female obesity among US women in the most recent decade [3], we assessed the blood lipid profiles of female C57BL/6 mice following HFD-consumption for short (6 weeks), long (22 weeks), and prolonged (36 weeks) periods to evaluate the persisting effects of feeding. To compare lipid alterations with metabolic and liver regulation, markers of liver homeostasis were assessed and correlations between them and indices of glucose tolerance and insulin sensitivity with the blood lipidome were determined. Circulating and liver levels of the two major endocannabinoids, 2-arachidonoylglycerol (2-AG) and anandamide (AEA), were also measured to determine the effects of HFD-consumption and age on the endocannabinoid system.

2. Materials and methods

2.1. *Animals*

Experiments were performed with female C57BL/6 mice (Harlan, Indianapolis, IN). The mice were housed (4-5/cage) and maintained at 22–24°C with food and water available *ad libitum* on a 12 h light/dark cycle in an AAALAC accredited facility throughout the

study. All experimental procedures were in accord with the latest National Institutes of Health (NIH) guidelines and the study was approved prior to initiation by the Institutional Animal Care and Use Committee (IACUC) of the University of Georgia.

2.2. *Dietary treatment*

The diets and dietary treatment are described in detail in our recent publication [17], where the body weight changes, metabolic and behavioral effects of the same experimental paradigm are reported. Briefly, 6-7 weeks old female mice weighing 16.0 ± 0.20 g (mean ± SEM) were randomly divided into two groups (n = 8/group/time point) and placed on either a low-fat diet (LFD; 10% kcal from fat, D12450J, Research Diets, Inc., New Brunswick, NJ) or a high-fat diet (HFD; 60% kcal from fat, D12492, Research Diets) for either 6, 22, or 36 weeks. The LFD diet (3.85 kcal/g) consisted of 70% carbohydrate, 20% protein, 10% fat, of which 23.5% were saturated fatty acids [SFA], 29.7% monounsaturated fatty acids [MUFA], and 46.8% polyunsaturated fatty acids [PUFA]) (***Table S3.4***). The HFD diet (5.24 kcal/g) consisted of 20% carbohydrate, 20% protein, 60% fat, of which 32.2% were SFA, 35.9% MUFA, 31.9% PUFA (***Table S3.4***).

2.3. *Blood, plasma, and liver tissue collection*

Mice were sacrificed at three time points (6, 22 and 36 weeks); considerations for the selection of these time points are explained in detailed in Krishna, *et al.,* body weights (BW) were recorded and liver was collected and quickly frozen at -80°C [17]. Blood (1 ml) was collected via cardiac puncture and immediately split into two aliquots: 500 µl was placed in Na citrate-containing tubes, mixed thoroughly, and the plasma was

separated by centrifugation (3,500 X g; 10 min; 4 ºC). Harvested plasma was then aliquoted and placed at -80 ºC until its use for endocannabinoid and esterase activity analyses as described in detail below. The other 500 µl of blood was immediately mixed, by vortexing, with 1 mL of methanol:water (1.0:0.4 v/v) and then placed at -80ºC until lipid extraction as described below. Liver (6, 22, and 36 weeks) samples were used for qPCR and endocannabinoid analyses (described below).

2.4. *Glucose tolerance test (GTT) and insulin sensitivity test (IST) areas under the curve (AUCs)*

Glucose tolerance (GTT) and insulin sensitivity (IST) tests were performed after 5, 20 and 33 weeks on respective diets as described in our recent study [17]. We used the blood glucose integrated areas under the curve (AUC) in the GTT and IST tests, as calculated using the trapezoidal method [24], to determine if mice's response to oral glucose challenge or to insulin correlates with specific lipid metabolites (described below).

2.5. *Bligh-Dyer blood lipid extraction*

Phospholipids were extracted using chloroform and methanol according to the method of Bligh and Dyer [25]. Briefly, blood samples designated for lipidomics analysis were suspended in 1.25 mL of methanol and 1.25 mL of chloroform. Tubes were vortexed for 30 secs, allowed to sit for 10 min on ice, centrifuged (213 x g; 5 min), and the bottom chloroform layer was transferred to a new test tube. The extraction steps were repeated a second time and the chloroform layers combined. The collected chloroform

layers were dried under nitrogen, reconstituted with 50 µL of methanol: chloroform (3:1 v/v), and stored at -80°C until analysis.

2.6. *Lipid phosphorus assay*

Lipid phosphorus was quantified using the phosphorus assay *[26]*. 400 µL of sulfuric acid (5M) was added to lipid extracts (10 µL) in a glass test tube, and heated at 180-200°C for 1 hr. 100 µL of 30% H_2O_2 was then added to the tube while vortexing, and heated at 180-200°C for 1.5 hrs. 4.6 mL of reagent (1.1 g ammonium molybdate tetrahydrate in 12.5 mL sulfuric acid in 500 mL dd$H_2$0) was added and vortexed, followed by 100 µL of 15% ascorbic acid and vortexing. The solution was heated for 7-10 minutes at 100°C, and a 150 µL aliquot was used to measure the absorbance at 830 nm.

2.7. *Phospholipid characterization with electrospray ionization-mass spectrometry (ESI-MS)*

Lipid extract samples (500 pmol/µl) were prepared by reconstitution in chloroform: methanol (2:1, v/v). ESI-MS was performed as described previously [27-29] using a Trap XCT ion-trap mass spectrometer (Agilent Technologies, Santa Clara, CA) with a nitrogen drying gas flow-rate of 8 L/min at 350ºC and a nebulizer pressure of 30 psi. The scanning range was from 200 to 1000 *m/z* on 5 µL of the sample scanned in positive and negative ion mode for 2.5 min with a mobile phase of acetonitrile: methanol: water (2:3:1) in 0.1% ammonium formate. As described previously [30], qualitative identification of individual phospholipid molecular species was based on their

calculated theoretical monoisotopic mass values, subsequent MS/MS analysis, and their level normalized to either the total ion count (TIC) or the most abundant phospholipid.

MS^{nth} fragmentation was performed on an Agilent Trap XCT ion-trap mass spectrometer equipped with an ESI source. Direct injection from the HPLC system was used to introduce the analyte. The nitrogen drying gas flow-rate was 8.0 L/min at 350°C. The ion source and ion optic parameters were optimized with respect to the positive molecular ion of interest. Initial identification was typically based on the loss of the parent head group followed by subsequent analysis of the lysophospholipid. In the event that neutral loss scanning could not confirm the species, the tentative ID was assigned based on the *m/z* value and the LIPIDMAPS database (http://www.lipidmaps.org).

2.8. *Multivariate statistical analysis of blood lipids*

Multivariate principal component analysis (PCA) was performed using MetaboAnalyst 3.0 (http://www.metaboanalyst.ca/). Automatic peak detection and spectrum deconvolution was performed using a peak width set to 0.5. Analysis parameters consisted of interquartile range filtering and sum normalization with no removal of outliers from the dataset. Features were selected based on volcano plot analysis and were further identified using MS/MS analysis. Significance for volcano plot analysis was determined based on a fold change threshold of 2.00 and $p \leq 0.05$. Following identification, total ion count was used to normalize each parent lipid level, and the change in the relative abundance of that phospholipid species as compared to its

control was determined. This method is standard for lipidomic analysis as reported in our previous studies [27, 29].

2.9. *Liver endocannabinoid (2-AG and AEA) levels*

2-AG and AEA were extracted from liver using a modification of the method of Kingsley and Marnett (2007). In brief, ~0.05-0.1 g of frozen liver tissue (exact weight recorded) was Dounce homogenized in 2:2:1 v/v/v ethyl acetate:hexane:0.1M potassium phosphate (pH 7.0) [total volume 5 mL; supplemented with butylated hydroxytoluene and triphenylphosphine, 0.05% w/v each (antioxidants)] containing deuterated standards for 2-AG and AEA (5.6 pmol d_8-AEA and 518 pmol d_8-2-AG). The mixture was vortexed (1 min) and centrifuged to separate organic and aqueous phases (1,400 x *g*, 10 min). The organic layer was removed, dried under a stream of N_2 and residues dissolved in 2:2:1 v/v/v water:methanol:isopropanol (200 µl). After filtration (0.1 µm), 10 µl of the resolubilized lipid was injected onto a Acquity UPLC BEH C18 column (2.1 x 50 mm, 1.7µm) equipped with VanGuard pre-column (2.1 x 5 mm, 1.7µm). The mobile phase was a blend of solvent A (2 mM ammonium acetate/0.1% acetic acid in water) and solvent B (2 mM ammonium acetate/0.1% acetic acid in methanol). Analytes are eluted with the following gradient program: 0 min (95% A, 5% B), 0.5 min (95% A, 5% B), 5 min (5% A, 95% B), 6 min (5% A, 95% B), 7 min (95% A, 5% B), 8 min (95% A, 5% B). The flow rate was 0.4 mL/min and the entire column eluate was directed into a Thermo Quantum Access triple quadrupole mass spectrometer (heated electrospray ionization in positive ion mode). Single reaction monitoring (SRM) of each analyte was as follows: 2-AG, $[M+NH_4]^+$ *m/z* 396.3>287.3; 2-AG-d_8, $[M+NH_4]^+$ *m/z* 404.3>295.3;

AEA, $[M+H]^+$ *m/z* 348>62; AEA-d_8, $[M+H]^+$ *m/z* 356>63. Endocannabinoids were quantified by measuring the area under each peak in comparison to the deuterated standards and normalized on tissue weight.

2.10. *Plasma endocannabinoid (2-AG and AEA) levels*

Plasma levels of the two endocannabinoids 2-arachidonoylglycerol (2-AG) and *anandamide* (N-arachidonoylethanolamine; AEA) were determined using mass spectrometry. First, 50 µL of mouse plasma was placed into a glass vial. Deuterated standards, 6 pmol AEA-d_8 and 52 pmol 2-AG-d_8 were added to each sample, followed by 2 mL of ethyl acetate for extraction. The mixture was vortexed (1 min) and centrifuged at 1,400 g for 10 min. The organic layer (~1.5 mL) was transferred into a clean glass vial and was dried under a stream of N_2. The residues were reconstituted in 1:1 v/v water: methanol (100 µL). After filtration (0.1 µm), 10 µL of samples was injected onto an Acquity UPLC system (Waters, Milford, MA) coupled to a TSQ Quantum Ultra tandem mass spectrometer equipped with a heated electrospray (H-ESI) source (Thermo Fisher). Chromatographic separation was carried out using an Acquity UPLC BEH C18 column (2.1 mm × 100 mm, 1.7 µm) equipped with a VanGuard precolumn (2.1 mm × 5 mm, 1.7 µm) at 40°C using column oven. The mobile phases used were water containing 0.1% acetic acid (A) and methanol containing 0.1% acetic acid (B). Mobile phase gradient conditions were as follows: hold at 15% A and 85% B for 0.5 min, linear increase of B to 95% in 2 min, hold at 95% B for 4 min, decrease of B to 5% in 1 min and re-equilibrate for 2 min at the starting conditions. The overall run time was 10 min and flow rate was 0.2 mL/min. Eluate from the LC was directly

electrosprayed into the mass spectrometer using an electrospray ionization interface in the positive mode. MS conditions were set as follows: spray voltage = 3500 V, vaporizer temperature = 350°C, sheath gas = 25 units, auxiliary gas = 2 and capillary temperature = 350°C. Samples were run in positive single reaction monitoring (SRM) mode and the following precursor-to-product ion transitions were used for quantification: 2-AG, $[M+H]^+$ *m/z* 379.2 > 287.1; AEA, $[M+H]^+$ *m/z* 348.2 > 287.2; 2-AG-d_8, $[M+H]^+$ *m/z* 387.2 > 292.3; AEA-d_8, $[M+H]^+$ *m/z* 356.2 > 294.2. Scan time was 0.2 s per SRM, and the scan width was *m/z* 0.01. Optimum collision energy and S-lenses conditions were determined for each compound by using autotune software for each analyte by post-column infusion of the individual compounds into a 50% A/50% B blend of the mobile phase being pumped at a flow rate of 0.2 mL/min. Xcalibur software was employed for data acquisition and processing. For quantification, each calibration standard was prepared ranging from 1 to 1000 nM by fortifying phosphate-buffered saline with stock standards of 2-AG or AEA prepared in methanol. Quality control samples were prepared at a concentration of 50 nM for each endocannabinoid in triplicate. Weighted calibration curves were constructed using 1/x as a weighting factor for 2-AG and AEA, respectively.

2.11. *Plasma esterase activity*

Plasma esterase activity was determined using the substrate *para*-nitrophenyl valerate, as previously described [31]. Production of *p*-nitrophenol liberated from *p*NPV was monitored at 405 nm on a spectrophotometer [32]. An extinction coefficient of 13 $cm^{-1}mM^{-1}$ [33] was used to convert the slopes of each activity curve to specific enzyme

activities. All enzymatic reaction rates were corrected for non-enzymatic hydrolysis rates as we have described previously [31].

2.12. *Real-time quantitative PCR (qPCR)*

qPCR was performed on liver samples as described in [17] and [34]. Briefly, total liver RNA (20 mg tissue) was isolated using a GeneJET ™ RNA Purification Kit (Thermo Fisher Scientific, Pittsburgh, PA) and quantified using a Take 3 plate and an Epoch microplate spectrophotometer (Bio-Tek, Winooski, VT). RNA was converted to cDNA using qScript cDNA SuperMix (Quanta Bioscience, Gaithersburg, MD) and a Peltier thermal cycler (Bio-Rad, Hercules, CA). Using 3 ng of cDNA per sample (with each sample run in duplicate), expression of peroxisome proliferator-activated receptor alpha (PPARα), peroxisome proliferator-activated receptor gamma (PPARγ), hepatic fatty acid transporter (CD36), fatty acid synthase (FAS), acetyl-CoA carboxylase (ACC), stearoyl-CoA desaturase (SCD), monoacylglycerol lipase (MGL), cannabinoid receptor type 1 (CB1), cannabinoid receptor type 2 (CB2) and 18S, was determined by qPCR using mouse-specific primers (Real Time Primers, Elkins Park, PA) and SYBR Green-based master mix (Qiagen, Valencia, CA). Amplifications were performed on a Mx3005P qPCR machine (Stratagene) and treatment differences were calculated as a fold change by the $^{\Delta\Delta}$ Ct method with 18S used as a house-keeping gene (HKG) as previously reported [17, 34]. Correlation between the results from the liver qPCR and the blood lipidome was investigated as described below.

2.13. *Regression analysis between lipid features, GTT/IST, plasma endocannabinoids, and liver homeostasis.*

GraphPad Prism for windows version 5.04 (GraphPad Software, Inc., La Jolla, CA) was used for all correlation analyses comparing the differential lipid expression via the relative abundance of features to multiple endpoints used in the study such as liver mRNA expression values, plasma endocannabinoid levels, and AUC values from GTT/IST. Reported correlations meet the fairly stringent cutoff correlation coefficient criteria of $R^2 \geq 0.6$.

2.14. *Statistical Analysis*

All statistical analyses were compiled using GraphPad Prism for windows version 5.04 (GraphPad Software, Inc., La Jolla, CA). For all analysis, the experimental unit was individual animals and samples from a total of 6-8 animals/diet/time point were assessed. For all analyses, significance was set at $p \leq 0.05$ where data are expressed as mean ± SEM based on t-test for pairwise analysis and/or ANOVA analysis (two-factor repeated-measures with Bonferroni *post hoc* test). Pairwise comparisons of data were performed with either an unpaired two-tailed Student's t-test or nonparametric test, depending on the outcomes of normality testing for Gaussian distributions.

3. Results

3.1 Morphometric, GTT, IST, and intestinal permeability data.

The lipid changes reported above were correlated to glucose tolerance (GTT) and insulin sensitivity (IST) outcomes, which were recently reported [17]. Briefly, HFD-fed

mice were significantly heavier than LFD mice at all three time points, and had impaired glucose tolerance. Interestingly, HFD-feeding had the greatest effect on glucose tolerance rather than insulin sensitivity [17]. On the other hand, while HFD decreased IST at the earlier time points, this trend was not seen at the end of the study due to age-dependent decreases in IST in LFD-fed mice [17]. HFD-consumption by the female C57BL/6 mice also increased the gastrointestinal permeability, more so after longer feeding durations [17].

3.2 Multivariate analysis of lipidome

Multivariate, unsupervised principal component analysis (PCA) of spectral data comparing high-fat diet (HFD) and low-fat diet (LFD) consumption showed distinct clustering within the blood lipidome where diet and age were the major effectors **(Fig. 3.1, Fig. 3.2)**. Scores plots of all groups, for both positive **(Fig. 3.1A)** and negative ion mode **(Fig. 3.2A)**, demonstrated a striking separation between 6-week vs. 22- and 36-week treatment groups. The separation of populations occurred regardless of dietary treatment indicating a significant role for age on the lipidome. However, HFD-consumption altered lipid profiles within each respective time point where 6-week treatment **(Fig. 3.1C, Fig. 3.2C)** had the most pronounced effect. Urine lipid profiles demonstrated a similar trend ***(Fig. S3.1)***. The baseline lipidome was also assessed with PCA analysis comparing blood lipid profiles of ~5-6-week-old mice to 6-week HFD/LFD-fed mice, indicating group differences along with variability in the baseline lipidome, which diminished following 6 weeks of dietary treatment ***(Fig. S3.4)***.

Volcano plots identified and ranked potentially important features based on fold change and statistical significance level for age- **(Fig. 3.3, *Fig. S3.2*)** and diet-related **(Fig. 3.4, *Fig. S3.3*)** effects. Age-related pairwise comparisons within dietary treatment groups for short vs. long/prolonged (6-week vs. 22- and 36-week) **(Fig. 3.3A-3.3B, *Fig. S3.2A-S3.2B*)** yielded the greatest number of features while 22-week vs. 36-week **(Fig. 3.3C, *Fig. S3.2C*)** resulted in very few. Based on the number of features altered, diet-related pairwise comparisons of LFD- vs. HFD-consumption indicated that HFD-induced alterations were most robust following a short consumption period **(Fig. 3.4A)** with fewer alterations following longer periods of exposure **(Fig. 3.4B, 3.4C)**.

3.3 Phospholipid species

Diet- and age-dependent alterations elevated the relative abundances of phospholipid (PL) species in blood lipid profiles of HFD-fed mice after 6 weeks of consumption **(Fig. 3.5A)**, and presented the most changes following 22 weeks of treatment where HFD-fed mice had decreased relative abundances of various PL species, differing from those species affected after 6 weeks on the diet **(Fig. 3.5A)**. None of the age-/diet- changes persisted after 36 weeks of HFD feeding **(Fig. 3.5A)**.

Significance analysis of lipid features was performed for all time points within each dietary group (i.e. 6 weeks vs. 22 weeks of LFD feeding) to identify age-/diet-alterations. These age-/diet- features were subsequently excluded during analysis of LFD vs. HFD treatment to characterize the effects of HFD feeding alone. Interestingly, the effects of HFD-consumption alone did not appear following 6 weeks of feeding **(Fig. 3.6A)**. 22-week consumption demonstrated the greatest effect, much like that observed

in features altered due to diet-/age-, although differences in PL relative abundances were bidirectional and did not show a class-specific uniform trend **(Fig. 3.6A)**. Following 36 weeks of feeding, the relative abundance of only one feature (*m/z* 578.3) changed due to HFD-consumption alone **(Fig. 3.6A)**. MS/MS analysis and neutral loss scanning was performed to validate phospholipid class identities **(*Table S3.1-S3.2*)**.

3.4 Fatty acyl species

Fatty acyl (FA) species altered based on diet- and age-related effects demonstrated bidirectional effects at all three time points where the majority of features identified were in blood profiles of mice following 22 weeks of treatment **(Fig. 3.5B)**. One feature (*m/z* 562.8) persisted between short- and long-term feeding, demonstrating an increase in relative abundance in HFD-fed animals after 6-weeks followed by a decrease after 22-weeks **(Fig. 3.5B)**.

Diet alone altered the blood lipidome of the 6-week treatment group in which HFD-consumption decreased the relative abundances of FAs by ~2-fold **(Fig. 3.6B)**. This was also observed in urine lipid profiles of the 6-week treatment group where three features (*m/z* 337, *m/z* 385*, m/z* 381) detected and altered in blood were also detected in urine with comparable magnitudes of differences between LFD- and HFD-fed mice **(Fig. 3.6B)**. The effects of HFD-consumption alone did not persist after 22-weeks and 36-weeks **(Fig. 3.6B)**. MS/MS analysis and neutral loss scanning was performed to validate fatty acyl class identities **(*Table S3.1-S3.2*)**.

3.5 Glycerolipid species

Most diet- and age-dependent feature alterations in glycerolipids occurred after short- (6 weeks) and long-term feeding (22 weeks) where changes were primarily bidirectional across groups **(Fig. 3.5C)**. 22-week feeding displayed a trend of general decreases in glycerolipid (GL) relative abundances in HFD-fed mice **(Fig. 3.5C)**. We identified one feature that was altered after 36-weeks of dietary treatment, (*m/z* 708.6), which was decreased in HFD-mice **(Fig. 3.5C)**.

Resembling the pattern observed across FA species **(Fig. 3.6B)**, the majority of features altered due to HFD-consumption alone were identified in the 6-week treatment group. Further, GL features demonstrated species-specific increases and decreases in both blood and urine profiles **(Fig. 3.6C)**. Long-term feeding affected a few GL features with net decreases in HFD-mice, which were no longer present after 36 weeks **(Fig. 3.6C)**. MS/MS analysis and neutral loss scanning was performed to validate glycerolipid class identities **(*Table S3.1-S3.2*)**.

3.6 Liver endocannabinoids.

Given that many of the species altered in HFD-fed mice were phospholipids containing polyunsaturated fatty acids (PUFAs), and because many of the fatty acyls correlated to derivatives of fatty acids, we focused on arachidonic acid-containing metabolites, including 2-arachidonoylglycerol (2-AG) and N-arachidonoylethanolamide (AEA). Upon release, these endocannabinoids target cannabinoid receptors (CB1 and CB2) and work together to play a role in energy homeostasis [22]. Liver 2-AG levels decreased after 6 and 36 weeks of HFD-consumption **(Appendix Fig. 1A)**. Interestingly, an age-related effect was observed where 36 weeks of HFD-feeding decreased liver 2-AG

levels **(Appendix Fig. 1A)**. The decrease of 2-AG levels on the liver after 36 weeks was accompanied by a significant increase of AEA **(Appendix Fig. 1B)**. The only significant effect of HFD on liver AEA levels was a significant decrease after 6 weeks on the diet **(Appendix Fig. 1B)**. CB1 expression did not change while CB2 expression showed time-dependent increases in HFD-fed mice, although these were not significant **(Appendix Fig. 1C)**.

3.7 Plasma endocannabinoids.

Plasma levels of 2-AG and AEA in the LFD-fed mice were quite stable, apart from a slight increase after 36 weeks of feeding **(Appendix Fig. 2)**. In contrast, HFD-consumption increased plasma levels of 2-AG, but the effects were bi-phasic where a significant increase was only observed at 6 and 36 weeks, but not after 22 weeks of HFD-consumption **(Appendix Fig. 2A)**. There also appeared to be an effect of age on plasma 2-AG within the HFD-fed mice as shown by an increase in 2-AG levels following 36 weeks compared to 22 weeks of feeding **(Appendix Fig. 2A)**. The effects of HFD-consumption on the other endocannabinoid, AEA, resembled the diet's effects on plasma 2-AG, with the only significant effect being an increase of plasma AEA levels after 36 weeks on HFD **(Appendix Fig. 2B)**.

3.8 Plasma esterase activity.

The increase in fatty acyls and lysophospholipid species suggests increased esterase activity. This hypothesis was addressed by assessing esterase activity at all time points in the plasma. HFD-consumption increased plasma esterase activity at all time points,

with the most pronounced effect following 6 weeks of feeding **(Appendix Fig. 3)**. Although plasma esterase activity increased following both 22 and 36 weeks, the effect at 36 weeks was not significant **(Appendix Fig. 3)**. It appeared that age alone affected plasma esterase activity, indicated by heightened esterase activity after 6 weeks of HFD-consumption followed by lower levels at later time points **(Appendix Fig. 3)**.

3.9 Liver qPCR data of key lipid homeostasis genes.

There are many genes that encode for protein regulating energy balance and lipid metabolism, including peroxisome proliferator-activated receptors (PPARs) [35, 36]. PPARα is best known for its major role in lipid and lipoprotein metabolism while PPARγ is involved in adipogenesis and insulin sensitivity [35, 37]. HFD-consumption increased expression of liver mRNA levels of PPARα, PPARγ, and CD36, a known target of PPARγ [38], significantly at 6 weeks of HFD **(Fig. 3.7A)**. Interestingly, PPARα and PPARγ levels increased after 36 weeks of HFD-consumption, but not after 22 weeks. Liver CD36 mRNA was elevated at all three time points **(Fig. 3.7A)**, with the magnitude of elevation greatest after 36 weeks on HFD.

PPARγ has been shown to increase during lipogenesis, thus we assessed the expression of fatty acid synthase (FAS), acetyl-CoA carboxylase (ACC), and stearoyl-CoA desaturase (SCD) **(Fig. 3.7B)**. HFD-fed mice demonstrated a numerical trend of time-dependent increases, although not significant, in SCD, ACC, and FAS expression **(Fig. 3.7B)**. MGL demonstrated increased expression in mice fed HFD for 6 weeks; however, this effect was tapered after long- and prolonged-feeding **(Fig. 3.7B)**.

3.10 Correlation between lipids, GTT/IST, plasma endocannabinoids, liver homeostasis.

We performed regression analysis to determine if changes in the blood lipidome correlated to changes in GTT or IST, plasma endocannabinoid levels, or gene expression of liver homeostasis markers. **Table 3.1A** lists correlations ($R^2 \geq 0.6$) between several lipid features and the expression of CD36, PPARα, and PPARγ mRNA in the liver. There were only a few lipid species whose abundance correlated to changes in these genes, including two unidentifiable FA species. Correlations occurred at all time points with increases in TG (52:4 or 52:5) [PPARγ] in HFD-mice at 6 weeks, decreases of DG (40:6) [CD36], PE (42:7) [CD36], and FA (*m/z* 562.8) [PPARα] at 22 weeks, and an increase in FA (*m/z* 438.8) [PPARα] at 36 weeks **(Fig. 3.8)**. Lipid species indicated by only their *m/z* value were unable to be fully characterized by subsequent MS/MS analysis.

Regression analyses also demonstrated quite a few relationships between changes in select blood lipids and changes in AUC from glucose tolerance and insulin sensitivity tests after 6 weeks **(Table 3.1B)**. Fewer correlations were identified for changes in the blood lipidome at 22 or 36 weeks **(*Table S3.3*)**, which is not surprising given the robust differences observed after 6-weeks of treatment. Interestingly, several lipids such as PC (44:3) and DG (34:3), which correlated to glucose tolerance, also demonstrated inverse correlates to insulin sensitivity.

Regarding plasma endocannabinoids, GL species (*m/z* 734.6, *m/z* 760.5) and FA species (*m/z* 353.2) correlated to changes in in 2-AG exclusively within HFD-mice, whereas AEA did not correlate to any lipid features **(Table 3.1C)**.

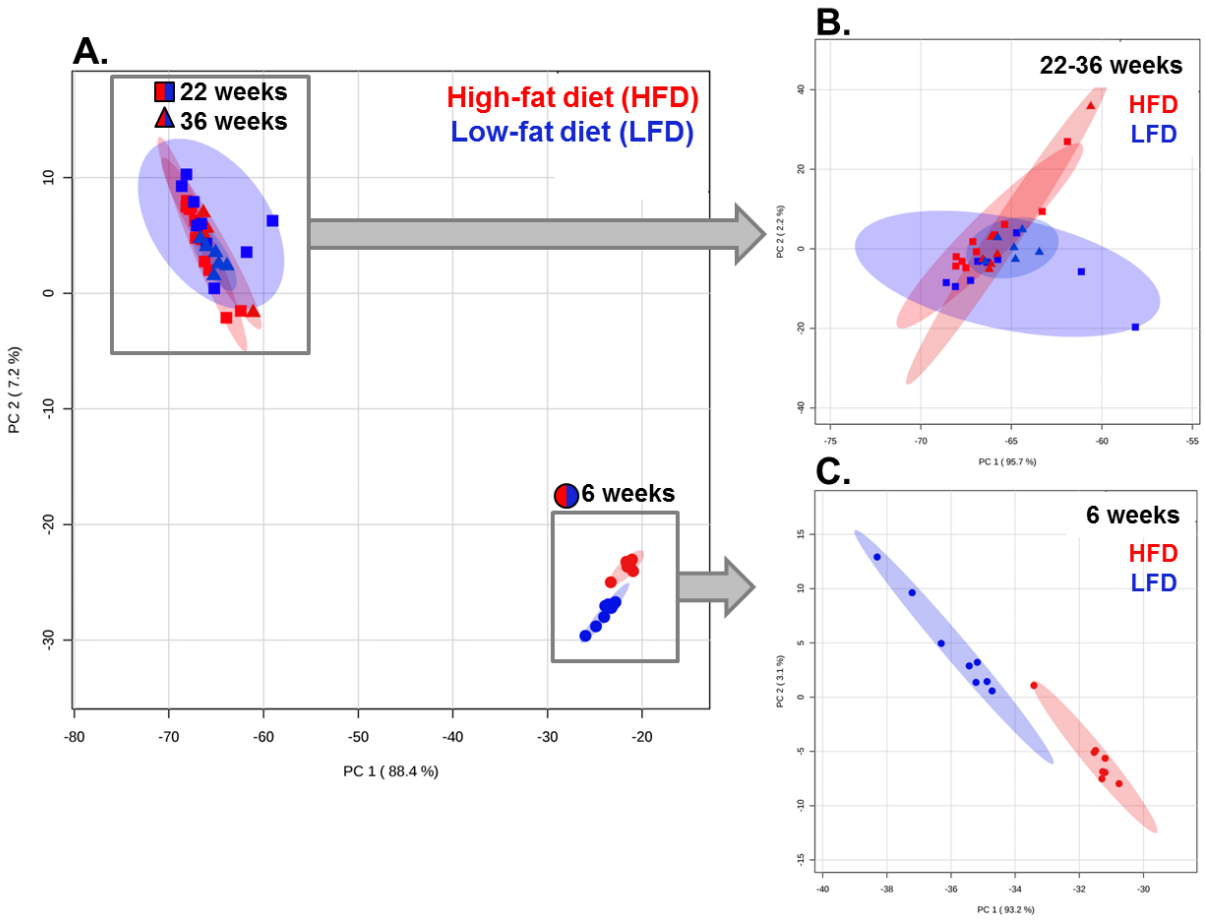

Figure 3.1. PCA scores plots of blood lipid profiles in positive ion mode. PCA scores plots comparing high-fat diet (HFD) and low-fat diet (LFD) consumption. Scores plots were generated based on mass spectrometric data acquired in the positive ion mode with comparisons of HFD and LFD for **(A)** 6, 22 or 36 weeks, **(B)** 22 and 36 weeks, and **(C)** 6 weeks only. 95.6%, 97.9%, and 96.3% of the total variance was explained by PC1 and PC2 in **(A-C)**, respectively. The ovals in the scores plots indicate a 95% confidence interval. Each data point represents an individual animal and a total of 6-8 animals/diet/time point were assessed.

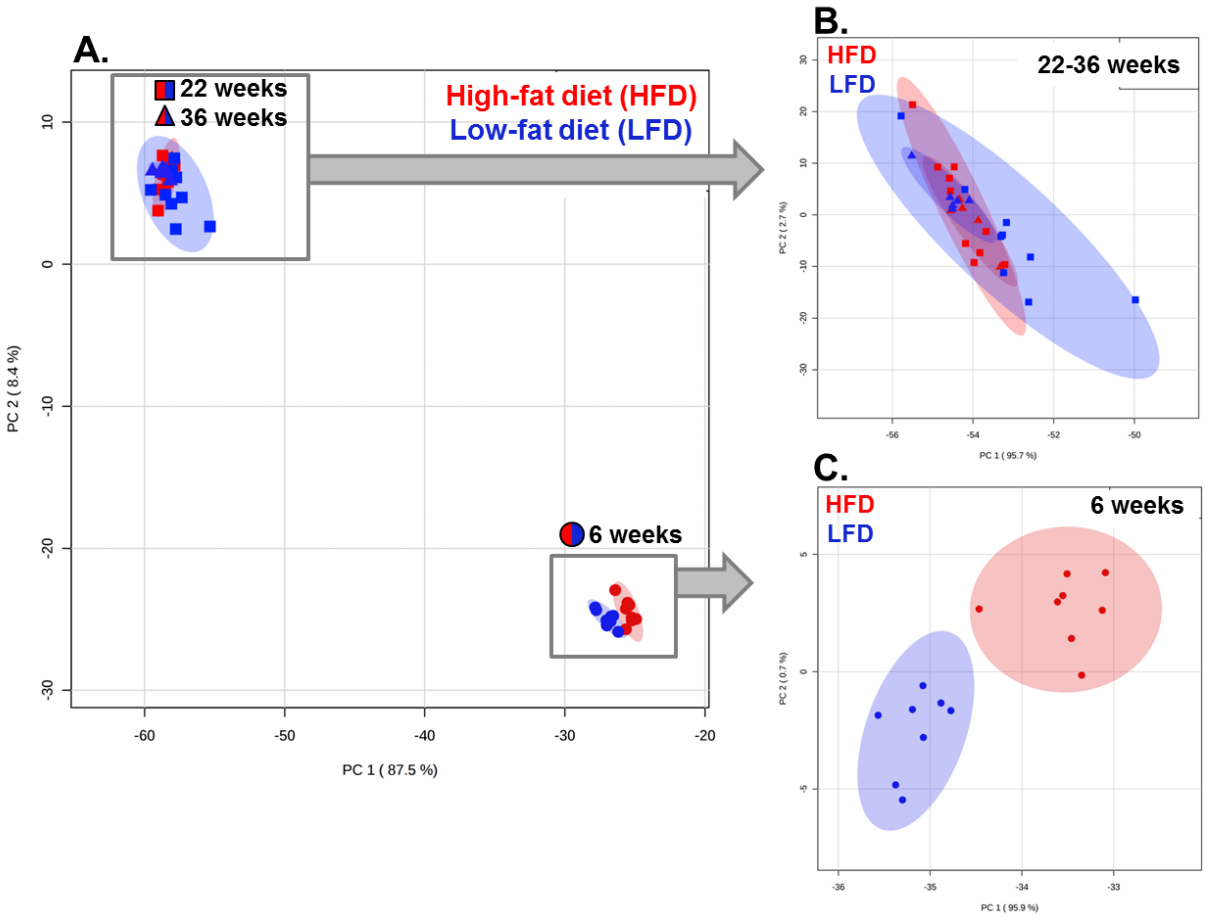

Figure 3.2. PCA scores plots of blood lipid profiles in negative ion mode. PCA scores plots comparing high-fat diet (HFD) and low-fat diet (LFD) consumption. Scores plots were generated based on mass spectrometric data acquired in the negative ion mode with comparisons of HFD and LFD for **(A)** 6, 22 or 36 weeks, **(B)** 22 and 36 weeks, and **(C)** 6 weeks only. 95.9%, 98.4%, and 96.6% of the total variance was explained by PC1 and PC2 in (**A-C**), respectively. The ovals in the scores plots indicate a 95% confidence interval. Each data point represents an individual animal and a total of 6-8 animals/diet/time point were assessed.

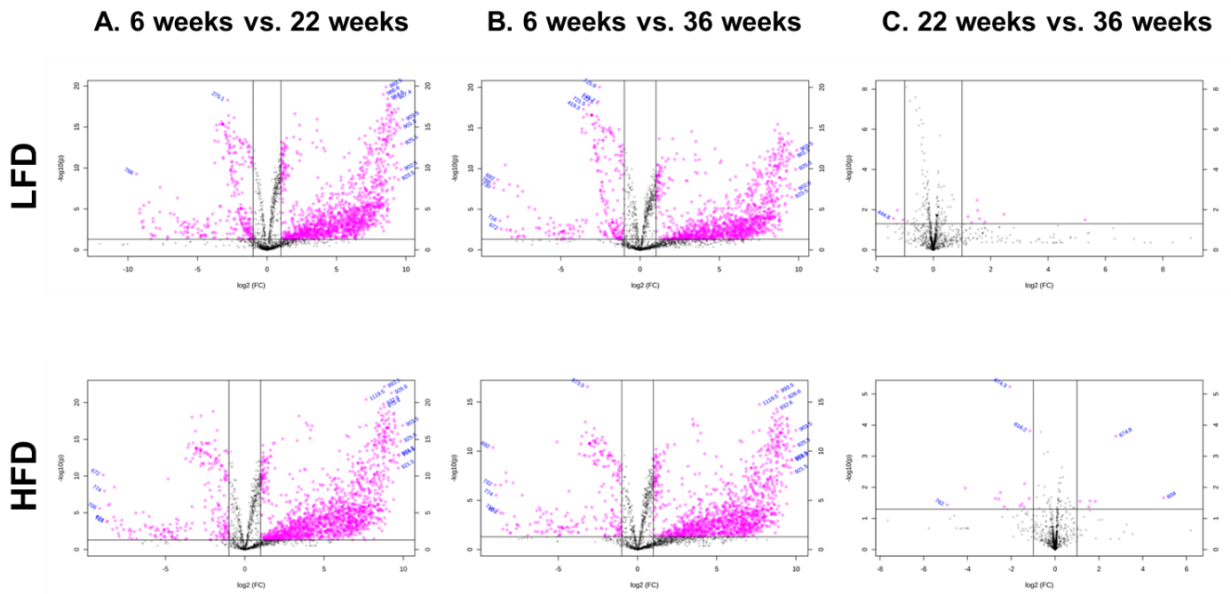

Figure 3.3. Volcano plot analysis of age-related effects in blood, positive ion mode. Positive ion mode volcano plot analysis of *m/z* values significantly altered for pairwise comparisons of age groups within dietary treatment groups: **(A)** 6 weeks vs. 22 weeks, **(B)** 6 weeks vs. 36 weeks, **(C)** 22 weeks vs. 36 weeks within HFD *(top row)* and LFD *(bottom row)*. All features presented are considered significant based on a fold change (FC) threshold = 2.00 and t-tests where *p*-value ≤ 0.05.

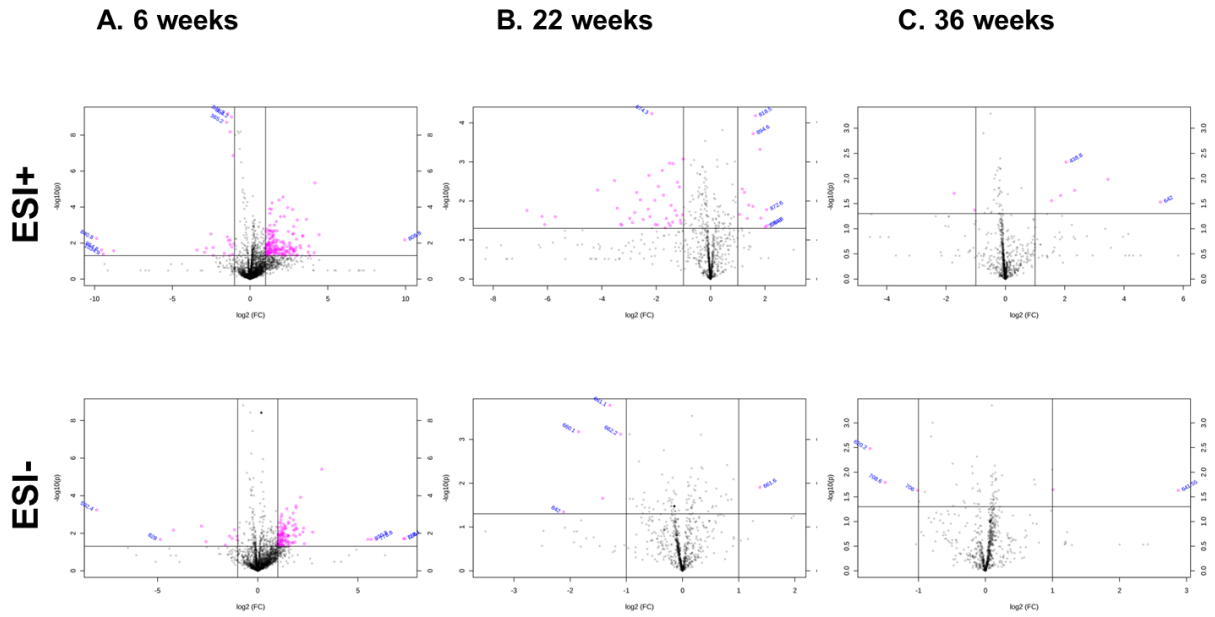

Figure 3.4. Volcano plot analysis of dietary effects in blood. Volcano plot analysis of *m/z* values significantly altered for pairwise comparisons of treatment with HFD vs LFD: **(A)** 6 weeks, **(B)** 22 weeks, **(C)** 36 weeks within positive ion mode *(top row)* and negative ion mode *(bottom row)*. All features presented are considered significant based on a fold change (FC) threshold = 2.00 and t-tests where *p*-value ≤ 0.05.

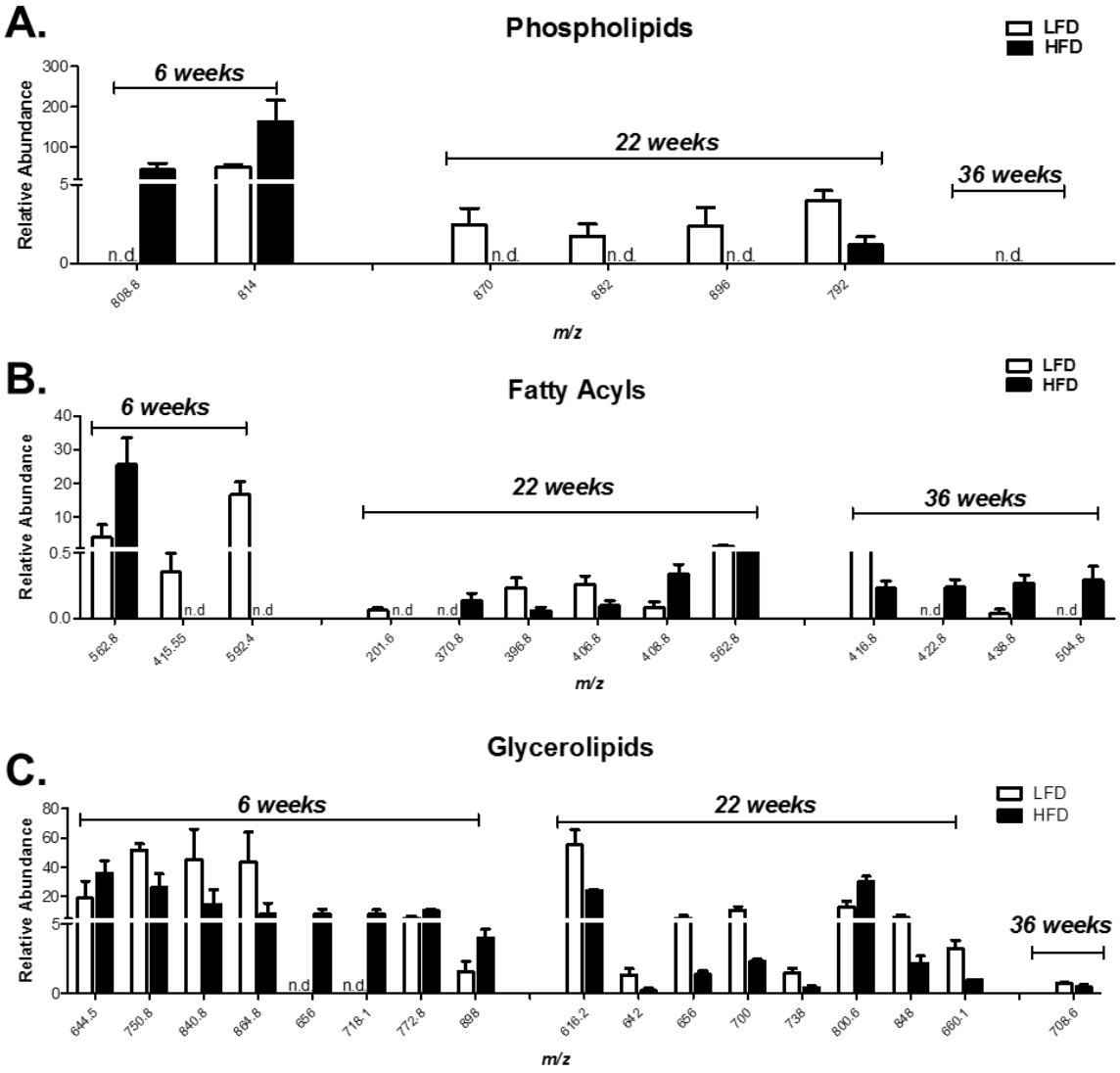

Figure 3.5. Features altered based on age- and diet-related effects in blood. Relative abundance of significant lipidomic features altered based on age and diet-related effects in blood of mice fed a high-fat diet (HFD) or low-fat diet (LFD) for a duration of 6, 22, and 36 weeks. Differential expression of features identified as **(A)** phospholipids, **(B)** fatty acyls, and **(C)** glycerolipids (see ***Table S3.2***) presented as the mean ± SEM of 6-8 animals per group (n=6–8). All features presented are considered significant based on ANOVA analysis (p-value ≤ 0.05, two-factor repeated measures with Bonferroni *post hoc* test). n.d. indicates not detected.

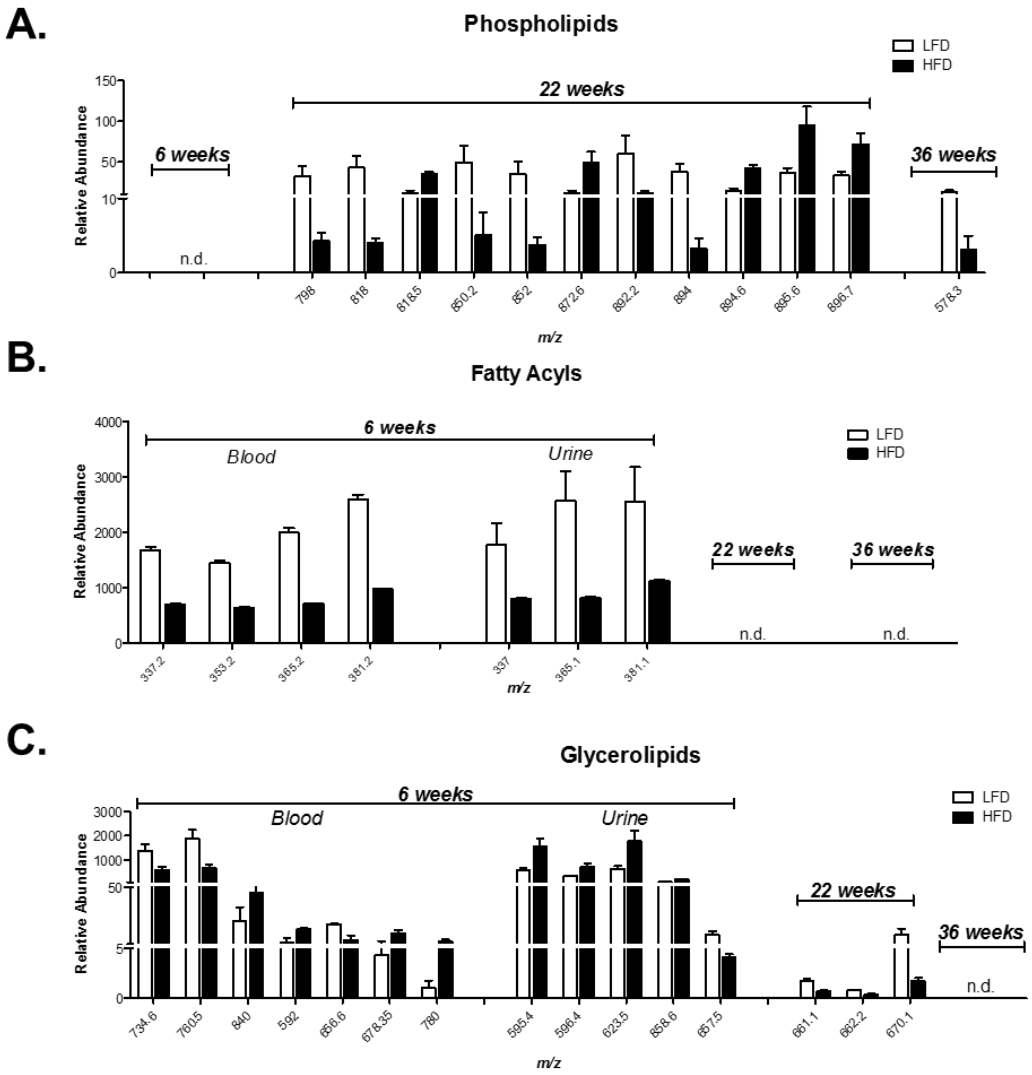

Figure 3.6. Features altered in blood and urine following dietary treatment for 6-36 weeks. Relative abundance of significant lipidomic features altered in blood and urine of mice fed a high-fat diet (HFD) or low-fat diet (LFD) for a duration of 6, 22, and 36 weeks. Differential expression of features identified as **(A)** phospholipids, **(B)** fatty acyls, and **(C)** glycerolipids (see ***Table S3.1***), presented as the mean ± SEM of 6-8 animals per group (*n*=6–8). All features presented are considered significant based on ANOVA analysis (*p*-value ≤ 0.05, two-factor repeated-measures with Bonferroni *post hoc* test). n.d. indicates not detected.

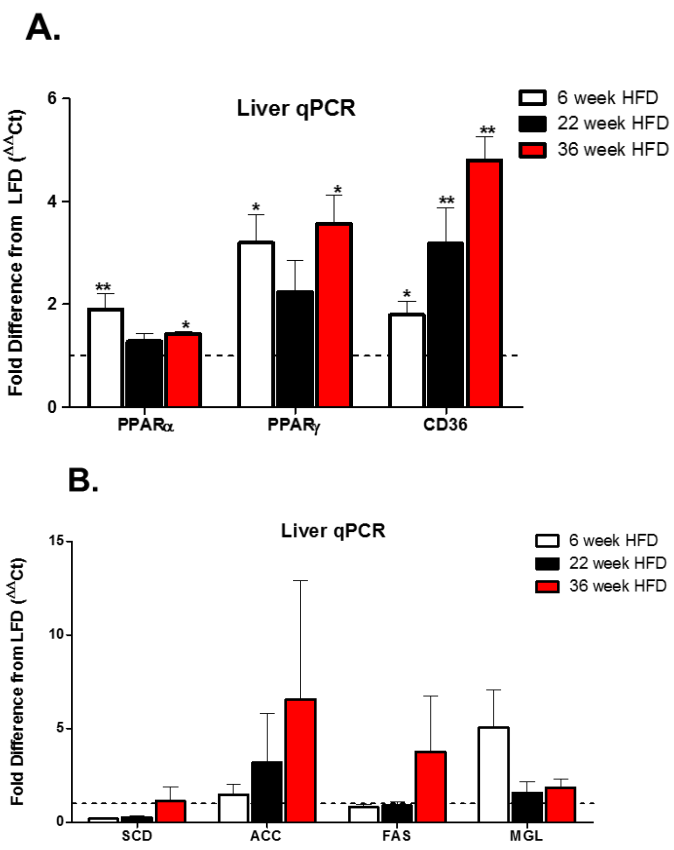

Figure 3.7. Effect of 6, 22 or 36 weeks of high-fat diet (HFD) consumption on liver mRNA levels of PPARα, PPARγ, and CD36. Effect of 6, 22 or 36 weeks of high-fat diet (HFD) consumption by female C57BL/6 mice on liver mRNA levels of: **(10A)** peroxisome proliferator-activated receptor alpha (PPARα), peroxisome proliferator-activated receptor gamma (PPARγ), and hepatic fatty acid transporter (CD36); **(10B)** stearoyl-CoA desaturase (SCD), acetyl-CoA carboxylase (ACC), fatty acid synthase (FAS), and monoacylglycerol lipase (MGL). The house keeping gene (HKG) 18S was used to normalize the mRNA data, which are presented as fold change relative to respective low-fat diet (LFD) group at each time point. Graphical representations are indicative of 6-8 animals per group (n = 6–8) and are expressed as mean ± SEM (*$p \leq 0.05$ compared across feeding durations).

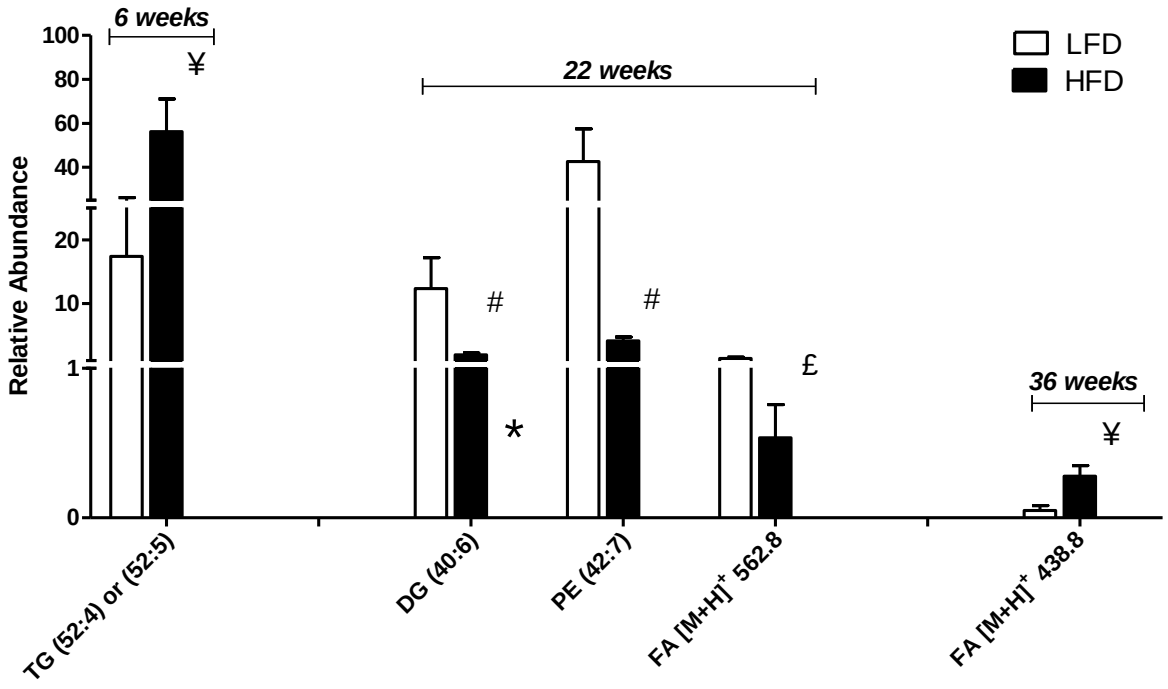

Figure 3.7. Differential expression of features correlating to markers of liver homeostasis. Differential expression of features correlating to mRNA expression of liver homeostasis markers with $R^2 \geq 0.6$ ($^{£}$PPARα, $^{¥}$PPARγ, $^{\#}$CD36, see **Table 3.1A**). Graphical representations are indicative of 6-8 animals per group (*n* = 6–8) and are expressed as mean ± SEM ($p \leq 0.05$ compared within each time point). Lipid species indicated by only their *m/z* value were unable to be fully characterized by subsequent MS/MS analysis.

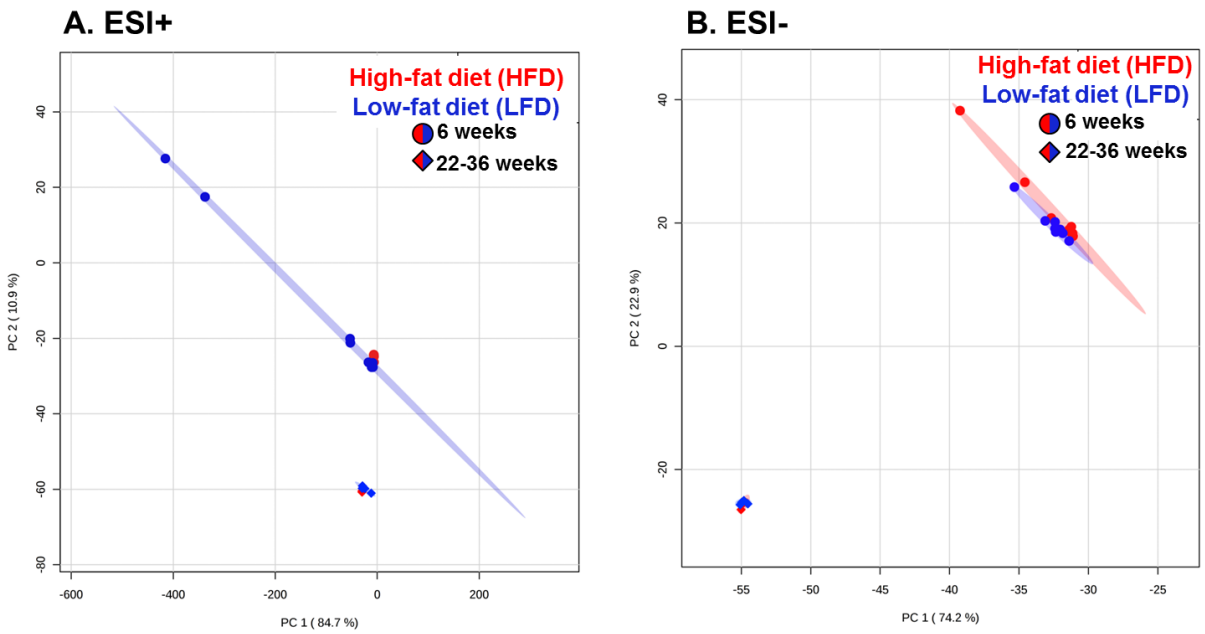

Figure S3.1. PCA scores plots of urine. PCA scores plots comparing high-fat diet (HFD) and low-fat diet (LFD) consumption. Scores plots were generated based on mass spectrometric data acquired in the **(A)** positive and **(B)** negative ion mode with comparisons of HFD and LFD for 6, 22 or 36 weeks. 95.6% and 97.1% of the total variance explained by PC1 and PC2 in (A) and (B), respectively. The ovals in the scores plots indicate a 95% confidence interval. Each data point represents an individual animal and a total of 6-8 animals/diet/time point were assessed.

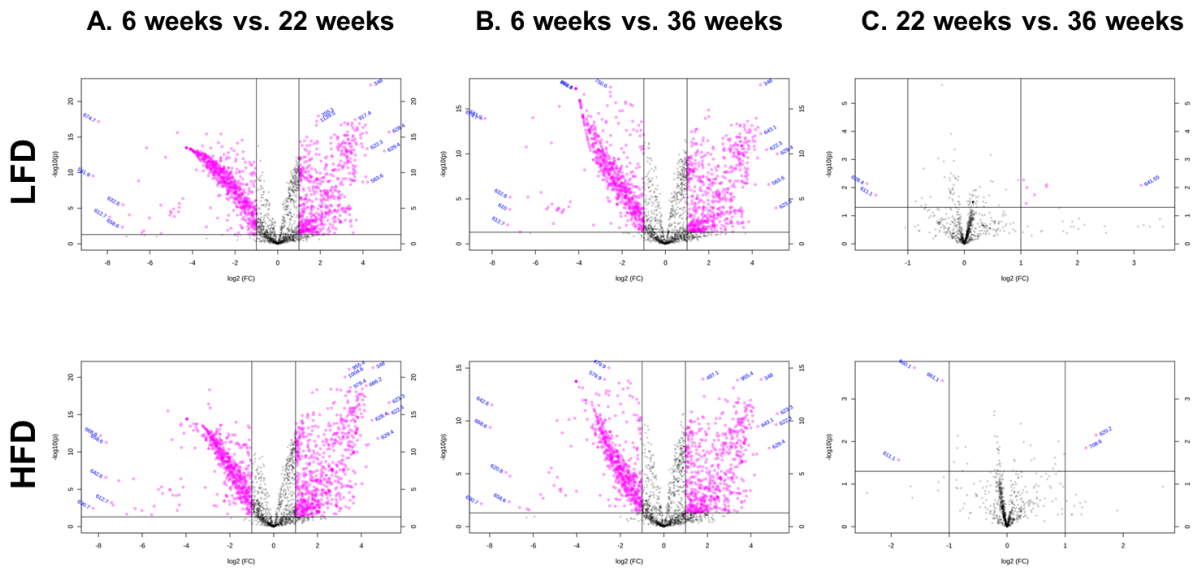

Figure S3.2. Volcano plot analysis of age-related effects in blood, negative ion mode. Negative ion mode volcano plot analysis of *m/z* values significantly altered for pairwise comparisons of age groups within dietary treatment groups: **(A)** 6 weeks vs. 22 weeks, **(B)** 6 weeks vs. 36 weeks, **(C)** 22 weeks vs. 36 weeks within HFD *(top row)* and LFD *(bottom row)*. All features presented are considered significant based on a fold change (FC) threshold = 2.00 and t-tests where p-value≤0.05.

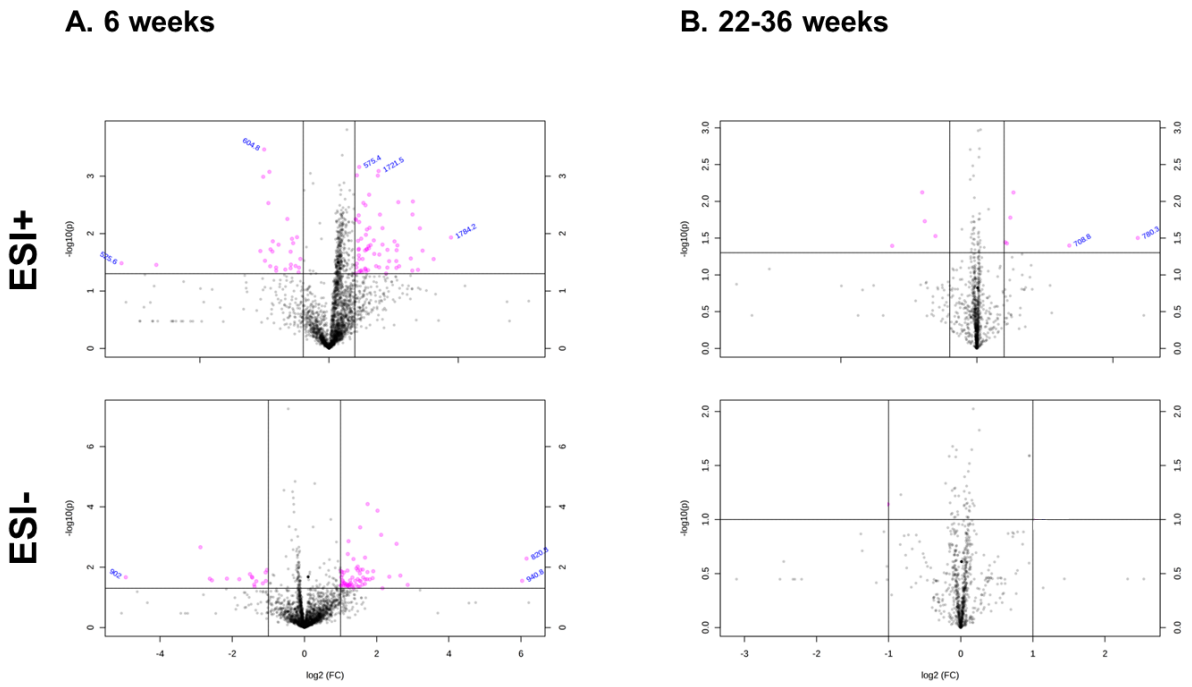

Figure S3.3. Volcano plot analysis of dietary effects in urine. Volcano plot analysis of *m/*z values significantly altered for pairwise comparisons of treatment with HFD vs LFD: **(A)** 6 weeks and **(B)** 22-36 weeks within positive ion mode *(top row)* and negative ion mode *(bottom row)*. All features presented are considered significant based on a fold change (FC) threshold = 2.00 and t-tests where *p*-value≤0.05.

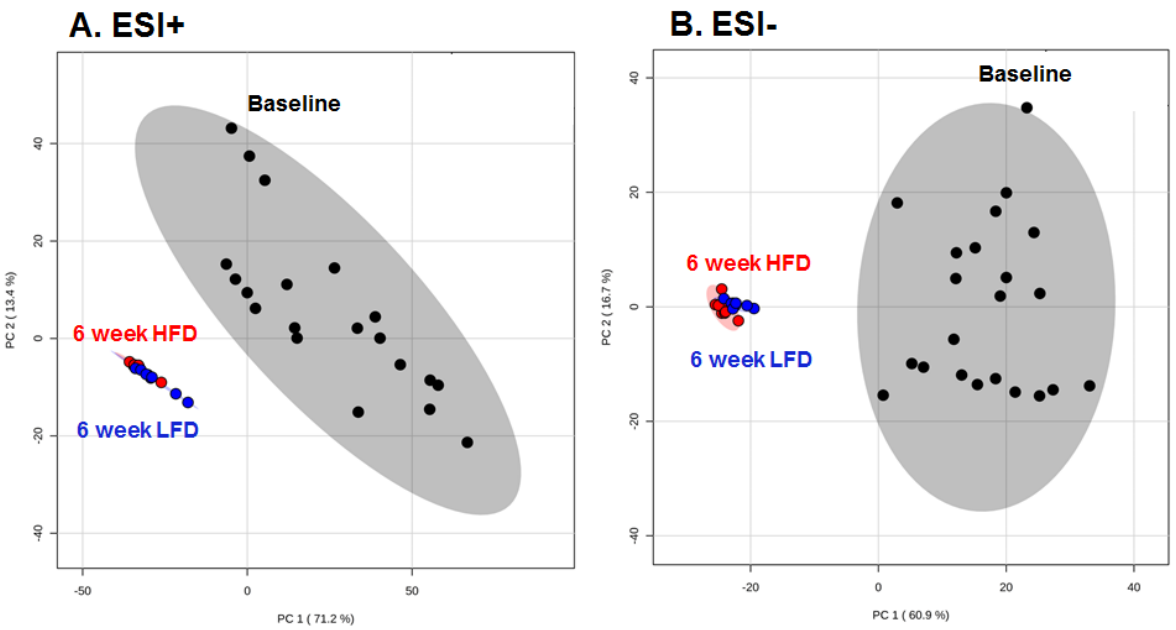

Figure S3.4. PCA scores plots of baseline blood lipidome. Scores plots were generated based on mass spectrometric data acquired in the **(A)** positive and **(B)** negative ion mode with comparisons of baseline blood lipid profile to 6-week HFD/LFD consumption. 84.6% and 77.6% of the total variance was explained by PC1 and PC2 in **(A)** and **(B)**, respectively. The ovals in the scores plots indicate a 95% confidence interval. Each data point represents an individual animal and a minimum of 6-8 animals/group were assessed.

Table 3.1. Correlation of lipid alterations with metabolic and liver regulation.

A. Correlation of differential lipid expression to markers of liver homeostasis

m/z	I.D.	R^2	Weeks on HFD	Liver mRNA Expression
$[M+H]^+$ 840	TG (52:4 or 52:5)	0.613	6 weeks	PPARγ
$[M+H]^+$ 670.1	DG (40:6)	0.743	22 weeks	CD36
$[M+H]^+$ 818	PE (42:7)	0.679	22 weeks	CD36
$[M+H]^+$ 562.8	*FA	0.688	22 weeks	PPARα
$[M+H]^+$ 438.8	*FA	0.754	36 weeks	PPARγ

B. Correlation of differential lipid expression identified at 6 weeks to GTT/IST

m/z	I.D.	R^2	Correlation	Diet	GTT/IST
$[M-H]^-$ 592	**DG (34:3)**	**0.606**	**Positive**	**HFD**	**Glucose**
		0.895	**Negative**	**LFD**	**Glucose**
		0.639	**Positive**	**LFD**	**Insulin**
$[M+H]^+$ 814	PC (38:2)	0.801	Positive	HFD	Insulin
$[M-H]^-$ 898	*GL	0.806	Negative	HFD	Insulin
$[M+H]^+$ 808.8	PC (38:5)	0.615	Positive	HFD	Glucose
$[M+H]^+$ 370.8	*FA	0.733	Negative	HFD	Glucose
$[M+H]^+$ 738	*GL	0.780	Negative	LFD	Glucose
		0.928	Positive	LFD	Insulin
$[M+H]^+$ 656	DG (40:6 or 40:5)	0.796	Negative	LFD	Glucose
		0.626	Positive	LFD	Insulin
$[M+H]^+$ 848	TG (52:8)	0.700	Negative	LFD	Glucose

$[M+H]^+$ 896	PC (44:3)	0.749	Negative	LFD	Glucose
		0.912	Positive	LFD	Insulin
$[M-H]^-$ 415.55	*FA	0.621	Negative	LFD	Glucose
$[M+H]^+$ 416.8	FA (28:4)	0.524	Negative	LFD	Insulin

C. Correlation of features identified at 6 weeks to 2-AG

m/z	I.D.	R^2	Duration of Consumption	Diet
$[M+H]^+$ 734.6	*GL	0.735	6 weeks	HFD
$[M+H]^+$ 760.5	*GL	0.765	6 weeks	HFD
$[M+H]^+$ 353.2	*FA	0.783	6 weeks	HFD

Highlighted rows indicate features altered based on age and diet-related effects
Asterisk (*) indicates tentative ID due to unconfirmed fragmentation
Bold text indicates features identified in urine

Table S3.1. Significant lipidomic features associated with dietary treatment.

Treatment Duration	Tissue	*m/z*	Ionization Mode	MS/MS Fragments	Lipid Class	Species
6 weeks	Blood	337.2	ESI+	304, 305, 319.1, 344.9	Fatty Acyl	$[M+H]^+$
	Blood	353.2	ESI+	112.9, 266.9, 294.9, 321, 335.2, 358.8	Fatty Acyl	$[M+H]^+$
	Blood	365.2	ESI+	218.9, 262, 307, 346.1, 347.1	Fatty Acyl	$[M+H]^+$
	Blood	381.2	ESI+	323, 363.1	Fatty Acyl	$[M+H]^+$
	Blood	592	ESI-	325.1, 326.1	Glycerolipid	$[M-H]^-$
	Blood	656.6	ESI-	---	*Glycerolipid	$[M-H]^-$
	Blood	678.35	ESI-	---	*Glycerolipid	$[M-H]^-$
	Blood	734.6	ESI+	227, 255, 256.1, 283, 453.2, 716.8, 725.3	Glycerolipid	$[M+H]^+$
	Blood	760.5	ESI+	268.8, 282.9, 298.9, 310.1, 324.8, 344.8, 358.9, 370.9, 416.9, 429.0, 505.0, 742.4, 751.8	Glycerolipid	$[M+H]^+$
	Blood	780	ESI-	---	*Glycerolipid	$[M-H]^-$
	Blood	840	ESI+	255, 283.1, 284.1, 552.4, 565.5, 566.5, 639.3, 821.5, 823, 830.4	Glycerolipid	$[M+H]^+$
	Urine	337	ESI+	278.9, 304.0, 305.0, 319.1	Fatty Acyl	$[M+H]^+$
	Urine	365.1	ESI+	307.0, 333.0, 347.1	Fatty Acyl	$[M+H]^+$
	Urine	381.1	ESI+	132.8, 174.8, 252.1, 287.2, 312.2, 320.2, 321.2, 349.1, 362.1, 363.1	Fatty Acyl	$[M+H]^+$
	Urine	595.4	ESI+	310.2, 576.5	Glycerolipid	$[M+H]^+$
	Urine	596.4	ESI+	281.2, 282.1, 309.2, 310.2, 311.2, 312.2, 327.1, 328.2, 537.5, 538.4, 577.4, 578.3, 579.4	Glycerolipid	$[M+H]^+$
	Urine	623.5	ESI+	281.1, 309.1, 310.2, 338.2, 565.5, 605.3	Glycerolipid	$[M+H]^+$
	Urine	657.5	ESI-	455.2	Glycerolipid	$[M-H]^-$
	Urine	858.6	ESI+	281, 481.4, 518, 783.4, 799.5, 826.1, 836, 839.5	Glycerolipid	$[M+H]^+$
22 weeks	Blood	661.1	ESI-	403.1, 571	Glycerolipid	$[M-H]^-$
	Blood	662.2	ESI-	441.1	Glycerolipid	$[M-H]^-$
	Blood	670.1	ESI+	283.1, 311.1,	Glycerolipid	$[M+H]^+$

				324.9, 354.9, 355.9, 358.9, 360.9, 369.2, 431, 445, 446, 542.4, 651.5		
	Blood	798	ESI+	339.3, 523.4, 613.4, 655.4, 656.4, 737.4, 738.3, 778.5, 780.5, 798.4	Phospholipid	$[M+H]^+$
	Blood	818	ESI+	678.3, 716.4, 718.4, 739.4, 758.5, 759.5, 760.5, 761.5, 796.6, 797.5, 798.5, 799.5, 800.5, 801.5	Phospholipid	$[M+H]^+$
	Blood	818.5	ESI+	355.9, 676.4, 716.4, 739.4, 758.5, 760.5, 782.5, 798.5, 800.5	Phospholipid	$[M+H]^+$
	Blood	850.2	ESI+	268.8, 298.9, 354.9, 371.0, 429.0, 445.0, 503.0, 549.4, 575.4, 603.4, 666.5, 781.4, 789.5, 813.5, 817.4, 831.6	Phospholipid	$[M+H]^+$
	Blood	852	ESI+	268.8, 298.9, 354.9, 371.0, 429.0, 446.0, 503.9, 551.4, 577.4, 668.4, 792.4, 816.1, 833.7	Phospholipid	$[M+H]^+$
22 weeks	Blood	872.6	ESI+	277.0, 313.1, 339.1, 506.3, 575.4, 589.4, 599.4, 615.4, 687.4, 812.5, 836.5, 853.5	Phospholipid	$[M+H]^+$
	Blood	892.2	ESI+	354.9, 429.0, 506.3, 524.3, 577.5, 591.4, 617.5, 836.5, 854.4, 872.5	Phospholipid	$[M+H]^+$
	Blood	894	ESI+	710.4, 808.5, 835.4, 874.5	Phospholipid	$[M+H]^+$
	Blood	895.6	ESI+	597.4, 711.4, 835.4, 836.5, 876.5, 877.6	Phospholipid	$[M+H]^+$
	Blood	896.7	ESI+	319.1, 593.5, 597.5, 599.4, 601.4, 613.4, 639.4, 711.4, 712.4, 713.4,	Phospholipid	$[M+H]^+$

				809.5, 835.4, 836.4, 837.5, 877.5, 878.5, 879.7, 880.6		
36 weeks	Blood	578.3	ESI+	238.8, 268.8, 298.8, 354.9, 356, 414.9, 415.9, 437.1, 559.3	Phospholipid	$[M+H]^+$

Asterisk (*) indicates tentative ID due to unconfirmed fragmentation

Table S3.2. Significant lipidomic features associated with dietary treatment and age in blood.

Treatment Duration	*m/z*	Ionization Mode	MS/MS Fragments	Lipid Class	Species
6 weeks	415.55	ESI-	---	Fatty Acyl*	$[M-H]^-$
	562.8	ESI+	227, 281.1, 283.1, 307.1, 309.1, 501.2, 544.6, 545.2, 553.7	Fatty Acyl	$[M+H]^+$
	592.4	ESI-	282, 325.1, 326.1	Fatty Acyl	$[M-H]^-$
	644.5	ESI+	226.9, 255.1, 311.2, 341.2, 342.2, 608.5, 626.3	Glycerolipid	$[M+H]^+$
	656	ESI-	---	*Glycerolipid	$[M-H]^-$
	718.1	ESI-	---	*Glycerolipid	$[M-H]^-$
	750.8	ESI+	226.9, 255.1, 283.1, 732.6, 733.3, 741.3, 741.8	Glycerolipid	$[M+H]^+$
	772.8	ESI-	---	*Glycerolipid	$[M-H]^-$
	808.8	ESI+	227, 255.1, 283.1, 309.1, 311.2, 509.3, 535.4, 537.4, 549.4, 551.3, 625.4, 715.9, 790.8, 791.4, 799.4	Phospholipid	$[M+H]^+$
	814	ESI+	227, 255, 283.1, 309.2, 531.5, 630.4, 795.5, 796.4, 804.3, 805	Phospholipid	$[M+H]^+$
	840.8	ESI+	283, 457.2, 538.4, 551.4, 552.4, 565.4, 566.4, 639.3, 823.1	Glycerolipid	$[M+H]^+$
	864.8	ESI+	255, 283, 354.9, 635.2, 636.2, 870.5	Glycerolipid	$[M+H]^+$
	898	ESI-	---	*Glycerolipid	$[M-H]^-$
22 weeks	201.6	ESI+	144.9, 158.9, 172.9	Fatty Acyl	$[M+H]^+$
	370.8	ESI+		Fatty Acyl	$[M+H]^+$
	396.8	ESI+	183.8, 268.8, 331, 335.1, 375.1, 376.2, 377.2, 378.2, 393.1	Fatty Acyl	$[M+H]^+$
	406.8	ESI+	150.8, 183.8, 284.1, 329.1, 342.9, 345.1, 346.1, 347.1, 349.1, 367.2, 369.3, 373.1, 385.2, 386.1, 387.1, 388.1, 389.1, 403	Fatty Acyl	$[M+H]^+$
	408.8	ESI+	183.8, 238.9, 257, 347.1, 349, 350.1, 363, 367, 375, 387, 388.2, 389.2, 391.1, 405.1	Fatty Acyl	$[M+H]^+$
	562.8	ESI+	227, 281.1, 283.1, 307.1, 309.1, 501.2, 544.6, 545.2, 553.7	Fatty Acyl	$[M+H]^+$
	616.2	ESI+	270.8, 271.8, 272.7, 355.9, 356.9, 357.9, 358.9, 359.9, 557.1, 558, 598.1	Glycerolipid	$[M+H]^+$
	642	ESI+	355, 624.4	Glycerolipid	$[M+H]^+$
	656	ESI+	311, 517.3, 607	Glycerolipid	$[M+H]^+$
	660.1	ESI-		Glycerolipid	$[M-H]^-$

	700	ESI+	228.8, 238.8, 294.9, 295.9, 298.9, 369, 370, 371, 561.3	Glycerolipid	$[M+H]^+$
	738	ESI+	---	*Glycerolipid	$[M+H]^+$
	792	ESI+	298.9, 606.4, 650.4, 690.4, 734.5, 772.5	Phospholipid	$[M+H]^+$
	800.6	ESI+	740.4, 781.5, 782.5, 784.5	Glycerolipid	$[M+H]^+$
	848	ESI+	268.8, 298.9, 354.9, 358.8, 369.1, 429, 478.2, 496.3, 547.4, 549.4, 551.4, 573.5, 575.4, 577.5, 590.4, 601.3, 787.4, 788.5, 789.5, 792.6, 800.5, 810.5, 811.5, 815.1, 828.5, 829.6	Glycerolipid	$[M+H]^+$
	870	ESI+	577.5, 686.4, 708.5, 809.4, 810.4, 850.5, 870.4	Phospholipid	$[M+H]^+$
	882	ESI+	579.5, 580.5, 581.6, 599.4, 607.5, 608.4, 697.3, 698.5, 821.5, 822.4	Phospholipid	$[M+H]^+$
	896	ESI+	593.4, 597.4, 599.4, 615.3, 711.3, 712.4, 713.5, 835.4, 844, 877.6, 879.6	Phospholipid	$[M+H]^+$
36 weeks	416.8	ESI+	283, 297.1, 344.8, 345.8, 346.8, 358.9, 359.9, 360.9, 398.1, 399.1, 399.9	Fatty Acyl	$[M+H]^+$
	422.8	ESI+	---	*Fatty Acyl	$[M+H]^+$
	438.8	ESI+	182.8, 227, 238.9,381.1 ,420.2, 421.2, 422.2	Fatty Acyl	$[M+H]^+$
	504.8	ESI+	239.9, 282.8, 283.8, 298.9, 299.9, 300.9, 345.8, 358.8, 359.9, 400.9, 414.9, 415.9, 416.9, 443.2, 487.2, 488.9	Fatty Acyl	$[M+H]^+$
	642	ESI+	355, 624.4	Glycerolipid	$[M+H]^+$
	708.6	ESI-	---	*Glycerolipid	$[M-H]^-$

Asterisk (*) indicates tentative ID due to unconfirmed fragmentation

Table S3.3. Correlation of differential lipid expression identified at 22-36 weeks to glucose tolerance and insulin sensitivity.

m/z	I.D.	R^2	Correlation	Duration of Consumption	Diet	GTT/ IST
$[M+H]^+$ 798	PC (38:3 or 38:2)	0.710	Positive	22 weeks	HFD	Insulin
$[M+H]^+$ 818.5	PE (42:7)	0.665	Positive	22 weeks	LFD	Glucose
$[M+H]^+$ 814	PC (38:2)	0.612	Positive	22 weeks	LFD	Glucose
$[M+H]^+$ 656	DG (40:6 or 40:5)	0.745	Positive	36 weeks	LFD	Glucose
$[M+H]^+$ 848	TG (52:8)	0.566	Positive	22 weeks	HFD	Glucose
$[M-H]^-$ 415.55	FA*	0.594	Positive	36 weeks	LFD	Glucose
$[M+H]^+$ 416.8	FA (28:4)	0.605	Positive	36 weeks	HFD	Insulin
$[M+H]^+$ 504.8	FA*	0.861	Positive	36 weeks	HFD	Glucose
		0.572	Positive	36 weeks	HFD	Insulin

Highlighted rows indicate features altered based on age and diet-related effects

Asterisk (*) indicates tentative ID due to unconfirmed fragmentation

Table S3.4. Dietary fatty acid profile.

	High-fat Diet (g) (D12492, Research Diets, Inc.)	Low-fat Diet (g) (D12450J, Research Diets, Inc.)
Lard	245	20
Soybean Oil	25	25
Total (g)	**270**	**45**
C10, Capric	0.148	0.012
C12, Lauric	0.225	0.018
C14, Myristic	2.83	0.25
C15	0.187	0.015
C16, Palmitic	49.9	6.45
C16:1, Palmitoleic	3.4	0.3
C17	0.928	0.087
C18, Stearic	26.9	3.08
C18:1, Oleic	86.3	12.32
C18:2, Linoleic	72.7	17.82
C18:3, Linolenic	5.1	2.12
C20, Arachidic	0.5	0.12
C20:1	1.58	0.19
C20:2	2.0	0.16
C20:3, n6	0.3	0.03
C20:4, Arachidonic	0.69	0.06
C22, Behenic	0.1	0.1
C22:5, Docosapentaenoic	0.209	0.017
Total (g)	**254.0**	**43.1**
Saturated (%)	*32.2*	*23.5*
Monounsaturated (%)	*35.9*	*29.7*
Polyunsaturated (%)	*31.9*	*46.8*

4. Discussion

The association between increased high-fat consumption and excess adiposity poses a major global health problem that heightens the risk of metabolic disorders, diabetes, heart disease, fatty liver, and some forms of cancer [39]. Growing evidence implicating a role for impaired lipid metabolism, coupled with the advent of bioinformatics tools has prompted efforts in characterizing the obese lipidome [40-42]. While these studies have highlighted alterations in the plasma and/or serum lipidome, there have been few studies examining the effects of age on the lipidome and/or the interaction between age and obesity. Further, the number of studies that address diet-induced obesity within female models is quite limited, although an increased linear trend of female obesity among US women within the last decade demonstrates the significant need [3, 43, 44]. Here, we used shotgun lipidomics to assess the effects of dietary fat consumption, age, and their interaction at the level of the blood lipidome. We correlated changes in the blood lipidome to changes in metabolic regulation, endocannabinoid levels, and plasma esterase activity.

One of the most interesting findings of this study is that the effect of age superseded the effect of HFD with regard to alterations in the blood lipidome. These data emphasize the need to characterize and stratify lipidomic alterations not only to diet, but also to age. The accentuated effect of age on the lipidome between 12-week-old (6-weeks on the diet) vs. 28-week-old (22 weeks on the diet) and 42-week-old (36 weeks on the diet) mice indicated distinct shifts in lipid composition and/or regulation, an interesting note since all ages fall within the mature adult phase of C57BL/6 mice. Although multivariate analysis indicated a slight difference between 28- and 42-week-

old animals, the separation was not as robust. With regard to dietary treatment, younger animals presented striking lipidomic responses to HFD-consumption while older animals had a more tapered shift, possibly a result of time-dependent homeostatic mechanisms in response from long-term feeding. In this regard, as we reported recently, it is interesting to note that in terms of insulin sensitivity, but not glucose tolerance, age appears to be a major driver of decreased insulin sensitivity to the point that the effects of prolonged HFD feeding are overpowered by the effects of age [17].

Given the limitations of the shotgun approach along with the sheer number of features identified in this study, we report general lipidomic changes in terms of lipid class with alterations falling into three classes: glycerolipids (GL), fatty acyls (FA), and phospholipids (PL). MS/MS analysis was employed to verify these lipid species (***Table S3.1***). Features changing at only a few time points showed a class-specific trend in terms of differential lipid expression; however, most changes indicated species-specific alterations.

A few studies have demonstrated alterations in lipid classes within rodent obesity where the majority of reported changes encompass ceramides, cholesterols, triglycerides, and phospholipids. For example, changes in lipid species such as lysophosphatidylcholines have been associated with obesity, insulin resistance, and type 2 diabetes [45-47]. In agreement with some of these studies, we report elevations in PC (38:5), PC (44:3), and PC (38:3) in the blood of HFD-fed mice, also reported in Eisinger *et al*. [40]. Changes in GL and FA reported in the current study are not in line with another study [48], but it should be noted that the sex of the mice, feeding durations, and importantly, the dietary composition in [48] and our study are different. It

should also be pointed out that several studies have demonstrated that HFD typically increases the levels of TAGs and DAGs [49]. The fact that not many of these lipids were detected in our own study is most likely a limitation of the shotgun approach used.

As mentioned above, lipidomic alterations identified by shotgun analysis revolved around three major lipid classes (GL, FA, and PL), which also happen to constitute the endocannabinoid system. Quantification of both 2-AG and AEA demonstrated several correlations with specific blood lipids. AEA and 2-AG, both derivatives of arachidonic acid, are signaling lipids that mediate their action via activation of cannabinoid receptors. Further, changes in plasma levels of 2-AG and AEA after 6 and 36 weeks associated with decreases in liver 2-AG. This suggests that increased 2-AG levels in circulation are due to increased mobilization from the liver, with/without concomitant decreased 2-AG breakdown [50]. In a study by Caraceni, *et al*, 2-AG levels were reported to be higher in the hepatic veins of cirrhosis patients when compared to peripheral blood, supporting the hypothesis that the liver contributes to circulating 2-AG levels [51]. This may also suggest that the source of the increase in plasma 2-AG is non-hepatic, i.e. dietary [20].

Plasma AEA levels were most affected by the diet after 36 weeks; however, as opposed to the decreases of liver 2-AG, liver AEA was increased after 36 weeks irrespective of diet. Together, these data indicate that in female C57BL/6 mice plasma 2-AG is more sensitive to HFD-consumption. Further, similar to other endpoints in this study, the effects of HFD diet are most prominent during early (6 weeks) and late phases (36 weeks) of the feeding trial. Circulating endocannabinoids also appear to be more sensitive to non-dietary liver pathology than their liver levels. For example, in

certain conditions, i.e. hepatitis C, plasma, but not liver, 2-AG was increased [52]. On the other hand, circulating AEA was significantly higher in cirrhotic patients [51].

A novel finding is the fact that age was associated with decreased 2-AG and increased AEA in the liver. At the end of the study (36 weeks on the diet, 42-43-week-old), the mice were middle-aged and close to becoming reproductively senescent [53]. While liver-specific endocannabinoid data for female C57BL/6 mice within the context of age are lacking, it is interesting that a recent study reported decreased 2-AG, but not AEA, levels in the hippocampus of aged mice [54]. In this study, the decrease in hippocampal 2-AG was attributed to a concomitant decrease of local 2-AG synthesis and increase of its breakdown [54]. With that in mind, our data suggest that the age-dependent metabolic changes in the 2-AG pathway that operate in the brain (hippocampus) do so in the liver as well. In addition, the increase in liver AEA levels at the end of the study highlights endocannabinoid metabolite-specific effects of age. Although Osei-Hyiaman, *et al.* previously showed that liver AEA levels increase following HFD, our data indicate lower levels of hepatic AEA in HFD-fed mice [55, 56]. However, it is important to note that the dietary feeding regimen in Osei-Hyiaman, *et al.* was initiated in slightly older mice, which may play a large role given our data demonstrating the interaction of age and diet. Moreover, the findings in the above study were based on the use of a combination of male and female mice and thus, does not reflect the effects within females alone. This would not be surprising since gender-specific responses to HFD-intake have been reported in rodents, and it has even been suggested that females are more susceptible to developing the secondary effects of HFD-induced obesity [57]. It should also be mentioned that adipose distribution and

function differs across males and females, so differences are expected to exist in mediators produced by adipocytes such as endocannabinoids [57-59].

The increased circulating 2-AG levels in the female C57BL/6 mice in our study are in line with multiple studies in obese human subjects. For example, obese men, especially those with increased intra-abdominal adiposity, have increased plasma 2-AG [60]. Interestingly, direct correlation between plasma endocannabinoids, insulin resistance and dyslipidemia has been suggested [61]. Moreover, chronic cannabinoid receptor 1 (CB1) stimulation exacerbates the metabolic dysregulation caused by HFD-consumption, suggesting key role for the endogenous endocannabinoids in the process [62]. Circulating endocannabinoids might contribute to obesity by their central and/or peripheral actions [20]. The key role of CB1-specific over-activation by excessive endocannabinoids is further emphasized by the fact that global CB1-/- mice are not susceptible to HFD and liver-specific CB1-/- mice are protected from some, but not all, of the adverse effects of HFD intake [63]. Treatments aimed at reducing plasma endocannabinoids are beneficial in re-balancing the metabolic dysregulation [64] and obesity-related inflammation [65], but not for reducing the body weight in obese subjects [64]. Interestingly, and in line with our current data, circulating 2-AG levels were significantly elevated in insulin-resistant obese women [66].

Peroxisome proliferator-activated receptors (PPARs) are members of the steroid hormone receptor superfamily of nuclear transcription factors that are involved in the regulation of various genes encoding proteins involved in energy balance and lipid metabolism [35, 36]. PPARα is best known for its major role in lipid and lipoprotein metabolism while PPARγ is involved in adipogenesis and insulin sensitivity [35, 37]. It

has also been suggested that hepatic PPARγ may mediate the accumulation of fat via the regulation of genes essential for *de novo* lipogenesis, i.e. fatty acid synthase (FAS), acetyl-CoA carboxylase (ACC), and stearoyl-CoA desaturase (SCD) [67]. Further, it is possible that glycerolipid alterations can be attributed to changes in lipolysis via monoacylglycerol lipase (MGL), one of the main lipases involved in the catabolism of TG.

In our study, we also observed HFD-induced increases in liver PPARα, PPARγ, and CD36. The increases in PPARα and PPARγ were biphasic (6 and 22 weeks) and more prominent after 6 weeks of HFD feeding, indicating that the activation of the PPAR pathways are time-dependent. PPARα regulates fatty acid β-oxidation, is activated by the AEA analogue oleoylethanolamide (OEA), and pharmacological increases of OEA are beneficial to diet-induced obese mice [68]. While we have not measured OEA in our study, it is conceivable that the lack of significant increase in liver PPARα after 22 weeks of HDF feeding was due to sensitization-dependent downregulation. Liver PPARγ, which showed similar kinetics to PPARα, regulates lipid and glucose homeostasis, is elevated by a HFD [69], and approaches aimed at curbing its activation are beneficial in obesity and type 2 diabetes [70]. Together, the changes in liver PPAR levels are in line with the time-dependent metabolic dysregulation of these mice, especially the sensitivity to insulin challenge, and reflects the changes in the blood lipidome reported here [17].

CD36 was the sole lipid homeostasis/inflammation molecule whose expression was increased by HFD throughout the study. Increases in CD36 were greatest at the end (36 weeks) of the experiment. CD36 is associated with obesity, diabetes, and liver

dysfunction; hence, our findings are not surprising. Liver CD36 was previously shown to increase due to aging [71]. Thus, the marked increase in liver CD36 at the end of the feeding duration could be a sum of the effects of age and HFD on its expression or, due to increased demand for hepatic lipid uptake in the face of continued HFD-consumption. In this regard, CD36 plays a major role on hepatic fat uptake [71].

Circulating esterases are predominantly investigated for their role in the metabolism of drugs and toxicants, though they also metabolize endogenous, i.e. dietary, and exogenous lipids [72]. The early robust increase in plasma esterase that we observed in the current study might be the result of host's attempt to maintain lipid homeostasis in the face of excessive dietary fat. Over time, the increases in esterase activity were still present, but less robust. This may reflect saturation of this likely protective mechanism. In support of this hypothesis, esterase-deficient mice are not only more susceptible to pesticides that are detoxified by it, but also to diet-induced metabolic dysregulation and atherosclerosis [73]. Our data indicating an age effect, i.e. decreased plasma esterase due to age, further supports the notion that this mechanism of metabolizing excessive dietary fat is less robust in older mice.

In conclusion, we demonstrated an interaction between dietary fat consumption and aging with widespread effects on the blood lipidome in female mice. This study indicates that the effects of HFD feeding occur in an age-dependent manner with robust responses at a younger age. Further, we identified several associations between lipids and metabolic and liver regulation, providing a basis for female-specific obesity- and age-related lipid biomarkers. These findings highlight the need for additional age-

dependent tracking studies, prior to sexual maturity into advanced age, to obtain comprehensive understanding of the evolving lipidome with regard to dietary changes.

References

[1] C. Buechler, J. Wanninger, M. Neumeier, Adiponectin, a key adipokine in obesity related liver diseases, World journal of gastroenterology: WJG, 17 (2011) 2801-2811.

[2] M.-R. Taskinen, Type 2 diabetes as a lipid disorder, Current molecular medicine, 5 (2005) 297-308.

[3] K.M. Flegal, D. Kruszon-Moran, M.D. Carroll, C.D. Fryar, C.L. Ogden, Trends in Obesity Among Adults in the United States, 2005 to 2014, JAMA, 315 (2016) 2284-2291.

[4] S.A. Khan, A. Ali, S.A. Khan, S.A. Zahran, G. Damanhouri, E. Azhar, I. Qadri, Unraveling the complex relationship triad between lipids, obesity, and inflammation, Mediators of inflammation, 2014 (2014).

[5] S. Yusuf, S. Hawken, S. Ôunpuu, T. Dans, A. Avezum, F. Lanas, M. McQueen, A. Budaj, P. Pais, J. Varigos, Effect of potentially modifiable risk factors associated with myocardial infarction in 52 countries (the INTERHEART study): case-control study, The Lancet, 364 (2004) 937-952.

[6] G. Boden, G. Shulman, Free fatty acids in obesity and type 2 diabetes: defining their role in the development of insulin resistance and β-cell dysfunction, European journal of clinical investigation, 32 (2002) 14-23.

[7] O. Quehenberger, A.M. Armando, A.H. Brown, S.B. Milne, D.S. Myers, A.H. Merrill, S. Bandyopadhyay, K.N. Jones, S. Kelly, R.L. Shaner, Lipidomics reveals a remarkable diversity of lipids in human plasma, Journal of lipid research, 51 (2010) 3299-3305.

[8] J.-P. Després, I. Lemieux, J. Bergeron, P. Pibarot, P. Mathieu, E. Larose, J. Rodés-Cabau, O.F. Bertrand, P. Poirier, Abdominal obesity and the metabolic syndrome:

contribution to global cardiometabolic risk, Arteriosclerosis, thrombosis, and vascular biology, 28 (2008) 1039-1049.

[9] D. Hu, J. Hannah, R.S. Gray, K.A. Jablonski, J.A. Henderson, D.C. Robbins, E.T. Lee, T.K. Welty, B.V. Howard, Effects of obesity and body fat distribution on lipids and lipoproteins in nondiabetic American Indians: The Strong Heart Study, Obesity research, 8 (2000) 411-421.

[10] A. Golay, E. Bobbioni, The role of dietary fat in obesity, International journal of obesity and related metabolic disorders: journal of the International Association for the Study of Obesity, 21 (1997) S2-11.

[11] B.B. Kahn, J.S. Flier, Obesity and insulin resistance, The Journal of clinical investigation, 106 (2000) 473-481.

[12] G. Riccardi, R. Giacco, A. Rivellese, Dietary fat, insulin sensitivity and the metabolic syndrome, Clinical nutrition, 23 (2004) 447-456.

[13] K.F. Petersen, D. Befroy, S. Dufour, J. Dziura, C. Ariyan, D.L. Rothman, L. DiPietro, G.W. Cline, G.I. Shulman, Mitochondrial dysfunction in the elderly: possible role in insulin resistance, Science, 300 (2003) 1140-1142.

[14] R.I. Fink, O.G. Kolterman, J. Griffin, J.M. Olefsky, Mechanisms of insulin resistance in aging, Journal of Clinical Investigation, 71 (1983) 1523.

[15] R.A. DeFronzo, Glucose intolerance and aging, Diabetes care, 4 (1981) 493-501.

[16] F. Amati, J.J. Dubé, P.M. Coen, M. Stefanovic-Racic, F.G. Toledo, B.H. Goodpaster, Physical inactivity and obesity underlie the insulin resistance of aging, Diabetes care, 32 (2009) 1547-1549.

[17] S. Krishna, Z. Lin, B. Claire, J.J. Wagner, D.H. Harn, L.M. Pepples, D.M. Djani, M.T. Weber, L. Srivastava, N.M. Filipov, Time-dependent behavioral, neurochemical, and metabolic dysregulation in female C57BL/6 mice caused by chronic high-fat diet intake, Physiology & behavior, 157 (2016) 196-208.

[18] W.L. Lim, S.M. Lam, G. Shui, A. Mondal, D. Ong, X. Duan, R. Creegan, I.J. Martins, M.J. Sharman, K. Taddei, G. Verdile, M.R. Wenk, R.N. Martins, Effects of a high-fat, high-cholesterol diet on brain lipid profiles in apolipoprotein E epsilon3 and epsilon4 knock-in mice, Neurobiol Aging, 34 (2013) 2217-2224.

[19] H.J. Mok, H. Shin, J.W. Lee, G.K. Lee, C.S. Suh, K.P. Kim, H.J. Lim, Age-Associated Lipidome Changes in Metaphase II Mouse Oocytes, PLoS One, 11 (2016) e0148577.

[20] S. Engeli, Dysregulation of the endocannabinoid system in obesity, J Neuroendocrinol, 20 Suppl 1 (2008) 110-115.

[21] M. Bluher, S. Engeli, N. Kloting, J. Berndt, M. Fasshauer, S. Batkai, P. Pacher, M.R. Schon, J. Jordan, M. Stumvoll, Dysregulation of the peripheral and adipose tissue endocannabinoid system in human abdominal obesity, Diabetes, 55 (2006) 3053-3060.

[22] C. Silvestri, V. Di Marzo, The Endocannabinoid System in Energy Homeostasis and the Etiopathology of Metabolic Disorders, Cell Metabolism, 17 475-490.

[23] V. Di Marzo, The endocannabinoid system in obesity and type 2 diabetes, Diabetologia, 51 (2008) 1356.

[24] J. Rodriguez-Rivera, L. Denner, K.T. Dineley, Rosiglitazone reversal of Tg2576 cognitive deficits is independent of peripheral gluco-regulatory status, Behav Brain Res, 216 (2011) 255-261.

[25] E.G. Bligh, W.J. Dyer, A rapid method of total lipid extraction and purification, Can J Biochem Physiol, 37 (1959) 911-917.

[26] G.R. Bartlett, Phosphorus assay in column chromatography, Journal of Biological Chemistry, 234 (1959) 466-468.

[27] G.R. Kinsey, J.L. Blum, M.D. Covington, B.S. Cummings, J. McHowat, R.G. Schnellmann, Decreased iPLA2gamma expression induces lipid peroxidation, cell death, and sensitizes cells to oxidant-induced apoptosis, J Lipid Res, (2008).

[28] L. Zhang, B.L. Peterson, B.S. Cummings, The effect of inhibition of Ca2+-independent phospholipase A2 on chemotherapeutic-induced death and phospholipid profiles in renal cells, Biochem Pharmacol, 70 (2005) 1697-1706.

[29] B. Peterson, K. Stovall, P. Monian, J.L. Franklin, B.S. Cummings, Alterations in phospholipid and fatty acid lipid profiles in primary neocortical cells during oxidant-induced cell injury, Chem Biol Interact, 174 (2008) 163-176.

[30] R. Taguchi, J. Hayakawa, Y. Takeuchi, M. Ishida, Two-dimensional analysis of phospholipids by capillary liquid chromatography/electrospray ionization mass spectrometry, J Mass Spectrom, 35 (2000) 953-966.

[31] J.A. Crow, A. Borazjani, P.M. Potter, M.K. Ross, Hydrolysis of pyrethroids by human and rat tissues: examination of intestinal, liver and serum carboxylesterases, Toxicol Appl Pharmacol, 221 (2007) 1-12.

[32] C.E. Wheelock, A.M. Wheelock, R. Zhang, J.E. Stok, C. Morisseau, S.E. Le Valley, C.E. Green, B.D. Hammock, Evaluation of alpha-cyanoesters as fluorescent substrates for examining interindividual variation in general and pyrethroid-selective esterases in human liver microsomes, Anal Biochem, 315 (2003) 208-222.

[33] E.W. Morgan, B. Yan, D. Greenway, D.R. Petersen, A. Parkinson, Purification and characterization of two rat liver microsomal carboxylesterases (hydrolase A and B), Arch Biochem Biophys, 315 (1994) 495-512.

[34] Z. Lin, C.A. Dodd, N.M. Filipov, Short-term atrazine exposure causes behavioral deficits and disrupts monoaminergic systems in male C57BL/6 mice, Neurotoxicol Teratol, 39 (2013) 26-35.

[35] M. Yoon, The role of PPARα in lipid metabolism and obesity: Focusing on the effects of estrogen on PPARα actions, Pharmacological Research, 60 (2009) 151-159.

[36] S.D. Clarke, P. Thuillier, R.A. Baillie, X. Sha, Peroxisome proliferator-activated receptors: a family of lipid-activated transcription factors, The American journal of clinical nutrition, 70 (1999) 566-571.

[37] E.D. Rosen, P. Sarraf, A.E. Troy, G. Bradwin, K. Moore, D.S. Milstone, B.M. Spiegelman, R.M. Mortensen, PPAR gamma is required for the differentiation of adipose tissue in vivo and in vitro, Mol Cell, 4 (1999) 611-617.

[38] P. Tontonoz, L. Nagy, J.G.A. Alvarez, V.A. Thomazy, R.M. Evans, PPARγ Promotes Monocyte/Macrophage Differentiation and Uptake of Oxidized LDL, Cell, 93 (1998) 241-252.

[39] J.M. Friedman, Obesity: Causes and control of excess body fat, Nature, 459 (2009) 340-342.

[40] K. Eisinger, G. Liebisch, G. Schmitz, C. Aslanidis, S. Krautbauer, C. Buechler, Lipidomic analysis of serum from high fat diet induced obese mice, International journal of molecular sciences, 15 (2014) 2991-3002.

[41] K. Eisinger, S. Krautbauer, T. Hebel, G. Schmitz, C. Aslanidis, G. Liebisch, C. Buechler, Lipidomic analysis of the liver from high-fat diet induced obese mice identifies changes in multiple lipid classes, Experimental and molecular pathology, 97 (2014) 37-43.

[42] E.L. Donovan, S.M. Pettine, M.S. Hickey, K.L. Hamilton, B.F. Miller, Lipidomic analysis of human plasma reveals ether-linked lipids that are elevated in morbidly obese humans compared to lean, Diabetology & metabolic syndrome, 5 (2013) 24.

[43] A.-M. Samuelsson, P.A. Matthews, M. Argenton, M.R. Christie, J.M. McConnell, E.H. Jansen, A.H. Piersma, S.E. Ozanne, D.F. Twinn, C. Remacle, Diet-induced obesity in female mice leads to offspring hyperphagia, adiposity, hypertension, and insulin resistance, Hypertension, 51 (2008) 383-392.

[44] N.A. Roza, L.F. Possignolo, A.C. Palanch, J.A. Gontijo, Effect of long-term high-fat diet intake on peripheral insulin sensibility, blood pressure, and renal function in female rats, Food & nutrition research, 60 (2016).

[45] A. Floegel, N. Stefan, Z. Yu, K. Mühlenbruch, D. Drogan, H.-G. Joost, A. Fritsche, H.-U. Häring, M.H. de Angelis, A. Peters, Identification of serum metabolites associated with risk of type 2 diabetes using a targeted metabolomic approach, Diabetes, 62 (2013) 639-648.

[46] K.H. Pietiläinen, M. Sysi-Aho, A. Rissanen, T. Seppänen-Laakso, H. Yki-Järvinen, J. Kaprio, M. Orešič, Acquired obesity is associated with changes in the serum lipidomic profile independent of genetic effects–a monozygotic twin study, PloS one, 2 (2007) e218.

[47] J.Y. Kim, J.Y. Park, O.Y. Kim, B.M. Ham, H.-J. Kim, D.Y. Kwon, Y. Jang, J.H. Lee, Metabolic profiling of plasma in overweight/obese and lean men using ultra performance liquid chromatography and Q-TOF mass spectrometry (UPLC− Q-TOF MS), Journal of proteome research, 9 (2010) 4368-4375.

[48] M.N. Barber, S. Risis, C. Yang, P.J. Meikle, M. Staples, M.A. Febbraio, C.R. Bruce, Plasma lysophosphatidylcholine levels are reduced in obesity and type 2 diabetes, PloS one, 7 (2012) e41456.

[49] B. Jacobs, G. De Angelis-Schierbaum, S. Egert, G. Assmann, M. Kratz, Individual serum triglyceride responses to high-fat and low-fat diets differ in men with modest and severe hypertriglyceridemia, The Journal of nutrition, 134 (2004) 1400-1405.

[50] I. Matias, T. Bisogno, V. Di Marzo, Endogenous cannabinoids in the brain and peripheral tissues: regulation of their levels and control of food intake, Int J Obes (Lond), 30 Suppl 1 (2006) S7-S12.

[51] P. Caraceni, A. Viola, F. Piscitelli, F. Giannone, A. Berzigotti, M. Cescon, M. Domenicali, S. Petrosino, E. Giampalma, A. Riili, Circulating and hepatic endocannabinoids and endocannabinoid-related molecules in patients with cirrhosis, Liver International, 30 (2010) 816-825.

[52] E. Patsenker, P. Sachse, A. Chicca, M.S. Gachet, V. Schneider, J. Mattsson, C. Lanz, M. Worni, A. de Gottardi, M. Semmo, J. Hampe, C. Schafmayer, R. Brenneisen, J. Gertsch, F. Stickel, N. Semmo, Elevated levels of endocannabinoids in chronic hepatitis C may modulate cellular immune response and hepatic stellate cell activation, Int J Mol Sci, 16 (2015) 7057-7076.

[53] M. Liu, Y. Yin, X. Ye, M. Zeng, Q. Zhao, D.L. Keefe, L. Liu, Resveratrol protects against age-associated infertility in mice, Hum Reprod, 28 (2013) 707-717.

[54] A. Piyanova, E. Lomazzo, L. Bindila, R. Lerner, O. Albayram, T. Ruhl, B. Lutz, A. Zimmer, A. Bilkei-Gorzo, Age-related changes in the endocannabinoid system in the mouse hippocampus, Mech Ageing Dev, 150 (2015) 55-64.

[55] J. Tam, J. Liu, B. Mukhopadhyay, R. Cinar, G. Godlewski, G. Kunos, Endocannabinoids in liver disease, Hepatology, 53 (2011) 346-355.

[56] D. Osei-Hyiaman, M. DePetrillo, P. Pacher, J. Liu, S. Radaeva, S. Bátkai, J. Harvey-White, K. Mackie, L. Offertáler, L. Wang, G. Kunos, Endocannabinoid activation at hepatic CB1 receptors stimulates fatty acid synthesis and contributes to diet-induced obesity, The Journal of Clinical Investigation, 115 (2005) 1298-1305.

[57] V. Mela, F. Piscitelli, A.L. Berzal, J. Chowen, C. Silvestri, M.P. Viveros, V. Di Marzo, Sex-dependent effects of neonatal maternal deprivation on endocannabinoid levels in the adipose tissue: influence of diet, Journal of Physiology and Biochemistry, (2017) 1-9.

[58] Z.C. Yan, D.Y. Liu, L.L. Zhang, C.Y. Shen, Q.L. Ma, T.B. Cao, L.J. Wang, H. Nie, W. Zidek, M. Tepel, Exercise reduces adipose tissue via cannabinoid receptor type 1 which is regulated by peroxisome proliferator-activated receptor-δ, Biochemical and biophysical research communications, 354 (2007) 427-433.

[59] X. Chen, R. McClusky, J. Chen, S.W. Beaven, P. Tontonoz, A.P. Arnold, K. Reue, The number of X chromosomes causes sex differences in adiposity in mice, PLoS genetics, 8 (2012) e1002709.

[60] M. Cote, I. Matias, I. Lemieux, S. Petrosino, N. Almeras, J.P. Despres, V. Di Marzo, Circulating endocannabinoid levels, abdominal adiposity and related cardiometabolic risk factors in obese men, Int J Obes (Lond), 31 (2007) 692-699.
[61] V. Di Marzo, A. Verrijken, A. Hakkarainen, S. Petrosino, I. Mertens, N. Lundbom, F. Piscitelli, J. Westerbacka, A. Soro-Paavonen, I. Matias, L. Van Gaal, M.R. Taskinen, Role of insulin as a negative regulator of plasma endocannabinoid levels in obese and nonobese subjects, Eur J Endocrinol, 161 (2009) 715-722.
[62] L. Geurts, G.G. Muccioli, N.M. Delzenne, P.D. Cani, Chronic endocannabinoid system stimulation induces muscle macrophage and lipid accumulation in type 2 diabetic mice independently of metabolic endotoxaemia, PLoS One, 8 (2013) e55963.
[63] D. Osei-Hyiaman, J. Liu, L. Zhou, G. Godlewski, J. Harvey-White, W.I. Jeong, S. Batkai, G. Marsicano, B. Lutz, C. Buettner, G. Kunos, Hepatic CB1 receptor is required for development of diet-induced steatosis, dyslipidemia, and insulin and leptin resistance in mice, J Clin Invest, 118 (2008) 3160-3169.
[64] K. Berge, F. Piscitelli, N. Hoem, C. Silvestri, I. Meyer, S. Banni, V. Di Marzo, Chronic treatment with krill powder reduces plasma triglyceride and anandamide levels in mildly obese men, Lipids Health Dis, 12 (2013) 78.
[65] J. Kim, M.E. Carlson, G.A. Kuchel, J.W. Newman, B.A. Watkins, Dietary DHA reduces downstream endocannabinoid and inflammatory gene expression and epididymal fat mass while improving aspects of glucose use in muscle in C57BL/6J mice, Int J Obes (Lond), 40 (2016) 129-137.
[66] J. Abdulnour, S. Yasari, R. Rabasa-Lhoret, M. Faraj, S. Petrosino, F. Piscitelli, D. Prud'homme, V. Marzo, Circulating endocannabinoids in insulin sensitive vs. insulin

resistant obese postmenopausal women. A MONET group study, Obesity, 22 (2014) 211-216.

[67] K. Matsusue, M. Haluzik, G. Lambert, S.-H. Yim, O. Gavrilova, J.M. Ward, B. Brewer, Jr., M.L. Reitman, F.J. Gonzalez, Liver-specific disruption of PPARγ in leptin-deficient mice improves fatty liver but aggravates diabetic phenotypes, The Journal of Clinical Investigation, 111 (2003) 737-747.

[68] N. Deblon, C. Veyrat-Durebex, L. Bourgoin, A. Caillon, A.L. Bussier, S. Petrosino, F. Piscitelli, J.J. Legros, V. Geenen, M. Foti, W. Wahli, V. Di Marzo, F. Rohner-Jeanrenaud, Mechanisms of the anti-obesity effects of oxytocin in diet-induced obese rats, PLoS One, 6 (2011) e25565.

[69] A. Vidal-Puig, M. Jimenez-Linan, B.B. Lowell, A. Hamann, E. Hu, B. Spiegelman, J.S. Flier, D.E. Moller, Regulation of PPAR gamma gene expression by nutrition and obesity in rodents, J Clin Invest, 97 (1996) 2553-2561.

[70] S. Fan, Y. Zhang, Q. Sun, L. Yu, M. Li, B. Zheng, X. Wu, B. Yang, Y. Li, C. Huang, Extract of okra lowers blood glucose and serum lipids in high-fat diet-induced obese C57BL/6 mice, J Nutr Biochem, 25 (2014) 702-709.

[71] F. Sheedfar, M.M. Sung, M. Aparicio-Vergara, N.J. Kloosterhuis, M.E. Miquilena-Colina, J. Vargas-Castrillon, M. Febbraio, R.L. Jacobs, A. de Bruin, M. Vinciguerra, C. Garcia-Monzon, M.H. Hofker, J.R. Dyck, D.P. Koonen, Increased hepatic CD36 expression with age is associated with enhanced susceptibility to nonalcoholic fatty liver disease, Aging (Albany NY), 6 (2014) 281-295.

[72] A.D. Quiroga, J. Lian, R. Lehner, Carboxylesterase1/Esterase-x regulates chylomicron production in mice, PLoS One, 7 (2012) e49515.

[73] D.M. Shih, L. Gu, Y.R. Xia, M. Navab, W.F. Li, S. Hama, L.W. Castellani, C.E. Furlong, L.G. Costa, A.M. Fogelman, A.J. Lusis, Mice lacking serum paraoxonase are susceptible to organophosphate toxicity and atherosclerosis, Nature, 394 (1998) 284-287.

CHAPTER 4

COCAINE USE AND SENSITIZATION ALTERS THE HUMAN LIPIDOME[1]

[1] S. Pati, S. Sahin-Bolukbasi, M. Furnari, K.A. Phillips, D.H. Epstein, K.L. Preston, J.J. Wagner and B.S. Cummings. ((2017) To be submitted to *Addiction Biology.*

Abstract

We recently reported that cocaine can induce lipidomic changes in the blood of rats and that some of these changes correlate to sensitization behavior. To determine whether these findings extend to humans, we extracted lipids from human blood (111 with drug use and 62 controls) and analyzed them using electrospray ionization-mass spectrometry (ESI-MS). Multivariate analysis indicated differences between the lipid profiles of control samples compared to drug use and suggested alterations in fatty acids, phospholipids and glycerolipids. We modified the Cocaine Response Scale (Davidson et al., 1993) to assess subjective responses to cocaine from the first lifetime use to typical current use. We then classified cocaine drug use (n = 80) as "sensitizers" if their score on either positive or negative effects changed by >5 across their using careers. Of these 80 individuals, there were 8 sensitizers, of whom 3 sensitized to positive effects only, 2 to negative effects only, and 2 to both. Partial least squares-discriminant analyses showed extensive differences in blood lipidomic profiles of the sensitized individuals compared to the nonsensitized group. These data suggest that sensitization to cocaine—positive, negative, or both—occurs approximately in 10% of frequent users as indicated by retrospective self-reporting. Similar to studies in rats, some changes in the blood lipidome correlated to sensitization. To our knowledge, this is the clearest demonstration to date that the psychostimulant sensitization observable in laboratory animals may have a human counterpart, and one of the first studies to suggest correlations to lipid changes in the blood.

Abbreviations: Electrospray ionization-mass spectrometry (ESI-MS), glycerolipid (GL), phosphatidylcholines (PC), phosphatidylethanolamines (PE), phospholipids (PLs), principal component analysis (PCA), tandem mass spectrometry (MS/MS).

1. Introduction

Cocaine dependence is a worldwide public health concern. Over 1.7 million people in the United States age 12 and over report current (within the past month) cocaine use (https://www.drugabuse.gov/drugs-abuse/cocaine), resulting in substantial medical, social and financial problems. An important research direction to address the problem of cocaine use disorder is the identification of biomarkers [1-4], as they could aid in the search for effective treatments. The current report builds on our recent studies in rats, and utilizes a lipidomics approach to identify novel markers of cocaine exposure in human blood using shotgun-based ESI-MS lipidomics.

We have recently reported that changes in lipidomic profiles in blood correlate to behavioral sensitization in rats [1]. Related studies to date in humans do not focus on sensitization and have evaluated a relatively small population. Nevertheless, these studies do suggest that lipid changes in the blood can predict some behavioral responses to cocaine [5-7]. For example, Buydens-Branchey et al, [5], demonstrated that decreases in fatty acids in the blood may serve as better predictors of relapse to cocaine use than drug use itself in humans.

Studies in humans have also suggested that changes in lipid metabolizing enzymes correlate to changes in craving for drugs of abuse. For example, Ross et al., [8], showed that cocaine exposure altered the level of calcium-independent

phospholipase A_2 as well as phosphocholine cytidylyltransferase (PCCT). These enzymes are important in the release of free fatty acids from glycerophospholipids and the remodeling of the resulting metabolites into the cell membrane. Although this earlier study suggested further links between changes in the blood lipidome and cocaine may be present in exposed individuals, it did not identify the specific lipids altered.

Our recent study in rats demonstrated that cocaine had distinct effects on the blood lipidome of rats [1]. Cocaine exposure tended to decrease specific lipids in blood. Behavioral responses to cocaine, specifically, the extent of locomotor sensitization across repeated exposures, were also strongly correlated with changes in the blood lipidome. Interestingly, the strongest correlations to sensitization were not between the lipids whose levels changed by the greatest amounts, but rather were more prominent in those who fold-change was somewhat modest (less than 0.5-fold). These correlations were especially strong for some species of glycerophospholipids (GL, *r* values in the range of .79 to .86). Additionally, sensitization scores correlated inversely with plasma levels of 20:3 lysophosphocholine (LPC), but positively with those of 32:0 phosphatidylcholine (PC), 34:1 PC, and 41:2 PE. These data were among the first to demonstrate that cocaine can alter the blood lipidome in manner that correlates with the extent of locomotor sensitization.

In the current study, we have translated our cocaine exposure findings in rats to humans by comparing people who use cocaine with controls who do not use cocaine (controls). Replicating our sensitization findings was more challenging: locomotor sensitization to acute administration of cocaine in rodents is well established, but its human homolog has been elusive. While, human sensitization has been examined in a

longitudinal prospective in healthy volunteers [9] and reported in cross-sectional studies in longtime psychostimulant users [10], these studies have not yet led to a standardized measure of sensitization in humans. Thus, for this study, we modified a published questionnaire on subjective effects of cocaine [11] to ask each respondent how the drug's effects had changed over their cocaine-using career. These retrospectively assessed trajectories provided a face-valid index of behavioral sensitization to acute effects of cocaine. An individual's trajectory was utilized as a human homolog of locomotor sensitization and compared with the corresponding blood-lipidome profile as a function of the presence or absence of a history of behavioral sensitization. We find that similar to our recent preclinical study demonstrating that repeated exposure to cocaine had distinct effects on the blood lipidome of rats [1], humans exposed to cocaine also exhibit alterations in the blood lipidome. Such alterations may collectively serve as a lipidomic biomarker profile that may be further used to differentiate sensitized from non-sensitized cocaine users.

2. Material and Methods

2.1. *Participants*

We collected blood from 173 participants (111 with drug use and 62 controls) in an ongoing IRB-approved protocol (#12-DA-N472) at the NIDA IRP in Baltimore, MD, USA. Participants gave written informed consent prior to study enrollment. **Table 4.1** shows their demographic information.

Drug use was defined using criteria from the DSM V and included those who had used cocaine more than 11 times in their life time. Average age among those with drug

use was 42.1 ± 10.1 years, and 33 (30%) were women. Men were overrepresented among those with drug use, but the outcome of interest, plasma lipid levels, did not differ by sex (data not shown). Samples were prepared and analyzed at the University of Georgia (Protocol IDMODO0000402).

2.2. *Blood collection*

We collected 1 mL of blood from each participant. After isolation, the blood was immediately vortexed with 1 mL of methanol:water (1.0:0.4 v/v) and then placed at -80ºC until shipment to the University of Georgia.

2.3. *Bligh-Dyer blood lipid extraction*

Lipids were extracted using chloroform and methanol according to the method of Bligh and Dyer [12]. Briefly, blood was suspended in 1.25 mL of methanol and 1.25 mL of chloroform. Tubes were vortexed for 30 seconds and allowed to sit for 10 minutes on ice. Tubes were centrifuged at 213 x g for 5 minutes, and the bottom chloroform layer was transferred to a new test tube. The extraction steps were repeated a second time, and the chloroform layers combined. The collected chloroform layers were dried under nitrogen, reconstituted with 50 µL of methanol: chloroform (3:1 v/v), and stored at -80°C.

2.4. *Lipid phosphorus assay*

Lipid phosphorus was quantified using the phosphorus assay [13]. Sulfuric acid (400 µL at 5M) was added to lipid extracts (10 µL) in a glass test tube, and heated at 180-200°C for 1 hr. H_2O_2 (100 µL of 30% v/v) was then added to the tube while

vortexing, and heated at 180-200°C for 1.5 hrs. Next, 4.6 mL of reagent (1.1 g ammonium molybdate tetrahydrate in 12.5 mL sulfuric acid in 500 mL ddH_20) was added and vortexed, followed by addition of 100 µL of 15% ascorbic acid and vortexing. The solution was heated for 7-10 minutes at 100°C, and a 150 µL aliquot was used to measure the absorbance at 830 nm.

2.5. *Lipid characterization with electrospray ionization-mass spectrometry (ESI-MS)*

Lipid extracts (500 pmol/µl) were prepared by reconstitution in chloroform: methanol (2:1, v/v). ESI-MS was performed as described previously [14-16] using a Trap XCT ion-trap mass spectrometer (Agilent Technologies, Santa Clara, CA) with a nitrogen drying gas flow-rate of 8 L/min at 350ºC and a nebulizer pressure of 30 psi. The scanning range was from 200 to 1000 *m/z* on 5 µL of the sample scanned in positive and negative ion mode for 2.5 min with a mobile phase of acetonitrile: methanol: water (2:3:1) in 0.1% ammonium formate. As described previously [17], qualitative identification of individual phospholipid molecular species was based on their calculated theoretical monoisotopic mass values, subsequent MS/MS analysis, and their level normalized to either the total ion count (TIC) or the most abundant phospholipid.

MS^{nth} fragmentation was performed on an Agilent Trap XCT ion-trap mass spectrometer equipped with an ESI source. Direct injection from the HPLC system was used to introduce the analyte. The nitrogen drying gas flow-rate was 8.0 L/min at 350°C. The ion source and ion optic parameters were optimized with respect to the positive molecular ion of interest. Initial identification was typically based on the loss of

the parent head group followed by subsequent analysis of the lysophospholipid. If neutral loss scanning could not confirm the species, the tentative ID was assigned based on the *m/z* value and the LIPIDMAPS database (http://www.lipidmaps.org).

2.6. Lipid Nomenclature

Phospholipids differ in terms of the numbers of carbons and double bonds and polar head groups. Typically, the nomenclature used to identify these traits is X:Y, where X = the number of carbons and Y = the number of double bonds; hence, 34:2 would indicate a lipid with 34 carbons and 2 double bonds. Polar head groups are referred to by their abbreviations. Lipid abbreviations are mentioned above and are standard.

2.7. *Assessment of human sensitization to cocaine*

We modified the Cocaine Response Scale [11] to assess subjective responses to cocaine in 80 participants whose blood lipidomes were assessed. The original version of the scale had 15 items, of which 8 assessed positive effects (“cocaine made me feel very happy”; “cocaine made me feel as though I was on top of things”) and 7 assessed negative effects (“I became fearful on cocaine”; “cocaine made my judgment worse”). Participants rated each item on a scale of 1 (“not at all”) to 4 (“very true”). Our modification was to have the participant rate each item once for “the first time I used cocaine” and once for “the most recent time I used cocaine.” We also gave items that were taken directly from the original version of the scale, including asking the time since first use, approximate number of times used, and how soon the second use followed the first use.

We scored responses by simple summation of positive and negative ratings, as recommended for the original version of the scale, additionally we calculated separate ratings for “first time” and “most recent” time cocaine was used. We classified cocaine “sensitizers” based on a score change >5, on either positive or negative effects, across their using careers.

2.8. *Multivariate statistical analysis of blood lipids*

Multivariate partial least squares-discriminant analysis (PLS-DA) was performed using MetaboAnalyst 3.0 (http://www.metaboanalyst.ca/). Automatic peak detection and spectrum deconvolution was performed using a peak width set to 0.5. Analysis parameters consisted of interquartile range filtering and sum normalization with no removal of outliers from the dataset. Features were selected based on volcano plot analysis and were further identified using MS/MS analysis. Significance for volcano plot analysis was determined based on a fold change threshold of 2.00 and $P \leq 0.05$. Following identification, total ion count was used to normalize each parent lipid level, and the change in the relative abundance of that phospholipid species as compared to its control was determined. This method is standard for lipidomic analysis as reported in our previous studies [14, 16].

2.9. *Regression analysis between lipid features and sensitization.*

GraphPad Prism for Windows version 5.04 (GraphPad Software, Inc., La Jolla, CA) was used for all correlation analyses comparing the differential lipid expression via the relative abundance of features to sensitization. Reported correlations meet the

stringent cutoff correlation coefficient criteria of $R^2 \geq 0.6$. For all analysis, the experimental unit was one sample from each patient. We used a two-tailed alpha of 0.05.

3. Results

3.1. *Drug Use vs. control*

Analysis of ESI-MS spectra of blood samples isolated from people with drug use and controls showed significant group differences in the overall abundance of several lipids (**Figure 4.1**). High-throughput multivariate analysis was performed on mass spectrometric data to identify group differences in blood lipid profiles. Multivariate partial least squares-discriminant analysis (PLS-DA) of spectral data comparing Controls and people with Drug Use demonstrated some separation between populations (**Figure 4.2A**).

To identify lipid alterations that may have attributed to PLS-DA separation, volcano plot analyses was performed to identify important features based on fold change and statistical significance level for drug-related effects. Pairwise comparison of Controls and people with Drug Use identified several lipids with lower abundances in people with drug use (**Figure 4.2B**). In general, lipids falling within the mass range of *m/z* 200-700 were lower across the board in people with drug use. This range includes several species of fatty acids (FA), lysophospholipids, and glycerolipids (GL). Species corresponding to phospholipids (PLs) did not differ between drug use and controls. Many of these lipids were FA (*m/z* values of 204.9 to 341.2, **Figure 4.3**). People with drug use also showed decreased levels in almost every single lipid species analyzed,

including those corresponding to those with lower molecular weights (i.e. those below a *m/z* of 600). Additionally, there were lower levels for a few GLs (**Figure 4.3**).

It is important to note that we stratified these differences by sex and, separately, by BMI (data not shown), and saw no indication that either of those accounted for the differences between people with drug use and controls.

3.2. *Sensitizers vs. nonsensitizers*

Responses on the sensitization scale are shown in **Figure 4.4**. Among the 80 participants who used cocaine and provided data, there were 8 sensitizers, of whom 3 sensitized to positive effects only, 3 to negative effects only, and 2 to both. With these data in hand, we used multivariate PLS-DA analysis and observed clustering of the 80 subjects into control, drug use and sensitized drug use groups (**Figure 4.5**). As observed previously, there was separation between the control and drug use groups (**Figure 4.5A**). Some separation was also evident between the sensitized and non-sensitized drug use groups; pairwise PLS-DA analysis showed a clear separation between these two groups (**Figure 4.5B**), suggesting that differences exist in the blood lipidome between sensitized and non-sensitized individuals.

Among the lipids that significantly differed between sensitized and nonsensitized drug use groups, we found several whose relative abundance positively correlated with changes in individual sensitization scores **(Table 4.2)**. The highest correlations were for lipids (*m/z* 733.4, *m/z* 715.4), identified as 36:0 and 34:3 phosphatidylethanolamine (PE), respectively, via subsequent *MS/MS* analysis. Other lipids strongly correlated with sensitization scores included 25:0 and 27:0 phosphatidic acid (PA). There were also a few *m/z* values whose identity could not be confirmed by *MS/MS* analysis,

including those corresponding to *m/z* 509.4, 619.4, 693.3 and 891.4. All correlations were in the positive direction (except *m/z* 579.4 in the participants who sensitized to positive effects of cocaine). Interestingly, the fold change of these lipids between sensitizers and nonsensitizers was not greater than 1.14. Nevertheless, these data suggest that changes in specific lipids correlate to changes with the degree of sensitization to cocaine.

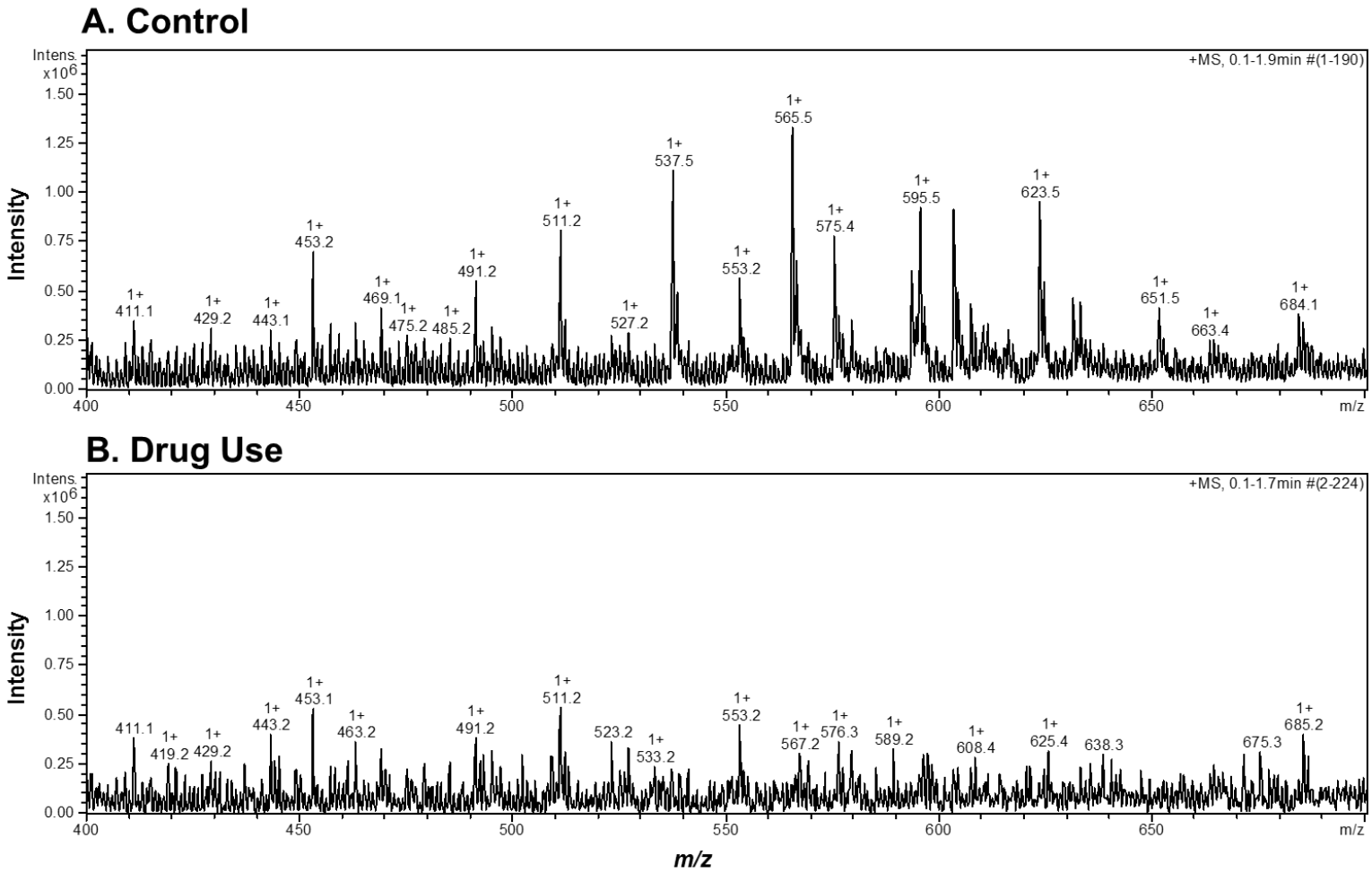

Figure 4.1. ESI-MS spectra of blood lipids extracted from one control (A) and one person who used cocaine (B) in the positive mode. The Y-axis indicated the intensity while the X-axis represents the *m/z* value of lipid analyzed. These data are representative of findings from 62 controls and 111 people who use drugs.

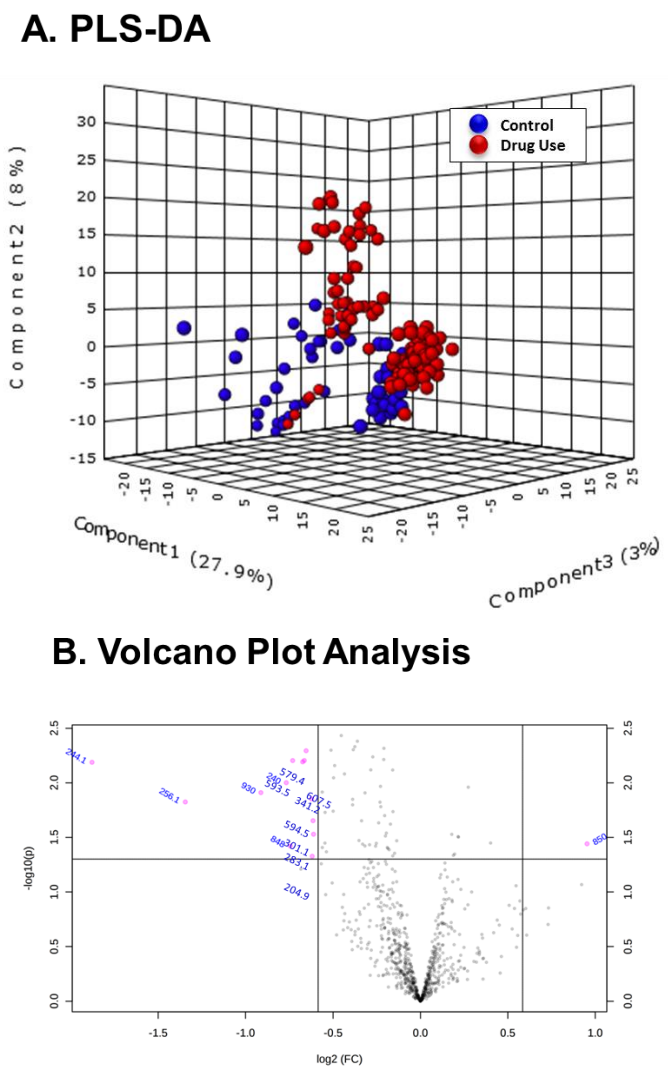

Figure 4.2. Multivariate analysis of human blood lipidome. (**A**) Partial-least-squares discriminant analysis (PLS-DA) of lipidomic data from human control and cocaine use groups as derived from ESI-MS in the positive mode. Each dot represents the calculated variance for the total lipidome of each individual assessed while the X, Y and Z axis represents compents analyzed and the total variance assessed. (**B**) Volcano blot analysis identifying specific *m/z* values of lipids whose expression were significantly altered. The fold change compared to controls is shown on the X-axis and significance is shown on y-axis.

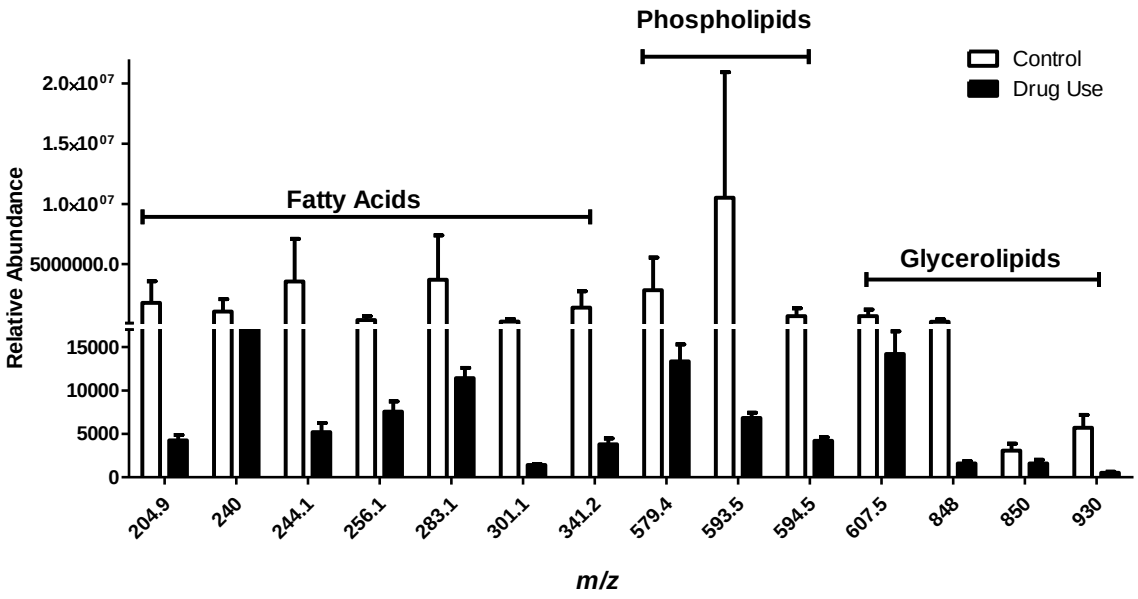

Figure 4.3. Comparison of significantly altered *m/z* features across ***controls*** and ***people who use drugs*** based on tentative identification of lipid classes detected in the positive mode and negative mode. Significant features were determined based on a fold change threshold of 1.00 and a p-value < 0.01.

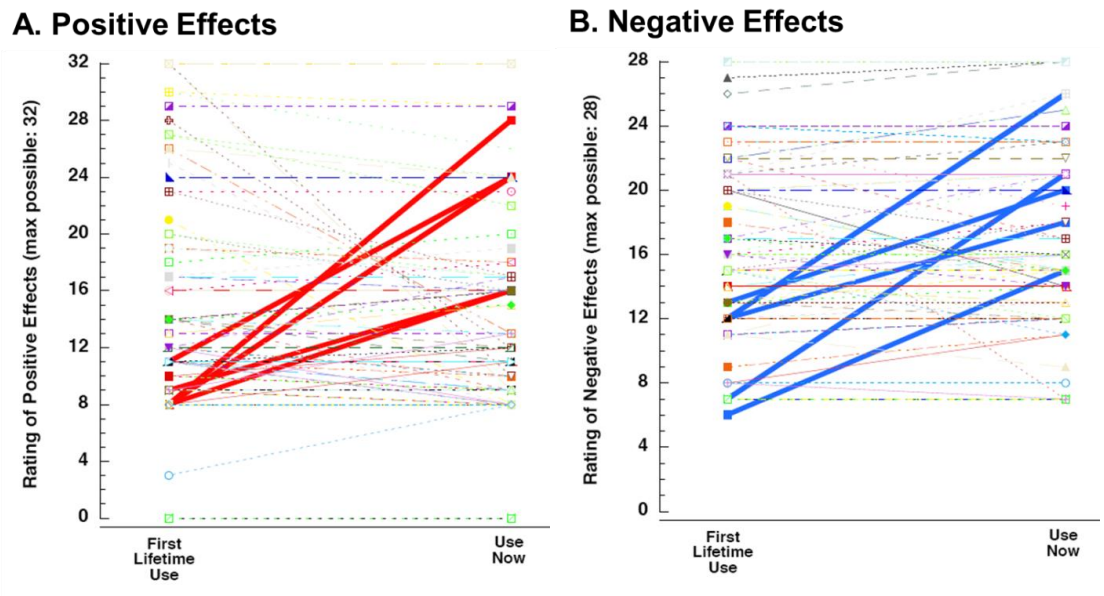

Figure 4.4. Self-reported responses to cocaine in terms of its positive (**A**) or negative (**B**) effects, from first lifetime use to most recent use. Each line in each panel shows data from one of 80 people who use cocaine. Bolded lines (red in panel **A**, blue in panel **B**) show participants whose ratings increase by at least 5 points, our *a priori* criterion for sensitization. There were 8 sensitizers in all (3 for positive effects only, 3 for negative effects only, and 2 who sensitized to both).

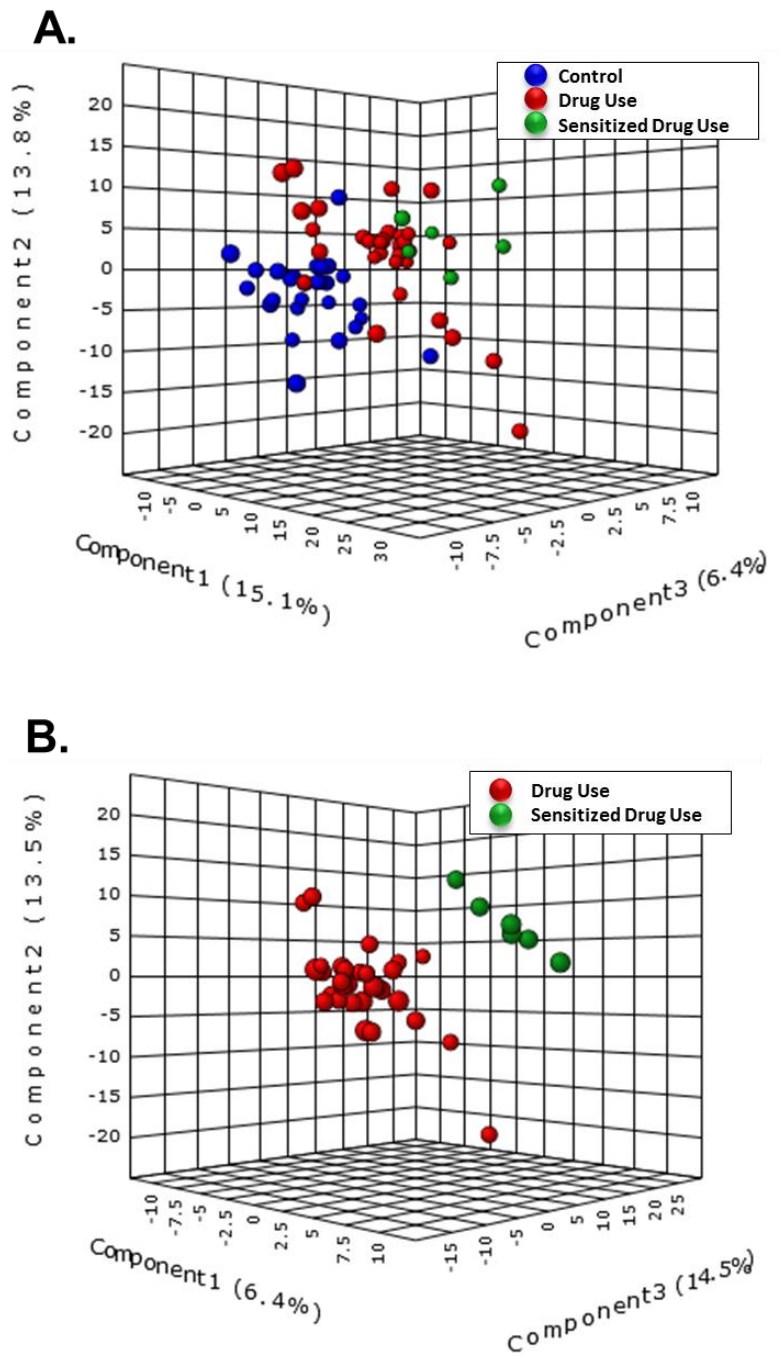

Figure 4.5. Partial-least-squares discriminant analyses (PLS-DA) of sensitization lipidome data from (**A**) control, nonsensitized cocaine use, and sensitized cocaine use groups, and (**B**) nonsensitized cocaine use group and sensitized cocaine use group.

Table 4.1. Demographic and clinical characteristics of drug users and nonusers.

	Control (n=62)	**Drug Use** (n=111)
Age	35.21 ±11.67 *Range (19-62)*	42.06 ±10.14 *Range (23-61)*
Gender		
Females	44 *(71.0%)*	33 *(29.7%)*
Males	18 *(29.0%)*	78 *(70.3%)*
Marital status		
Never married	34 *(54.8%)*	70 *(63.1%)*
Married	8 *(12.9%)*	6 *(5.4%)*
Separated/Divorced	7 *(11.3%)*	20 *(18.0%)*
Single or No Response	8 *(12.9%)*	8 *(7.2%)*
Educational level		
8th Grade or Less	1 *(1.6%)*	1 *(0.9%)*
GED	5 *(8.1%)*	13 *(11.7%)*
Some High School	4 *(6.5%)*	24 *(21.6%)*
H.S. Diploma	16 *(25.8%)*	42 *(37.8%)*
Some College	20 *(32.3%)*	26 *(23.4%)*
College Graduate	16 *(25.8%)*	5 *(4.5%)*
Body Mass Index (BMI)	29.21 ± 8.05	26.96 ± 6.09
Ethnicity		
American Indian/Alaska Native	1 *(1.61%)*	--
Asian	3 *(4.84%)*	--
Black or African American	40 *(64.52%)*	77 *(69.4%)*
More than one race	3 *(4.84%)*	3 *(2.7%)*
White	15 *(24.19%)*	31 *(27.9%)*

Table 4.2. Correlation of differential lipid expression to sensitization scores.

m/z	I.D.	R^2	Fold Change
$[M+H]^+$ 509.4	*Unidentified**	0.77	0.73
$[M+H]^+$ 551.4	PA(25:0)	0.81	0.79
$[M+H]^+$ 579.4	PA(27:0)	0.82	0.68
$[M+H]^+$ 619.4	*Unidentified**	0.75	0.78
$[M+H]^+$ 715.4	PE(34:3)	0.88	0.90
$[M-H]^-$ 566.2	PS(20:0)	0.68	1.14
$[M-H]^-$ 693.3	*Unidentified**	0.63	0.89
$[M-H]^-$ 733.4	PE(36:0)	0.95	0.86
$[M-H]^-$ 887.5	PS(44:1)	0.81	0.91
$[M-H]^-$ 891.4	*Unidentified**	0.91	0.91
$[M-H]^-$ 911.4	PI(40:5)	0.75	0.90
$[M-H]^-$ 919.4	PI(40:1)	0.80	0.91

Asterisk (*) indicates tentative ID due to unconfirmed fragmentation

4. Discussion

Our previous studies in rats showed that cocaine exposure lowered the plasma levels of several phospholipids and fatty acids, and that alterations in several of these lipids correlated to sensitization, as measured by changes in open-field activity after a challenge dose [1]. The current study extends these findings to humans and demonstrates several similar findings, including a general decrease in several phospholipids and fatty acid species in the blood of humans who use cocaine compared to those who do not. These results are consistent with earlier studies showing that cocaine can alter lipid metabolism in the brain in humans [8, 18].

While the current study is not the first to compare changes in plasma fatty acids or phospholipids in humans after cocaine use, it differs from previous work in that other studies tended to focus on cholesterol and lipoproteins [6, 19, 20] rather than on the total lipidome. Nevertheless, the current study replicated previous literature by demonstrating alterations in fatty acids between people who use cocaine and those who do not. The current study also demonstrated correlation between select lipids and behavioral sensitization. Interestingly, lower levels of cholesterol, linoleic acid, arachidonic acid, and n-3 polyunsaturated fatty acids (PUFAs) predicted greater likelihood of relapse to cocaine 12 months later in drug users [6]. In the same sample, lower levels of fatty acids at admission to treatment were associated with histories of cocaine-induced aggression [21].

The current study also demonstrated several similarities to our recent study in rats [1], including a decrease in several of the same fatty acid species, such as palmitic acid, oleic acid and derivatives of arachidonic acid. There were also some notable

differences between rats and humans, a major one being the number of lipid species altered: hundreds of lipids species were altered in cocaine-treated rats as compared to controls [1], whereas fourteen species of lipids were identified as significantly altered in the blood of the cocaine use versus control human participants. One reason for this may be that the human lipidome displayed considerably more variability than the rat lipidome, as would be expected due to differences in diet and lifestyle among humans. In mice, we have shown that experimentally imposed variations in diet (low and high-fat) do not alter the same fatty acids or lipids identified in this study (data submitted, under revision); this increases our confidence that the lipidome differences between human users and nonusers are not accounted for by dietary differences between those two groups.

Another similarity between the current study and our previous work is that a correlation was identified between alterations in select phospholipids and a measure of sensitization. As mentioned above, a human homolog of sensitization has been elusive despite some data [9, 10]. The approach used in the current study identified differences in the behavioral histories between users who did or did not report experiences consistent with the occurrence of sensitized responses. A relatively small minority of drug users were identified as being sensitized, and their sensitization scores were utilized for comparison to changes in their blood lipidome. As we had observed previously in rats, the lipids whose levels correlated to sensitization scores were not always those that exhibited the highest fold-change in cocaine exposed individuals. These lipids included several PE species, phosphatidic acids (PA), and phosphatidylserines (PS). Although we identified similar decreases in several fatty acid

species between rats and human (including a few common phospholipid species, such as PA, [1]; these agreements appeared to be an exception to the general trend. Overall, except for those mentioned above, there were few similarities between sensitization-associated lipid changes identified in humans as compared to rats with respect to specific lipid species.

Even though fatty acids have been demonstrated to be decreased in previous studies in humans, in our current study (and in recent studies in rats) we did not identify any fatty acid species whose level correlated with the sensitization score. We did identify several species whose m/z values correlate to phospholipid metabolites (*m/z* range 450-600). These species are similar to those shown to be associated with general cocaine use (**Figure 4.3)**. Similarly, we also identified some sensitization-associated phosphatidylinositols (PI) that were similar to the high-molecular-weight glycerolipids shown to be lower in people who use cocaine (**Figure 4.3;** *m/z* range 848, 850 and 930), but again, these were not the same exact lipid species. One reason for this lack of coherence may be that our analysis was not focused on the fold-change in lipids as much as it was on the correlation to behavior. Further, the analysis of lipid changes in the sensitized cocaine use group focused on comparison of the non-sensitized cocaine use group to the sensitized cocaine use group, as opposed to controls. As a result, the fold-changes in lipids reported in **Table 4.2** are quite modest compared to those reported in **Figure 4.3**. Interestingly, this is similar to our report in rats [1], where many lipids whose levels correlated to sensitization had fold-changes less than 0.5. Thus, one limitation of the metabolomic assessment of blood lipids is that the features with the greater fold-change may not necessarily reflect behavior. This

underscores the importance of assessing behavior when interpreting omics-based data, rather than simply relating the results to exposure level.

Results reported in the current study from human blood samples, combined with our previous studies in rats, help to establish lipidomic changes in the blood as potential biomarkers of sensitization following cocaine use/exposure. These results are limited in that neither the rat data nor the human data permit comparisons regarding behavioral aggression or susceptibility to relapse as reported previously. However, our use of sensitization as an outcome measure is both a limitation and a strength of the current work. The lack of a standardized approach to quantify sensitization in human drug users necessitated the creation of subjective scoring systems based on a modified questionnaire. It is important to point out that while this questionnaire has strong face validity, it was not put through a formal psychometric process of development. This limitation is not a severe as it would seem because the questionnaire would still retain all the uncertainties of a retrospective assessment even if it had been subjected to the above. Further, prospective data about drug effects from initiation onward may soon become available from a recent ambitious cohort studies [22], which would provide better information about such inherently longitudinal phenomena as sensitization. At this point, the findings of our questionnaire that sensitization was detectable by self-report in approximately ten percent of people who use cocaine, and that it encompassed positive effects, negative effects, or both, is to our knowledge a new contribution to this aspect of addiction research. The correlation of these findings with blood lipids presents compelling possibilities that are worthy of future studies in larger populations.

In conclusion, our findings suggest that exposure to cocaine alters the human blood lipidome and that some of the alterations correlate with self-reported sensitization to cocaine's effects. While this study is not the first study to demonstrate changes in the blood lipidome in response to cocaine, it does significantly extend previous reported results [5-7, 21], and translates our own findings in a rodent model of cocaine sensitization [1] to a human population of cocaine users. It will be interesting to determine whether the changes reported herein can be detected prospectively and if any such underlying mechanisms can be elucidated.

References

[1] B.S. Cummings, S. Pati, S. Sahin, N.E. Scholpa, P. Monian, P.M. Trinquero, J.K. Clark, J.J. Wagner, Differential effects of cocaine exposure on the abundance of phospholipid species in rat brain and blood, Drug and alcohol dependence, 152 (2015) 147-156.

[2] L. Pomierny-Chamiolo, A. Moniczewski, K. Wydra, A. Suder, M. Filip, Oxidative stress biomarkers in some rat brain structures and peripheral organs underwent cocaine, Neurotoxicity research, 23 (2013) 92-102.

[3] L.J. Porrino, M.D. Miller, H.R. Smith, S.H. Nader, M.A. Nader, Neural Correlates of Exposure to Cocaine Cues in Rhesus Monkeys: Modulation by the Dopamine Transporter, Biological psychiatry, 80 (2016) 702-710.

[4] J. Sharma, N. Rathnayaka, C. Green, F.G. Moeller, J.M. Schmitz, D. Shoham, A.H. Dougherty, Bradycardia as a Marker of Chronic Cocaine Use: A Novel Cardiovascular Finding, Behav Med, 42 (2016) 1-8.

[5] L. Buydens-Branchey, M. Branchey, J.R. Hibbeln, Higher n-3 fatty acids are associated with more intense fenfluramine-induced ACTH and cortisol responses among cocaine-abusing men, Psychiatry research, 188 (2011) 422-427.

[6] L. Buydens-Branchey, M. Branchey, Association between low plasma levels of cholesterol and relapse in cocaine addicts, Psychosom Med, 65 (2003) 86-91.

[7] L. Buydens-Branchey, M. Branchey, D.L. McMakin, J.R. Hibbeln, Polyunsaturated fatty acid status and relapse vulnerability in cocaine addicts, Psychiatry research, 120 (2003) 29-35.

[8] B.M. Ross, A. Moszczynska, F.J. Peretti, V. Adams, G.A. Schmunk, K.S. Kalasinsky, L. Ang, N. Mamalias, S.D. Turenne, S.J. Kish, Decreased activity of brain phospholipid metabolic enzymes in human users of cocaine and methamphetamine, Drug and alcohol dependence, 67 (2002) 73-79.

[9] I. Boileau, A. Dagher, M. Leyton, R.N. Gunn, G.B. Baker, M. Diksic, C. Benkelfat, Modeling sensitization to stimulants in humans: an [11C]raclopride/positron emission tomography study in healthy men, Archives of general psychiatry, 63 (2006) 1386-1395.

[10] M. Leyton, Conditioned and sensitized responses to stimulant drugs in humans, Progress in neuro-psychopharmacology & biological psychiatry, 31 (2007) 1601-1613.

[11] E.S. Davidson, J.F. Finch, S. Schenk, Variability in subjective responses to cocaine: initial experiences of college students, Addict Behav, 18 (1993) 445-453.

[12] E.G. Bligh, W.J. Dyer, A rapid method of total lipid extraction and purification, Can J Biochem Physiol, 37 (1959) 911-917.

[13] G.R. Bartlett, Phosphorus assay in column chromatography, Journal of Biological Chemistry, 234 (1959) 466-468.

[14] G.R. Kinsey, J.L. Blum, M.D. Covington, B.S. Cummings, J. McHowat, R.G. Schnellmann, Decreased iPLA2gamma expression induces lipid peroxidation, cell death, and sensitizes cells to oxidant-induced apoptosis, J Lipid Res, (2008).

[15] L. Zhang, B.L. Peterson, B.S. Cummings, The effect of inhibition of Ca2+-independent phospholipase A2 on chemotherapeutic-induced death and phospholipid profiles in renal cells, Biochem Pharmacol, 70 (2005) 1697-1706.

[16] B. Peterson, K. Stovall, P. Monian, J.L. Franklin, B.S. Cummings, Alterations in phospholipid and fatty acid lipid profiles in primary neocortical cells during oxidant-induced cell injury, Chem Biol Interact, 174 (2008) 163-176.
[17] R. Taguchi, J. Hayakawa, Y. Takeuchi, M. Ishida, Two-dimensional analysis of phospholipids by capillary liquid chromatography/electrospray ionization mass spectrometry, J Mass Spectrom, 35 (2000) 953-966.
[18] B.M. Ross, A. Moszczynska, K. Kalasinsky, S.J. Kish, Phospholipase A2 activity is selectively decreased in the striatum of chronic cocaine users, Journal of neurochemistry, 67 (1996) 2620-2623.
[19] T. Massardo, V. Araya, C. Ibanez, J. Veliz, R. Fernandez, R. Jaimovich, J. Pallavicini, R. Chandia, K. Pereira, J. Pereira, [Serum lipid levels in a group of cocaine dependent subjects in recent abstinence], Rev Med Chil, 143 (2015) 697-706.
[20] S.H. Lin, Y.K. Yang, S.Y. Lee, P.C. Hsieh, P.S. Chen, R.B. Lu, K.C. Chen, Association between cholesterol plasma levels and craving among heroin users, J Addict Med, 6 (2012) 287-291.
[21] L. Buydens-Branchey, M. Branchey, D.L. McMakin, J.R. Hibbeln, Polyunsaturated fatty acid status and aggression in cocaine addicts, Drug and alcohol dependence, 71 (2003) 319-323.
[22] J.M. Bjork, L.K. Straub, R.G. Provost, M.C. Neale, The ABCD Study of Neurodevelopment: Identifying Neurocircuit Targets for Prevention and Treatment of Adolescent Substance Abuse, Current Treatment Options in Psychiatry, 4 (2017) 196-209.

CHAPTER 5

LOCALIZATION AND EXPRESSION OF CTP:PHOSPHOCHOLINE CYTIDYLYLTRANSFERASE IN RAT BRAIN FOLLOWING COCAINE EXPOSURE[1]

[1]Sumitra Pati, Min K. Sun, John J. Wagner, Brian S. Cummings. (2017) To be submitted to *Brain Research.*

Abstract

Phosphatidylcholine (PC) is a primary phospholipid, a major source of secondary lipid messengers, and also serves as a biosynthetic precursor for other membrane phospholipids. Phosphocholine cytidylyltransferase [CCT] is the rate-limiting enzyme responsible for catalyzing the formation of PC. Alterations in CCT activity have been associated with lipid dysregulation across some neurological disorders and CDP-choline, the essential intermediate in PC synthesis, has suggested beneficial effects in attenuating drug craving in cocaine addiction. We recently demonstrated the persisting effects of cocaine conditioning on brain PC alterations where the majority of changes occurred region-specifically in the cerebellum and hippocampus. In this study, we attempted to identify a potential mechanism mediating these changes by examining the expression of CCT, including both of its isoforms; alpha (CCTα) and beta (CCTβ). Immunohistochemical analysis did not detect any staining of CCTα throughout the rat brain. In contrast, CCTβ expression was detected in the Purkinje cells of the cerebellum and its expression decreased after rats were exposed to cocaine. Collectively, these data demonstrate the region- and cell-specific localization of CCTα and CCTβ in the rat brain as well as the altered expression of CCTβ in the cerebellum following cocaine exposure.

Abbreviations: bovine serum albumin (BSA); cytidine triphosphate (CTP); CTP:phosphocholine cytidylyltransferase (CCT); CCT alpha (CCTα); CCT beta (CCTβ); 3,3'-diaminobenzidine (DAB); diacylglycerol (DAG); immunohistochemistry (IHC); matrix-assisted laser desorption/ionization (MALDI); nuclear localization sequence

(NLS); optical density (OD); phosphatidylcholine (PC); polyunsaturated fatty acid (PUFA); region of interest (ROI).

1. Introduction

Phosphatidylcholine (PC) is a primary membrane phospholipid in eukaryotes and major source of secondary lipid messengers (i.e. diacylglycerol [DAG], phosphatidic acid) as well as the biosynthetic precursor for other membrane phospholipids [1, 2]. The major pathway responsible for PC biosynthesis is the CDP-choline or Kennedy pathway, where the main regulator is cytidine triphosphate (CTP):phosphocholine cytidylyltransferase [CCT] [3]. CCT is the rate-limiting, enzyme responsible for catalyzing the transfer of choline from phosphocholine to CDP-choline, which can proceed to donate the phosphocholine moiety to DAG and result in the formation of PC [3]. Thus, the regulation of PC homeostasis in mammalian cells is heavily reliant on CCT.

CCT proteins are characterized by their N- and C-termini depending on the presence (CCTα) or absence (CCTβ) of a nuclear localization signal (NLS), extent of phosphorylation, or charge [1, 4]. Regarding cellular localization, CCT is an amphitropic enzyme distributed between the cytosol and membrane. Generally, the NLS directs most of CCTα to the nucleus but it can also be found in the cytoplasm associated with other organelle membranes, although this can differ across cells and tissues [4, 5]. CCTβ, however, is reported to exclusively localize outside of the nucleus in HeLa cells [6].

Regulation of CCT activity is well-characterized by the translocation from the inactive, soluble form to the active, membrane-bound form, which becomes subject to

lipid-dependent feed-forward and feedback mechanisms [7]. All isoforms maintain the same biochemical function; however, expression varies across tissue type [5]. CCTα is ubiquitously expressed throughout various tissues whereas CCTβ expression is generally low, with the exception of the brain and gonadal tissue [4, 8]. The heightened expression of CCTβ in the brain suggests an important functional role in this tissue.

Alterations in CCT activity have been associated with lipid dysregulation across some neurological disorders [4, 9]. The accumulation of cellular glucosylceramide observed in Gaucher disease has been shown to directly activate PC synthesis [10]. CCT has also been implicated in neuronal development with an essential role in the PC biosynthesis of axons [11]. The essential intermediate in PC synthesis, cytidine-5'-diphosphocholine (CDP-choline or citicholine), has been extensively studied for its potential to remedy membrane damage and provide therapeutic effects across a variety of CNS disorders and injury [9]. For example, CDP-choline demonstrated beneficial effects in cocaine addiction where treatment attenuated drug craving in cocaine-dependent subjects, suggesting a role for PC synthesis within the context of drug dependence [12]. Furthermore, Ross *et al*., demonstrated reduced CCT activity in postmortem brain tissue obtained from cocaine users [13], identifying a potential rationale for the efficacy of CDP-choline treatment.

We previously demonstrated the persisting effects of cocaine conditioning on brain phospholipid alterations where the majority of changes occurred in PC species, region-specifically in the cerebellum and hippocampus [14]. The hippocampus, characterized by its role in learning and memory, is directly involved in the reinstatement of drug-seeking behavior as well as the retention of memories of addiction, including those

related to membrane remodeling and lipid alterations [14-16]. Although the cerebellum has not received much attention in the addiction literature, quite a few studies have suggested a role for the cerebellum in drug reward and reinstatement of drug-seeking [17-20]. These studies report consistent cerebellar activation in response to drug-cues via neuroimaging, bidirectional connections with regions mediating drug reward such as the striatum and ventral tegmental area, involvement in nonmotor function [19, 20], and more recently, Wagner, *et. al* demonstrated that granule cells can convey information about the expectation of reward [18].

To identify a potential mechanism mediating these changes, we further investigated the effects of cocaine exposure on region-specific CCT expression in the hippocampus and cerebellum. Additionally, while the distribution of CCT isoforms in human tissues has been reported, there is little information available pertaining to the abundance as well as localization of CCT isoforms in the rodent brain [6, 21]. To address this gap, we assessed the localization and expression of CCT isoforms in the rat brain using immunohistochemical analyses.

2. Experimental Procedures

2.1 Animals

Adult (12-13 weeks) male Sprague-Dawley rats (Harlan, Indianapolis, IN, USA) were housed in pairs in clear plastic cages and maintained on a 12-hour light/dark cycle (0700/1900 hours) with food and water available *ad libitum.* Animals were allowed to acclimate to their home cages for at least 1 week and were habituated to handling (3 days) prior to testing. All studies were approved by the University of Georgia

Institutional Animal Care and Use Committee and were conducted in accordance with the Guide for the Care and Use of Laboratory Animals. Cocaine hydrochloride was obtained from the National Institutes of Health National Institute on Drug Abuse (RTI International, Research Triangle Park, NC), and was dissolved in 0.9% saline and filter sterilized prior to use. Animals were injected intraperitoneally with either cocaine (15 mg/kg on conditioning days, 10 mg/kg on reinstatement days) or 0.9% saline.

2.2 Conditioned place preference

Behavioral testing took place in 43.2-cm × 43.2-cm chambers with clear plastic walls and a smooth solid floor (Med Associates Inc., St. Albans, VT), as described previously [22]. Briefly, each chamber was located in a sound-attenuating box equipped with two house lights, ventilation fan, and photo beam banks for horizontal activity detection. Beam breaks were counted using Activity Monitor software (Med Associates, Inc.). The chamber was divided into two compartments with a black partition containing a guillotine door. Removal of the door permitted the rat access to either compartment. For conditioning sessions, the door was closed in order to confine the animal's activity. To obtain equal preference between compartments, one compartment contained rod-like steel bar flooring and black plastic walls while the other compartment contained a wire mesh grid floor and transparent walls.

The experimental design for the behavioral regimen was modified based on that described in previous studies [22, 23]. Following a pretest session, conditioning sessions took place for 4 consecutive days. Rats were divided into two groups: saline-treated (n=8) and cocaine-treated (n=19). Animals were injected with either saline or

cocaine (15 mg/kg, I.P.), placed in one of the two insert compartments for 15 minutes, and then returned to their home cage. Four hours later, animals were injected with either saline or cocaine and were confined to the opposite compartment for the second daily conditioning session. After the 4 days of conditioning, the rats underwent a drug-free place preference post-test to determine the shift in time spent in the drug-paired compartment as compared with the pretest session assessed prior to conditioning. Over the next 7 days, these animals then experienced six consecutive days of extinction (saline conditioning) followed by a cocaine-primed reinstatement assessment. Rats were then housed in their home cage environment for 30 days of abstinence, followed by a final reinstatement session. The results from these behavioral assessments are currently submitted elsewhere and are under review.

2.3 Tissue extraction

Region-specific brain tissue was extracted 7 days after the final exposure to cocaine, as described previously [22]. Briefly, animals were anesthetized with halothane prior to decapitation in compliance with protocols approved by the University of Georgia Animal Care and Use guidelines. The brain was removed and regions of interest were extracted and flash frozen in liquid nitrogen. For immunohistochemistry studies ($n \geq 3$ rats per group), the left hemisphere was placed midline down on a coverslip, flash frozen in liquid nitrogen, and kept at -80°C until cryosectioning.

2.4 Immunohistochemistry

Immunohistochemical staining was performed on sagittal, 10-µm frozen sections fixed in 2% paraformaldehyde at room temperature for 20 min. The manufacturer's protocol was

followed using the Vectastain Universal Elite ABC HRP Kit (Vector Laboratories, Burlingame, CA) as described previously [22]. Sections were incubated overnight with primary antibody against CCTβ and/or CCTα (1:50 dilution; obtained as a generous gift from Dr. S. Jackowski) in 0.1% bovine serum albumin (BSA) in PBS. Secondary staining was performed with 3,3'-diaminobenzidine (DAB) as substrate (Vector Laboratories), which were subsequently counterstained using Gill's hematoxylin. Sections were mounted with Fluoromount (SigmaAldrich, St. Louis, MO) and visualized using a Nikon AZ100 microscope (Tokyo, Japan). Quantification and image analysis was subsequently performed using the ImageJ-based software package FIJI [24]. Using the 'colour deconvolution' with 'H DAB' settings, DAB and Gill's hematoxylin staining were deconvoluted, inverted, and converted into 8-bit gray scale images. Regions of interest (ROI) were defined to ensure uniform quantitative comparisons across sections and structures. For example, the entire hippocampus and Purkinje cell layer were set as the ROIs for hippocampal and cerebellar comparisons, respectively. Relative optical density (O.D.) was calculated based on DAB staining values where mean intensity was calculated using the 'Measure' function. A reciprocal intensity was derived based on the maximum intensity of an 8-bit image (250) and log transformed to yield an O.D. directly proportional to the amount of chromogen present.

2.5 Immunoblot analysis

Protein isolation was performed region specifically using 10–15 mg flash-frozen tissue as described previously [22]. Protein concentrations were determined using the BCA assay and samples (40 mg) were separated on SDS-PAGE gels and transferred to

nitrocellulose membranes. The membranes were blocked in 5% (w/v) milk powder in Tris-buffered saline/Tween 20 for 2 hours and exposed to primary antibodies against CCTβ or CCTα (1:2000 dilution; obtained as a generous gift from Dr. S. Jackowski) overnight. Membranes were then incubated with secondary antibody (1:2500 dilution; Promega, Madison, WI) for 2 hours and bands were visualized using SuperSigna Chemiluminescent Substrate (Thermo Scientific, Waltham, MA). Intensities were quantified using an Alpha Innotech FluorChem HD2 system (ProteinSimple, Santa Clara, CA) and normalized to *β*-actin (1:2000 dilution).

2.6 Statistical Analysis

All statistical analyses were compiled using GraphPad Prism for windows version 5.04 (GraphPad Software, Inc., La Jolla, CA). For all analysis, the experimental unit was one tissue section from an individual animal and sections obtained from a total of 4-5 animals/group point were assessed. For all analyses, significance was set at $p \leq 0.05$ where data are expressed as mean ± SEM based on t-test for pairwise analysis. Pairwise comparisons of data were performed with either an unpaired two-tailed Student's t-test or nonparametric test, depending on the outcomes of normality testing for Gaussian distributions.

3. Results

3.1 Expression of CCT Isoforms

Immunohistochemistry (IHC) was performed on 10-µm sagittal rat brain sections and detected the expression of CCTβ in both the hippocampus and cerebellum (**Figure 5.1)**.

CCTβ expression was also detected in the corpus callosum along with structures throughout the midbrain (data not shown). However, little, if any staining of CCTα was detected throughout the brain **(Figure 5.1)**.

3.2 Cerebellar Localization

IHC analysis indicated region-specific expression of CCTβ throughout the cerebellum **(Figure 5.2A)**, where localization appeared to be predominately in Purkinje cells **(Figure 5.2B)**, a class of inhibitory projection neurons. Further, CCTβ expression appears to be cytosolic within these Purkinje cells **(Figure 5.2B, inset 2)**. Although levels of CCTβ expression are known to be more abundant in the brain, there is little information regarding the cellular localization of CCTβ throughout neural structures. Previously, CCTβ has been reported to be localized outside of the nucleus [6]; however, our IHC analysis indicates region-specific cellular localization throughout the rat brain. While cerebellar CCTβ is cytosolic, IHC analysis indicates nuclear CCTβ expression throughout the peripheral midbrain **(Figure 5.2B, inset 1)**.

3.3 Protein Expression of CCTβ following Cocaine Exposure

Previous studies, including our own [14], have implicated a role for altered phosphatidylcholine (PC) metabolism within the context of addiction. Thus, we examined the effects of cocaine exposure on region-specific CCT protein expression in the hippocampus and cerebellum **(Figures 5.3 & 5.4)**. IHC analysis demonstrated significantly decreased CCTβ expression in the cerebellar Purkinje cell layer **(Figure 5.4)** following cocaine exposure, although no significant change was detected in the

hippocampus **(Figure 5.3)**. Immunoblot analysis of whole tissue samples did not demonstrate altered CCTβ expression between cocaine- and saline-treated rats in either the cerebellum or hippocampus brain regions **(Figure 5.5)**.

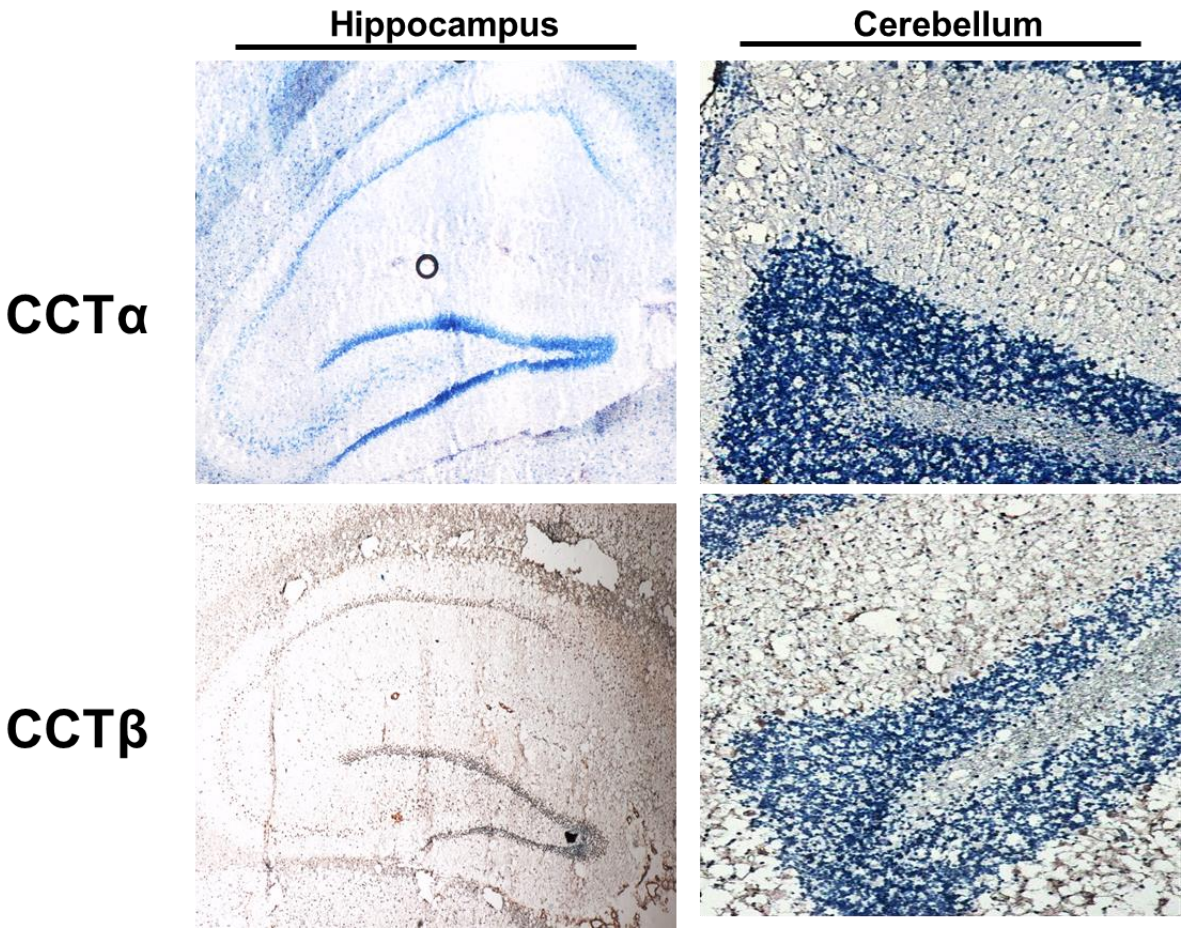

Figure 5.1. Distribution of CCT isoforms throughout the rat brain. Immunohistochemical analysis of 10-μm sagittal sections (magnification: X20) demonstrated detection of CCTβ but not CCTα, in both the hippocampus and cerebellum where positive staining is indicated by DAB (brown). Images are representative of sections analyzed from at least 3 (n = 3) animals.

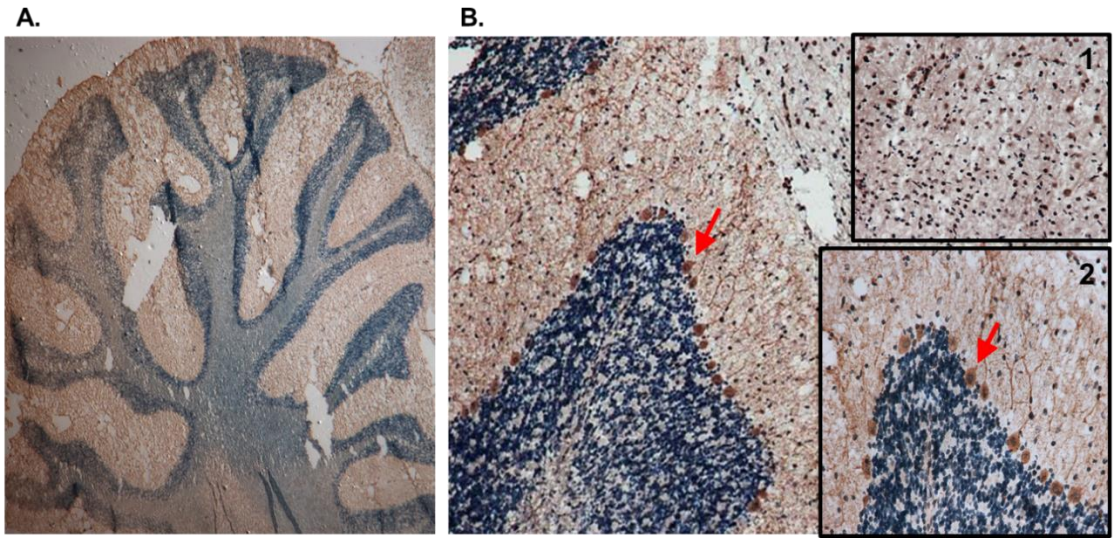

Figure 5.2. Localization of CCTβ in cerebellar Purkinje cells of rat brain. Immunohistochemical analysis (magnification: X20) of 10-μm sagittal sections demonstrated a relatively high expression of CCTβ in Purkinje cells of the cerebellum, which are indicated by red arrows, with enlarged inset view (magnification: X50). Top inset (magnification: X50) indicates nuclear CCT staining throughout peripheral midbrain. Images are representative of sections analyzed from at least 3 (n = 3) separate animals.

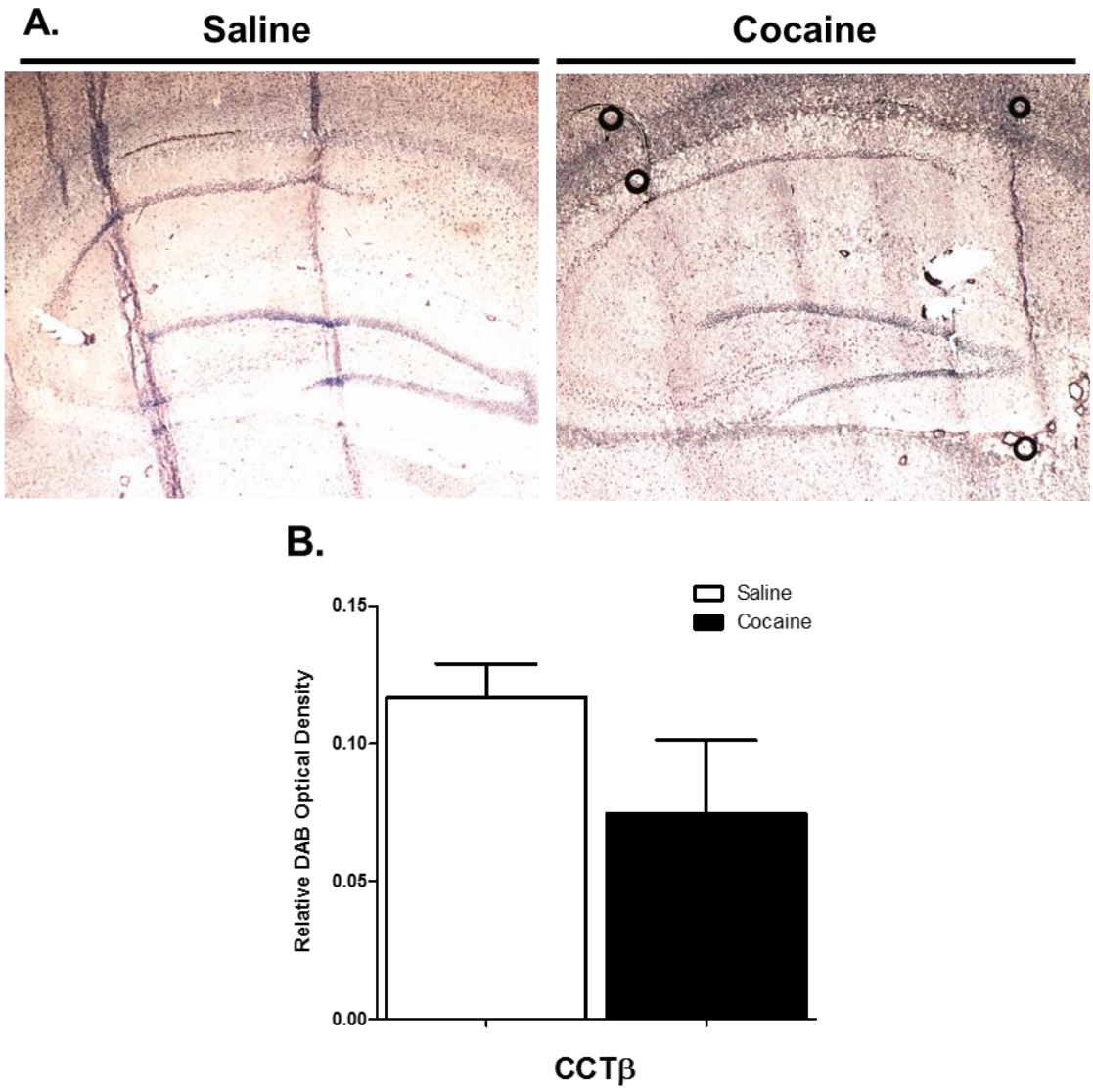

Figure 5.3. Immunohistochemical analysis of cocaine exposure on hippocampal CCTβ expression. (A) IHC was performed on 10-μm sagittal sections to assess CCTβ protein expression in the hippocampus of saline- and cocaine-treated rats (magnification: X20). **(B)** Quantification and image analysis was performed using the ImageJ-based software package FIJI to obtain the relative optical density of DAB staining values. Data indicate results from 3 separate animals (n=3) per group and are expressed as mean values ± SEM.

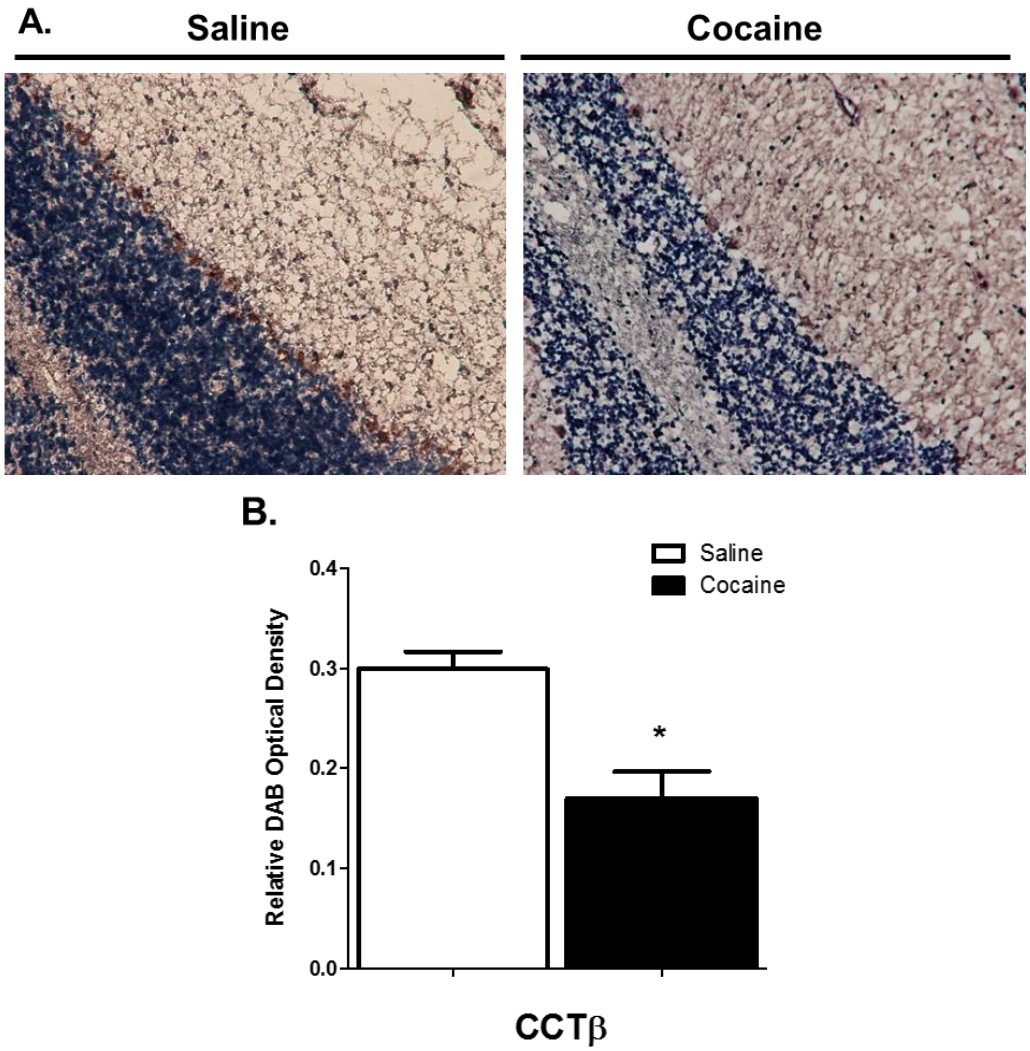

Figure 5.4. Immunohistochemical analysis of cocaine exposure on cerebellar CCTβ expression. (A) IHC was performed on 10-µm sagittal sections to assess CCTβ protein expression in the Purkinje layer of the cerebellum in saline- and cocaine-treated rats (magnification: X20). **(B)** Quantification and image analysis was performed using the ImageJ-based software package FIJI to obtain the relative optical density of DAB staining values. Data indicate results from 3 separate animals (n=3) per group and are expressed as mean values ± SEM. *Indicates a significant difference ($p < 0.05$) as compared to saline control rats.

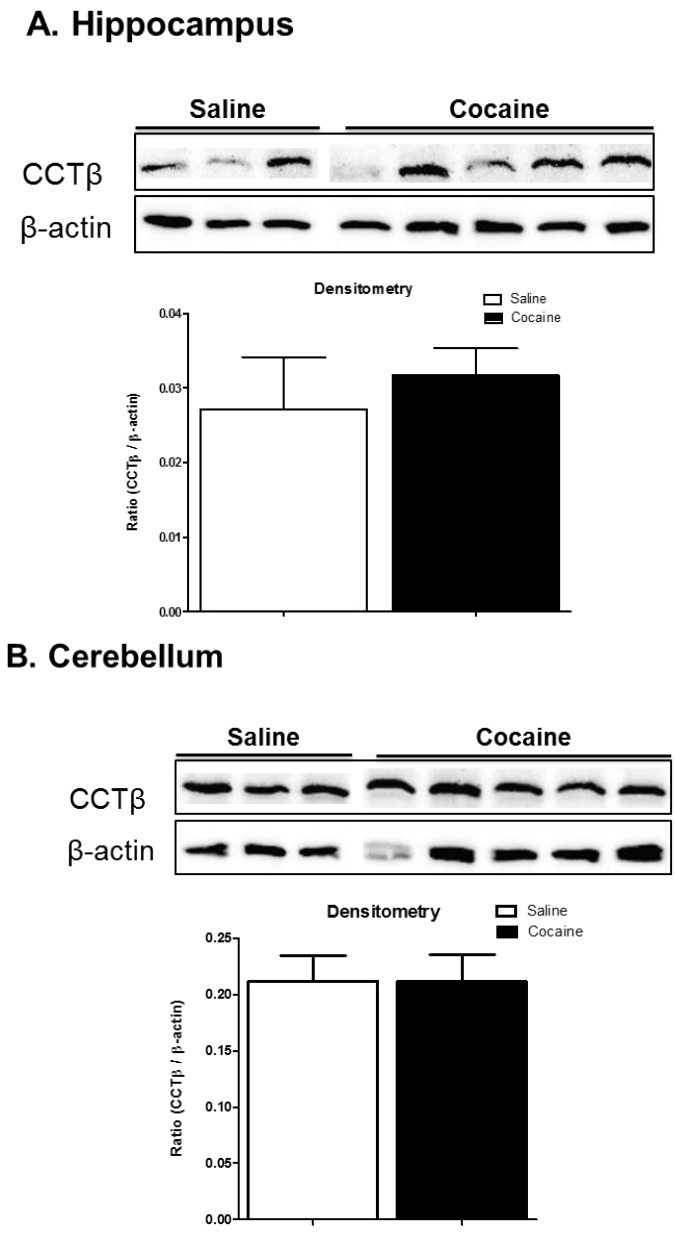

Figure 5.5. Effect of cocaine exposure on hippocampal and cerebellar CCTβ protein expression. CCTβ protein expression was assessed in the **(A)** hippocampus and **(B)** cerebellum of saline- and cocaine-treated rats using immunoblot analysis. Quantitative densitometry is presented as the CCTβ/β-actin ratio. Data indicate results from 3 separate animals (n=3) per group and are expressed as mean values ± SEM.

4. Discussion

CCT, the rate-limiting enzyme in PC synthesis, is responsible for the regulation of PC homeostasis within mammalian cells. CCT has been well studied across various pathologies including neurological disorders such as ischemia and addiction. However, there is little information regarding the basic distribution and cellular localization of CCT isoforms in the rodent brain. Within the context of cocaine dependence, Ross *et al*. reported a reduction of CCT activity in cocaine users [13]. Additionally, we previously demonstrated the effects of cocaine conditioning on region-specific alterations of PC species in the rat brain [14]. With these studies in mind, we examined the expression of the PC synthesis protein, CCT, including both isoforms alpha (CCTα) and beta (CCTβ), as well as region-specific alterations following cocaine exposure.

To our knowledge, this is the first report to use immunohistochemistry to determine the expression of CCTα and CCTβ in the brain as well as to assess its regional distribution. Although significant CCTα was not detected in either the hippocampus of the cerebellum, this does not preclude the possibility that CCTα is expressed in other areas of the rat brain or at different levels compared to CCTβ. This possibility is supported by earlier studies suggesting that rodent brains may contain a mixture of both α and β isoforms, possibly varying in different ratios in different brain regions [10, 25]. The finding that CCTβ is the dominantly expressed isoform within the hippocampus and cerebellum supports the assertion that CCTβ has an essential biological role in the brain [4, 8].

The cytosolic expression of CCTβ in Purkinje cells, which are located between the molecular and granule layers of the cerebellar cortex, was interesting given that its

expression was predominantly nuclear in the hippocampus, corpus callosum, and structures throughout the midbrain. The expression of CCTβ in the cytosol in the cerebellum agrees with previously published studies demonstrating the exclusive cytosolic expression of CCTβ [6]. The nuclear localization of CCTβ is intriguing since CCTβ lacks a NLS and was previously reported to be located outside the nucleus in HeLa cells [6]. These differences cannot be attributed to the CCTβ antibody as the same antibody was used in both studies. These differences may arise due to differences in the cell-types being studied along with the use of tissue for IHC analysis as opposed to cells. It should also be mentioned that HeLa cells are cancerous in origin and the differential expression and localization of CCT isoforms between normal and cancerous tissues is not well known.

Regardless of its nuclear or cytosolic localization, the expression of CCTβ in Purkinje cells raises questions relating to its functional role. As mentioned above, CCT is responsible for regulating PC synthesis. Studies using mass spectrometric imaging with matrix-assisted laser desorption/ionization (MALDI) have reported abundant PC levels in the cerebellum of rodent brains [26, 27]. For example, Sugiura, *et al*. showed that polyunsaturated fatty acid (PUFA)-containing PCs are distributed in cerebellar Purkinje cells [26], while Mikawa, *et al*. reported very high levels of PC 32:0 and PC 34:1 in the molecular layer of the cerebellum [27]. It is possible that higher levels of CCT expression within Purkinje cells is needed to maintain the cellular distribution of these lipids.

The discrepancy between IHC and immunoblot analysis with regard to the persisting effects of cocaine exposure on CCT expression is puzzling. Although IHC

staining demonstrated a decrease in CCTβ expression in the Purkinje cell layer of the cerebellum, this was not supported by immunoblot analysis of the whole cerebellum tissue. Thus, the cellular-specific decrease in CCTβ expression observed within Purkinje cells may not be abundant enough to alter the overall protein expression in the cerebellum when assessed as a whole, which would also include CCTβ expression throughout the molecular and granule layers.

In summary, we have demonstrated the region- and cell-specific localization of CCTα and CCTβ in the rat brain as well as the altered expression of CCTβ in the cerebellum following cocaine exposure. Specifically, we have demonstrated the ubiquitous nuclear expression of the CCTβ throughout the brain with cytosolic expression exclusively in the cerebellar Purkinje layer.

References

[1] R.B. Cornell, N.D. Ridgway, CTP: phosphocholine cytidylyltransferase: Function, regulation, and structure of an amphitropic enzyme required for membrane biogenesis, Progress in lipid research, 59 (2015) 147-171.

[2] D.E. Vance, Phospholipid biosynthesis in eukaryotes, New comprehensive biochemistry, 36 (2002) 205-232.

[3] C. Kent, CTP: phosphocholine cytidylyltransferase, Biochimica et Biophysica Acta (BBA)-Lipids and Lipid Metabolism, 1348 (1997) 79-90.

[4] S. Jackowski, P. Fagone, CTP: phosphocholine cytidylyltransferase: paving the way from gene to membrane, Journal of Biological Chemistry, 280 (2005) 853-856.

[5] M. Karim, P. Jackson, S. Jackowski, Gene structure, expression and identification of a new CTP: phosphocholine cytidylyltransferase β isoform, Biochimica et Biophysica Acta (BBA)-Molecular and Cell Biology of Lipids, 1633 (2003) 1-12.

[6] A. Lykidis, I. Baburina, S. Jackowski, Distribution of CTP: phosphocholine cytidylyltransferase (CCT) isoforms identification of a new CCTβ splice variant, Journal of Biological Chemistry, 274 (1999) 26992-27001.

[7] S.L. Pelech, D.E. Vance, Regulation of phosphatidylcholine biosynthesis, Biochimica et Biophysica Acta (BBA)-Reviews on Biomembranes, 779 (1984) 217-251.

[8] S. Jackowski, J.E. Rehg, Y.-M. Zhang, J. Wang, K. Miller, P. Jackson, M.A. Karim, Disruption of CCTβ2 expression leads to gonadal dysfunction, Molecular and cellular biology, 24 (2004) 4720-4733.

[9] R.M. Adibhatla, J. Hatcher, Cytidine 5′-diphosphocholine (CDP-choline) in stroke and other CNS disorders, Neurochemical research, 30 (2005) 15-23.

[10] J. Bodennec, D. Pelled, C. Riebeling, S. Trajkovic, A.H. Futerman, Phosphatidylcholine synthesis is elevated in neuronal models of Gaucher disease due to direct activation of CTP: phosphocholine cytidylyltransferase by glucosylceramide, The FASEB Journal, 16 (2002) 1814-1816.

[11] J. Strakova, L. Demizieux, R.B. Campenot, D.E. Vance, J.E. Vance, Involvement of CTP: phosphocholine cytidylyltransferase-β2 in axonal phosphatidylcholine synthesis and branching of neurons, Biochimica et Biophysica Acta (BBA)-Molecular and Cell Biology of Lipids, 1811 (2011) 617-625.

[12] P.F. Renshaw, S. Daniels, L.H. Lundahl, V. Rogers, S.E. Lukas, Short-term treatment with citicoline (CDP-choline) attenuates some measures of craving in cocaine-dependent subjects: a preliminary report, Psychopharmacology, 142 (1999) 132-138.

[13] B.M. Ross, A. Moszczynska, F.J. Peretti, V. Adams, G.A. Schmunk, K.S. Kalasinsky, L. Ang, N. Mamalias, S.D. Turenne, S.J. Kish, Decreased activity of brain phospholipid metabolic enzymes in human users of cocaine and methamphetamine, Drug and Alcohol Dependence, 67 (2002) 73-79.

[14] B.S. Cummings, S. Pati, S. Sahin, N.E. Scholpa, P. Monian, P.M. Trinquero, J.K. Clark, J.J. Wagner, Differential effects of cocaine exposure on the abundance of phospholipid species in rat brain and blood, Drug and alcohol dependence, 152 (2015) 147-156.

[15] G. Buzsaki, E.I. Moser, Memory, navigation and theta rhythm in the hippocampal-entorhinal system, Nature neuroscience, 16 (2013) 130-138.

[16] S.R. Vorel, X. Liu, R.J. Hayes, J.A. Spector, E.L. Gardner, Relapse to cocaine-seeking after hippocampal theta burst stimulation, Science, 292 (2001) 1175-1178.
[17] G.F. Koob, N.D. Volkow, Neurocircuitry of addiction, Neuropsychopharmacology : official publication of the American College of Neuropsychopharmacology, 35 (2010) 217-238.
[18] M.J. Wagner, T.H. Kim, J. Savall, M.J. Schnitzer, L. Luo, Cerebellar granule cells encode the expectation of reward, Nature, (2017).
[19] E.A. Moulton, I. Elman, L.R. Becerra, R.Z. Goldstein, D. Borsook, The cerebellum and addiction: insights gained from neuroimaging research, Addiction biology, 19 (2014) 317-331.
[20] J. Moreno-Rius, M. Miquel, The cerebellum in drug craving, Drug and Alcohol Dependence, 173 (2017) 151-158.
[21] K.Y. Xu, Y. Xiong, Z.Q. Xie, W. Bian, N.H. Jing, Y.C. Du, Localization of CCTbeta in rat brain and overexpression in insect cells, Acta pharmacologica Sinica, 23 (2002) 349-354.
[22] N.E. Scholpa, S.B. Briggs, J.J. Wagner, B.S. Cummings, Cyclin-Dependent Kinase Inhibitor 1a (p21) Modulates Response to Cocaine and Motivated Behaviors, Journal of Pharmacology and Experimental Therapeutics, 357 (2016) 56-65.
[23] C.M. Seymour, J.J. Wagner, Simultaneous expression of cocaine-induced behavioral sensitization and conditioned place preference in individual rats, Brain research, 1213 (2008) 57-68.
[24] J. Schindelin, I. Arganda-Carreras, E. Frise, V. Kaynig, M. Longair, T. Pietzsch, S. Preibisch, C. Rueden, S. Saalfeld, B. Schmid, J.-Y. Tinevez, D.J. White, V. Hartenstein,

K. Eliceiri, P. Tomancak, A. Cardona, Fiji: an open-source platform for biological-image analysis, Nat Meth, 9 (2012) 676-682.

[25] Y. Xiong, X.-l. Liu, Y. Wang, Y.-c. Du, Cloning of cytidine triphosphate: phosphocholine cytidylyltransferase mRNA upregulated by a neuropeptide arginine-vasopressin (4–8) in rat hippocampus, Neuroscience letters, 283 (2000) 129-132.

[26] Y. Sugiura, Y. Konishi, N. Zaima, S. Kajihara, H. Nakanishi, R. Taguchi, M. Setou, Visualization of the cell-selective distribution of PUFA-containing phosphatidylcholines in mouse brain by imaging mass spectrometry, Journal of lipid research, 50 (2009) 1776-1788.

[27] S. Mikawa, M. Suzuki, C. Fujimoto, K. Sato, Imaging of phosphatidylcholines in the adult rat brain using MALDI-TOF MS, Neuroscience letters, 451 (2009) 45-49.

CHAPTER 6

LIPIDOMIC CHANGES IN THE RAT BRAIN AND BLOOD AFTER LONG TERM AND REPEATED COCAINE EXPOSURE[1]

[1]Sumitra Pati, Peggi Angel, Richard R. Drake, John J. Wagner, Brian S. Cummings. (2017) To be submitted to *Journal of Lipid Research.*

Abstract

Cocaine-dependence affects millions of individuals worldwide; however, there are no pharmacotherapeutic and/or diagnostic solutions. Recent evidence suggests a role for lipid signaling in the development and maintenance of addiction, highlighting the need to understand how lipid remodeling mediates neuroadaptation after cocaine exposure. This study utilized shotgun lipidomics to assess cocaine-induced lipid remodeling in rats using a novel behavioral regimen that incorporated multiple sessions of extinction and reinstatement. Repeated cocaine exposure selectively altered the relative abundance of specific phospholipids, glycerolipids, and fatty acyl species in the blood. Interestingly, blood lipid profiles demonstrated the greatest differences after a drug-induced reinstatement following a prolonged period of abstinence. Mass spectrometric imaging demonstrated region-specific decreases in phospholipid abundances throughout the brain and high spatial resolution MALDI-FTICR-MS indicated hippocampus-specific phospholipid alterations following cocaine exposure. We analyzed the expression of genes involved in hippocampal lipid metabolism and demonstrate region-specific regulation. In addition, we found that cocaine exposure differentially regulates mitochondrial biogenesis in the brain. This work presents a comprehensive lipidomic assessment of cocaine-induced lipid remodeling in the profiles of rat blood and brain. Further, these findings indicate a potential interplay between CNS energetics and differential lipid regulation and suggest a role for cocaine in the maintenance of energy homeostasis.

Abbreviations: 2,4-Dienoyl-CoA Reductase (Decr1), Acetyl-CoA Acetyltransferase, Acat2), Acyl-CoA Dehydrogenase (Acadl), Acyl-coenzyme A Thioesterase 12 (Acot12), Carnitine Palmitoyltransferase 1C (Cpt1c), Cocaine use disorder (CUD), Conditioned place preference (CPP), Electrospray ionization (ESI), Fatty acyls (FA), Mahalanobis distance (D_M), mass spectrometric imaging (MSI), mass spectrometry (MS), matrix-assisted laser desorption/ionization Fourier-transform ion cyclotron resonance (MALDI-FTICR), mitochondria transcription factor A (Tfam), nuclear respiratory factors (NRFs), peroxisome proliferation-activated receptor coactivator 1 α (PGC-1α), phospholipids (PL), polyunsaturated fatty acids (PUFA).

1. Introduction

Cocaine-dependence is a worldwide public health concern that affects more than a million users in the United States alone *(National Survey on Drug Use and Health)*. Presently, there are no FDA-approved pharmacotherapies available for the treatment of cocaine dependence nor are there early detection strategies for its diagnosis. This highlights the need to search and identify new therapeutic targets as well as markers of exposure and dependence.

Recent studies have suggested roles for lipid signaling in the development and maintenance of addiction [1]. This has led to the hypothesis that a better understanding of lipid signaling can offer new therapeutic targets for cocaine addiction [2]. Lipids are essential biomolecules that play a major role in brain through their participation in signaling, as modulators of synaptic transmission, and are thought to play a role in the synaptic changes that are hypothesized to underlie the process of drug addiction [3].

Several studies have suggested that aberrant lipid metabolism occurs following exposure to drugs of abuse such as cocaine [4-7]. A study in human patients suggested an association between cocaine-dependence and increases in brain phospholipid precursors, suggesting that phospholipids may mediate some of the cocaine-induced effects of dopamine receptor stimulation [8]. Additionally, pathways that stimulate the release of arachidonic acid, such as activators of phospholipase A_2, were shown to exhibit inhibitory effects on dopamine uptake, while dietary deficiency in α-linolenic acid, the precursor of long-chain n–3 polyunsaturated fatty acids (PUFA), altered dopaminergic neurotransmission [6, 7].

Remarkably, studies have reported links between blood lipids and addictive drug use, suggesting that blood lipids may serve as indices of peripheral tissue status for clinical diagnosis and prognosis. Buydens-Branchey and Branchey, *et al*. reported a link between n-6 or n-3 PUFA status and relapse vulnerability in cocaine addicts where early relapsing subjects possessed lower baseline levels of total n-6 PUFAs, linoleic acid, arachidonic acid, and total n-3 PUFAs compared to non-relapsing subjects [4]. The same group also showed an association between low total cholesterol level and relapse rates in detoxified cocaine addicts [5]. Lipid remodeling following cocaine exposure has also been linked with behaviors such as drug relapse and behavioral sensitization [4, 9]. Our prior work was the first to report that cocaine induces region-specific changes in select lipid species in the rat brain and the blood using a preclinical model for behavioral sensitization [9]. Interestingly, many of these blood lipids correlated to locomotor sensitization [9]. Huston, et al. previously suggested a role for the acid sphingomyelinase (ASM)-ceramide pathway in the brain in the involvement of the

learning of extinction behavior [10]. Moreover, the association between blood lipids and neurological dysfunction has also been demonstrated with other neuropathologies including a recent study that identified ten phospholipids in human plasma that can serve as biomarkers for the onset of amnestic mild cognitive impairment or Alzheimer's disease [11].

The above studies suggest that cocaine can induce lipid remodeling, which would correlate with cocaine's ability to induce neuroadaptation. Recent work has also revealed that lipids are also essential for mediating mitochondrial dynamics [12]. These organelles carry critical enzymes for multiple biosynthetic processes including those essential for lipid metabolism [13]. Further, efficient mitochondrial function is essential for proper central nervous system performance. Interestingly, it has been suggested that drugs of abuse may directly influence the mitochondria and that mitochondrial perturbations are involved in the neurological changes associated with drug addiction [14, 15]. In a clinical study, cocaine abusers exhibited altered mitochondrial biogenesis, inhibited oxidative phosphorylation, along with energy consumption and metabolic deficits resulting in neuronal impairment [16]. Although the mechanisms that underlie these drug-induced alterations are not well understood, they suggest the hypothesis that the cocaine exposure mediates alterations to lipid metabolism and mitochondrial function.

Our previous work [9] has led to growing interest [17, 18] for investigating cocaine-induced lipid alterations within specific regions of the brain. The present study assesses the onset and progression of lipid alterations as a framework for lipid remodeling regarding cocaine-induced responses within a rodent model. We utilized shotgun

lipidomics, a powerful approach for comprehensive lipid profiling, and mass spectrometric imaging to elucidate alterations in the rat lipidome along with theirneuroanatomical localization following cocaine exposure. Finally, we investigated the region-specific effects of repeated cocaine exposure on the regulation of fatty acid metabolism and mitochondrial biogenesis.

2. Methods

2.1. Animal Maintenance

Adult (12-13 weeks) male Sprague-Dawley rats (Harlan, Indianapolis, IN, USA) were housed in pairs in clear plastic cages and maintained on a 12-hour light/dark cycle (0700/1900 hours) with food and water available *ad libitum.* Animals were allowed to acclimate to their home cages for at least 1 week and were habituated to handling (3 days) prior to testing. All studies were approved by the University of Georgia Institutional Animal Care and Use Committee and were conducted in accordance with the Guide for the Care and Use of Laboratory Animals.

2.2. Drug

Cocaine hydrochloride was obtained from the National Institutes of Health National Institute on Drug Abuse (RTI International, Research Triangle Park, NC), and was dissolved in 0.9% saline and filter sterilized prior to use. Animals were injected intraperitoneally with either cocaine (15 mg/kg on conditioning days, 10 mg/kg on reinstatement days) or 0.9% saline.

2.3. Conditioned Place Preference Apparatus

Behavioral testing took place in 43.2-cm × 43.2-cm chambers with clear plastic walls and a smooth solid floor (Med Associates Inc., St. Albans, VT), as described previously [19]. Briefly, each chamber was located in a sound-attenuating box equipped with two house lights, ventilation fan, and photo beam banks for horizontal activity detection. Beam breaks were counted using Activity Monitor software (Med Associates, Inc.). A modified open field chamber with two-compartments (Med Associates, Inc.) was used for conditioned place preference (CPP) testing. The chamber was divided into two compartments with a black partition containing a guillotine door. Removal of the door permitted the rat access to either compartment. For conditioning sessions, the door was closed in order to confine the animal's activity. To obtain equal preference between compartments, one compartment contained rod-like steel bar flooring and black plastic walls while the other compartment contained a wire mesh grid floor and transparent walls.

2.4. Conditioned Place Preference Training

The experimental design for the behavioral regimen (**Figure 6.1**) was modified based on that described in previous studies [19, 20]. Reinstatement, extinction, and prolonged abstinence intervals were incorporated to establish a model resembling the pattern of repeat relapse observed in humans. For the place preference assay, rats were first tested in a pretest session (day 4), during which each rat was placed in the lighter/grid floor compartment and the guillotine door was removed, allowing free access to both

compartments for 15 minutes. The time spent in each compartment was measured to ensure that no animals had a strong bias (>65%) toward one side or another.

Conditioning sessions took place for 4 consecutive days (day 5-8). Rats were divided into two groups: saline-treated (*n*=8) and cocaine-treated (*n*=19). Animals were injected with either saline or cocaine (15 mg/kg, I.P.), placed in one of the two insert compartments for 15 minutes, and then returned to their home cage. Four hours later, animals were injected with either saline or cocaine and were confined to the opposite compartment for the second daily conditioning session. After the 4 days of conditioning, the rats underwent a drug-free place preference post-test on experiment day 9.

Extinction and reinstatement are commonly used to model relapse, as reviewed in Aguilar, *et al* [21]. Following the post-test on experiment day 9, rats were injected with saline and allowed to move freely between compartments for 15 minutes. This extinction phase took place for 6 consecutive days (day 10-15) to extinguish place preference. Reinstatement was performed the day following the extinction phase (day 16). The reinstatement day was identical to the post-test session; however, rats were injected with a cocaine prime (10 mg/kg, IP) for drug-induced reinstatement. Following injection, rats were placed in the apparatus and allowed to move freely between compartments for 15 minutes. Following the reinstatement session on day 16, rats were left in their home cage for 30 consecutive days, with weekly handling, for a month-long abstinence period. A repeat drug-induced reinstatement session took place on experiment day 49.

2.5. Tissue Harvesting

Tail vein blood (0.75 mL) was collected on Baseline (day 3), Post-test (day 9), Extinction (day 15), Post-Reinstatement (day 17), Post-Abstinence, 30 days later (day 48), Post-Abstinence Reinstatement (day 50), and Sacrifice (day 57). Following isolation, samples were immediately mixed, by vortexing, with 1 mL of methanol:water (1.0:0.4 v/v) and then placed at -80ºC until lipid extraction. Region-specific brain and liver tissues were extracted 7 days after the final exposure to cocaine, as described previously [19]. Briefly, animals were anesthetized with halothane prior to decapitation in compliance with protocols approved by the University of Georgia Animal Care and Use guidelines. The brain was removed from the cranium and regions of interest were extracted and flash frozen in liquid nitrogen. For immunohistochemical and MALDI-FTICR-MS studies ($n \geq 3$ rats per group), the left hemisphere was placed midline down on a coverslip, flash frozen in liquid nitrogen, and kept at -80°C until cryosectioning.

2.6. Bligh-Dyer Blood Lipid Extraction

Phospholipids were extracted using chloroform and methanol according to the method of Bligh and Dyer [22]. Briefly, blood samples designated for lipidomics analysis were suspended in 1.25 mL of methanol and 1.25 mL of chloroform. Tubes were vortexed for 30 secs, allowed to sit for 10 min on ice, centrifuged (213 x g; 5 min), and the bottom chloroform layer was transferred to a new test tube. The extraction steps were repeated a second time and the chloroform layers combined. The collected chloroform layers were dried under nitrogen, reconstituted with 50 µL of methanol: chloroform (3:1 v/v), and stored at -80°C until analysis.

2.7. Lipid Phosphorus Assay

Lipid phosphorus was quantified using the phosphorus assay *[23]*. 400 µL of sulfuric acid (5M) was added to lipid extracts (10 µL) in a glass test tube, and heated at 180-200°C for 1 hr. 100 µL of 30% H_2O_2 was then added to the tube while vortexing, and heated at 180-200°C for 1.5 hrs. 4.6 mL of reagent (1.1 g ammonium molybdate tetrahydrate in 12.5 mL sulfuric acid in 500 mL ddH_2O) was added and vortexed, followed by 100 µL of 15% ascorbic acid and vortexing. The solution was heated for 7-10 minutes at 100°C, and a 150 µL aliquot was used to measure the absorbance at 830 nm.

2.8. ESI-MS Analysis of Blood Lipids

Lipid extract samples (500 pmol/µl) were prepared by reconstitution in chloroform: methanol (2:1, v/v) and spiked with a commercial mix of internal standards (Avanti Polar Lipids, Inc.). Electrospray ionization mass spectrometry (ESI-MS) was performed as described previously [24-26] using a Trap XCT ion-trap mass spectrometer (Agilent Technologies, Santa Clara, CA) with a nitrogen drying gas flow-rate of 8 L/min at 350ºC and a nebulizer pressure of 30 psi. The scanning range was from 200 to 1000 *m/z* on 5 µL of the sample scanned in positive and negative ion mode for 2.5 min with a mobile phase of acetonitrile: methanol: water (2:3:1) in 0.1% ammonium formate. Samples were run in triplicate runs (n=3) and overlap of confident identifications or most abundant species was defined as the core lipid pool [27]. As described previously [28], qualitative identification of individual phospholipid molecular species was based on their calculated theoretical monoisotopic mass values, subsequent MS/MS analysis, and

their level normalized to either the total ion count (TIC) or the most abundant phospholipid.

MS^{nth} fragmentation was performed on an Agilent Trap XCT ion-trap mass spectrometer equipped with an ESI source. Direct injection from the HPLC system was used to introduce the analyte. The nitrogen drying gas flow-rate was 8.0 L/min at 350°C. The ion source and ion optic parameters were optimized with respect to the positive molecular ion of interest. Initial identification was typically based on the loss of the parent head group followed by subsequent analysis of the lysophospholipid. In the event that neutral loss scanning could not confirm the species, the tentative ID was assigned based on the *m/z* value from literature data and the LIPIDMAPS database (http://www.lipidmaps.org).

2.9. 2-D Imaging with Matrix-Assisted Laser Desorption/Ionization Fourier-Transform Ion Cyclotron Resonance (MALDI-FTICR MS)

Fresh frozen tissue was cryosectioned into sagittal sections (10-12 µm) and thaw mounted on indium tin oxide coated slides. Tissues were sprayed with the matrix 5 mg/mL 2,5-diaminonaphthalene in 90% acetonitrile. Matrix was applied using a TM Sprayer (HTX Imaging) with 10 passes at a 1300 mm/min velocity and spray maintained at 60°C. Images were collected by MALDI-FTICR (7.0 solariX Legacy, Bruker Daltonics) equipped with a Smartbeam2 laser using 200 laser shots per pixel at a 125 µm stepsize. Data were acquired in negative or positive ion mode on the same tissue, offsetting x and y steps by 75 µm. Transients of 1 Mega word were acquired in broadband mode over m/z 200-1800 resulting in an estimated 118,000 resolving power

on tissue at m/z 790 calculated at full width half max (FWHM). Data were visualized in flexImaging 4.1 build 116 (Bruker Daltonics) and analyzed for regional distribution in SCiLS Lab software version 2016b.

2.10. Multivariate Analysis

Multivariate principal component analysis (PCA) was performed on spectral data acquired from blood lipid analysis using MetaboAnalyst 3.0 (http://www.metaboanalyst.ca/). Automatic peak detection and spectrum deconvolution was performed using a peak width set to 0.5. Analysis parameters consisted of interquartile range filtering and sum normalization with no removal of outliers from the dataset. PCA analysis was quantified by calculating the Mahalanobis distance (D_M) value of the distances between the centroids of the clusters as described in [29]. Statistical significance was assessed using the Hotelling's two-sample T^2 statistic and F-value (F_{true}), which was followed by an F-test to determine significance of the separation across scores clustering.

2.11. Feature Selection of Spectral Data

For ESI-MS analysis of blood, features were selected based on volcano plot analysis and were further identified using MS/MS analysis. Significance for volcano plot analysis was determined based on a fold change threshold of 2.00 and $p \leq 0.05$. Following identification, total ion count was used to normalize each parent lipid level, and the change in the relative abundance of that phospholipid species as compared to its

control was determined. This method is standard for lipidomic analysis as reported in our previous studies [24, 26].

For MALDI-FTICR-MS imaging of brain tissue, technical replicate analysis calculated values on all spectra in order to consider technical variability where individual spectra represent technical replicates. The maximum area under the curve (AUC) was obtained based off the receiver operating curve characteristic (ROC) and an ROC cutoff ≥0.7 was used to filter for species that discriminate between biological states. P-values calculated based on the Wilcoxon Rank Sum (WRS) were classified based on a significance rating. Mean intensities from each region and area under the peak are reported per region. Values were normalized to combined total ion current and number of spectral counts, equal to number of pixels, to minimize sampling variability.

2.12. Real-time Quantitative PCR (qPCR)

RNA was isolated region-specifically from flash frozen tissue using the TRIzol (Invitrogen, Carlsbad, CA), which was followed by the RNeasy MinElute Cleanup Kit (Qiagen) according to the manufacturer's instructions. For array analyses, RNA concentration and quality were assessed using the Bioanalyzer 2100 (Aglient Technologies) following the manufacturer's protocol and samples with RNA scores > 8.0 were used for quantitative PCR. First strand cDNA synthesis was performed using the RT^2 First Strand Kit (SABiosciences, Frederick, MD) following the manufacturer's protocol.

Real-time PCR was performed using the RT^2 Profiler^{TM} PCR Array: Rat Fatty Acid Metabolism Plate (SABiosciences^{TM}, Frederick, MD) according to the

manufacturer's instructions and quantitative PCR was carried out using the CFX Connect (BioRad, Hercules, CA). Treatment differences were calculated as a fold change by the $^{\Delta\Delta}$Ct method and normalized by the house-keeping genes Actb, B2m, Hprt1, Ldha, and Rplp1. Unsupervised hierarchical clustering of the dataset was perfomed by clustergram analysis to display a heat map with dendrograms indicating co-regulated genes across groups and samples with using the RT^2 profiler RT-PCR array data analysis software, version 3.5.

Array results were validated with qPCR on altered fatty acid metabolism targets and mitochondrial biogenesis genes. Total RNA (100 ng) was used for cDNA synthesis using the iScript cDNA Synthesis Kit (Biorad, Hercules, CA). cDNA (100 ng) with a 260:280 >1.8 was used for quantitative PCR using iTaq Universal SYBR Green Supermix (BioRad, Hercules, CA) with specific primers (***Table S6.1***).

2.13. Statistical Analyses

All statistical analyses were compiled using GraphPad Prism for windows version 5.04 (GraphPad Software, Inc., La Jolla, CA). For all analysis, the experimental unit was individual subjects and samples obtained from a minimum of 4-5 subjects/group were assessed. For all analyses, significance was set at $p \leq 0.05$ where data are expressed as mean ± SEM based on t-test for pairwise analysis and/or ANOVA analysis (two-factor repeated-measures with Bonferroni *post hoc* test). Pairwise comparisons of data were performed with either an unpaired two-tailed Student's t-test or nonparametric test, depending on the outcomes of normality testing for Gaussian distributions.

3. Results

3.1. Conditioned place preference model

We modified a behavioral model based on that described in previous studies [19, 20] that incorporated reinstatement, extinction, and prolonged abstinence in order to recapitulate the pattern of repeat relapse observed in humans (**Figure 6.1**). Cocaine-treated rats exhibited place preference following conditioning as indicated by more time spent in the designated drug-paired compartment during the CPP Post-test than during the Pretest (**Figure 6.2**). Interestingly, cocaine-treated rats demonstrated varied CPP response, which was stratified into sub-behavioral cohorts such as no, low, and high CPP using CPP scores normalized to Pretest (**Figure 6.2B, 1**). This was performed for subsequent Extinction and Reinstatement assays where animals were divided into *extinction resistant* and *extinguished* CPP as well as *did not reinstate*, *low reinstaters*, and *high reinstaters* CPP, respectively (**Figure 6.2B, 2-4**). The behavioral outcomes from this grouping were used as inclusion criteria for lipidomic analyses.

3.2. Assessment of repeated cocaine exposure on the blood lipidome

Lipid analysis using direct infusion mass spectrometry was performed on rat blood, which was collected and analyzed throughout the conditioned place preference model to elucidate the onset and progression of blood lipid changes. Pairwise multivariate comparisons of cocaine- and saline-treated rat blood lipid profiles were quantified to assess similarities at each time point in the positive and negative ion modes (**Figure 6.3**). As expected, Baseline blood lipid profiles were almost identical across treatment groups as given by a Mahalanobis distance (D_M) close to zero. Post-test and Extinction lipid profiles indicated increased variability between cocaine- and saline-treated rats;

however, this variability slightly diminished by Post-Reinstatement (**Figure 6.3**). Blood lipid profiles regressed to very similar states between cocaine- and saline-treated animals after a 30-day abstinence period (**Figure 6.3**). Interestingly, blood lipid profiles showed striking differences at the Post-Abstinence Reinstatement, and demonstrated the greatest variability across all time points (**Figure 6.3**). However, these lipid alterations did not persist and were not detected at Sacrifice (**Figure 6.3**).

Volcano plot analyses identified significant changes in quite a few lipids at each time point in the positive and negative ion mode (**Table 6.1**). Positively charged lipid species demonstrated a general trend of increased relative abundance in cocaine-treated rats at Post-test, Extinction, and Post-Abstinence Reinstatement (**Table 6.1**). However, this was not observed in the profiles at Reinstatement and Post-Abstinence, 30 days later, in which cocaine-treated rats showed net decreases in the relative abundances of lipid species falling in the range of *m/z* 600-900 (**Table 6.1**). Notably, only two lipid species recurred with significant alterations at multiple time points. These were *m/z* 939.6 and *m/z* 973.7, which showed decreased levels at Reinstatement and Post-Abstinence, 30 days later, and can be classed as triglyceride species based on theoretical *m/z* values Fewer negatively charged lipids were altered; however, like the positive ion mode, the majority of lipids demonstrated a general trend of increases in relative abundance in cocaine-treated rats. Extinction blood lipid profiles were the exception, displaying decreases in the relative abundances of lipids identified in the negative ion mode (**Table 6.1**). *M/z* 941.5 was the only species to be altered at more than one time point, which was elevated in both Reinstatement profiles. This species was also classed as a triglyceride based on its *m/z* value (**Table 6.1**).

3.3. Localization of cocaine-induced brain lipid alterations with mass spectrometric imaging

Low spatial resolution matrix-assisted laser desorption/ionization Fourier-transform ion cyclotron resonance mass spectrometry (MALDI-FTICR-MS) imaging was performed on entire, sagittal brain sections from saline- and cocaine-treated rats to understand relative lipid expression and distribution. This analysis demonstrated decreases in lipid species in the *m/z* range from 700-1000 in cocaine-treated rats as compared to saline controls (**Figure 6.4**). The representative two-dimensional images of spectral data indicate decreases in the relative abundance of lipid species throughout structures such as the cerebellum, hippocampus, striatum, corpus callosum, frontal cortex, and the thalamus (**Figure 6.4**).

3.4. Hippocampus-specific phospholipid alterations following cocaine exposure

High spatial resolution MALDI-FTICR-MS analyses of the hippocampal region showed decreases in lipid abundances for species in the *m/z* range from 700-900 along with a lower molecular weight lipid at *m/z* 455.2113 following cocaine exposure (**Figure 6.5**). Statistical feature identification of hippocampal lipids was based on ROC filtering and *p*-value comparisons between cocaine- and saline-treated rats. Five lipids were significantly decreased in cocaine-treated rats: *m/z* 782.5828, *m/z* 807.5703, *m/z* 815.6987, *m/z* 832.5908, and *m/z* 834.6097 (**Figure 6.5**).

Hippocampus-specific lipid features identified with MS imaging were screened at all time points in rat blood to assess a potential link between blood and brain alterations (**Figure 6.6**). Significant differences were observed in only two lipids, with decreased

levels of *m/z* 782.5828 and *m/z* 807.5703 as compared to controls, in Post-Abstinence, 30 days later (day 48) profiles (**Figure 6.6**).

3.5. Effect of cocaine exposure on fatty acid metabolism regulation

Although we demonstrate brain region-specific decreases in PL abundance following repeat cocaine exposure, lipidomic analyses did not indicate fatty acid alterations that would accompany PL lipid remodeling. This phenomenon suggested a potential role for perturbed regulation of genes involved in fatty acid metabolism. We analyzed the gene expression of hippocampal fatty acid metabolism using a gene expression array of tissue comparing cocaine- and saline-treated rats. Based on the expression of 84 fatty acid metabolism genes (**Figure 6.7**), a pattern of upregulation was observed in 68 genes in the hippocampal tissue of cocaine-treated rats with respect to saline-treated controls (***Table S6.2***). Sixteen genes were downregulated in cocaine-treated rats, many of which with regulatory functions for protein kinases and fatty acid transporters, e.g. members of the solute carrier family (***Table S6.2***). Protein class and cellular compartmentalization was also determined for the upregulated genes via biological function analyses (http://www.pantherdb.org), indicating that many of the upregulated genes encode for transferase proteins, specifically acetyltransferases (**Figure 6.8A**), several of which are mitochondrial (**Figure 6.8B**).

Significantly altered genes identified from the hippocampal array analyses were individually validated with qPCR (**Figure 6.9**). These genes consisted of: (1) Carnitine Palmitoyltransferase 1C (Cpt1c), (2) Acyl-CoA Dehydrogenase (Acadl), (3) Acetyl-CoA Acetyltransferase (Acat2), (4) 2,4-Dienoyl-CoA Reductase (Decr1), and (5). Acyl-

coenzyme A Thioesterase 12 (Acot12). qPCR analyses of these genes (**Figure 6.9A**) confirmed findings from the array analysis, while analysis of gene expression in the cerebellum (**Figure 6.9B**) demonstrated a significant ~2-fold downregulation of the Acat2 gene in cocaine-treated rats. The effects of cocaine exposure were also assessed in peripheral liver tissue (**Figure 6.9C**) of the 5 targets identified in the brain. These data showed a trend of numerical decreases, with significant downregulation of the Acadl gene following cocaine exposure, and undetected expression of Cpt1c (**Figure 6.9C**).

3.6. Regulation of mitochondrial biogenesis in the brain and liver following cocaine exposure

We assessed the effect of repeated cocaine exposure on mitochondrial biogenesis, the growth and division of pre-existing mitochondria to accommodate increases in ATP production as a response to greater energy expenditure [30]. Specifically, we assessed markers of mitochondrial biogenesis, a highly regulated process mediated by peroxisome proliferation-activated receptor coactivator 1 α (PGC-1α), PGC-1α-dependent nuclear respiratory factors (NRFs), and mitochondria transcription factor A (Tfam). Gene expression of these markers were all significantly upregulated in the hippocampus in cocaine-treated rats (**Figure 6.10A**). This was not paralleled in the cerebellum, which indicated a trend of numerical decreases in tissue from cocaine-treated rats (**Figure 6.10B**). Remarkably, these genes were all significantly downregulated in the liver following cocaine exposure with the most pronounced decrease in PGC-1α (**Figure 6.10C**).

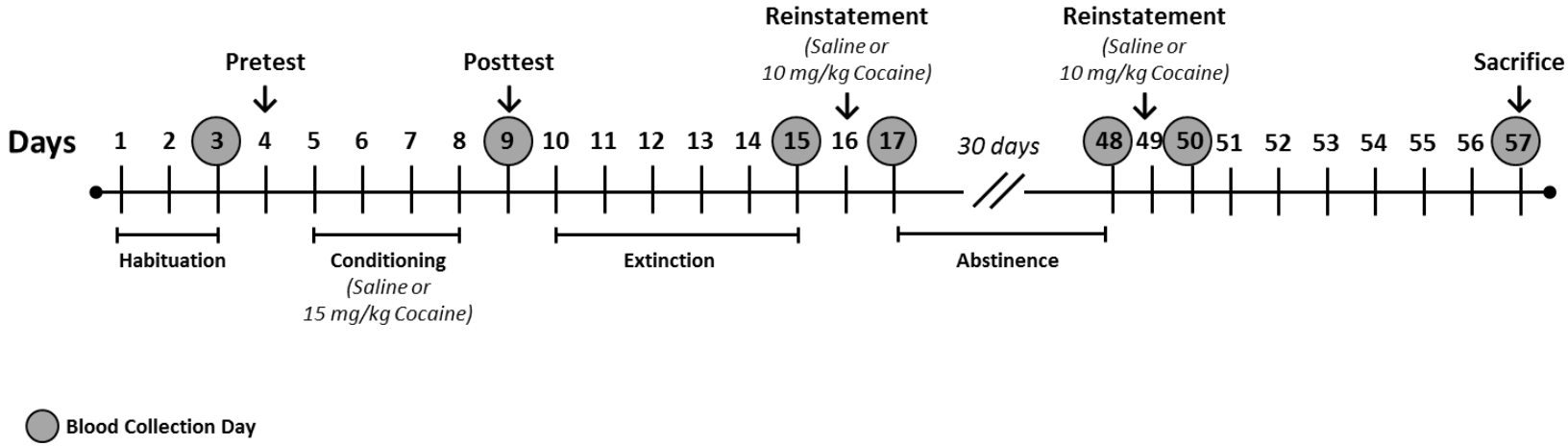

Figure 6.1. Non-contingent behavioral and drug exposure protocol. Gray shaded circles indicate blood collection via tail vein. Reinstatement, extinction, and prolonged abstinence intervals were incorporated to model the pattern of repeat relapse observed in humans. Shaded circles indicate days on which tail vein blood was isolated from saline- and cocaine-treated rats.

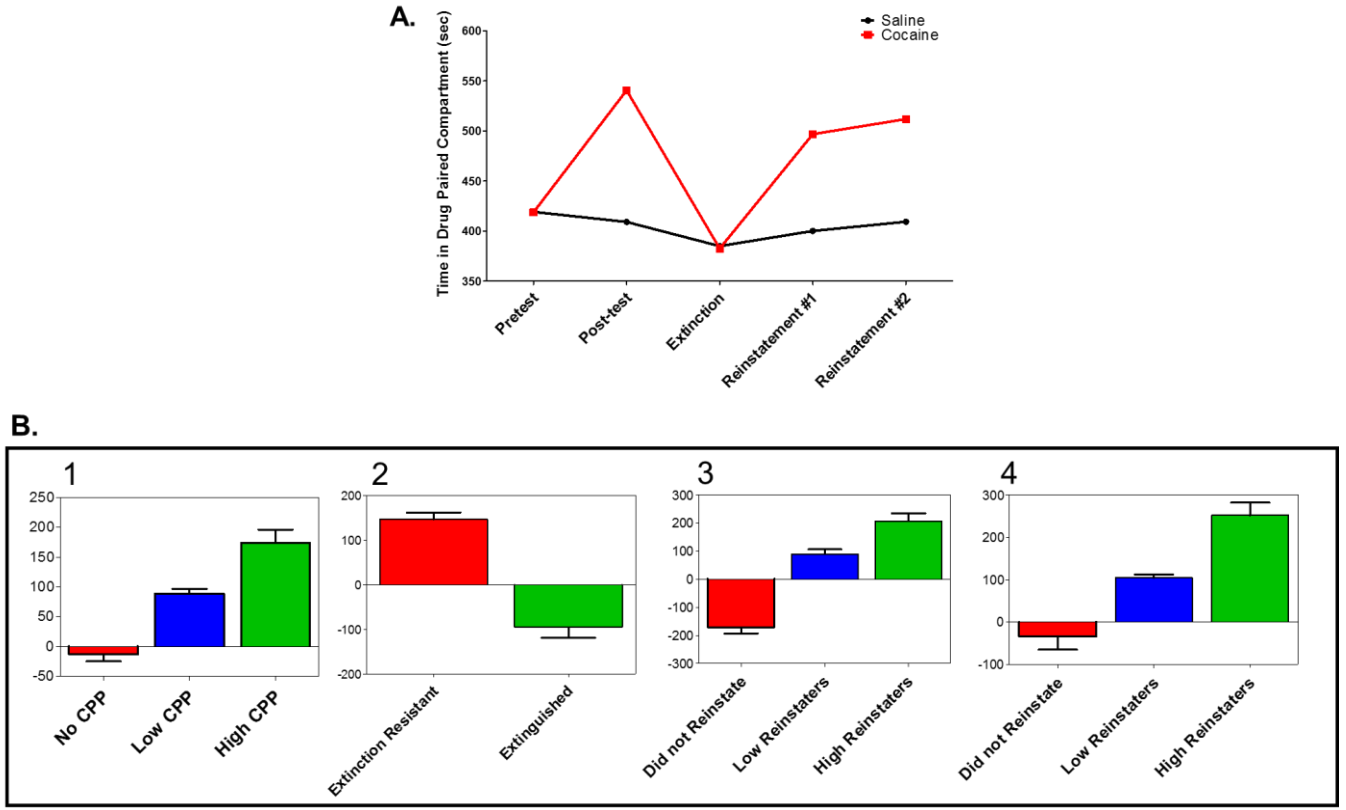

Figure 6.2. Effect of cocaine on conditioned place preference. Rats were injected i.p. with either saline or cocaine under conditions shown to induce conditioned place preference (CPP). (A) Cocaine-induced CPP was examined in saline- and cocaine-treated rats. Behavioral data are indicative of a total of 8 saline-treated (n=8) and 19 cocaine-treated (n=19) rats. (**B)** Pretest performance was subtracted from subsequent assays to obtain CPP scores and animals were stratified based on varied behavioral response during (1) Post-test, (2) Extinction, (3) Reinstatement #1, and (4) Reinstatement #2. Animal cohorts represented are expressed as mean ± SEM.

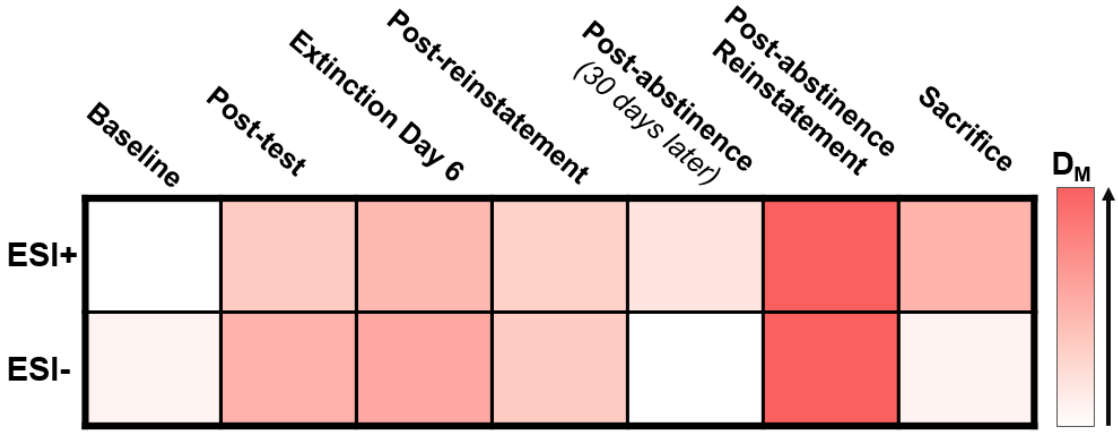

Figure 6.3. Color scale representation of multivariate analysis of blood lipids. Rats were injected i.p. with either saline or cocaine as described previously. Blood was collected on Baseline (day 3), Post-test (day 9), Extinction (day 15), Post-Reinstatement (day 17), Post-Abstinence, 30 days later (day 48), Post-Abstinence Reinstatement (day 50), and Sacrifice (day 57). Lipids were extracted using the Bligh-Dyer method and subsequent principal component analysis (PCA) of mass spectrometric blood lipid data was performed to assess pairwise comparisons of saline- and cocaine-treated rats. Similarities between blood lipid profiles were calculated and are represented with a color scale based on the Mahalanobis distance (D_M) values obtained from principal components 1 and 2 from generated PCA scores plots. Positive ion mode analysis is represented by ESI+ ***(top row)*** and negative ion mode analysis is represented by ESI- ***(bottom row)***. The data are indicative of at least 8 different rats per group.

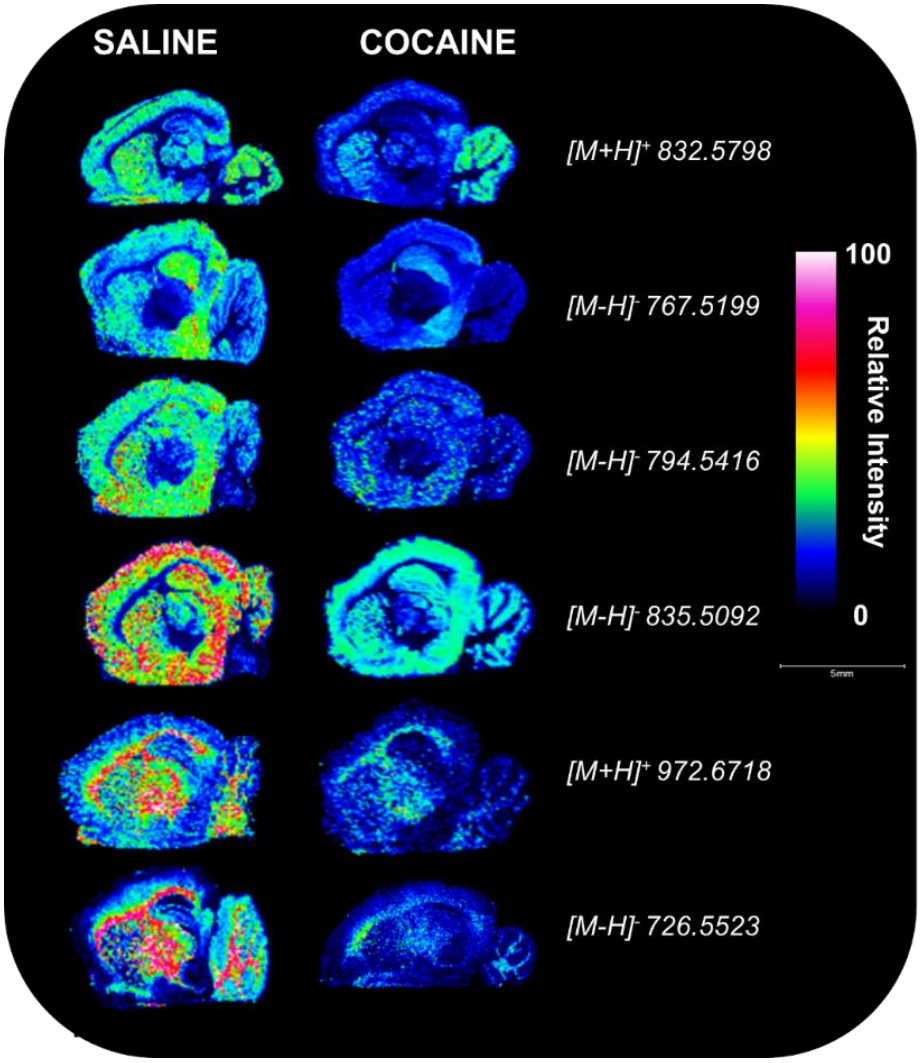

Figure 6.4. Differential abundance and distribution of phospholipid species throughout the rat brain following cocaine exposure with MALDI-FTICR-MS analysis. Rats were injected i.p. with either saline or cocaine as described previously. The left-brain hemisphere was extracted seven days after the final treatment (day 57) and sagittal sections were analyzed by MALDI-FTICR-MS analysis. Sections were assessed from saline-treated ***(left)*** and cocaine-treated ***(right)*** rats. Representative images are shown from each group to illustrate trends observed in tissue sections from at least 3 different rats. Color scale represents the relative intensity normalized to total ion count. Scale bar: 5 mm.

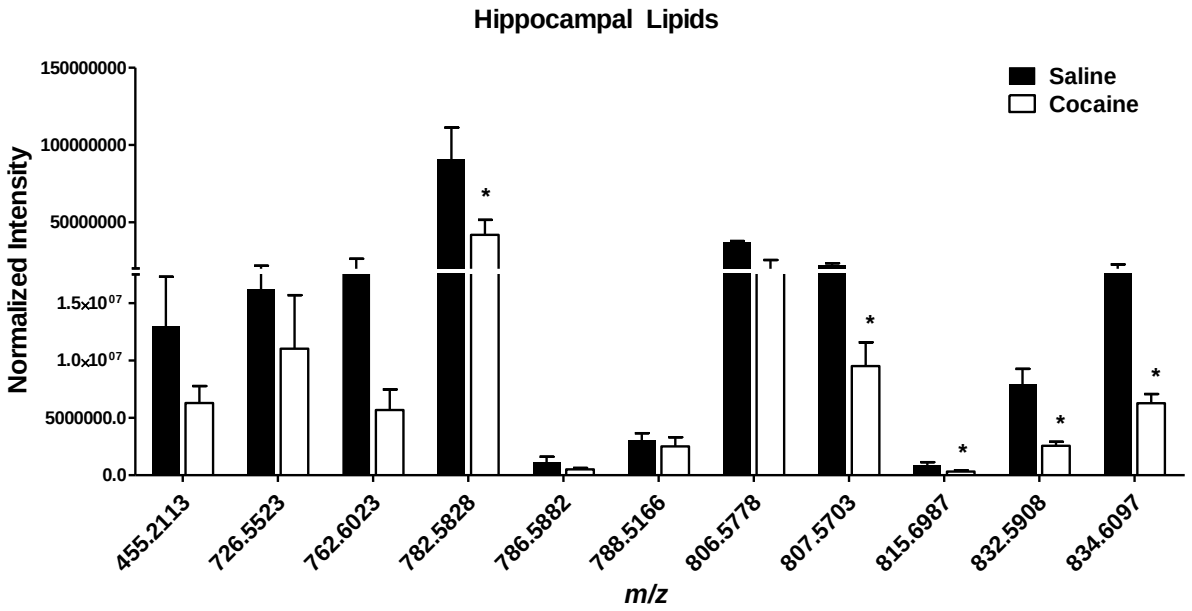

Figure 6.5. Normalized abundance of hippocampus-specific lipid features altered following cocaine exposure. Rats were injected i.p. with either saline or cocaine as described previously. The left-brain hemisphere was extracted seven days after the final treatment (day 57) and sagittal sections were analyzed by MALDI-FTICR-MS analysis. Mean intensities from each region and area under the peak were obtained from high-spatial resolution MALDI-FTICR-MS analysis of the hippocampus and normalized to combined total ion current and number of spectral counts, equal to number of pixels. Features were filtered based on an ROC cutoff ≥0.7 and/or p-value≤0.05 (*Indicates a significant difference based on both ROC and p-value as compared to saline-treated rats). The data are presented as the mean ± SEM of tissue sections from at least 3 different rats.

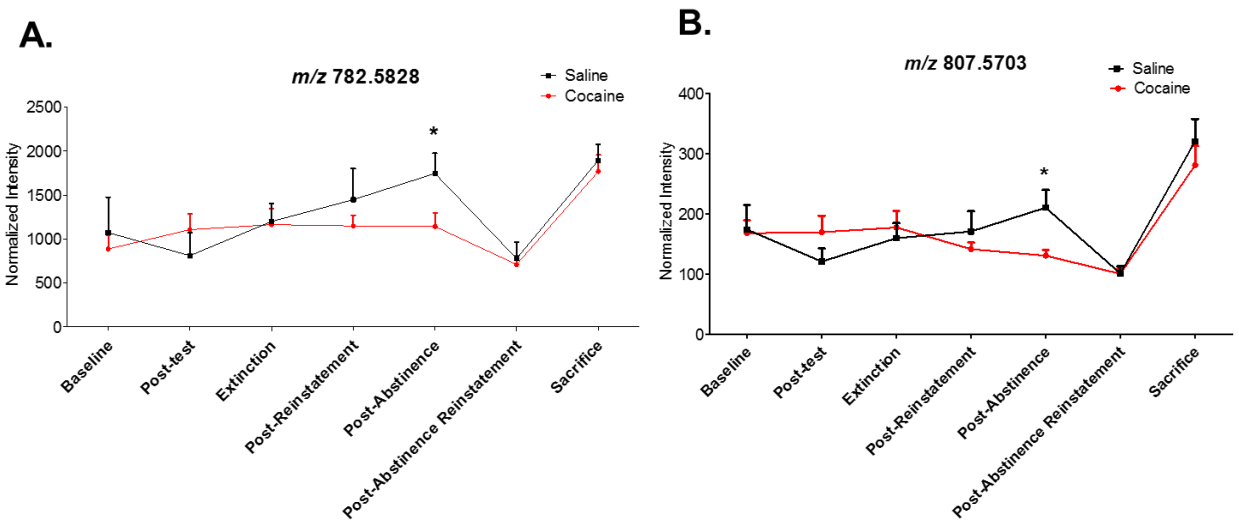

Figure 6.6. Effect of cocaine exposure on relative abundances of blood lipid features identified from high-spatial resolution analysis of the hippocampus. Rats were injected i.p. with either saline or cocaine as described previously. Blood was collected on Baseline (day 3), Post-test (day 9), Extinction (day 15), Post-Reinstatement (day 17), Post-Abstinence, 30 days later (day 48), Post-Abstinence Reinstatement (day 50), and Sacrifice (day 57). Lipids were extracted using the Bligh-Dyer method and subsequent ESI-MS analysis. Hippocampus-specific lipid features identified using MALDI-FTICR-MS were screened in rat blood, which indicated significant differences in **A.** *m/z* 782.5828 and **B.** *m/z* 807.5703 on day 48 (Post-Abstinence, 30 days later). The data are presented as the mean ± SEM of at least 8 different rats. *Indicates a significant difference ($p < 0.05$) as compared to saline-treated rats.

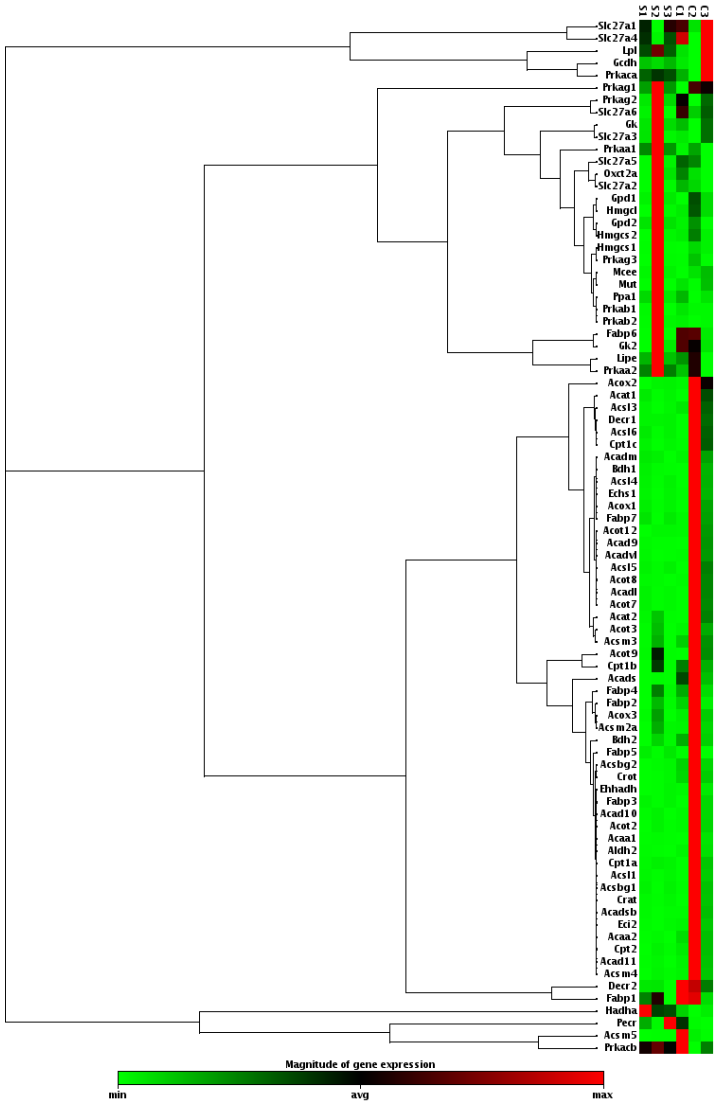

Figure 6.7. Clustergram analysis and heatmap of gene expression data. Hippocampal expression of 84 fatty acid metabolism-related genes are represented as a heatmap graph with genes clustered according to their expression patterns. Rats were injected i.p. with either saline or cocaine as described previously. Hippocampal tissue was extracted from the right-brain hemisphere seven days after the final treatment and assessed for mRNA expression of an 84-set list of genes related to fatty acid metabolism using qPCR. The data are indicative of tissue from at least 3 different rats per group.

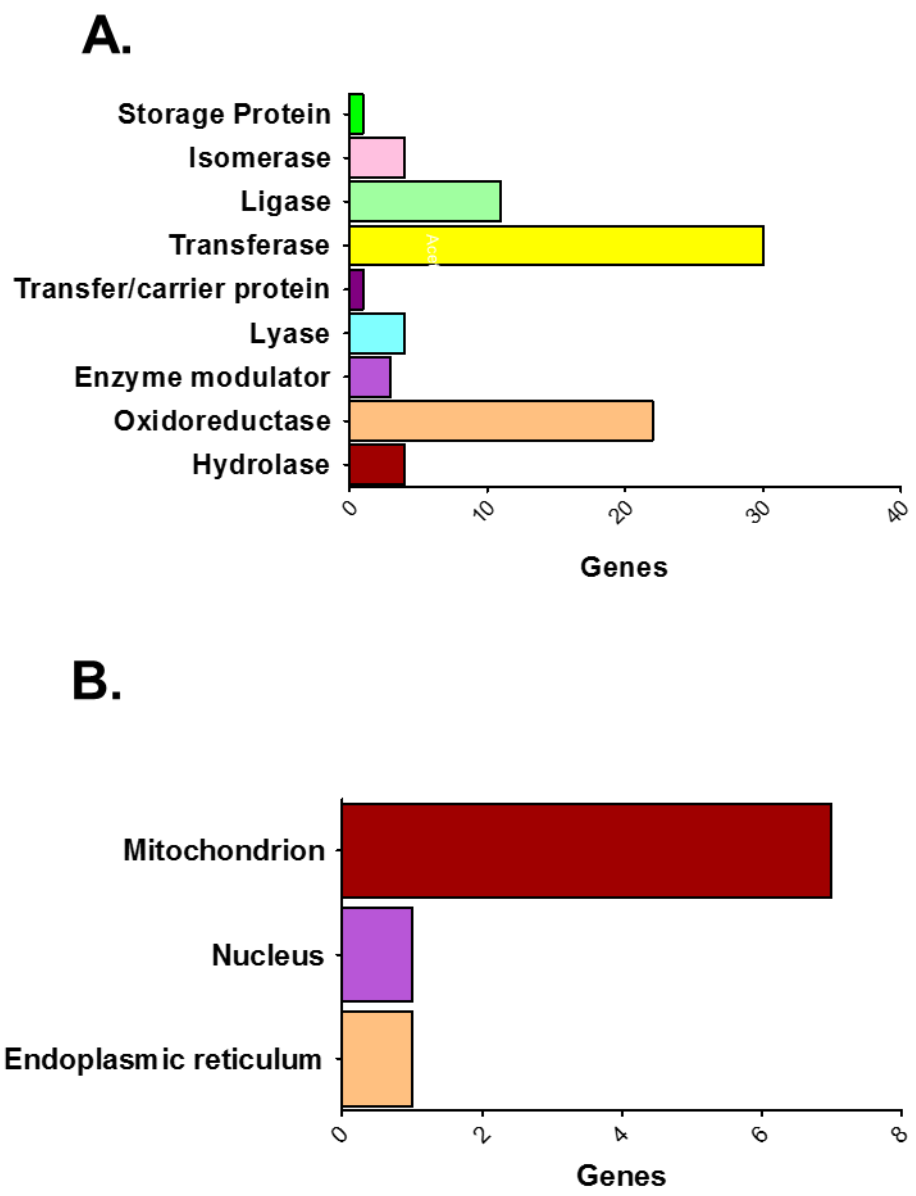

Figure 6.8. Pathway analysis of upregulated genes in the rat hippocampus following cocaine exposure. The PANTHER database was used to analyze the list of fatty acid metabolism-related genes that were upregulated in the rat hippocampus to identify **A.** protein class and **B.** cellular compartmentalization.

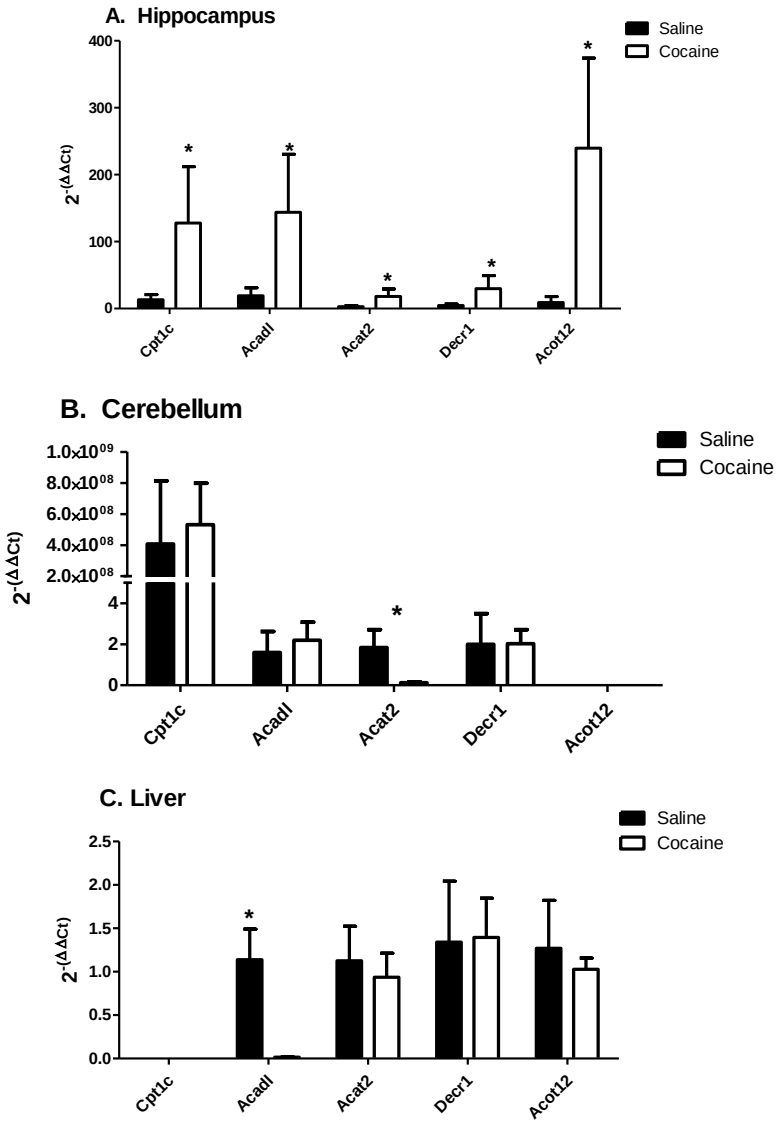

Figure 6.9. Effect of cocaine exposure on genes related to fatty acid metabolism in the rat brain and liver. The indicated tissues were extracted seven days after the final treatment and assessed for mRNA expression of Carnitine Palmitoyltransferase 1C (Cpt1c), Acyl-CoA Dehydrogenase (Acadl), Acetyl-CoA Acetyltransferase (Acat2), 2,4-Dienoyl-CoA Reductase (Decr1), and Acyl-coenzyme A Thioesterase 12 (Acot12) in the **A.** hippocampus, **B.** cerebellum, and **C.** liver using qPCR. The data are indicative of tissue from at least 3 different rats per group and are expressed as $2^{-(\Delta\Delta Ct)}$ ± SEM ΔCt. *Indicates a significant difference ($p < 0.05$) as compared to saline-treated controls.

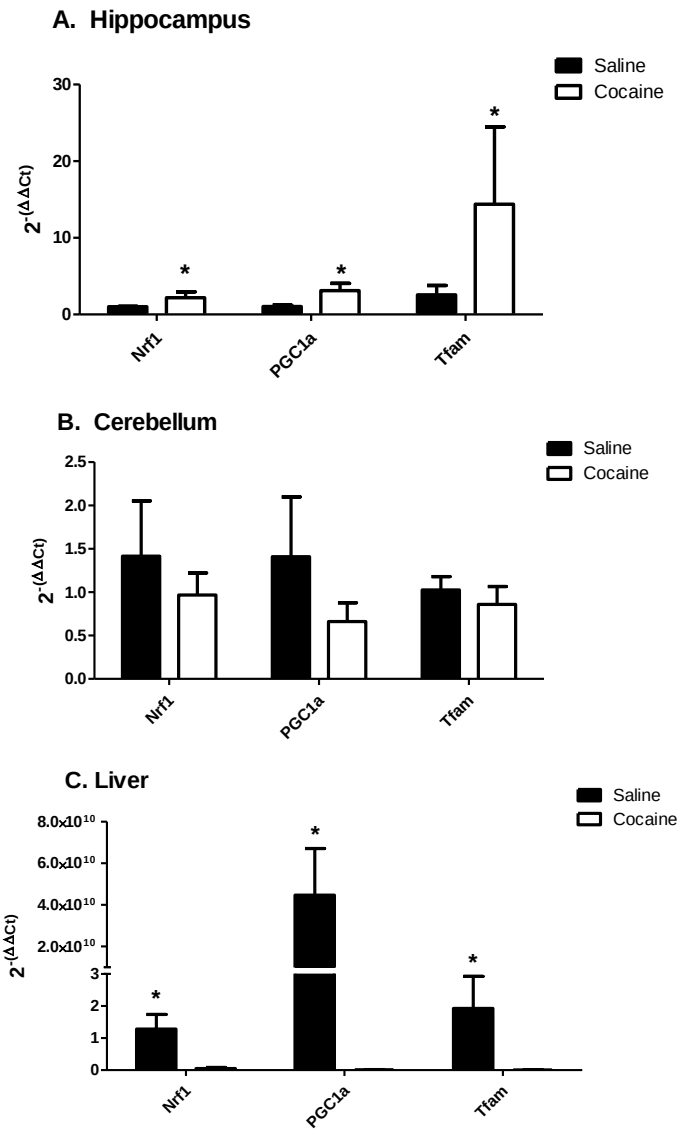

Figure 6.10. Effect of cocaine exposure on mitochondrial biogenesis genes in the rat brain and liver. The indicated tissues were extracted seven days after the final treatment and assessed for mRNA expression of Nuclear respiratory factor 1 (Nrf1), Peroxisome proliferator-activated receptor gamma coactivator 1-alpha (PGC-1α), and transcription factor A, mitochondrial (Tfam) in the **A.** hippocampus and **B.** cerebellum using qPCR. The data are indicative of tissue from at least 3 different rats per group and are expressed as $2^{-(\Delta\Delta Ct)}$ ± SEM ΔCt. *Indicates a significant difference ($p < 0.05$) as compared to saline-treated controls.

Table 6.1. **Effect of cocaine on differential lipid feature abundance in rat blood**. Rats were injected i.p. with either saline or cocaine as described previously. Blood was collected on Baseline (day 3), Post-test (day 9), Extinction (day 15), Post-Reinstatement (day 17), Post-Abstinence, 30 days later (day 48), and Post-Abstinence Reinstatement (day 50). Significant lipid features were identified from volcano plot analysis of spectral data, which are presented as a fold change (FC) comparing the cocaine to saline ratio, and are indicative of blood from at least 8 different rats. FC cells are colored according to differential abundance: Yellow, increased FC>1.5; Blue, decreased FC<-1.5; White, FC≈1.

Day	*m/z*	FC	p-value	ESI Mode	Lipid Class
Post-test	465.2	-1.05	1.07E-03	+	FA
	467.1	1.63	2.75E-03	-	FA
	562.3	2.68	2.05E-02	+	SL
	615.1	1.26	2.46E-02	-	GL
	640.4	1.39	7.64E-05	+	SL
	659.4	1.14	3.63E-03	+	GL
	936.6	1.31	3.02E-02	+	FA
	996.7	1.18	2.65E-04	+	GL
Extinction	353.1	34.30	2.13E-02	+	FA
	397.2	47.99	9.56E-03	+	FA
	409.2	1.30	2.41E-03	+	FA
	441.2	1.11	1.50E-03	+	FA
	677.4	-1.10	4.63E-02	-	GL
	930.8	-1.14	2.63E-03	-	GL
	962.5	-1.02	1.61E-03	-	PL
Post-Reinstatement	604.3	-1.54	1.36E-02	+	GL
	621.2	-1.02	3.00E-02	-	GL
	864.4	-1.37	2.87E-03	-	PL
	875.7	-2.13	1.32E-02	+	GL
	876.7	-2.38	1.85E-02	+	GL

	900.7	-2.38	2.13E-02	+	PL
	938.6	-1.45	3.63E-04	+	FA
	939.6	-1.28	1.41E-04	+	GL
	940.6	-1.10	3.13E-08	+	FA
	941.5	1.02	2.29E-02	-	GL
	965.6	-1.25	1.64E-03	+	GL
	973.7	-1.18	1.80E-02	+	GL
Post-Abstinence (30 days)	222.7	2.14	2.27E-02	-	FA
	223.7	1.71	1.91E-02	-	FA
	622.4	-50.00	3.02E-02	+	PL
	637.4	35.68	1.30E-02	+	GL
	647.5	-1.08	4.24E-02	+	GL
	656.4	38.68	1.45E-02	+	PL
	668.5	43.65	2.29E-03	+	SL
	939.6	-1.39	1.53E-03	+	GL
	973.7	-1.30	4.21E-02	+	GL
Post-Abstinence Reinstatement	312.9	1.01	1.55E-02	-	FA
	462	1.02	1.07E-02	-	FA
	608.2	1.02	1.05E-02	-	SL
	616.1	4.11	1.64E-02	+	GL
	617.1	3.77	1.83E-02	+	GL
	636.2	1.29	1.99E-02	-	PL
	651.3	1.82	4.74E-02	+	GL
	660.1	5.14	1.81E-02	-	PL
	661.1	2.69	1.74E-02	-	GL
	867	1.94	4.59E-02	-	PL
	941.5	1.09	2.19E-02	-	GL
	970.6	1.36	3.08E-05	+	GL
	972.7	-1.08	4.92E-02	+	GL

*PL, phospholipid; FA, fatty acyl; GL, glycerolipid; SL, sphingolipid.

Table S6.1. Primer sequences for fatty acid metabolism and mitochondrial biogenesis genes.

Gene Name		Primer Sequence
Nrf1	Sense	5’-CCT CTG GGC TGT TGT GAA TTA
	Anti-sense	3’-GTC CGA GTC ATC GTA AGA AGT G
Tfam	Sense	5’-TGA AGT TCT TAC ACT GAT GGC
	Anti-sense	3’-CCA CGT CAT CTA GTA AAG CC
PGC-1α	Sense	5’-AGG CTC AAG AGG GAC GAA TA
	Anti-sense	3’-CAC AGG TGT AAC GGT AGG TAA TG
Acadl	Sense	5’-TGA TTC CCT ACC ACG AAG AAT G
	Anti-sense	3’-GAG AAT CCA ATC ACT CCC AGA C
Acat2	Sense	5’-GGA CCG ATT CCA GCC ATA AA
	Anti-sense	3’-GGT GTG TAA CAA GGT CAC TAG AA
Decr1	Sense	5’-GTG ACG TTC GAG ATC CTG ATA TG
	Anti-sense	3’-ATA GGC CCT GGC TGA ATT ATG
Acot12	Sense	5’-CCA CCA CCT TGG AGA AGA TAA A
	Anti-sense	3’-CAC CGA GCA GGT GAT GTA AT
Cpt1c	Sense	5’-GAC TGG TGG GAA GAG TTT GT
	Anti-sense	3’-GAC GAT GAG GGT GAA GGA TTT
β-actin	Sense	5’-CAC CCG CGA GTA CAA CCT T
	Anti-sense	3’-CCC ATA CCC ACC ATC ACA CC

Table S6.2. Fold change for expression analysis of rat fatty acid metabolism genes. Fold change (FC) analysis was performed based on the FC of $2^{-(\Delta\Delta Ct)}$ values comparing cocaine- and saline-treated rats. The data are indicative of tissue from at least 3 different rats per group.

Symbol	Description	Fold Change
Acaa1	Acetyl-Coenzyme A acyltransferase 1A	5.30
Acaa2	Acetyl-Coenzyme A acyltransferase 2	4.63
Acad10	Acyl-Coenzyme A dehydrogenase family, member 10	4.70
Acad11	Acyl-Coenzyme A dehydrogenase family, member 11	7.43
Acad9	Acyl-Coenzyme A dehydrogenase family, member 9	10.10
Acadl	Acyl-Coenzyme A dehydrogenase, long-chain	7.53
Acadm	Acyl-Coenzyme A dehydrogenase, C-4 to C-12 straight chain	5.31
Acads	Acyl-Coenzyme A dehydrogenase, C-2 to C-3 short chain	8.57
Acadsb	Acyl-Coenzyme A dehydrogenase, short/branched chain	3.79
Acadvl	Acyl-Coenzyme A dehydrogenase, very long chain	8.87
Acat1	Acetyl-coenzyme A acetyltransferase 1	4.84
Acat2	Acetyl-Coenzyme A acetyltransferase 3	6.37
Acot12	Acyl-CoA thioesterase 12	26.27
Acot2	Acyl-CoA thioesterase 2	9.37
Acot3	Acyl-CoA thioesterase 3	7.52
Acot7	Acyl-CoA thioesterase 7	8.67
Acot8	Acyl-CoA thioesterase 8	6.25
Acot9	Acyl-CoA thioesterase 9	7.94
Acox1	Acyl-Coenzyme A oxidase 1, palmitoyl	4.70
Acox2	Acyl-Coenzyme A oxidase 2, branched chain	17.41
Acox3	Acyl-Coenzyme A oxidase 3, pristanoyl	5.09
Acsbg1	Acyl-CoA synthetase bubblegum family member 1	2.82
Acsbg2	Acyl-CoA synthetase bubblegum family member 2	13.78

Acsl1	Acyl-CoA synthetase long-chain family member 1	3.26
Acsl3	Acyl-CoA synthetase long-chain family member 3	10.42
Acsl4	Acyl-CoA synthetase long-chain family member 4	5.11
Acsl5	Acyl-CoA synthetase long-chain family member 5	6.30
Acsl6	Acyl-CoA synthetase long-chain family member 6	5.85
Acsm2a	Acyl-CoA synthetase medium-chain family member 2	14.05
Acsm3	Acyl-CoA synthetase medium-chain family member 3	6.54
Acsm4	Acyl-CoA synthetase medium-chain family member 4	9.30
Acsm5	Acyl-CoA synthetase medium-chain family member 5	43.92
Aldh2	Aldehyde dehydrogenase 2 family (mitochondrial)	4.46
Bdh1	3-hydroxybutyrate dehydrogenase, type 1	3.65
Bdh2	3-hydroxybutyrate dehydrogenase, type 2	3.97
Cpt1a	Carnitine palmitoyltransferase 1a, liver	4.49
Cpt1b	Carnitine palmitoyltransferase 1b, muscle	4.96
Cpt1c	Carnitine palmitoyltransferase 1c	9.64
Cpt2	Carnitine palmitoyltransferase 2	8.43
Crat	Carnitine acetyltransferase	4.63
Crot	Carnitine O-octanoyltransferase	6.10
Decr1	2,4-dienoyl CoA reductase 1, mitochondrial	6.59
Decr2	2,4-dienoyl CoA reductase 2, peroxisomal	2.88
Echs1	Enoyl Coenzyme A hydratase, short chain, 1, mitochondrial	3.05
Eci2	Enoyl-Coenzyme A delta isomerase 2	3.57
Ehhadh	Enoyl-Coenzyme A, hydratase/3-hydroxyacyl Coenzyme A dehydrogenase	6.60
Fabp1	Fatty acid binding protein 1, liver	-1.87
Fabp2	Fatty acid binding protein 2, intestinal	2.52
Fabp3	Fatty acid binding protein 3, muscle and heart	2.42
Fabp4	Fatty acid binding protein 4, adipocyte	2.33
Fabp5	Fatty acid binding protein 5, epidermal	1.30
Fabp6	Fatty acid binding protein 6, ileal	4.98
Fabp7	Fatty acid binding protein 7, brain	1.94

Gcdh	Glutaryl-Coenzyme A dehydrogenase	2.59
Gk	Glycerol kinase	-2.17
Gk2	Glycerol kinase 2	2.10
Gpd1	Glycerol-3-phosphate dehydrogenase 1 (soluble)	1.38
Gpd2	Glycerol-3-phosphate dehydrogenase 2, mitochondrial	-4.28
Hadha	Hydroxyacyl-Coenzyme A dehydrogenase/3-ketoacyl-Coenzyme A thiolase/enoyl-Coenzyme A hydratase (trifunctional protein), alpha subunit	-10.52
Hmgcl	3-hydroxymethyl-3-methylglutaryl-Coenzyme A lyase	2.73
Hmgcs1	3-hydroxy-3-methylglutaryl-Coenzyme A synthase 1 (soluble)	1.86
Hmgcs2	3-hydroxy-3-methylglutaryl-Coenzyme A synthase 2 (mitochondrial)	1.97
Lipe	Lipase, hormone sensitive	-2.77
Lpl	Lipoprotein lipase	1.32
Mcee	Methylmalonyl CoA epimerase	1.75
Mut	Methylmalonyl-Coenzyme A mutase	3.49
Oxct2a	3-oxoacid CoA transferase 2A	-4.15
Pecr	Peroxisomal trans-2-enoyl-CoA reductase	-7.66
Ppa1	Pyrophosphatase (inorganic) 1	-2.14
Prkaa1	Protein kinase, AMP-activated, alpha 1 catalytic subunit	-7.54
Prkaa2	Protein kinase, AMP-activated, alpha 2 catalytic subunit	-4.01
Prkab1	Protein kinase, AMP-activated, beta 1 non-catalytic subunit	-1.14
Prkab2	Protein kinase, AMP-activated, beta 2 non-catalytic subunit	-2.26
Prkaca	Protein kinase, cAMP-dependent, catalytic, alpha	1.31
Prkacb	Protein kinase, cAMP dependent, catalytic, beta	-3.51
Prkag1	Protein kinase, AMP-activated, gamma 1 non-catalytic subunit	1.28
Prkag2	Protein kinase, AMP-activated, gamma 2 non-catalytic subunit	2.17
Prkag3	Protein kinase, AMP-activated, gamma 3 non-	1.75

	catalytic subunit	
Slc27a1	Solute carrier family 27 (fatty acid transporter), member 1	-1.14
Slc27a2	Solute carrier family 27 (fatty acid transporter), member 2	-1.46
Slc27a3	Solute carrier family 27 (fatty acid transporter), member 3	1.69
Slc27a4	Solute carrier family 27 (fatty acid transporter), member 4	1.06
Slc27a5	Solute carrier family 27 (fatty acid transporter), member 5	-1.01
Slc27a6	Solute carrier family 27 (fatty acid transporter), member 6	1.38

4. Discussion

Cocaine is a powerfully addictive stimulant drug whose abuse can lead to dependence, a chronic relapsing disease caused by changes in the brain, and is lacking in pharmacotherapeutic and diagnostic solutions. There is increasing evidence that implicates a role for lipids as related to drugs of abuse, highlighting the need for lipidomic research that may reveal new targets for drug development and/or biomarker detection [4-7]. Such research is also essential for expanding our current understanding of how lipids are involved in signal transduction processes accompanying the neurobiology of addiction. Recent advances in the development of mass spectrometric tools to characterize molecular lipids have made it possible to unravel the complexity of the plasma lipidome along with the perturbations in lipid metabolism that occur in numerous diseases such as obesity, diabetes, and Alzheimer's disease [31-33].

The novel behavioral regimen used in this study was intended to recapitulate the pattern of repeat relapse often observed in humans by incorporating intervals of reinstatement, extinction, and prolonged abstinence, which were assessed using conditioned place preference (CPP). Using this model, cocaine-treated rats exhibited place preference within each behavioral session, although, rats displayed differential CPP response. While variability in CPP is a common behavioral phenomenon in drugs of abuse studies conducted in rodents, these outcomes are rarely reported outside of group trend data. However, our previous work demonstrating correlations between lipid relative abundance and differential locomotor sensitization suggest that in some instances, behavioral variability is reflected downstream in peripheral biological processes [9]. Thus, the conventional grouping of animals based on treatment rather

than response may interfere with molecular and analytical analyses. The behavioral variation observed in animal models is expected and may resemble the variation in drug response observed in human addicts. Currently, there are no established strategies to acknowledge this across datasets and to address this phenomenon. As such, we stratified animals into sub-behavioral cohorts based on the behavioral outcomes of CPP assays. The tracking of individual animal behavior was essential and was used as an inclusion criteria metric for subsequent lipidomic analyses.

We previously showed that cocaine exposure selectively alters the relative abundance of specific phospholipids (PLs) in the blood and that cocaine-induced locomotor sensitization results in the remodeling of specific PLs in a region-specific manner in the rat brain [9]. The use of the repeated exposure model discussed above permitted continual analysis of the lipidome, facilitating the detection of blood lipid changes from onset to progression. We previously used a behavioral sensitization rat model to demonstrate an overall trend of decreased PL relative abundance in the blood profiles of cocaine-treated rats [9]. The current study validates these findings, but further demonstrates that an expanded exposure protocol induced a similar decrease in PL species after cocaine exposure. We also identified alterations in glycerolipids and decreases in fatty acyl species. Interestingly, PL alterations demonstrated little to no persistence, and we observed bidirectional trends that were time point-specific. The fact that only two lipids were detected at more than one timepoint in the protocol suggests that multiple factors influence the regulation of blood lipids. Another recent study also discerned a complicated scheme in the persistence and directionality of lipidomic changes relating to cocaine exposure [17]. Differences between our previous studies

and the current observations likely result from slight differences in the behavioral models and more importantly, time of blood collection when comparing studies. The lack of overlap in blood lipidomic studies supports the hypothesis that cocaine exposure along with behaviors, such as extinction, reinstatement, and sensitization, illicit differential lipid alterations. It also suggests that changes in blood lipids assessed using shotgun lipidomics may not be useful for predicting behavioral changes in rats. It is certainly possible that more advanced and sensitive techniques may yield more success.

A striking overlap between both our current and previous studies [9] was that the majority of lipid alterations occurred in the hippocampus and cerebellum, with relatively few changes in the striatum. However, our previous study used shotgun ESI-MS to assess whole-scale changes in the isolated regions. The use of mass spectrometric imaging (MSI) confirms these data and demonstrates that lipid alterations were region-specific. Specific changes in the hippocampus were not surprising given the involvement of this region in dopaminergic signaling and reward. The hippocampus is a region involved with learning and memory, which is associated with drug-seeking behavior through the conditioned cues or environmental context that accompany drug experiences [34, 35]. The phospholipid alterations detected in the hippocampus suggest a role for lipids in the retention of the memories of addiction, possibly due to membrane remodeling. Cerebellar lipid changes were surprising since this region had been previously presumed to lack relevance to the mechanisms underlying addictive behavior. However, the current study, along with our previously mentioned work, are among the first to suggest a role for the cerebellum in drug reward and reinstatement of

drug-seeking [36-39]. Recently, studies have reported consistent cerebellar activation in response to drug-cues via neuroimaging and bidirectional connections with regions mediating drug reward, and involvement in nonmotor function [37-39].

As mentioned above, MSI clearly demonstrated region-specific cocaine-induced lipid remodeling throughout rat brain substructures. The finding that cocaine exposure reduces PL levels throughout the brain and hippocampus was interesting given the findings of Ross, *et al*. who showed decreased activity of key phospholipid-metabolizing enzymes, calcium-stimulated phospholipase A_2 and phosphatidylcholine cytidylyltransferase, in dopaminergic brain regions of human cocaine users [8]. Another novel finding is the alteration of two PLs (*m/z* 782.5828 and *m/z* 807.5703) in both peripheral blood and hippocampus. Hippocampal MSI-analysis indicated significant decreases in the abundance of these lipids in brain sections from Sacrifice (day 57). The relative abundances of these lipids were assessed at each time point in peripheral blood, which generally displayed equitable levels across cocaine- and saline-treatment except during Post-Abstinence, 30 days later (day 48). We detected significant decreases in these lipid levels during Post-Abstinence, 30 days later, correlating to that observed in the hippocampus almost a week later, which may serve as potential indicators of neuroadaptation.

Although absolute quantitation was not performed for phospholipid features, the data are assumed to be a proper indication of the trend occurring between states. Lipid concentrations obtained by MALDI-MSI signals recently showed successful comparisons to those assessed by LC-MS/MS in brain tissue [40]. A few studies have used MSI to analyze cocaine drug and metabolites [41, 42]; however, this study is one

of the first to report the persisting effects of cocaine on differential lipid abundance with MSI. A recent study by Bodzon-Kulakowska, *et al*. demonstrated the influence of cocaine, morphine, and amphetamine on select PL species throughout limbic structures using desorption electrospray MSI [17]. Comparison of this study to ours demonstrated a few of the same PLs alterations (*m/z* 834.5, *m/z* 786.5, *m/z* 806.6). These similarities occurred despite differences between the behavioral regimen used as well as differences in the dose and frequency of cocaine administration [17]. Another recent study showed the profound effect of cocaine on the brain lipidome in mice using behavioral models of CPP and locomotor sensitization [18]. Lin, *et al*. demonstrated significant decreases in ceramide and lysophospholipids accompanied by increases in PLs and polyunsaturated fatty acid (PUFA)-containing PLs in the nucleus accumbens [18].

While our data demonstrate the novel finding that cocaine persistently induces decreases in PLs throughout various brain structures, it does not show a corresponding increase in fatty acid (FA) species. We have previously demonstrated that oxidant-induced damage in neurons results in increased FA release that is accompanied by PL remodeling, as indicated by increased levels of phospholipids with PUFAs [26]. The absence of such remodeling in the current study begs the question regarding the synthesis and metabolism these fatty acids. The mitochondria are a key site for fatty acid metabolism, and recent work suggest that energy deficits plays a regulatory role in drug addiction and in the development of neurodegenerative diseases [43, 44]. Studies have also shown that cocaine impacts glucose metabolism with subsequent effects the brain [45]. These findings coupled with the active involvement of the mitochondria in

the regulation of synaptic plasticity [46, 47] led us to investigate the role of cocaine on the differential regulation of mitochondrial biogenesis and fatty acid metabolism. Our finding that cocaine exposure upregulates hippocampal FA metabolism supports the hypothesis that cocaine alters the maintenance of energy homeostasis. Moreover, the differences between hippocampal and cerebellar expression of genes involved in FA metabolism indicates that such regulation occurs region-specifically. The trend of downregulation observed for these FA gene targets in the liver was interesting, although the effect of cocaine on peripheral FA metabolism remains elusive.

Recent studies suggest that mitochondrial energetics are altered during neuronal injury and protective mechanisms can be initiated by increasing mitochondrial biogenesis [48]. Little attention has been given to understanding the effect of cocaine on energy expenditure via mitochondrial biogenesis. The finding that cocaine exposure upregulates markers of mitochondrial biogenesis in the hippocampus is surprising, but in line with changes in the expression of mitochondrial fatty acid regulatory genes. Further, these changes appear to be region-specific as cerebellar and liver biogenesis was downregulated, with striking decreases in the liver. These findings are in agreement with Sadakierska-Chudy, *et al*. who reported significant elevation in mtDNA copy number and concomitant increased expression of mitochondrial genes including Tfam in the hippocampus and prefrontal cortex of rats following cocaine self-administration [49]. However, these responses may vary based on behavior, drug exposure, and may not extend to other drugs of abuse. For example, Feng, *et al*. reported an association between opioid addiction with mtDNA copy number reduction and neurostructural remodeling [15]. Further, the influence of cocaine exposure on the

mitochondria has been shown to differentially affect ROS production, superoxide dismutase activity, and mitochondrial gene transcription at a variety of doses, ranging from acute to chronic, and is reviewed in detail [14].

In summary, the above work presents a comprehensive lipidomic assessment of cocaine-induced lipid remodeling in rat blood and brain. We report differential alterations in multiple lipid classes in the blood and hippocampus-specific changes in the rat brain. These data suggest that addictive behaviors, e.g. sensitization, extinction, and reinstatement, are involved in the induction of widespread lipid alterations. We also show region-specific regulation of genes involved in fatty acid metabolism and mitochondrial biogenesis in the brain and liver, indicating a potential interplay between CNS energetics and differential lipid regulation. Our findings link cocaine exposure to the induction of lipidomic changes in both the CNS and periphery and suggest a role for cocaine in the maintenance of energy homeostasis, providing novel insight into the link between lipids and drugs of abuse.

References

[1] E. Leishman, K.J. Kokesh, H.B. Bradshaw, Lipids and addiction: how sex steroids, prostaglandins, and cannabinoids interact with drugs of abuse, Annals of the New York Academy of Sciences, 1282 (2013) 25-38.

[2] L. Orio, F. Javier Pavon, E. Blanco, A. Serrano, P. Araos, M. Pedraz, P. Rivera, M. Calado, J. Suárez, F. Rodríguez de Fonseca, Lipid transmitter signaling as a new target for treatment of cocaine addiction: new roles for acylethanolamides and lysophosphatidic acid, Current pharmaceutical design, 19 (2013) 7036-7049.

[3] C.J. Hillard, Lipids and drugs of abuse, Life Sciences, 77 (2005) 1531-1542.

[4] L. Buydens-Branchey, M. Branchey, D.L. McMakin, J.R. Hibbeln, Polyunsaturated fatty acid status and relapse vulnerability in cocaine addicts, Psychiatry research, 120 (2003) 29-35.

[5] L. Buydens-Branchey, M. Branchey, Association between low plasma levels of cholesterol and relapse in cocaine addicts, Psychosomatic medicine, 65 (2003) 86-91.

[6] L. Zhang, M.E. Reith, Regulation of the functional activity of the human dopamine transporter by the arachidonic acid pathway, European journal of pharmacology, 315 (1996) 345-354.

[7] L. Zimmer, S. Delion-Vancassel, G. Durand, D. Guilloteau, S. Bodard, J.-C. Besnard, S. Chalon, Modification of dopamine neurotransmission in the nucleus accumbens of rats deficient in n–3 polyunsaturated fatty acids, Journal of Lipid Research, 41 (2000) 32-40.

[8] B.M. Ross, A. Moszczynska, F.J. Peretti, V. Adams, G.A. Schmunk, K.S. Kalasinsky, L. Ang, N. Mamalias, S.D. Turenne, S.J. Kish, Decreased activity of brain phospholipid

metabolic enzymes in human users of cocaine and methamphetamine, Drug and alcohol dependence, 67 (2002) 73-79.

[9] B.S. Cummings, S. Pati, S. Sahin, N.E. Scholpa, P. Monian, P.M. Trinquero, J.K. Clark, J.J. Wagner, Differential effects of cocaine exposure on the abundance of phospholipid species in rat brain and blood, Drug and alcohol dependence, 152 (2015) 147-156.

[10] J.P. Huston, J. Kornhuber, C. Mühle, L. Japtok, M. Komorowski, C. Mattern, M. Reichel, E. Gulbins, B. Kleuser, B. Topic, A sphingolipid mechanism for behavioral extinction, Journal of neurochemistry, 137 (2016) 589-603.

[11] M. Mapstone, A.K. Cheema, M.S. Fiandaca, X. Zhong, T.R. Mhyre, L.H. MacArthur, W.J. Hall, S.G. Fisher, D.R. Peterson, J.M. Haley, M.D. Nazar, S.A. Rich, D.J. Berlau, C.B. Peltz, M.T. Tan, C.H. Kawas, H.J. Federoff, Plasma phospholipids identify antecedent memory impairment in older adults, Nat Med, 20 (2014) 415-418.

[12] C.U. Mårtensson, K.N. Doan, T. Becker, Effects of lipids on mitochondrial functions, Biochimica et Biophysica Acta (BBA) - Molecular and Cell Biology of Lipids, 1862 (2017) 102-113.

[13] M.B. Hock, A. Kralli, Transcriptional control of mitochondrial biogenesis and function, Annual review of physiology, 71 (2009) 177-203.

[14] A. Sadakierska-Chudy, M. Frankowska, M. Filip, Mitoepigenetics and drug addiction, Pharmacology & Therapeutics, 144 (2014) 226-233.

[15] Y.-M. Feng, Y.-F. Jia, L.-Y. Su, D. Wang, L. Lv, L. Xu, Y.-G. Yao, Decreased mitochondrial DNA copy number in the hippocampus and peripheral blood during opiate

addiction is mediated by autophagy and can be salvaged by melatonin, Autophagy, 9 (2013) 1395-1406.

[16] T. Samikkannu, V.S. Atluri, M.P. Nair, HIV and Cocaine Impact Glial Metabolism: Energy Sensor AMP-activated protein kinase Role in Mitochondrial Biogenesis and Epigenetic Remodeling, Scientific reports, 6 (2016) 31784.

[17] A. Bodzon-Kulakowska, A. Antolak, A. Drabik, M. Marszalek-Grabska, J. Kotlinska, P. Suder, Brain lipidomic changes after morphine, cocaine and amphetamine administration - DESI - MS imaging study, Biochimica et biophysica acta, 1862 (2017) 686-691.

[18] Y. Lin, H. Gu, L. Jiang, W. Xu, C. Liu, Y. Li, X. Qian, D. Li, Z. Li, J. Hu, H. Zhang, W. Guo, Y. Zhao, X. Cen, Cocaine modifies brain lipidome in mice, Molecular and Cellular Neuroscience, (2017).

[19] N.E. Scholpa, S.B. Briggs, J.J. Wagner, B.S. Cummings, Cyclin-Dependent Kinase Inhibitor 1a (p21) Modulates Response to Cocaine and Motivated Behaviors, Journal of Pharmacology and Experimental Therapeutics, 357 (2016) 56-65.

[20] C.M. Seymour, J.J. Wagner, Simultaneous expression of cocaine-induced behavioral sensitization and conditioned place preference in individual rats, Brain research, 1213 (2008) 57-68.

[21] M.A. Aguilar, M. Rodriguez-Arias, J. Minarro, Neurobiological mechanisms of the reinstatement of drug-conditioned place preference, Brain research reviews, 59 (2009) 253-277.

[22] E.G. Bligh, W.J. Dyer, A rapid method of total lipid extraction and purification, Can J Biochem Physiol, 37 (1959) 911-917.

[23] G.R. Bartlett, Phosphorus assay in column chromatography, Journal of Biological Chemistry, 234 (1959) 466-468.
[24] G.R. Kinsey, J.L. Blum, M.D. Covington, B.S. Cummings, J. McHowat, R.G. Schnellmann, Decreased iPLA2gamma expression induces lipid peroxidation, cell death, and sensitizes cells to oxidant-induced apoptosis, J Lipid Res, (2008).
[25] L. Zhang, B.L. Peterson, B.S. Cummings, The effect of inhibition of Ca2+-independent phospholipase A2 on chemotherapeutic-induced death and phospholipid profiles in renal cells, Biochem Pharmacol, 70 (2005) 1697-1706.
[26] B. Peterson, K. Stovall, P. Monian, J.L. Franklin, B.S. Cummings, Alterations in phospholipid and fatty acid lipid profiles in primary neocortical cells during oxidant-induced cell injury, Chem Biol Interact, 174 (2008) 163-176.
[27] E. Maes, D. Valkenborg, G. Baggerman, H. Willems, B. Landuyt, L. Schoofs, I. Mertens, Determination of variation parameters as a crucial step in designing TMT-based clinical proteomics experiments, PloS one, 10 (2015) e0120115.
[28] R. Taguchi, J. Hayakawa, Y. Takeuchi, M. Ishida, Two-dimensional analysis of phospholipids by capillary liquid chromatography/electrospray ionization mass spectrometry, J Mass Spectrom, 35 (2000) 953-966.
[29] A.M. Goodpaster, M.A. Kennedy, Quantification and statistical significance analysis of group separation in NMR-based metabonomics studies, Chemometrics and Intelligent Laboratory Systems, 109 (2011) 162-170.
[30] F.R. Jornayvaz, G.I. Shulman, Regulation of mitochondrial biogenesis, Essays in biochemistry, 47 (2010) 10.1042/bse0470069.

[31] D. Steinberg, An interpretive history of the cholesterol controversy: Part II: the early evidence linking hypercholesterolemia to coronary disease in humans, J Lipid Res, 46 (2005) 179-190.
[32] A.D. Watson, Thematic review series: systems biology approaches to metabolic and cardiovascular disorders. Lipidomics: a global approach to lipid analysis in biological systems, Journal of lipid research, 47 (2006) 2101-2111.
[33] M.R. Wenk, The emerging field of lipidomics, Nature reviews. Drug discovery, 4 (2005) 594.
[34] R.A. Fuchs, K.A. Evans, C.C. Ledford, M.P. Parker, J.M. Case, R.H. Mehta, R.E. See, The role of the dorsomedial prefrontal cortex, basolateral amygdala, and dorsal hippocampus in contextual reinstatement of cocaine seeking in rats, Neuropsychopharmacology, 30 (2005) 296-309.
[35] W. Sun, G.V. Rebec, Lidocaine inactivation of ventral subiculum attenuates cocaine-seeking behavior in rats, Journal of Neuroscience, 23 (2003) 10258-10264.
[36] G.F. Koob, N.D. Volkow, Neurocircuitry of addiction, Neuropsychopharmacology, 35 (2010) 217-238.
[37] M.J. Wagner, T.H. Kim, J. Savall, M.J. Schnitzer, L. Luo, Cerebellar granule cells encode the expectation of reward, Nature, (2017).
[38] E.A. Moulton, I. Elman, L.R. Becerra, R.Z. Goldstein, D. Borsook, The cerebellum and addiction: insights gained from neuroimaging research, Addiction biology, 19 (2014) 317-331.
[39] J. Moreno-Rius, M. Miquel, The cerebellum in drug craving, Drug and Alcohol Dependence, 173 (2017) 151-158.

[40] J.A. Hankin, R.C. Murphy, Relationship between MALDI IMS intensity and measured quantity of selected phospholipids in rat brain sections, Analytical chemistry, 82 (2010) 8476-8484.

[41] H.-Y.J. Wang, S.N. Jackson, J. McEuen, A.S. Woods, Localization and analyses of small drug molecules in rat brain tissue sections, Analytical chemistry, 77 (2005) 6682-6686.

[42] D.A. Pirman, R.F. Reich, A.s. Kiss, R.M. Heeren, R.A. Yost, Quantitative MALDI tandem mass spectrometric imaging of cocaine from brain tissue with a deuterated internal standard, Analytical chemistry, 85 (2012) 1081-1089.

[43] S. Cunnane, S. Nugent, M. Roy, A. Courchesne-Loyer, E. Croteau, S. Tremblay, A. Castellano, F. Pifferi, C. Bocti, N. Paquet, Brain fuel metabolism, aging, and Alzheimer's disease, Nutrition, 27 (2011) 3-20.

[44] P.K. Thanos, M. Michaelides, H. Benveniste, G.J. Wang, N.D. Volkow, The effects of cocaine on regional brain glucose metabolism is attenuated in dopamine transporter knockout mice, Synapse, 62 (2008) 319-324.

[45] W. Renthal, E.J. Nestler, Epigenetic mechanisms in drug addiction, Trends in molecular medicine, 14 (2008) 341-350.

[46] M. Levy, G.C. Faas, P. Saggau, W.J. Craigen, J.D. Sweatt, Mitochondrial regulation of synaptic plasticity in the hippocampus, Journal of Biological Chemistry, 278 (2003) 17727-17734.

[47] D. Ben-Shachar, D. Laifenfeld, Mitochondria, Synaptic Plasticity, And Schizophrenia, in: International Review of Neurobiology, vol. 59, Academic Press, 2004, pp. 273-296.

[48] S.-D. Chen, D.-I. Yang, T.-K. Lin, F.-Z. Shaw, C.-W. Liou, Y.-C. Chuang, Roles of oxidative stress, apoptosis, PGC-1α and mitochondrial biogenesis in cerebral ischemia, International journal of molecular sciences, 12 (2011) 7199-7215.

[49] A. Sadakierska-Chudy, A. Kotarska, M. Frankowska, J. Jastrzębska, K. Wydra, J. Miszkiel, E. Przegaliński, M. Filip, The alterations in mitochondrial DNA copy number and nuclear-encoded mitochondrial genes in rat brain structures after cocaine self-administration, Molecular neurobiology, (2016) 1-11.

CHAPTER 7

SUMMARY

The link between lipid signaling and the development and maintenance of addiction suggests that discoveries in lipid research may offer new therapeutic targets for treatment of prediction of cocaine addiction. Although several studies report associations between lipids and addiction, few have assessed the onset and persistence of global lipid alterations. To our knowledge, no studies have characterized cocaine-induced changes in the lipidome using multiple models of exposure including preclinical and clinical models. Furthermore, none have examined the interaction between drug exposure and other factors that influence the lipidome such as diet and age, nor suggested mechanisms that may mediate changes in the lipidome. Herein, we present a series of studies that attempts to address these gaps in knowledge within the context of addiction and test the overall hypothesis that cocaine-induced lipidomic alterations can serve as indicators of addictive behaviors.

Initially, we assessed analytical strategies for shotgun lipid analysis and used cross-platform method validation to address the issue of methodological variability in metabolomic research. This focused our efforts toward standardizing protocols to ensure reproducibility in terms of detection, sensitivity, and feature identification across experimental models. A common phenomenon in the use of shotgun lipidomics is the

inability to regulate lipid identification across runs. We tackled this by defining matrix-specific pools comprised of overlapping and most abundant lipid species.

It is widely accepted that circulating lipid composition in the plasma and blood can be altered by dietary intake, lifestyle, genetics, and metabolism. Of these, dietary intake is among the most important. Recent advances in metabolomics methods have revealed that changes in lipid signatures are often a result of the interactions between such factors, and likely contribute to the interindividual variation observed in clinical lipidomics studies. Our findings support this hypothesis and suggest that characterizing dietary responses and their interactions is an essential prerequisite for assessing the effect of any stimuli on lipidomic changes in the blood. We demonstrated a link between dietary fat intake with changes in the blood lipidome in female mice. We also showed the unique finding that there is a fundamental interaction between dietary fat intake and aging, which is reflected in circulating lipid profiles. Specifically, the effects of high fat consumption occur in an age-dependent manner with robust responses at a younger age. We also showed that some lipid changes correlated to changes in the gene expression of markers of metabolic and lipid regulation as well as liver homeostasis. These findings provide a basis for female-specific obesity and age-related lipid biomarkers. Remarkably, the effect of age on the blood lipidome was not only observed in mice, but also occurred in a stimuli-independent manner in rat and human models. These outcomes demonstrate that age and/or time-related factors are detectable at the level of the lipidome. Further, these factors emphasize the need for substantial consideration of the effect of age in experiments utilizing lipidomics-based biomarker discovery.

With regards to cocaine, we first explored changes in the lipidome using a clinical model of illicit drug use and demonstrated the widespread effects of such exposure on phospholipid, glycerolipid, and fatty acyl lipid remodeling in human blood. The finding that drug exposure lowered lipid abundances, mainly in fatty acyl lipids, recapitulated the findings of several epidemiological studies; however, we were the first to report these changes using untargeted global lipidomics. Interestingly, several of the lipid changes detected in the blood correlated to behavioral sensitization to cocaine that was observed in approximately 10% of frequent users. These outcomes are noteworthy for multiple reasons: first, this is the clearest demonstration to date that the psychostimulant sensitization observable in laboratory animals may have a human counterpart; second, this is one of the first studies to suggest correlations between human behavior and lipid changes that can be detected in circulation.

Although the results from our clinical study have implications for drug-induced responses in lipid metabolism and behavior, diversity among human participants due to the variation in background and drug exposure posed challenges in elucidating cocaine-specific lipidomic responses. We addressed this by using preclinical models of cocaine exposure and behavioral sensitization in rats. These studies demonstrated that cocaine-induced lipid remodeling in the rat blood and brain in a region-specific manner. Hippocampus- and cerebellum-specific alterations in multiple lipid classes suggested a role for addictive behaviors, i.e. sensitization, extinction, and reinstatement, in the induction of widespread lipid alterations. Moreover, we observed that human and rodent models demonstrate similar correlations between sensitization to cocaine, specifically with many of the same blood lipids. This implies that lipidomic responses induced by

diet and age, as well as cocaine, are somewhat conserved across these species. This finding increases the translation potential of these models and could have a profound impact on the field of addiction research.

Initially, we postulated that cocaine induces brain lipid alterations that parallel similar changes in blood lipids, and that this would allow for blood lipids to serve as indicators of addictive behaviors. However, the relationship between blood and brain lipids remains elusive. Blood lipid changes rarely persisted throughout repeated drug exposure, suggesting that changes in lipids only offer a glimpse into an evolving state of lipid metabolism in response to cocaine. Nevertheless, we were able to show that cocaine primarily decreases the phospholipidome in the brain and differentially alters fatty acyl and glycerolipid composition in the blood. It is plausible that these differences are attributed to a combination of responses that are independently regulated by metabolic and/or CNS processes. For example, systemic liver regulation may be partially responsible for the induction of lipid changes in the blood. This would not be surprising given the breadth of literature on the regulation of lipid and lipoprotein metabolism through peroxisome proliferator-activated receptors in the liver. Nonetheless, the full implication of these differences between the effects of cocaine on the blood and brain lipidome remains to be fully discerned. Regardless, the outcomes of our preclinical and clinical studies begged the question of what regulators are driving lipid remodeling following cocaine exposure.

Despite some published studies reporting lipid remodeling following exposure to drugs of abuse, none have identified or suggested mechanisms by which these responses occur. Our first attempt to address this question focused on assessing CCT,

a key enzymatic regulator of PC synthesis. This target was selected based on our studies showing persistent effects of cocaine on PC lipids. Our data were the first to demonstrate the region- and cell-specific localization of CCT isoforms in the rat brain and to show that that cocaine exposure decreased cerebellar CCTβ expression. This discovery, along with our lipidomic studies, strongly support a novel role for the cerebellum in drug reward and reinstatement of drug-seeking.

Although cocaine exposure decreased a number of phospholipids in the brain, these decreases were not accompanied by increases in any corresponding fatty acids. This suggests perturbations in the synthesis and metabolism these fatty acids. In support of this hypothesis, we showed that genes involved in fatty acid metabolism are differentially expressed in a region-specific manner in brain as well as the liver, indicating a potential interplay between CNS energetics and lipid regulation. Further, our finding that cocaine-induced hippocampus-specific changes in mitochondrial biogenesis suggests a regulatory role for energy deficits in drug addiction and in the development of neurodegenerative diseases.

The series of studies presented here provides novel insight into the link between lipids and drugs of abuse. Our findings lay the foundation for further studies assessing the mechanism by which cocaine induces lipid remodeling. The limitations of the shotgun approach fuel the need for future studies involving targeted validation and absolute quantitation of lipids identified in this work. Our results also highlight the need to correct for both diet- and age in such studies, as well as to assess the effect of exposures prior to sexual maturity, or into advanced age, to obtain a comprehensive understanding of the evolving lipidome. Moreover, while we suggest a role for cocaine

in the maintenance of energy homeostasis, more mechanistic studies are needed to probe up- and downstream regulators. Lastly, it will be essential to establish causal roles for lipids in addictive behaviors. Such studies are critical for revealing the impact of lipid signaling in addiction and for providing a platform to understand how changes in the lipidome mediate some of the molecular and cellular adaptions of the brain in response to drugs of abuse.

APPENDIX A: APPENDIX FIGURES FOR CHAPTER 3

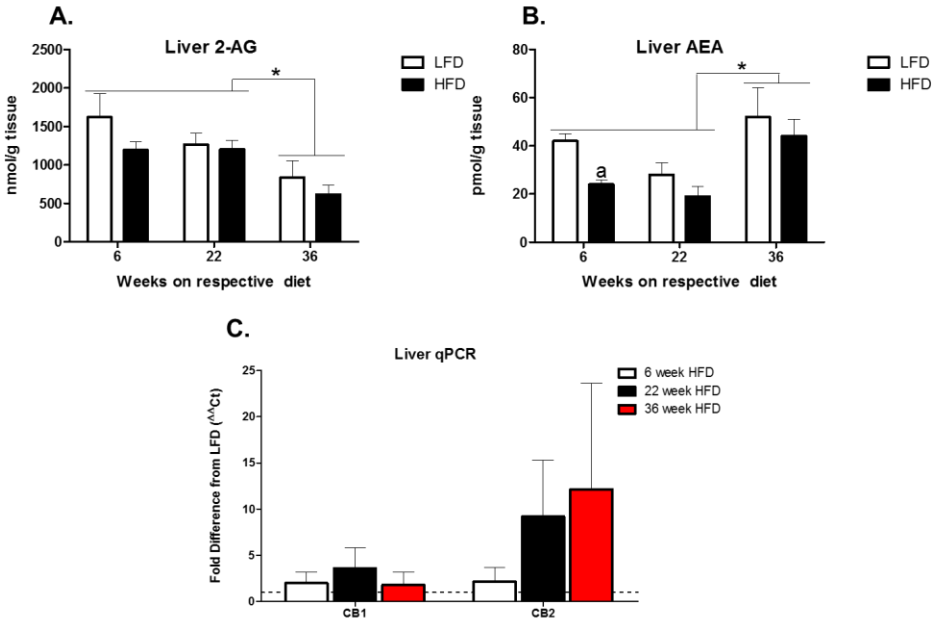

Appendix Figure 1. Effect of 6, 22 or 36 weeks of high-fat diet (HFD) consumption on liver endocannabinoid levels. Liver concentration of 2-arachidonoylglycerol (2-AG; nmol/g tissue; **7A**) and N-arachidonoylethanolamide (AEA; pmol/g tissue; **7B**) was determined after 6, 22 or 36 weeks of high-fat diet (HFD) consumption by female C57BL/6 mice with a triple quadrupole mass spectrometer. **(7C)** Effect of 6, 22 or 36 weeks of high-fat diet (HFD) consumption by female C57BL/6 mice on liver mRNA levels of cannabinoid receptor type 1 (CB1) and type 2 (CB2). The house keeping gene (HKG) 18S was used to normalize the mRNA data, which are presented as fold change relative to respective low-fat diet (LFD) group at each time point. Graphical representations are indicative of 6-8 animals per group (n=6–8) and are expressed as mean ± SEM. *Indicate significant ($p \leq 0.05$) differences between feeding durations; [a]Indicates a significant ($p \leq 0.05$) diet effect within a feeding duration.

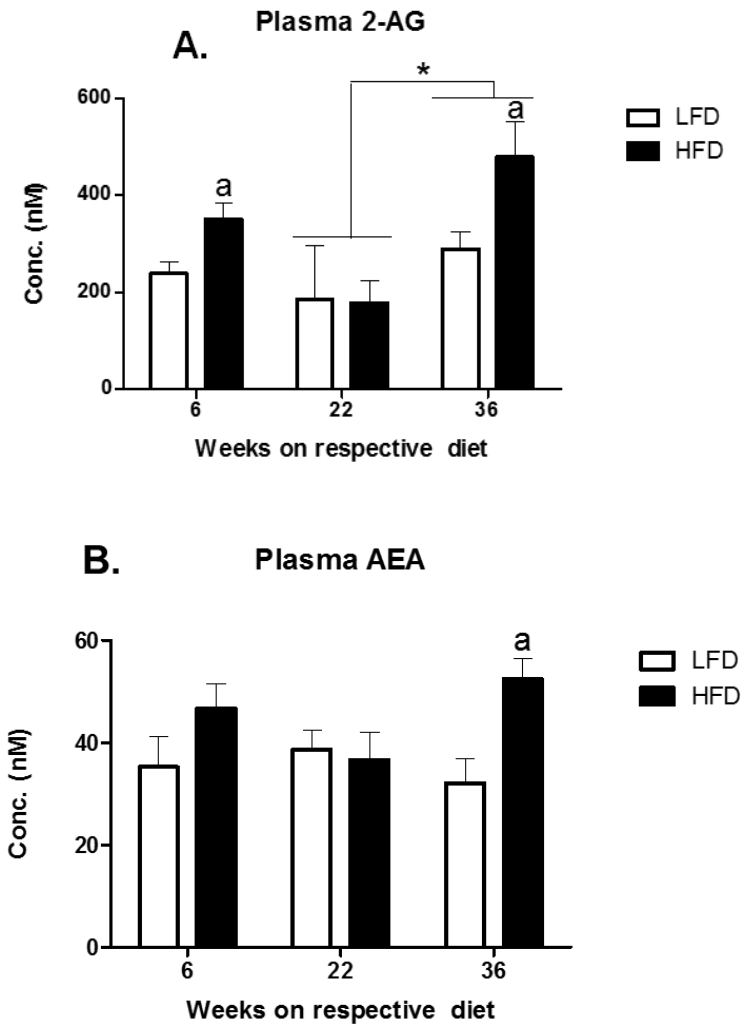

Appendix Figure 2. Effect of 6, 22 or 36 weeks of high-fat diet (HFD) consumption on plasma endocannabinoid levels. Plasma levels of 2-arachidonoylglycerol (2-AG; nM; **8A**) and N-arachidonoylethanolamide (AEA; nM; **8B**) were determined after 6, 22 or 36 weeks of high-fat diet (HFD) consumption by female C57BL/6 mice with a triple quadrupole mass spectrometer. Graphical representations are indicative of 6-8 animals per group (n=6–8) and are expressed as mean ± SEM. *Indicates a significant ($p \leq 0.05$) difference between feeding durations; [a]Indicates a significant ($p \leq 0.05$) diet effects within a feeding duration.

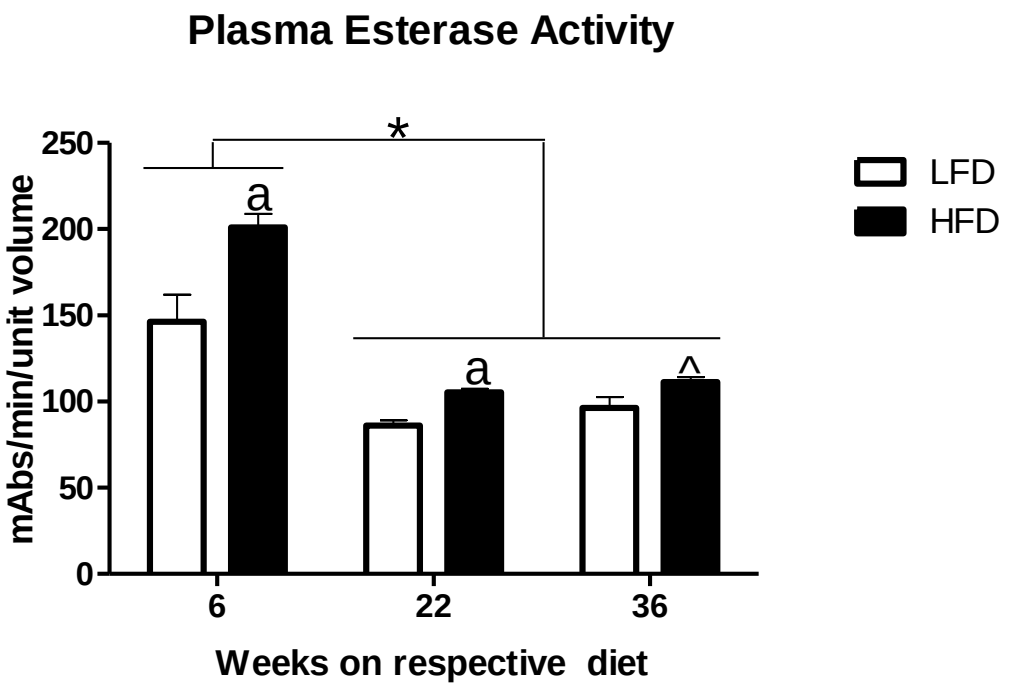

Appendix Figure 3. Effect of 6, 22 or 36 weeks of high-fat diet (HFD) consumption on plasma esterase activity. Plasma esterase activity (mAbs/min/unit volume) was determined after 6, 22 or 36 weeks of high-fat diet (HFD) consumption by female C57BL/6 mice using *para*-nitrophenyl valerate as substrate. Graphical representations are indicative of 6-8 animals per group (*n*=6–8) and are expressed as mean ± SEM. * Indicates significant ($p \leq 0.05$) differences between feeding durations; [a]Indicates a significant ($p \leq 0.05$) diet effects within a feeding duration; ^ Indicates non-significant ($p > 0.05 < 0.1$) diet effect within a feeding duration.

APPENDIX B: DIFFERENTIAL EFFECTS OF COCAINE EXPOSURE ON THE ABUNDANCE OF PHOSPHOLIPID SPECIES IN RAT BRAIN AND BLOOD[1]

[1] Brian S. Cummings, Sumitra Pati, Serap Sahin, Natalie E. Scholpa, Prashant Monian, Paul O. Trinquero, Jason K. Clark, and John J. Wagner. (2015) *Drug and Alcohol Dependence.* Reprinted with permission from publisher.

Abstract

Background: Lipid profiles in the blood have been shown to be altered in humans who have abused cocaine, consistent with the hypothesis that cocaine-dependence can induce lipid remodeling.

Methods: We have addressed this hypothesis using the rat model of cocaine-induced locomotor sensitization followed by shotgun lipidomics using electrospray ionization-mass spectrometry (ESI-MS). To determine if any lipidomic changes were also reflected in the blood, we performed principal component analysis (PCA) of lipidomic spectra of samples isolated from cocaine treated animals.

Results: Behavioral sensitization altered the relative abundance of several phospholipid species in the hippocampus and cerebellum measured one week following the final exposure to cocaine. In contrast, relatively few effects on phospholipids in either the dorsal or the ventral striatum regions of the brain were observed. PCA analysis demonstrated that cocaine altered the relative abundance of several glycerophospholipid species as compared to saline injected controls. Subsequent MS/MS analysis identified some of these lipids as plasmenyl phosphatidylcholines, phosphatidylcholines and sphingomyelins.

Conclusion: Taken together, these data demonstrate the novel finding that cocaine-induced locomotor sensitization results in the remodeling of specific phospholipids in rat brain tissue in a region-specific manner and also altered the intensities and types of phospholipid species in rat blood.

1. Introduction

The National Survey on Drug Use and Health [1] estimates 1.4 million people over the age 12 used cocaine in 2011, and that over 820,000 of these individuals met the Diagnostic and Statistical Manual of Mental Disorders criteria for dependence or abuse of cocaine [1]. Cocaine is responsible for more emergency room visits in the US than any other illegal drug (http://www.oas.samhsa.gov/) and there are currently no FDA approved treatments for cocaine substance use disorder.

Although an extensive effort has been made to characterize and evaluate various mechanisms involved in cocaine-induced alterations of brain function, few studies have assessed the effect of cocaine use on brain lipid metabolism in humans [2, 3] and none have identified the specific lipid species that are altered following drug exposure. It is also known that a history of cocaine use alters blood levels of cholesterol [4] and fatty acids [5]. These findings are consistent with the premise that altered cell membrane remodeling activity is occurring in these individuals exposed to cocaine. Given that lipid remodeling would be inherent to the changes in neuronal morphology and synaptic plasticity thought to underlie the neuroadaptations associated with substance use disorder, it is somewhat surprising that such few studies have assessed changes in lipid profiles after cocaine exposure, and that none have been described using animal models of addiction.

One practical consideration impeding the progress of such studies is that thousands of lipids exist in biological tissues, making it difficult to identify specific changes in select lipid species. Furthermore, until recently the methods used to isolate and characterize such lipids could be somewhat laborious and time consuming. One productive approach has been to use matrix-assisted laser desorption/ionization–time-

of-flight mass spectrometry (MALDI-TOF MS) imaging in rat brain tissue sections to identify lipid species [6, 7]. Subsequent studies have described discrete localization of lipids throughout both the rat [8, 9] and the human brain [10, 11]. These observations suggest that heterogeneity in the relative abundance of lipid species both within and between brain regions may have functional relevance.

We performed shotgun lipidomics using electrospray ionization-mass spectrometry (ESI-MS) to assess the persisting effects of cocaine on the relative abundance of phospholipid species in tissues obtained from both the brain and the blood of rats that had been repeatedly exposed to the drug. The resulting data significantly informs our understanding of how cocaine alters lipid remodeling within specific brain regions and further suggests that changes in the blood lipidome may be useful as prognostic and/or diagnostic indicators of behavioral responses to cocaine and of drug exposure history.

2. Methods

2.1 *Behavior Assays*

Induction of locomotor sensitization

Male Sprague-Dawley rats, 8 weeks of age (Harlan, Indianapolis, IN, USA) were housed in pairs in clear plastic cages and maintained on a 12 hr light/dark cycle (0700/1900 hr). Food and water was available *ad libitum* except during the behavioral sessions. Animals were allowed to adapt to the lab conditions for a week before behavioral testing began. Behavioral sessions were conducted daily between 0900 and 1600 hr.

The apparatus and measurement of activity have been described in detail elsewhere [12, 13]. Briefly, locomotor (LM) activity was measured in four 43.2 x 43.2 cm chambers with clear plastic walls and a solid smooth floor (Med Associates, St. Albans, VT, USA). The chambers were individually housed in sound-attenuating cubicles equipped with a house light and a ventilation fan. Two banks of 16 infrared photobeams and detectors, mounted at right angles 3.5 cm above the floor, detected horizontal activity. Activity Monitor software (Med Associates) was used to count photobeam breaks.

Animals were subjected to a locomotor sensitization protocol over a period of twelve days (**Figure 1A**). Following 3 days of habituation to experimenter handling, on day 4 animals were placed in the center of the open field activity chamber for 30 minutes to establish a baseline LM activity for each animal. At that time they were given an i.p. injection of either 10 mg/kg cocaine or saline and returned to the chamber for an additional 60 minutes of monitoring (**Figure 1B**, cocaine/saline activity). During conditioning sessions (days 5-8), animals were injected i.p. with either cocaine (15 mg/kg) or 0.9% saline using the same open field procedure. Seven days after the last conditioning session animals were again challenged (day 15) with either cocaine (10mg/kg) or saline in the open field activity chamber as described above for protocol day 4.

Isolation of specific brain areas and blood

All experimental protocols were performed following approval by the University of Georgia Animal Care and Use Committee. Rats were anesthetized with halothane prior

to decapitation. Brains were removed and cooled in ice-cold oxygenated (95% O_2/5% CO_2) dissection artificial cerebrospinal fluid containing 120 mM NaCl, 3 mM KCl, 4 mM $MgCl_2$, 1 mM NaH_2PO_4, 26 mM $NaHCO_3$ and 10 mM glucose. Brain regions were dissected and the tissue was either processed immediately with the Bligh-Dyer lipid extraction or flash frozen in liquid N_2. Blood was isolated via cardiac puncture prior to decapitation and immediately mixed, by vortexing, with 1 mL of methanol:water (2.0:0.8 v/v) and then placed at -20ºC until lipid extraction.

2.2 *Lipidomic Analysis*

Lipid nomenclature

Phospholipids differ in terms of the numbers of carbons and double bonds and polar head groups. Typically, the nomenclature used to identify these traits is X:Y, where X = the number of carbons and Y = the number of double bonds; hence, 34:2 would indicate a lipid with 34 carbons and 2 double bonds. Polar head groups are referred to by their abbreviations.

Bligh-Dyer lipid extraction

Phospholipids were extracted using chloroform and methanol according to the method of Bligh and Dyer [14]. After treatment, tissues and blood were isolated as explained above, and tissue was washed with PBS and homogenized in 3 mL of methanol: water (2.0:0.8 v/v). Blood was suspended in 1.25 mL of methanol and 1.25 mL of chloroform. Tubes were vortexed for 30 seconds and allowed to sit for 10 minutes on ice. Tubes were centrifuged at 213 x *g* for 5 minutes and the bottom chloroform layer was

transferred to a new test tube. The extraction steps were repeated a second time and the chloroform layers combined. The collected chloroform layers were dried under nitrogen, reconstituted with 50 μL of methanol: chloroform (2:1 v/v), and stored at -20°C.

Lipid phosphorus assay

Lipid phosphorus was quantified using malachite green [15]. Lipids extracts (10 μL) were dried down under nitrogen in a glass test tube, 200 μL of perchloric acid was added to the tube, and heated at 130°C for 2-3 hr. After this time, 1 mL of dH_2O was added to the tube while vortexing, then 1.5 mL of reagent C (4.2 grams ammonium molybdate tetrahydrate in 100 mL 5 N HCl and 0.15 grams malachite green oxalate in 300 mL dd H_20) was added and vortexed, followed by 200 μL of 1.5% v/v Tween 20 and vortexing. After 25 minutes of sitting at room temperature, a 200 μL aliquot was used to measure the absorbance at 590 nm.

Characterization and quantitation of phospholipids using electrospray ionization-mass spectrometry (ESI-MS)

Lipid extract samples (500 pmol/μl) were prepared by reconstitution in chloroform: methanol (2:1, v/v). ESI-MS was performed as described previously [16-18] using a Trap XCT ion-trap mass spectrometer (Agilent Technologies, Santa Clara, CA) with a nitrogen drying gas flow-rate of 8 L/min at 350ºC and a nebulizer pressure of 30 psi. The scanning range was from 100 to 2200 *m/z* on 5 μL of the sample scanned in negative ion mode for 2.5 min with a mobile phase of acetonitrile: methanol: water (2:3:1) in 0.1% ammonium formate. As previously described [19], qualitative

identification of individual phospholipid molecular species was based on their calculated theoretical monoisotopic mass values, subsequent MS/MS analysis, and their level normalized to either the total ion count (TIC) or the most abundant phospholipid.

MS^{nth} fragmentation was performed on an Agilent Trap XCT ion-trap mass spectrometer equipped with an ESI source. The analyte was introduced by direct injection from the HPLC system. The nitrogen drying gas flow-rate was 8.0 L/min at 350°C. The ion source and ion optic parameters were optimized with respect to the positive molecular ion of interest. Initial identification was typically based on the loss of the parent head group followed by subsequent analysis of the lysophophosolipid.

Multivariate Statistical Analysis of Blood Lipids: Multivariate techniques, such as principal component analysis (PCA), were performed using MetaboAnalyst 2.0 (http://www.metaboanalyst.ca/MetaboAnalyst/faces/Home.jsp) using default algorithms. Automatic peak detection and spectrum deconvolution was performed using a peak width set to 0.5. Data were normalized to the total ion count, and scaled to the z-value. No outliers were removed from the analysis.

Select lipids that were identified using a volcano plot analysis (**Supplemental Table 1**) were further studied and identified using MS/MS analysis. Following identification, the level of each parent lipid was normalized to the total ion count, and the change in the relative abundance of that phospholipid species as compared to its control was determined. This method is standard for lipidomic analysis as reported in our previous studies [16, 18].

Statistical Analysis

All statistical analysis for locomotor data were compiled using SigmaStat for windows version 3.11 (SPSS Science, Chicago, IL). Behavioral sensitization data was analyzed by combining the ambulatory counts and stereotypic counts to get the total horizontal counts (i.e. the total number of horizontal beam breaks) for each animal. The data were binned in 10 min blocks and planned comparisons made at each time point between the treatment activity vs. treatment challenge results using an unpaired Student's t-test. All statistical analysis for lipid data were also compiled using SigmaStat for windows version 3.11 (SPSS Science, Chicago, IL). Lipids isolated from one animal source (blood or tissue) equaled an n of 1, samples from a total of six animals were assessed.

3. Results

Induction of Locomotor Sensitization (LMS)

Using the protocol outlined in Figure 1A. We assessed locomotor movement as an indicator of behavioral sensitization to cocaine in rats by comparing locomotion after the initial "Activity" administration of the drug (10mg/kg, i.p.) on day 4, with the movement observed following a second "Challenge" administration on day 15. Following habituation to the open field environment during the first 30 minutes, cocaine caused an increase in total horizontal movement in rats compared to those treated with saline (Figure 1B). One week following conditioning with four daily doses (15mg/kg, i.p.), a cocaine challenge on day 15 again increased movement compared to saline-treated controls. In addition, cocaine-induced movement at each of the 40, 50, & 60 minute time points also was significantly increased ($p<0.05$, $n=6$) on the Challenge day as

compared to the initial drug-induced movement observed on the Activity day (Figure 1B). This increase in cocaine-induced locomotion following conditioning exposures is indicative of behavioral sensitization (see [20] for recent review).

Seven days after the final exposure to cocaine or saline (protocol day 22), rats were euthanized and specific brain regions and blood were isolated and prepared for lipidomic analysis as explained in the Methods. Brain tissues analyzed following cocaine-induced behavioral sensitization included hippocampus, ventral striatum, dorsal striatum and cerebellum. The areas were chosen as they are known to be involved with drug reward and reinstatement of drug-seeking, and the cerebellum was chosen as a brain region not directly involved with these behaviors [21].

Differential abundance of phospholipids in the hippocampus, frontal cortex and cerebellum of control (drug naïve) rats

We used ESI-MS to analyze over 1,000 *m/z* values representing multiple phospholipid classes. Prior to assessing the effect of repeated cocaine exposure on the level of phospholipids, we first determined the relative abundance of phospholipid species between brain structures. These data are shown in Supplemental Figures 1 and 2. Phosphatidylcholines (PCs) were generally the highest expressed lipids in these tissues and their relative abundance did not appear to vary greatly between the different brain regions studied. Relatively low levels of 16:0 lysophosphatidylcholine (LPC) were also detected in all regions. The pattern an intensities of these lipids is in general agreement with several studies assessing regional distribution of phospholipids in the brain [6, 7, 9]. Two lipid species with *m/z* values of 815-817 and 824.5 had relative abundance

levels 2-fold higher than baseline; however, the identity of these lipids could not be confirmed by subsequent MS/MS analysis.

The relative abundance of select sphingomyelins (SM) was also determined in the hippocampus, frontal cortex and cerebellum (Supplemental Figure 2). In general, the cerebellum had higher levels of 20:0, 22:1, 24:1 and 26:4 SM, as compared to the hippocampus and frontal cortex regions. The levels of all SM species studied were similar in the hippocampus and frontal cortex tissues. For the subsequent cocaine studies, we chose to add assessments of the dorsal and ventral striatum regions.

Effect of repeated cocaine exposure on the relative abundance of phospholipid species in the hippocampus

Analysis of spectra derived from the hippocampus of control and cocaine treated rats showed significant differences in the intensities of *m/z* values ranging from 300 to 600, which can indicate lysophospholipids or low molecular weight phospholipids (Figure 2). Changes were also detected in intensities for *m/z* values correlating to higher molecular weight phospholipids (spectra not shown). Cocaine treatment specifically increased the intensities of peaks with *m/z* values of 565.6 and 593.6 (Figure 2A and B). Subsequent MS/MS analysis identified these peaks to contain 26:0 and 28:0 phosphatidic acid (PA) (Figure 2C), which were increased 2-4-fold in cocaine treated rats compared to saline treated animals. Significant increases in the levels of 27:1 PC and 18:2/18:1 SM were also identified, as well as modest decreases in the levels of 34:1 plasmenyl PC and 34:2 PC.

Effect of repeated cocaine exposure on the relative abundance of phospholipid species in the dorsal and ventral striatum

Analysis of spectra derived from the ventral and dorsal striatum of cocaine and saline treated rats showed few drug-induced differences with regards to phospholipid levels (Figure 3). The intensity of only three *m/z* values differed significantly among these two regions, corresponding to 27:1 PC and 30:0 PC in the ventral striatum and 32:1 PC in the dorsal striatum (Figure 3E). In the ventral striatum, the level of 27:1 PC was increased about 2-fold after cocaine treatment, as compared to saline control, while 30:0 PC was increased about 1.5-fold. In contrast, in the dorsal striatum the level of 32:1 PC was decreased in cocaine treated rats about 20%, as compared to saline treated rats.

Effect of repeated cocaine exposure on the relative abundance of phospholipid species in the cerebellum

Analysis of spectra derived from the cerebellum of rats exposed to cocaine showed several *m/z* values whose intensities significantly decreased compared to control rats (Figure 4). These *m/z* values corresponded to several phospholipids including 546.6, unable to be identified by subsequent MS/MS, and 28:1 PA (Figure 4C). Additionally, the data showed decreases in 30:1, 30:0 and 40:3 PC. All of these phospholipids decreased approximately 20% in cocaine treated rats, as compared to saline treated rats.

Effect of repeated cocaine exposure on the blood lipidome

The above data demonstrate the novel finding that cocaine exposure induces region specific changes in the relative abundance of phospholipid species in the rat brain. To determine if the relative abundance of phospholipids were also changed in blood after cocaine exposure, we analyzed spectra derived from the blood of rats (Figure 5A and B). Subsequent PCA analysis demonstrated that cocaine significantly altered the variability of the blood lipidome compared to saline exposed rats (Figure 5C). A volcano plot analysis demonstrated several *m/z* values whose relative abundance was significantly ($p < 0.05$) altered compared to saline treated animals (Figure 5D and Supplemental Table 1). In general, cocaine treatment decreased the relative abundance of most lipid species, although increases were seen in some species. We validated some of these data by comparing the relative abundance of select lipids (Figure 6) and by performing MS/MS analysis (Supplemental Figure 4). This analysis demonstrated increases in 40:0 plasmenyl PC, 40:0 PG and *m/z* 546.6. The level of 40:0 plasmenyl PC in cocaine treated rats was almost 3-fold higher than controls, while 40:0 PG and 20:3 LPC were only increased about 60 and 20%, respectively. In contrast, and in agreement with the volcano plot, the majority of lipids decreased in cocaine treated animals, compared to saline treated animals. A majority of these lipids were identified as PCs; however, significant decreases were also detected for several SM species, including 18:1/22:0, 18:1/24:1 and 18:1/24:0 SM.

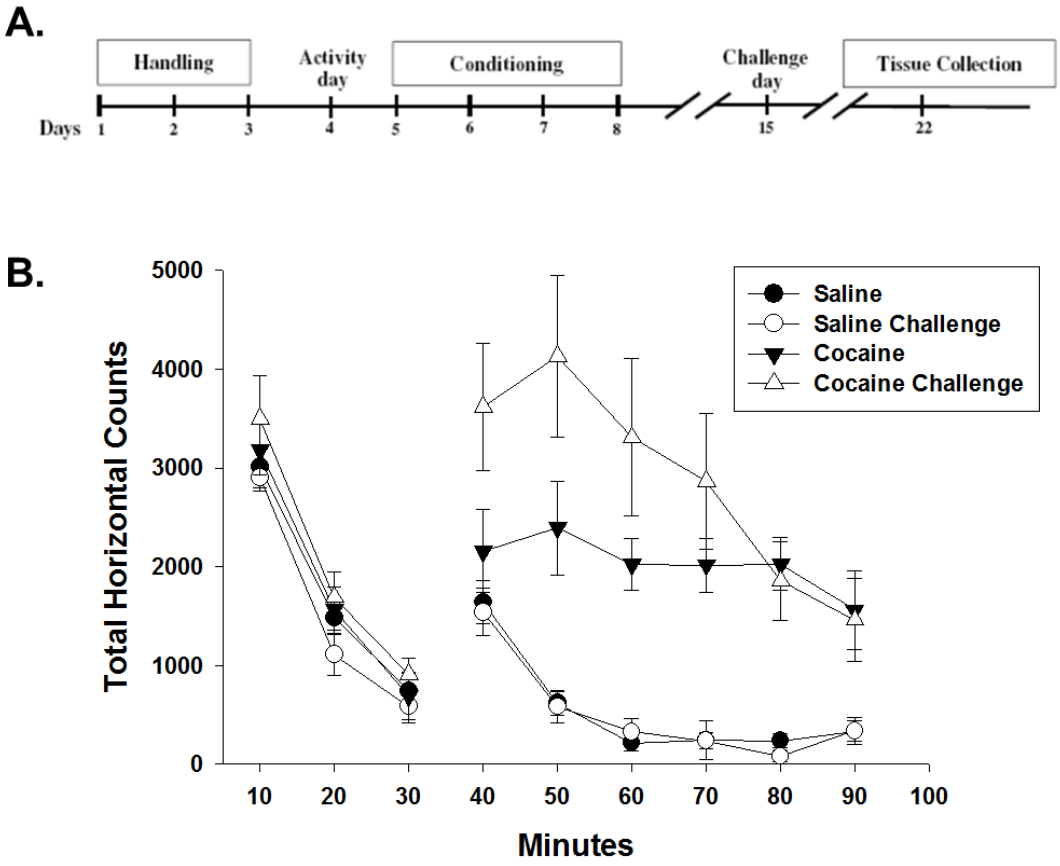

Figure 1. Effect of cocaine conditioning on open-field locomotor activity. **A.** Rats were treated according to a standard locomotor sensitization protocol, as indicated. Activity and Challenge day test dose of cocaine was 10mg/kg i.p., conditioning dose on days 5-8 was 15mg/kg. **B.** Time course quantification of total horizontal counts during the open-field Activity day (filled symbols) and Challenge day (open symbols) sessions prior (10-30 minutes) and post (40-90 minutes) i.p. injection with either saline (circles) or cocaine (triangles). Data represent the mean ± the SEM from groups of n=6 rats.

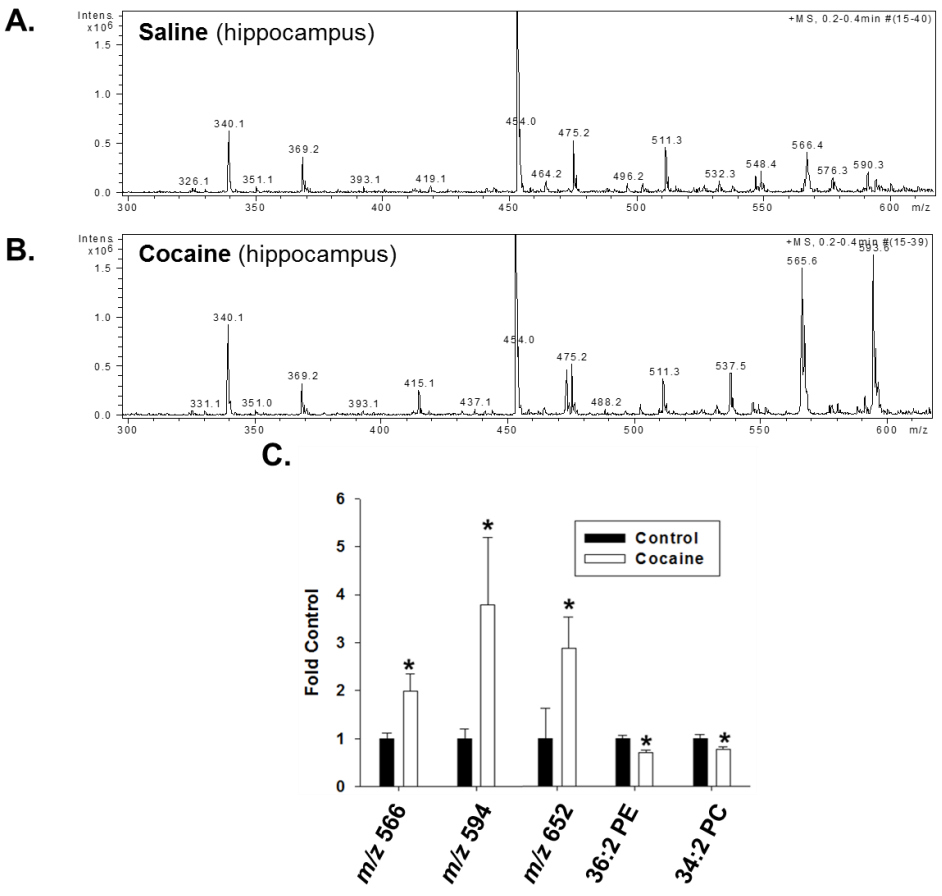

Figure 2. Effect of cocaine exposure on the relative abundance of phospholipids in the hippocampus. Rats were treated with either saline or cocaine as described in Figure 1A. Seven days after the final treatment (Day 22) hippocampal tissue was isolated, subjected to Bligh-Dyer extraction and analyzed by ESI-MS. **A.** represents positive ion ESI-MS spectra from control rats while **B.** represents positive ion ESI-MS spectra from cocaine exposed rats. **C.** represents changes in the relative abundance of select phospholipids in cocaine treated rats compared to saline controls and is presented as the mean ± the SD of at least 6 different rats. *Indicates a significant difference ($p < 0.05$) as compared to saline control rats.

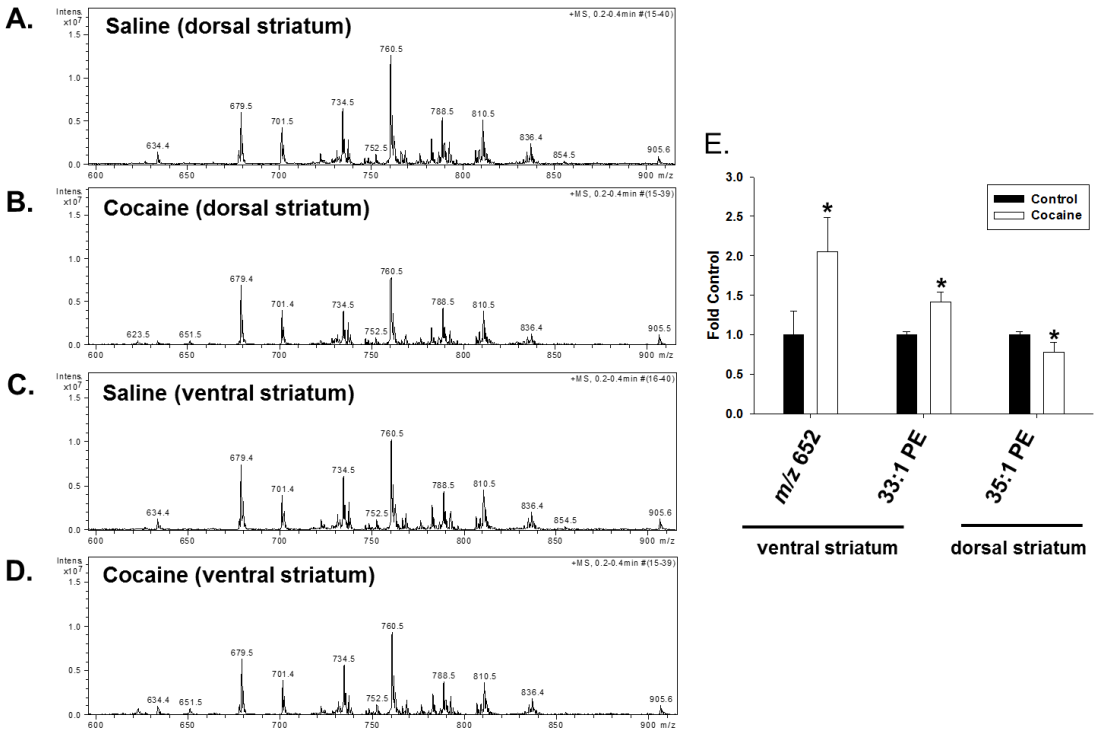

Figure 3. Effect of cocaine exposure on the relative abundance of phospholipids in the dorsal and ventral striatum. Rats were treated with either saline or cocaine as described in Figure 1A. Seven days after the final treatment (Day 22) ventral and dorsal striatal tissue was isolated, subjected to Bligh-Dyer extraction and analyzed by ESI-MS. **A.** and **C.** represent positive ion ESI-MS spectra from control rats for the indicated tissues, while **B.** and **D.** represent spectra from cocaine exposed rats. **E.** represents changes in the relative abundance of select phospholipids in cocaine treated rats as compared to saline controls, and is presented as the mean ± the SD of at least 6 different rats. *Indicates a significant difference ($p < 0.05$) as compared to saline control rats.

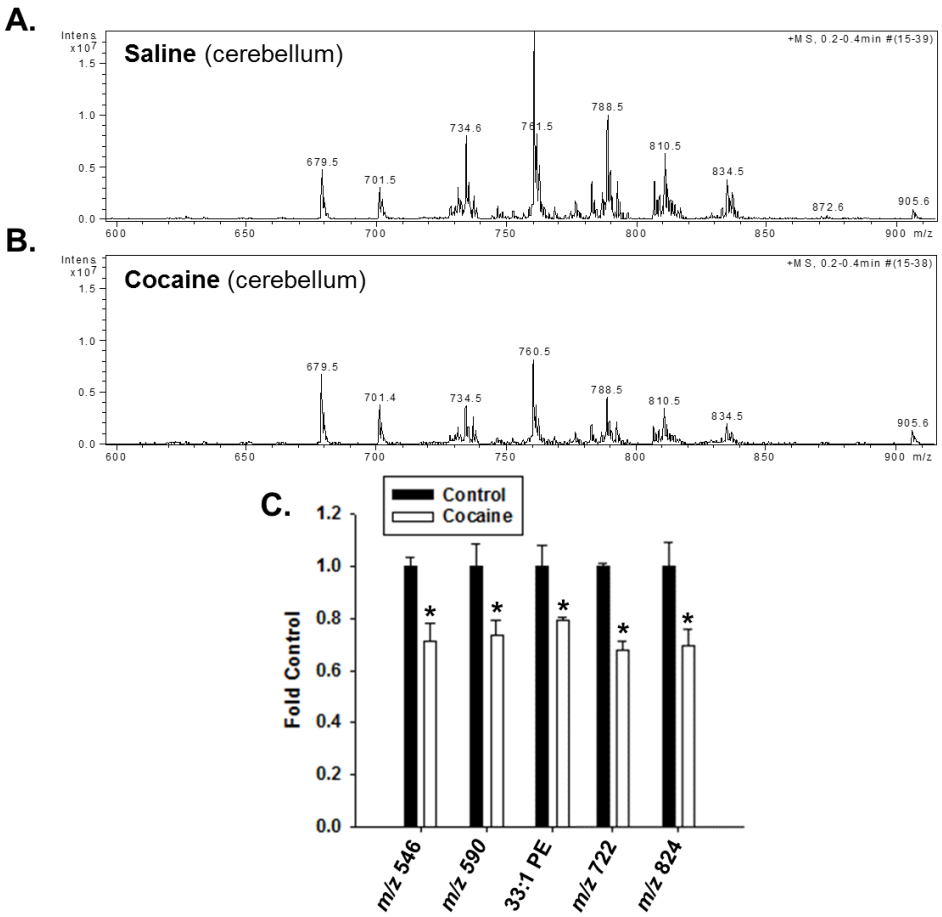

Figure 4. Effect of cocaine exposure on the relative abundance of phospholipids in the cerebellum. Rats were treated with either saline or cocaine as described in Figure 1A. Seven days after the final treatment (Day 22) cerebellar tissue was isolated, subjected to Bligh-Dyer extraction and analyzed by ESI-MS. **A.** represents positive ion ESI-MS spectra from control rats for the indicated tissues, while **B.** represents spectra from cocaine exposed rats. **C.** represents changes in the relative abundance of select phospholipids in cocaine treated rats as compared to saline controls, and is presented as the mean ± the SD of at least 6 different rats. The lipid species present at *m/z* 546.6 was unable to be identified by subsequent MS/MS. *Indicates a significant difference ($p < 0.05$) as compared to saline control rats.

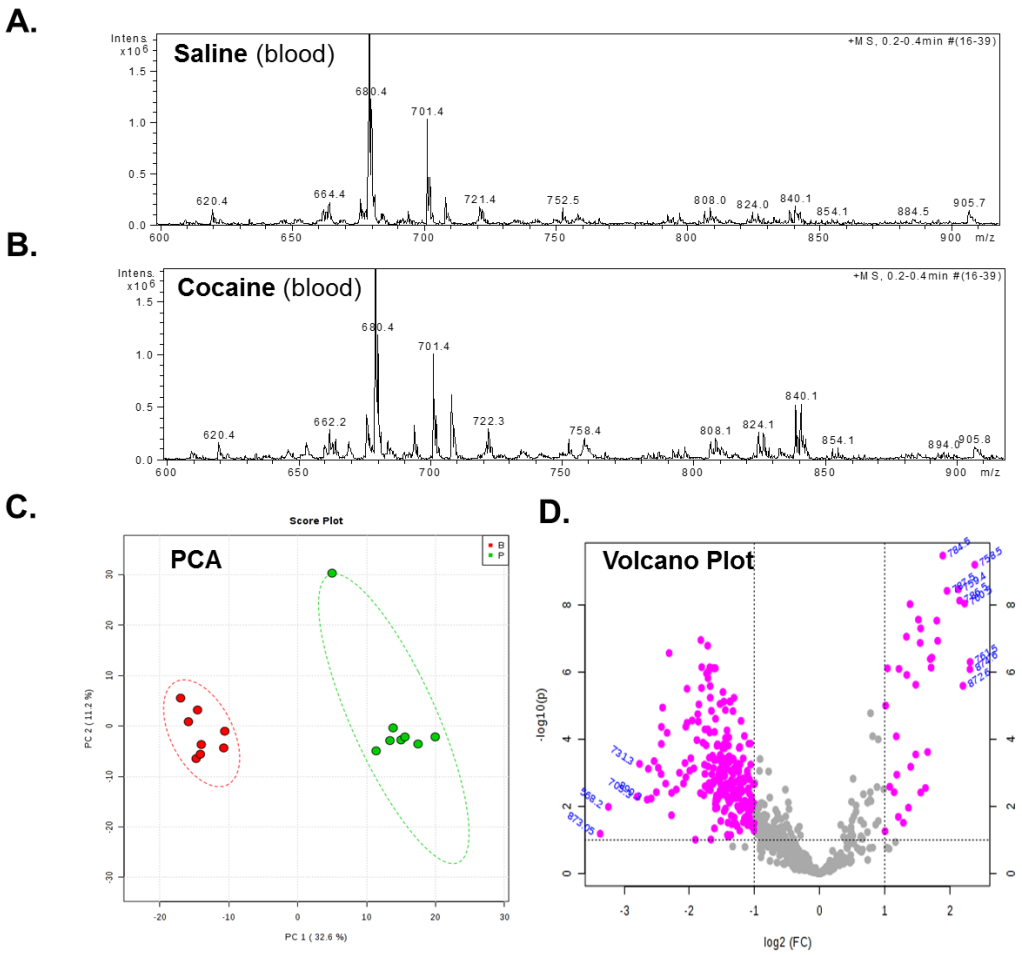

Figure 5. Effect of cocaine exposure on the relative abundance of phospholipids in the blood. Rats were treated with either saline or cocaine as described in Figure 1A. Seven days after the final treatment (Day 22) blood was collected, subjected to Bligh-Dyer extraction and analyzed by ESI-MS. **A.** represents positive ion ESI-MS spectra from saline treated rats for the indicated tissue, while **B.** represents spectra from cocaine exposed rats. **C.** represents PCA analysis of lipids extracted from saline treated rats (green) and cocaine treated rats (red). The circles represent the 95% confidence intervals. **D.** Represents a volcano plot analysis comparing the log change in each *m/z* value (X-axis) to the significance value (Y-axis). The identity of select *m/z* values are indicated next to each data point.

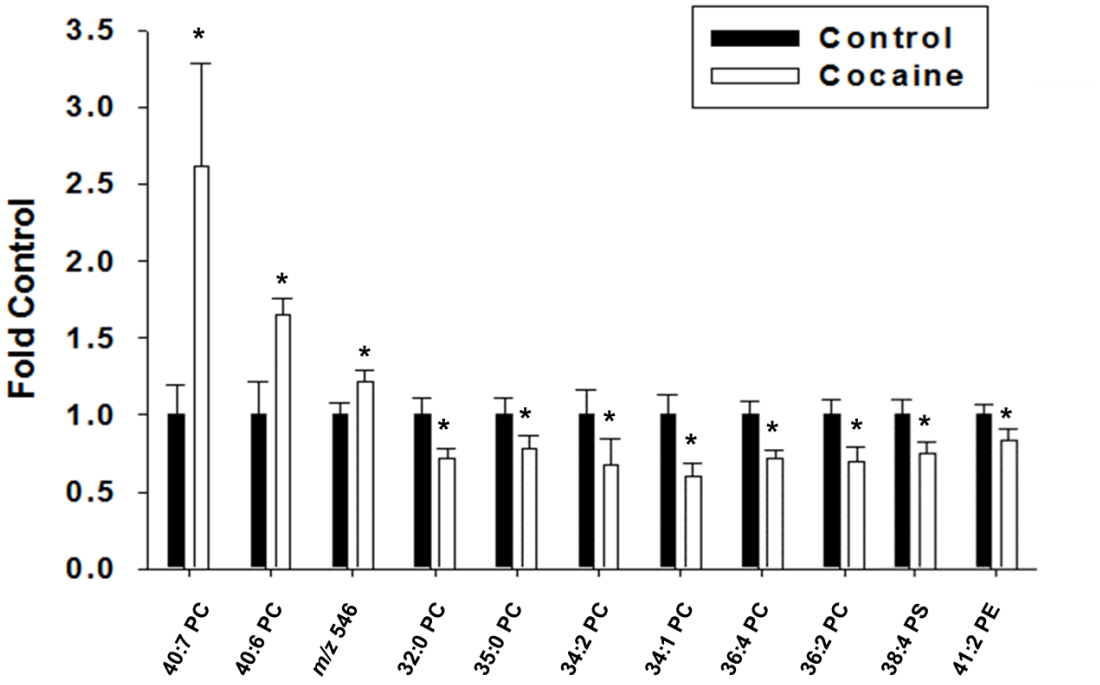

Figure 6. Identification of blood phospholipids altered after cocaine exposure. Rats were treated with either saline or cocaine as described in Figure 1A. Seven days after the final treatment (Day 22) blood was collected, subjected to Bligh-Dyer extraction and analyzed by ESI-MS and subsequent PCA analysis using a volcano plot. Select *m/z* values that demonstrated significant changes in the volcano plot were identified using MS/MS analysis and the fold-change in relative abundance between the saline treated controls and the cocaine treated rats determined. Lipids present at the *m/z* values of 546.6 and 734.5 were unable to be identified by subsequent MS/MS. The data are presented as the mean ± the SD of at least 6 different rats. *Indicates a significant difference ($p < 0.05$) as compared to saline control rats.

Table 1. Correlation between Initial Response and Sensitization to Cocaine and Changes in the Expression of Select Glycerophospholipids in Rat Blood.

m/z	Tentative Lipid[b]	R^2 Initial Response	R^2 Sensitization
546.6	20:3 LPC[b]	0.44	−0.75
734.5	32:0 PC[c]	0.75	0.66
735.5	35:0 PC[c]	0.83	0.23
758.8	34:2 PC[c]	0.76	0.57
760.6	34:1 PC[c]	0.64	0.63
782.3	36:4 PC[c]	0.52	0.13
786.6	36:2 PC[c]	0.89	0.23
813.6	38:4 PS[c]	0.59	0.53
815.3	41:2 PE	0.77	0.63
832.4	40:7 PC[c]	−0.36	−0.48
834.6	40:6 PC[c]	0.08	−0.39

[a]As determined by comparing the percent change in lipid to initial response to cocaine

[b]Based on theoretical m/z reported in Lipids Maps (www.lipidmaps.org)

[c]Based on theoretical m/z reported in Lipids Maps (www.lipidmaps.org) and MS/MS analysis with neutral loss scanning

Supplemental Table 1. Volcano plot analysis of *m/z* values significantly changed in rat blood after cocaine reinstatement. The log2(FC) and the – log10(p) indicate the size change and the significance value as determined by PCA analysis.

m/z	Fold Change (FC)	log2(FC)	p-value	-log10(p)
784.5	3.7198	1.895	3.309E-10	9.4803
758.5	5.2324	2.387	6.179E-10	9.2091
759.4	4.3937	2.135	3.344E-09	8.4757078
787.5	3.8915	1.96	3.731E-09	8.4281864
786.5	4.4516	2.154	7.322E-09	8.1353762
760.5	4.6936	2.23	8.904E-09	8.0504148
812.5	2.6235	1.3915	9.337E-09	8.0298066
814.5	2.869	1.52	2.689E-08	7.5704092
783.5	3.4904	1.803	2.888E-08	7.5394329
788.5	2.938	1.554	4.915E-08	7.3084942
369.15	2.5245	1.336	8.729E-08	7.0590305
1349.7	0.28267	-1.82	1.096E-07	6.9602687
782.5	3.5228	1.816	1.157E-07	6.9365916
762.5	2.9227	1.547	1.333E-07	6.875235
197.8	0.30391	-1.71	1.608E-07	6.793822
624.3	0.20161	-2.31	2.684E-07	6.5712337
734.5	3.31	1.726	3.652E-07	6.4374573
813.5	3.2562	1.703	4.018E-07	6.3960009
761.5	4.9778	2.315	4.935E-07	6.3067216
631.3	0.2853	-1.8	7.06E-07	6.1511768
940.5	0.31118	-1.68	7.121E-07	6.1474895
815.6	3.285	1.715	7.255E-07	6.1393446
580.3	0.33003	-1.59	7.598E-07	6.1193236
579.3	0.32424	-1.62	7.6E-07	6.1192093
811.5	2.0632	1.044	7.676E-07	6.1148481
816.5	2.3326	1.222	7.943E-07	6.10001
874.6	4.9669	2.312	8.152E-07	6.0887412
560.3	0.30655	-1.7	9.334E-07	6.0299462
276.5	0.3004	-1.73	1.087E-06	5.9636107
735.5	2.5353	1.342	1.201E-06	5.9203485
432.1	0.30486	-1.71	1.496E-06	5.8249813
785.5	2.7899	1.48	2.35E-06	5.6288767
872.6	4.6139	2.206	2.532E-06	5.5965363
955.5	0.31211	-1.67	2.572E-06	5.5898135
627.4	0.28449	-1.81	2.945E-06	5.5308705
636.4	0.24395	-2.03	3.114E-06	5.5066396
595.3	0.35773	-1.48	3.904E-06	5.4085458
460.1	0.3124	-1.67	5.723E-06	5.2423914

543.2	0.40242	-1.31	5.781E-06	5.237997
209.8	0.38452	-1.37	7.529E-06	5.1232858
649.4	0.38631	-1.37	7.537E-06	5.1227842
667.4	0.36124	-1.46	7.542E-06	5.1224962
695.4	0.3467	-1.52	8.855E-06	5.0528311
333	0.27673	-1.85	9.106E-06	5.0406724
789.5	2.0241	1.0173	9.868E-06	5.0057709
153.8	0.18805	-2.4108	1.134E-05	4.9455785
710.4	0.3672	-1.4454	1.339E-05	4.8732194
626.3	0.31617	-1.6612	1.419E-05	4.8480788
309	0.39782	-1.3298	1.447E-05	4.8395915
645.3	0.27337	-1.871	1.776E-05	4.7505815
1009.3	0.33063	-1.5967	2.446E-05	4.6115968
405.1	0.25766	-1.9564	2.741E-05	4.5621543
641.3	0.43376	-1.205	2.838E-05	4.546957
248.85	0.27513	-1.8618	2.964E-05	4.5280925
316.95	0.24386	-2.0359	3.222E-05	4.4919014
555.3	0.24086	-2.0537	4.217E-05	4.3749758
374.05	0.18569	-2.429	4.27E-05	4.3695823
606.3	0.30418	-1.717	5.044E-05	4.2972594
198.8	0.29533	-1.7596	5.068E-05	4.2951891
411.1	0.37331	-1.4216	5.437E-05	4.2646327
582.3	0.32703	-1.6125	6.064E-05	4.2172695
505.1	0.3107	-1.6864	6.246E-05	4.2044189
377.9	0.19725	-2.3419	6.403E-05	4.1936165
685.3	0.44955	-1.1534	7.981E-05	4.0979318
772.5	2.266	1.1801	8.188E-05	4.086801
586.3	0.38048	-1.3941	8.787E-05	4.0561693
557.3	0.36799	-1.4423	9.061E-05	4.0428047
587.3	0.27094	-1.884	0.0001055	3.9768711
385.1	0.3692	-1.4375	0.0001093	3.9615388
589.3	0.28908	-1.7905	0.0001262	3.8990439
547.3	0.4793	-1.061	0.0001343	3.8719887
750.4	0.47144	-1.0848	0.000135	3.8696019
794.3	0.18556	-2.43	0.0001378	3.8606247
435.15	0.33776	-1.5659	0.0001415	3.8493663
572.3	0.36004	-1.4738	0.0001453	3.8377344
574.3	0.29882	-1.7427	0.0001504	3.8228388
216.8	0.37885	-1.4003	0.0001531	3.8149681
518.2	0.33579	-1.5744	0.0001556	3.8080462
490.2	0.42785	-1.2248	0.0001699	3.7697044
486.2	0.4255	-1.2328	0.0001818	3.74043
515.2	0.3564	-1.4884	0.0001827	3.7383565
509.2	0.36315	-1.4614	0.0001848	3.733392
876.6	3.167	1.6631	0.0002396	3.6204407

902.6	2.7888	1.4796	0.0002842	3.5464218
272.9	0.34742	-1.5252	0.0002927	3.5335328
504.2	0.32014	-1.6432	0.0003099	3.5088485
447.2	0.38203	-1.3882	0.0003213	3.4931433
581.3	0.35314	-1.5017	0.0003458	3.461175
424.1	0.30943	-1.6923	0.0003555	3.4491726
694.4	0.37269	-1.424	0.0003682	3.4339634
166.7	0.25404	-1.9768	0.0003688	3.4331973
692.4	0.39716	-1.3322	0.0003723	3.4291186
650.4	0.44349	-1.173	0.0003725	3.4288621
466.1	0.33425	-1.581	0.0003998	3.3981572
240.9	0.35573	-1.4911	0.0004062	3.3912387
614.3	0.39985	-1.3225	0.0004112	3.3859575
487.2	0.32651	-1.6148	0.0004184	3.3784602
1074.8	0.17188	-2.5405	0.0004493	3.3474249
425.1	0.36776	-1.4432	0.000455	3.3420363
628.3	0.38363	-1.3822	0.0004716	3.3264446
519.2	0.35255	-1.5041	0.0004943	3.3060445
683.4	0.23873	-2.0666	0.0005098	3.2926428
484.2	0.41955	-1.2531	0.0005348	3.2718411
731.3	0.1471	-2.7652	0.0005394	3.268073
573.3	0.42917	-1.2204	0.0005606	3.2513856
368.1	0.48098	-1.0559	0.0005679	3.2457511
338.1	0.29395	-1.7663	0.0005732	3.2417165
657.3	0.36788	-1.4427	0.0005754	3.2400452
302.9	0.41215	-1.2788	0.0006096	3.2149265
594.3	0.30523	-1.712	0.0006443	3.1909119
901.6	2.6424	1.4018	0.0006618	3.1792667
256.8	0.41215	-1.2788	0.0006682	3.175074
706.3	0.17968	-2.4765	0.0007086	3.1496234
339.1	0.32335	-1.6288	0.0007215	3.1417938
973.4	0.26235	-1.9304	0.0007369	3.1326091
1133.8	0.37365	-1.4202	0.0007453	3.127698
583.3	0.40206	-1.3145	0.0007493	3.1253732
851.4	0.16164	-2.6292	0.0007628	3.1175722
347	0.34706	-1.5268	0.0007677	3.1147915
728.5	0.42257	-1.2427	0.0007775	3.109294
1005.3	0.3875	-1.3677	0.0008651	3.0629588
362.1	0.25112	-1.9936	0.0008666	3.0622014
421.1	0.46392	-1.1081	0.0008777	3.0566786
349	0.34553	-1.5331	0.0008792	3.0559321
417.1	0.42302	-1.2412	0.0009259	3.0334218
260.8	0.35827	-1.4809	0.0009514	3.0216505
651.3	0.22507	-2.1515	0.000997	3.0013136
537.2	0.34273	-1.5449	0.001047	2.9800533

396.2	0.29519	-1.7603	0.0010782	2.9673007
632.2	0.18509	-2.4337	0.0010904	2.9624142
423.1	0.46448	-1.1063	0.0010906	2.9623345
960.3	0.3176	-1.6547	0.0011008	2.9582916
561.2	0.39823	-1.3283	0.0011012	2.9581338
375.05	0.34136	-1.5506	0.0011204	2.9506269
706.5	2.2791	1.1885	0.0011389	2.9435144
535.3	0.36007	-1.4737	0.0011823	2.9272723
556.2	0.36465	-1.4554	0.0012072	2.9182208
653.3	0.35921	-1.4771	0.0012406	2.9063682
332.1	0.24084	-2.0538	0.0013607	2.8662376
311	0.34593	-1.5314	0.0013896	2.8571102
715.4	0.44184	-1.1784	0.0014872	2.8276306
304.9	0.42611	-1.2307	0.0015429	2.8116622
489.2	0.47459	-1.0752	0.0015534	2.8087167
335	0.33108	-1.5948	0.0016319	2.7873065
387.1	0.39037	-1.3571	0.0016956	2.7706766
395.1	0.44764	-1.1596	0.0017964	2.745597
1050.55	0.32312	-1.6299	0.0018223	2.7393801
437.1	0.40898	-1.2899	0.0018702	2.7281119
389.1	0.39148	-1.353	0.001908	2.7194216
181.8	0.34742	-1.5252	0.0020116	2.6964584
357	0.30889	-1.6949	0.0020282	2.6928892
529.2	0.3702	-1.4336	0.0020722	2.6835683
225.8	0.32149	-1.6371	0.0020885	2.6801655
1020.65	0.23482	-2.0904	0.0020948	2.6788574
302.2	0.19432	-2.3635	0.0020988	2.6780289
431.1	0.32173	-1.6361	0.0021108	2.6755529
480.2	0.49294	-1.0205	0.0021424	2.6690994
307	0.31219	-1.6795	0.0021697	2.6636003
623.4	0.49853	-1.0042	0.0021921	2.6591396
514.25	0.37441	-1.4173	0.0022977	2.6387067
430.1	0.38479	-1.3778	0.0023407	2.6306542
445.1	0.43083	-1.2148	0.00251	2.6003263
1028.65	0.2955	-1.7588	0.0025224	2.598186
961.2	0.35224	-1.5054	0.0025539	2.5927961
818.5	2.1135	1.0796	0.0025972	2.5854946
688.3	0.39139	-1.3533	0.0026643	2.5744169
615.3	0.38353	-1.3826	0.0026684	2.5737491
1073.7	0.30163	-1.7292	0.002731	2.5636783
904.6	3.0932	1.6291	0.0028511	2.5449875
714.4	0.39855	-1.3272	0.0028552	2.5443635
913.5	0.37807	-1.4033	0.002901	2.5374523
689.3	0.46875	-1.0931	0.0029137	2.5355552
939.5	0.43406	-1.204	0.0029432	2.5311802

670.3	0.42537	-1.2332	0.0030296	2.5186147
348.1	0.30584	-1.7092	0.0031461	2.5022275
646.3	0.36991	-1.4348	0.0031522	2.5013862
912.3	0.21742	-2.2014	0.0031614	2.5001206
950.5	0.41402	-1.2722	0.0032812	2.4839673
1103.5	0.31286	-1.6764	0.0032837	2.4836365
398.1	0.46771	-1.0963	0.0033014	2.4813019
312	0.3964	-1.335	0.0033231	2.4784566
506.2	0.34657	-1.5288	0.0034252	2.4653141
1031.7	0.34945	-1.5169	0.0034877	2.4574609
409.1	0.43936	-1.1865	0.0035683	2.4475386
774.5	2.2153	1.1475	0.0037684	2.423843
829.3	0.17592	-2.507	0.0037764	2.422922
875.6	2.94	1.5558	0.0038765	2.4115602
901.45	0.20702	-2.2721	0.0039687	2.4013517
336	0.28144	-1.8291	0.004015	2.3963145
404.1	0.47366	-1.0781	0.0041367	2.383346
353.1	0.35111	-1.51	0.0044022	2.3563302
258.9	0.42589	-1.2315	0.004458	2.3508599
530.2	0.39828	-1.3281	0.0044717	2.3495273
609.3	0.2917	-1.7774	0.0046298	2.3344378
660.25	0.34836	-1.5214	0.0046942	2.3284384
314	0.33365	-1.5836	0.0047433	2.3239194
630.3	0.36956	-1.4361	0.004757	2.3226668
517.2	0.40544	-1.3024	0.0049434	2.3059742
1080.7	0.37468	-1.4163	0.0050639	2.2955149
705.3	0.14328	-2.8031	0.0051529	2.2879483
559.3	0.4853	-1.043	0.0052156	2.2826957
671.3	0.42299	-1.2413	0.0055374	2.2566941
1200.7	0.40706	-1.2967	0.0056956	2.2444605
777.3	0.16667	-2.5849	0.0058099	2.2358313
588.3	0.3868	-1.3703	0.0059632	2.2245206
450.1	0.33186	-1.5914	0.0060248	2.2200574
687.3	0.39058	-1.3563	0.0061125	2.2137811
603.3	0.33782	-1.5657	0.0061611	2.2103417
474.1	0.37847	-1.4018	0.0061883	2.2084286
890.3	0.15953	-2.6481	0.0062826	2.2018606
1199.7	0.45104	-1.1487	0.0067881	2.1682518
436.1	0.33152	-1.5928	0.0069758	2.156406
558.2	0.47236	-1.0821	0.0075681	2.1210131
356.1	0.38284	-1.3852	0.0077892	2.1085071
1030.5	0.4417	-1.1789	0.0078646	2.1043234
1078.6	0.47463	-1.0751	0.0081652	2.0880332
214.8	0.49858	-1.0041	0.008202	2.0860802
1350.7	0.33003	-1.5993	0.0084438	2.0734621

618.3	0.4807	-1.0568	0.0085716	2.0669381
991.55	0.43699	-1.1943	0.0087883	2.0560951
644.3	0.48814	-1.0346	0.0089527	2.048046
992.6	0.45638	-1.1317	0.0095225	2.021249
534.2	0.43606	-1.1974	0.0095862	2.0183535
765.4	0.41815	-1.2579	0.0097806	2.0096345
1006.4	0.43975	-1.1852	0.01012	1.9948195
563.3	0.47591	-1.0712	0.010202	1.9913147
568.2	0.10556	-3.2439	0.01039	1.9833845
578.3	0.4224	-1.2433	0.010796	1.9667371
407.1	0.33592	-1.5738	0.010958	1.9602687
319	0.46331	-1.1099	0.010995	1.9588048
878.6	2.5813	1.3681	0.011004	1.9584494
672.4	0.49612	-1.0112	0.011077	1.9555778
238.8	0.47516	-1.0735	0.011386	1.9436288
658.4	0.43929	-1.1868	0.01141	1.9427144
328	0.33012	-1.599	0.011661	1.9332642
969.5	0.42926	-1.2201	0.011674	1.9327803
1059	0.36757	-1.4439	0.011736	1.9304799
536.2	0.47969	-1.0598	0.012533	1.901945
1000.7	0.42852	-1.2226	0.013147	1.8811733
365	0.47288	-1.0805	0.01376	1.8613816
941.5	0.4886	-1.0333	0.013998	1.853934
956.5	0.36224	-1.465	0.014028	1.8530042
629.35	0.49455	-1.0158	0.014248	1.8462461
1077.7	0.47132	-1.0852	0.015028	1.8230988
361.1	0.46878	-1.093	0.015987	1.796233
1328.6	0.20677	-2.2739	0.01853	1.7321246
410.1	0.48401	-1.0469	0.018535	1.7320074
1327.5	0.39056	-1.3564	0.019044	1.7202418
448.2	0.49613	-1.0112	0.019579	1.7082095
903.7	2.3173	1.2125	0.020658	1.6849117
966.5	0.40325	-1.3102	0.021219	1.6732751
989.6	0.45353	-1.1407	0.021284	1.6719467
1104.5	0.4764	-1.0698	0.022567	1.6465262
686.3	0.44991	-1.1523	0.022887	1.6404111
700.35	0.45816	-1.1261	0.023712	1.6250318
341.9	0.3494	-1.517	0.027402	1.5622177
377.1	0.48497	-1.044	0.029687	1.5274337
510.3	0.44417	-1.1708	0.029722	1.526922
640.3	0.37734	-1.4061	0.030784	1.5116749
947.5	2.4442	1.2894	0.030948	1.5093674
1036.5	0.49936	-1.0018	0.032651	1.4861035
162.7	0.4097	-1.2874	0.032853	1.483425
1076.5	0.40604	-1.3003	0.033476	1.4752664

1022.5	0.39329	-1.3463	0.034113	1.4670801
329	0.47224	-1.0824	0.034297	1.4647439
775.4	0.46492	-1.1049	0.036526	1.4373979
910.5	0.41571	-1.2663	0.03894	1.4096041
593.4	0.48497	-1.044	0.039618	1.4021075
638.3	0.32671	-1.6139	0.045609	1.3409494
990.7	0.49732	-1.0077	0.046067	1.3366101
1075.5	0.4976	-1.007	0.052752	1.2777611
831.5	0.42772	-1.2253	0.053021	1.2755521
871.6	2.0111	1.008	0.055321	1.25711
873.05	0.096733	-3.3698	0.065639	1.182838
878.4	0.37523	-1.4142	0.071401	1.1462957
903.5	0.38839	-1.3644	0.072174	1.1416192
1344.4	0.37785	-1.4041	0.080282	1.0953818
566.7	0.31486	-1.6672	0.097868	1.0093593
947.7	0.26661	-1.9072	0.098723	1.0055817

Supplemental Table 2. Lipid phosphorus assay. Lipids extracted from brain and blood samples were analyzed for inorganic phosphorus content based on analysis of standards ranging from 1 ug to 5 ug at λ=590 nm. Concentrations of samples were diluted to 500 pmol/ul for mass spectrometry.

Sample	Absorbance (nm)	Concentration (ug)
1	0.8996	14.55
2	1.4414	27.48
3	0.4351	3.47
4	0.4989	4.99
5	0.9898	16.70
6	1.6206	31.76
7	0.4676	4.24
8	0.5283	5.69
9	0.946	15.66
10	1.0229	17.49
11	0.4837	4.63
12	0.5898	7.16
13	0.5869	7.09
14	1.1309	20.07
15	0.4221	3.16
16	0.5075	5.19
17	1.1614	20.80
18	1.822	36.57
19	0.3565	1.59
20	0.3346	1.07
21	1.4187	26.94
22	1.743	34.68
23	0.3726	1.97
24	0.4354	3.47
25	1.1532	20.60
26	1.4641	28.02
27	0.4839	4.63
28	0.5417	6.01
29	1.5024	28.94
30	1.4122	26.79
31	0.5225	5.55
32	0.6048	7.52
33	0.3742	2.01
34	0.3829	2.22
35	0.3771	2.08
36	0.3883	2.35

37	0.3483	1.39
38	0.3459	1.34
39	0.3526	1.50
40	0.3701	1.91
41	0.3684	1.87
42	0.3729	1.98
43	0.3029	0.31
44	0.4028	2.69
45	0.4016	2.67
46	0.4135	2.95
47	0.3081	0.43
48	0.4298	3.34

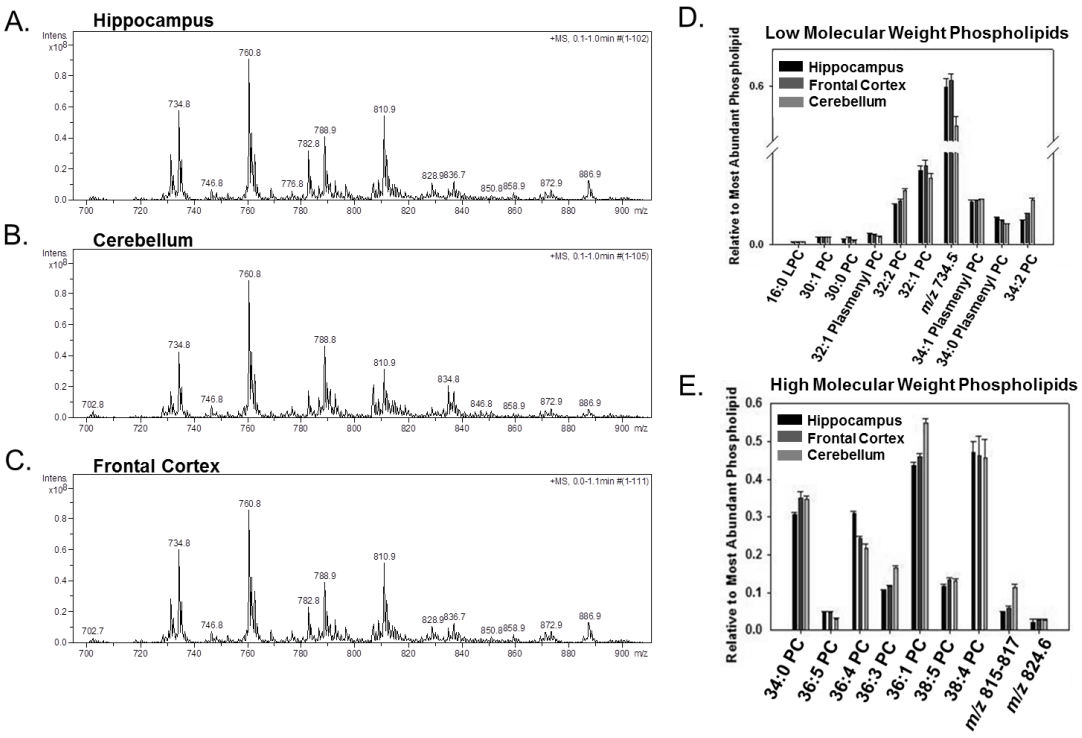

Supplemental Figure 1. Positive ion ESI-MS spectra of lipids isolated from rat brain. The hippocampus **A**., cerebellum **B**. and frontal cortex **C**. were isolated from control rat brains and subjected to Bligh-Dyer extraction after which an equal amount of lipids were analyzed by ESI-MS. Panels **D.** and **E.** represent the relative expression of phospholipids in each area based on the expression of 34:2 PC. Spectra in **A.**-**C.** are representative of at least 6 different animals, while data in **D.** and **E.** are presented as the mean ± the SD of at least 3 different rats. Lipids present at the *m/z* values of 734.5 in **D.** 815-817 and 824.6 in **E.** were unable to be identified by subsequent MS/MS.

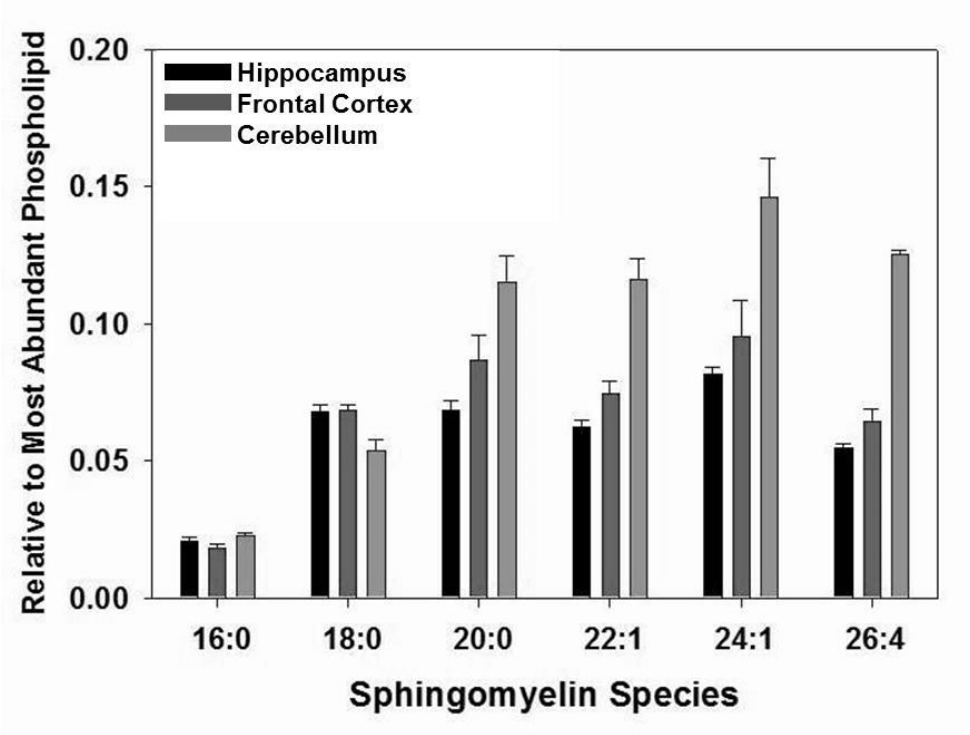

Supplemental Figure 2. Differential expression of sphingomyelins in the rat brain. The hippocampus, cerebellum and frontal cortex were isolated from rat brain and subjected to Bligh-Dyer extraction prior to analysis of sphingomyelin expression using ESI-MS. The first number represents the number of carbons in the sn-2 fatty acid and second number represents the number of double bonds. Data are presented as the mean ± the SD of at least 3 different rats.

A. 20:4 PC *(m/z 546)*

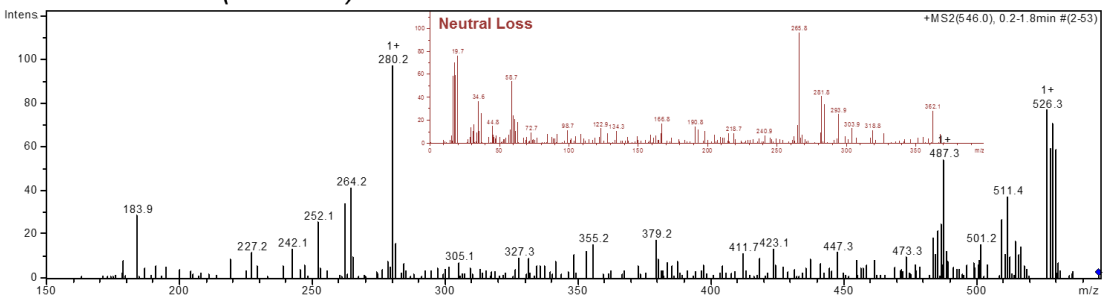

B. 33:1 PE *(m/z 704)*

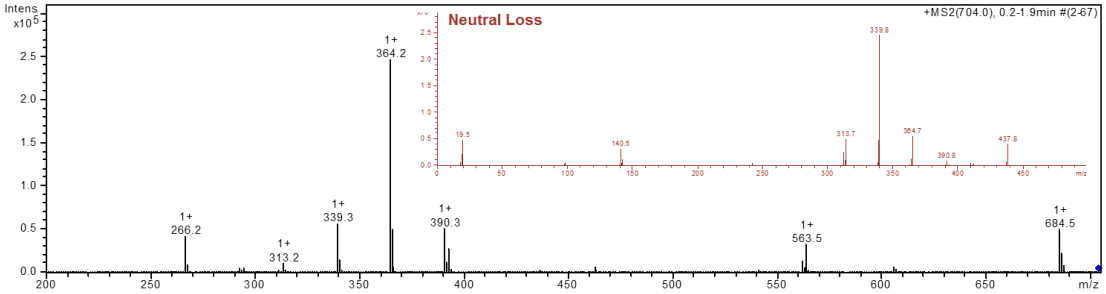

C. 35:6 PE *(m/z 722)*

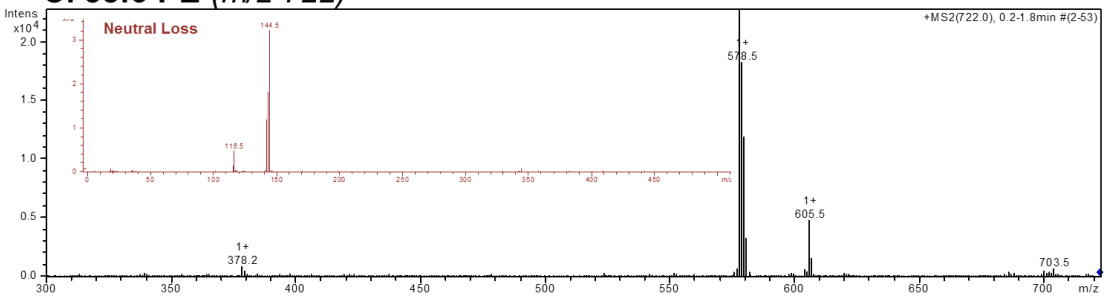

D. 42:4 PE *(m/z 824)*

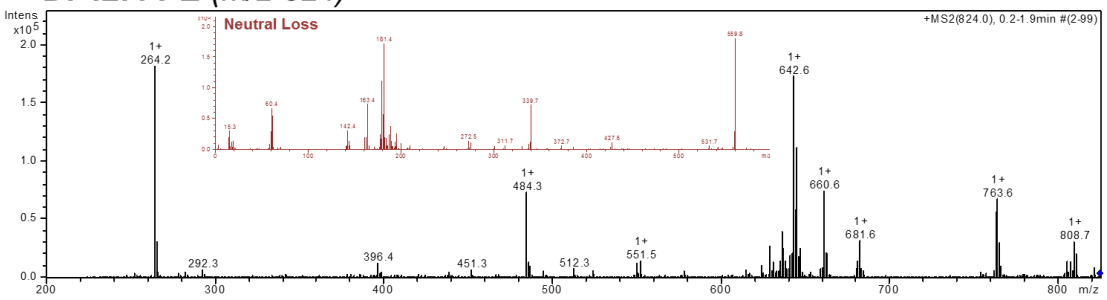

Supplemental Figure 3. MS/MS spectra and neutral loss fragmentation. MS/MS was performed to validate the identity of lipid species shown to be altered in the **cerebellum** of rats treated with cocaine compared to those treated with saline. Lipid species present at the *m/z* value of 590 were unable to be identified.

A. 20:0 PC *(m/z 566)*

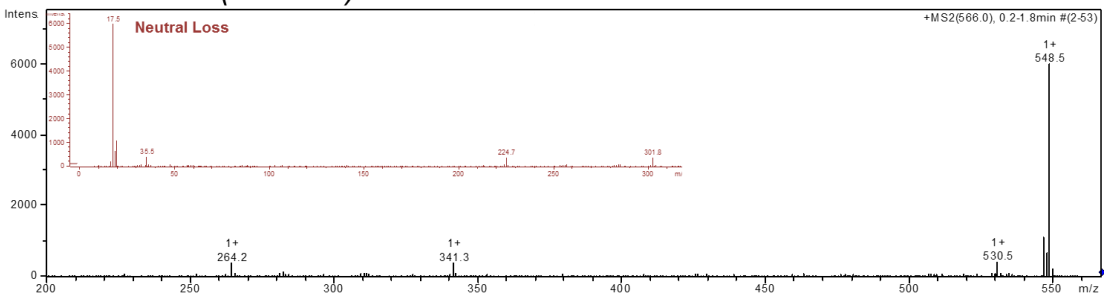

B. 22:0 PC *(m/z 594)*

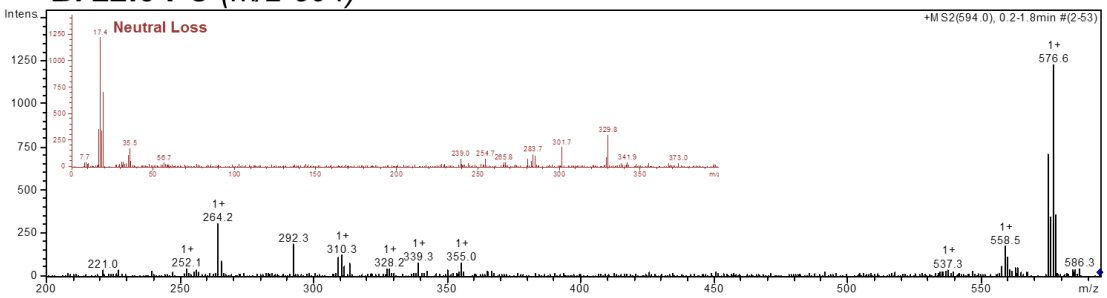

C. 27:1 PG *(m/z 652)*

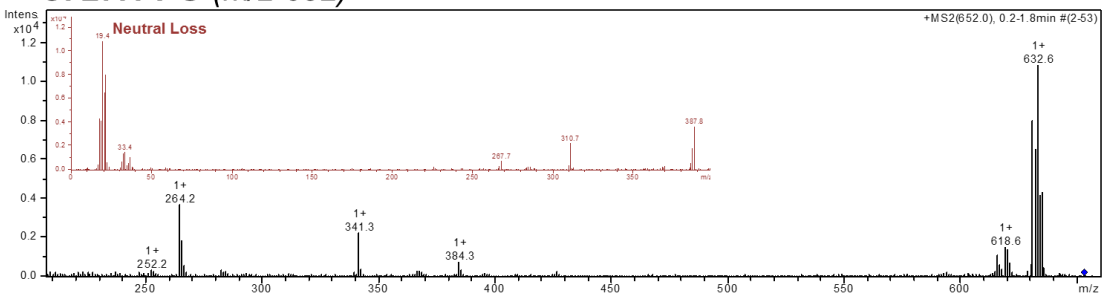

D. 36:2 PE *(m/z 744)*

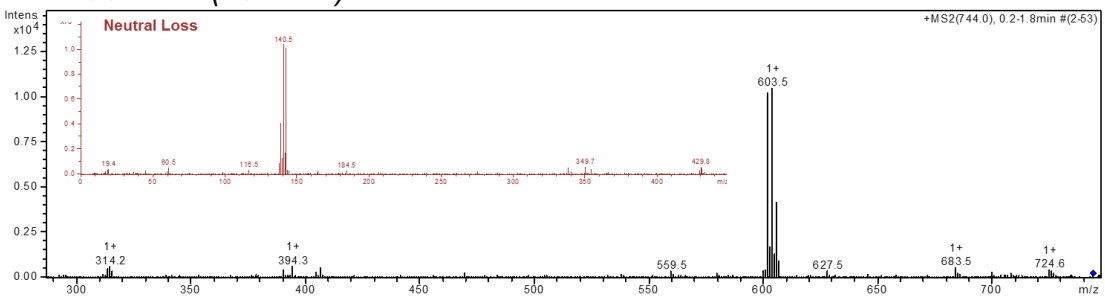

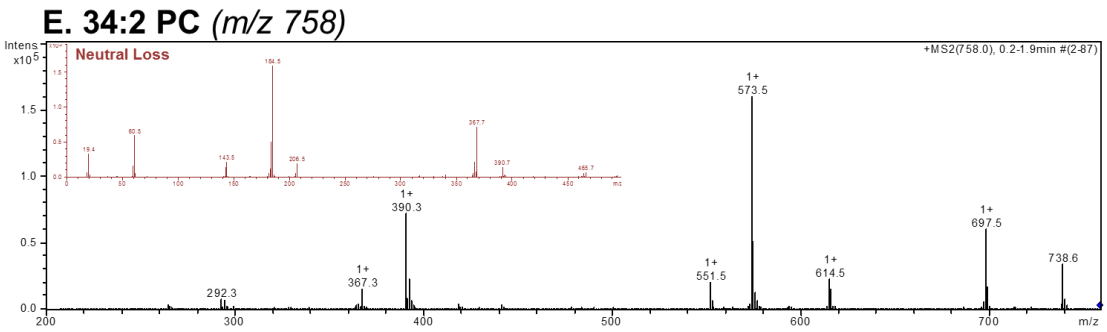

Supplemental Figure 4. MS/MS spectra and neutral loss fragmentation. MS/MS was performed to validate the identity of lipid species shown to be altered in the **hippocampus** of rats treated with cocaine compared to those treated with saline.

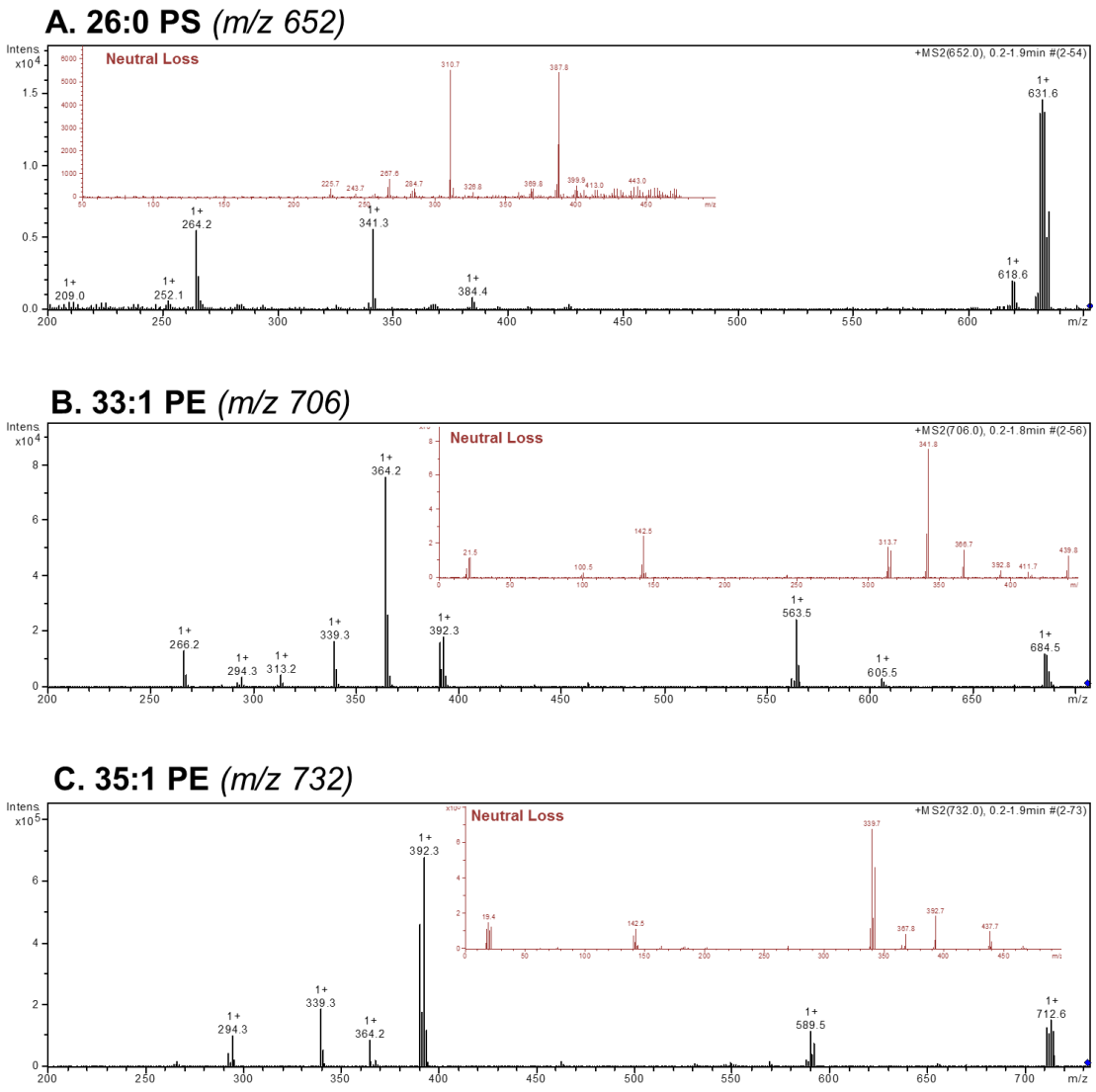

Supplemental Figure 5. MS/MS spectra and neutral loss fragmentation. MS/MS was performed to validate the identity of lipid species shown to be altered in the **striatum** of rats treated with cocaine compared to those treated with saline.

A. 20:3 PC *(m/z 546)*

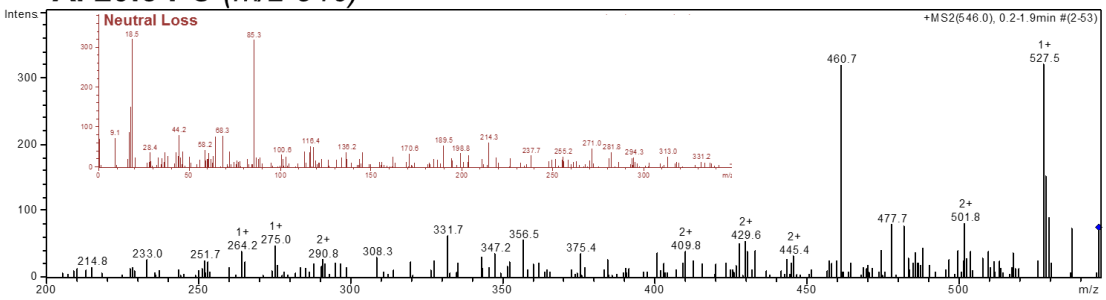

B. 32:0 PC *(m/z 734)*

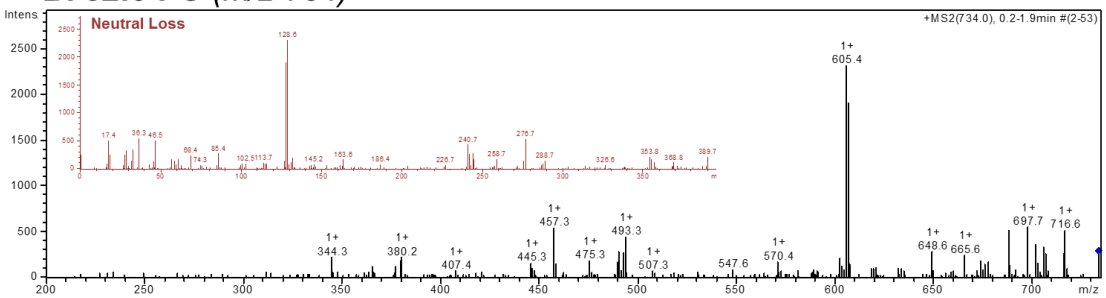

C. 35:0 PC *(m/z 735.5)*

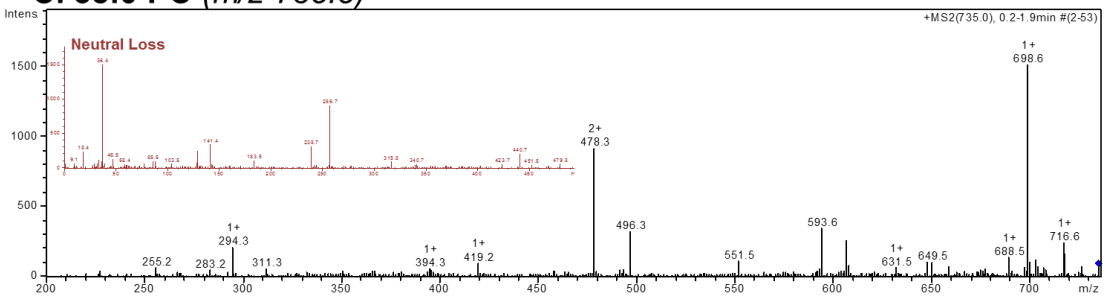

D. 34:2 PC *(m/z 758)*

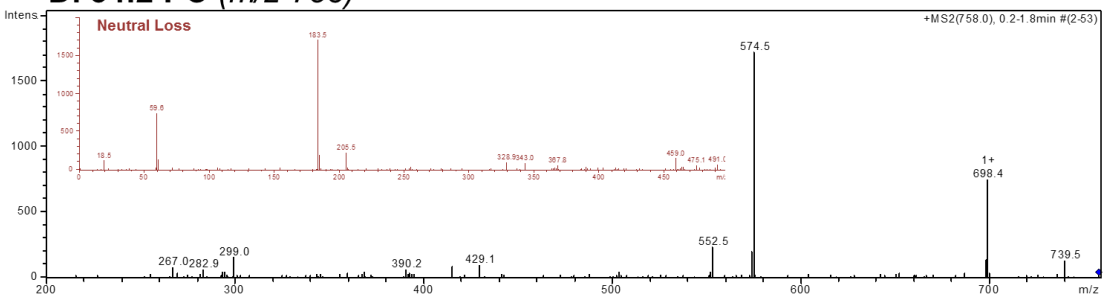

E. 34:1 PC *(m/z 760)*

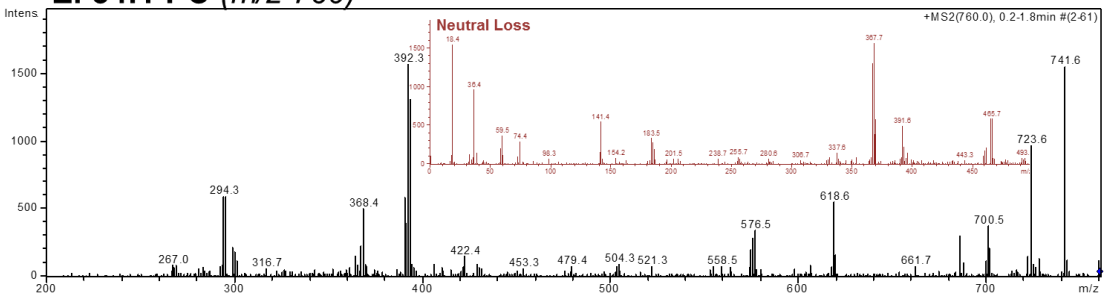

F. 36:4 PC *(m/z 782)*

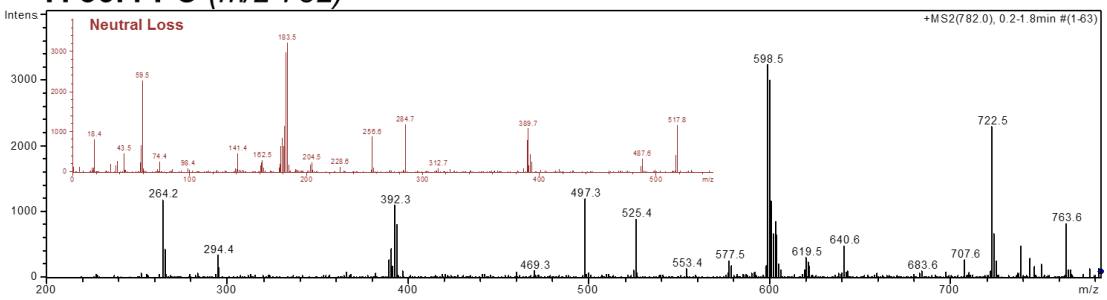

G. 36:2 PC *(m/z 786)*

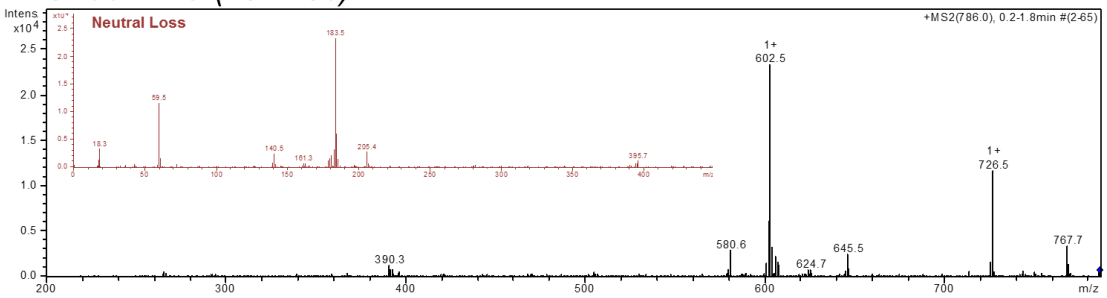

H. 38:4 PS *(m/z 813.6)*

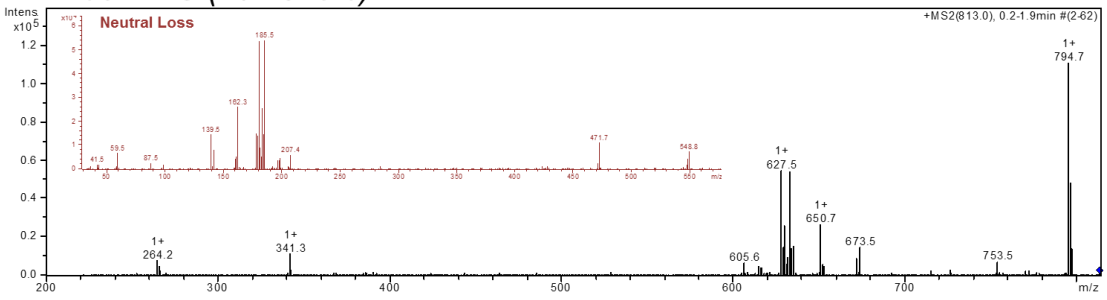

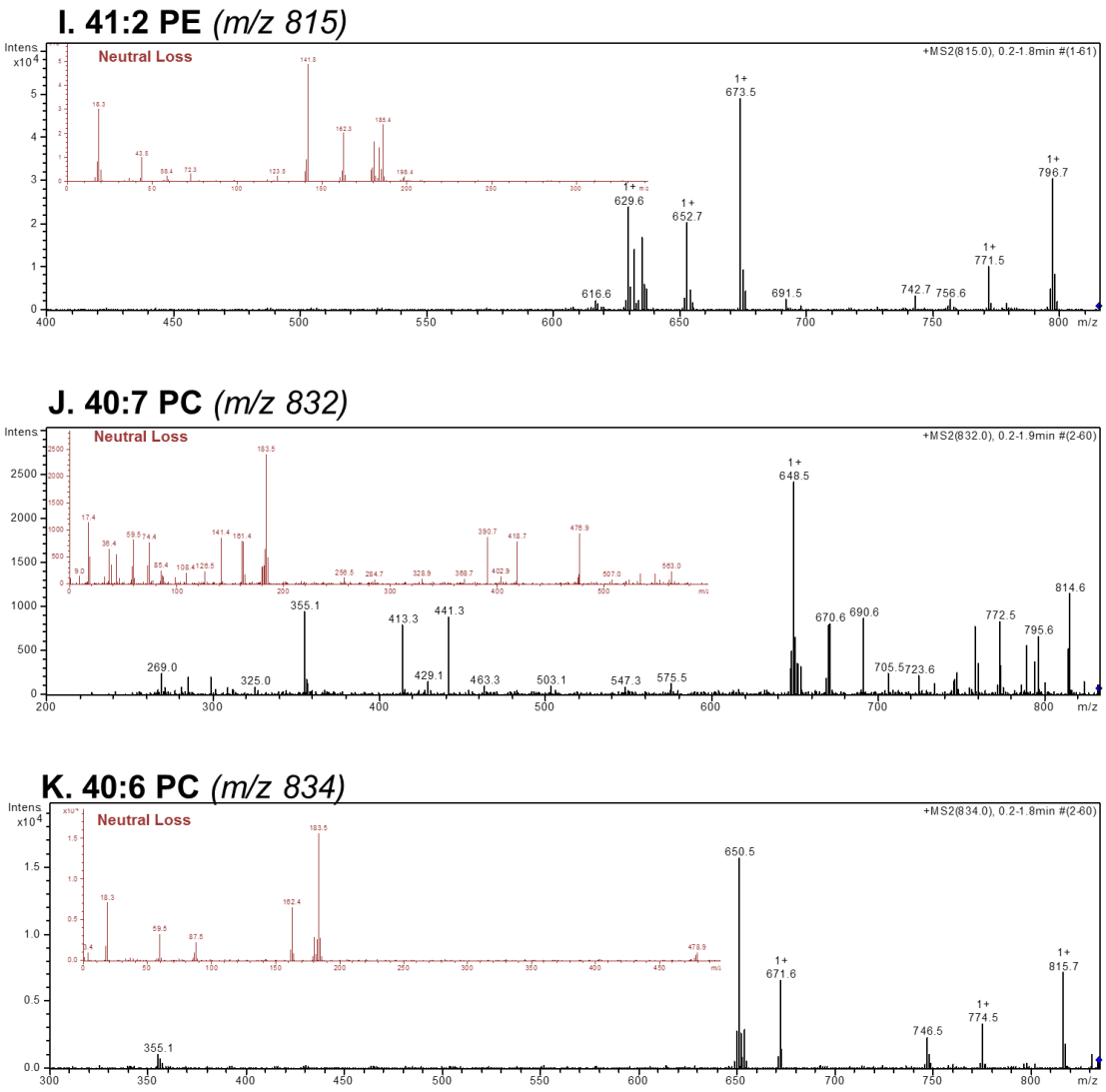

Supplemental Figure 6. MS/MS spectra and neutral loss fragmentation. MS/MS was performed to validate the identity of lipid species shown to be altered in the **blood** of rats treated with cocaine compared to those treated with saline.

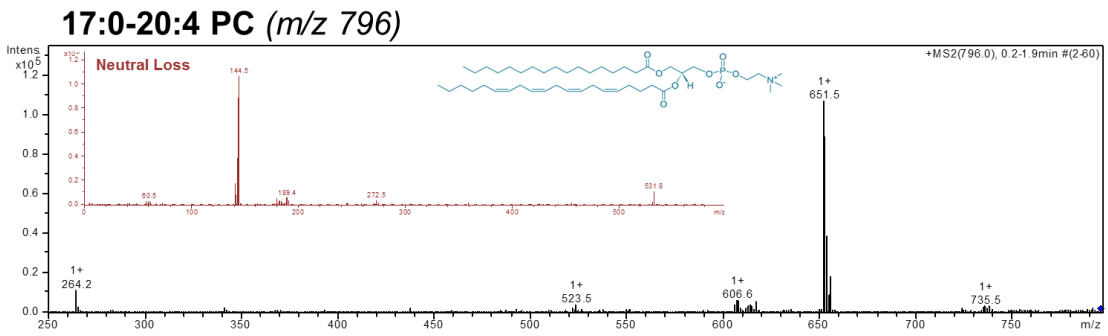

Supplemental Figure 7. MS/MS spectra and neutral loss fragmentation. MS/MS was performed on a known phosphatidylcholine standard, 17:0-20:4 PC (Avanti Polar Lipids, Inc.).

4. Discussion

This study shows that cocaine-induced locomotor sensitization resulted in region-specific changes in select lipid species in the rat brain. The repeated cocaine conditioning protocol also changed the lipidomic profile of the blood. Importantly, the changes in the lipidome of these tissues were present one week following the final administration of cocaine, suggesting that these effects are not merely acute responses following drug exposure. Rather, these lipidomic alterations may reflect some of the persisting consequences of using drugs such as cocaine and may therefore serve as markers of drug history and of the resulting behavioral adaptations.

The relative abundance of phospholipid species were significantly changed in the hippocampus, a prominent brain region involved with various aspects of learning and memory [22]. Changes in phospholipids in this brain region may coincide with the role of the hippocampus in drug-seeking behavior that is primed by either conditioned cues [23] or environmental context [24], as such stimuli are activating memories associated with prior drug experience. Given that the hippocampus is directly involved in the reinstatement of drug-seeking behavior in extinguished rats with a history of cocaine self-administration [25], this brain region is a likely site for persisting changes that are related to the memories of addiction, some of which may include membrane remodeling and related lipidomic changes. By comparison, the relatively few changes in phospholipids occurring in either the dorsal or ventral striatum may seem unexpected given the involvement of these areas in dopaminergic signaling and reward. However, it is important to consider the timing of our tissue collections for our assessments. By sampling one week following the final drug exposure, lipidomic changes in brain regions

involved with persisting memories associated with drug exposure would be favored as opposed to those involved in mediating acute drug effects.

The observed changes in phospholipids in the cerebellum were unexpected. Originally, the cerebellum was chosen because of its presumed lack of relevance to the mechanisms underlying addictive behavior. However, it has been suggested that the cerebellum may be involved in such behavior, as several subregions within the cerebellum have bidirectional connections with brain areas mediating drug reward, including the striatum [26] and the ventral tegmental area [27]. The ventral tegmental area also sends dopaminergic projections to the cerebellum [28], forming a midbrain-cerebellar circuit [29]. These and other structural findings have challenged the traditional view of the cerebellum as being independent from the effects of drugs of abuse [29, 30]. In light of these considerations, it is not surprising that we observed cocaine-induced changes in phospholipid intensities in the cerebellum, albeit modest in magnitude (less than 30%).

The relative abundance of numerous phospholipids in the blood of cocaine treated rats was altered, with most of them being decreased. Interestingly, an early magnetic resonance spectroscopy study has reported decreases in phospholipid metabolites in the brains of cocaine dependent patients [31, 32], and decreases in post mortem brain phospholipid metabolizing enzymes, such as phospholipase A_2 (PLA_2) have also been noted [2, 3] in cocaine users. PLA_2 enzymes metabolize phospholipids, releasing fatty acid and lysophospholipid moieties, and are important mediators of phospholipid remodeling [33]. Thus, alterations in these enzymes may mediate some changes in lipid profiles in both blood and brain tissues, and such decreases could

result in corresponding decreases in blood fatty acid levels, as has been observed in relapsing cocaine addicts [5]. Decreases in blood cholesterol levels have also been reported in patients that had relapsed to cocaine [4], a finding that is also consistent with a decrease in lipid membrane remodeling activity. It remains to be seen if the specific phospholipids identified in our current study using the behavioral sensitization model for cocaine effects in the rat will similarly translate to the human condition, but it is notable that i.p. cocaine administration has previously been shown to reduce PLA_2 activity in the rat [34], as was mentioned above for human cocaine users. Our results provide further evidence supporting the hypothesis that changes in lipid membrane remodeling and associated levels of these lipids and their metabolites are a consequence of cocaine exposure in both rats and humans.

The lipid isolation procedure used in this study certainly extracts more than just phospholipids; however, we chose to focus our effort on phospholipids due to their important role in the function of plasma membrane, and because the few studies that have assessed the effect of cocaine on the lipid profile in humans suggest that this class is altered. In total, over 1,000 different *m/z* values were evaluated, representing as many lipids, yet we only detected significant changes in approximately 10% of these lipids. This suggests that phospholipid changes induced by cocaine using this model are not systemic. A variety of other lipids could certainly originate from the metabolism of the phospholipids identified in this study, including fatty acids, such as arachidonic acid. Future studies will focus on additional characterization of the specific phospholipids and the metabolites being altered, as well as further refinement of the identification of the specific brain regions where these changes are taking place.

A limitation to this study was that the lipids analyzed were compared based on relative abundance, as opposed to actual quantitation. Direct quantitation of lipids is a goal of future work, but would have been impractical in this current study due to the vast numbers of lipids species initially identified using a shotgun approach. Another limitation is the shotgun approach used in this study did not involve any separation of the lipids prior to analysis. As such, it's possible that other lipid species may also be represent by a single *m/z* value, and that these species may be altering the ionization of other lipids. Finally, while the use of MS/MS allowed for identification of polar head groups, fatty acyl chain lengths and double bond numbers, it did not allow us to determine the positions of these double bonds. Future studies, focusing on the specific lipids identified in this study, are needed to address these limitations.

To our knowledge, this is the first report demonstrating that repeated cocaine exposure selectively alters the relative abundance of specific phospholipids in the blood, and that in some instances, these changes can be related to lipidomic changes in specific regions of the rat brain. The data reported in this study represents one of the most comprehensive analyses of changes in rat brain phospholipids after exposure to cocaine described to date, and support the hypothesis that cocaine can induce lipid remodeling in the brain and blood.

References

[1] Substance Abuse and Mental Health Services Administration, in: Results from the 2011 National Survey on Drug Use and Health: Summary of National Findings, Substance Abuse and Mental Health Services Administration Rockville, MD, 2012.

[2] B.M. Ross, A. Moszczynska, F.J. Peretti, V. Adams, G.A. Schmunk, K.S. Kalasinsky, L. Ang, N. Mamalias, S.D. Turenne, S.J. Kish, Decreased activity of brain phospholipid metabolic enzymes in human users of cocaine and methamphetamine, Drug and alcohol dependence, 67 (2002) 73-79.

[3] B.M. Ross, A. Moszczynska, K. Kalasinsky, S.J. Kish, Phospholipase A2 activity is selectively decreased in the striatum of chronic cocaine users, Journal of neurochemistry, 67 (1996) 2620-2623.

[4] L. Buydens-Branchey, M. Branchey, Association between low plasma levels of cholesterol and relapse in cocaine addicts, Psychosom Med, 65 (2003) 86-91.

[5] L. Buydens-Branchey, M. Branchey, D.L. McMakin, J.R. Hibbeln, Polyunsaturated fatty acid status and relapse vulnerability in cocaine addicts, Psychiatry research, 120 (2003) 29-35.

[6] S.N. Jackson, H.Y. Wang, A.S. Woods, In situ structural characterization of phosphatidylcholines in brain tissue using MALDI-MS/MS, Journal of the American Society for Mass Spectrometry, 16 (2005) 2052-2056.

[7] S.N. Jackson, H.Y. Wang, A.S. Woods, M. Ugarov, T. Egan, J.A. Schultz, Direct tissue analysis of phospholipids in rat brain using MALDI-TOFMS and MALDI-ion mobility-TOFMS, Journal of the American Society for Mass Spectrometry, 16 (2005) 133-138.

[8] S. Mikawa, M. Suzuki, C. Fujimoto, K. Sato, Imaging of phosphatidylcholines in the adult rat brain using MALDI-TOF MS, Neuroscience letters, 451 (2009) 45-49.

[9] A.M. Delvolve, B. Colsch, A.S. Woods, Highlighting anatomical sub-structures in rat brain tissue using lipid imaging, Analytical methods : advancing methods and applications, 3 (2011) 1729-1736.

[10] A. Veloso, E. Astigarraga, G. Barreda-Gomez, I. Manuel, I. Ferrer, M.T. Giralt, B. Ochoa, O. Fresnedo, R. Rodriguez-Puertas, J.A. Fernandez, Anatomical distribution of lipids in human brain cortex by imaging mass spectrometry, Journal of the American Society for Mass Spectrometry, 22 (2011) 329-338.

[11] A. Veloso, R. Fernandez, E. Astigarraga, G. Barreda-Gomez, I. Manuel, M.T. Giralt, I. Ferrer, B. Ochoa, R. Rodriguez-Puertas, J.A. Fernandez, Distribution of lipids in human brain, Analytical and bioanalytical chemistry, 401 (2011) 89-101.

[12] B.A. Gosnell, Sucrose intake enhances behavioral sensitization produced by cocaine, Brain research, 1031 (2005) 194-201.

[13] C.M. Seymour, J.J. Wagner, Simultaneous expression of cocaine-induced behavioral sensitization and conditioned place preference in individual rats, Brain research, 1213 (2008) 57-68.

[14] E.G. Bligh, W.J. Dyer, A rapid method of total lipid extraction and purification, Can J Biochem Physiol, 37 (1959) 911-917.

[15] X. Zhou, G. Arthur, Improved procedures for the determination of lipid phosphorus by malachite green, J Lipid Res, 33 (1992) 1233-1236.

[16] G.R. Kinsey, J.L. Blum, M.D. Covington, B.S. Cummings, J. McHowat, R.G. Schnellmann, Decreased iPLA2gamma expression induces lipid peroxidation, cell death, and sensitizes cells to oxidant-induced apoptosis, J Lipid Res, (2008).
[17] L. Zhang, B.L. Peterson, B.S. Cummings, The effect of inhibition of Ca2+-independent phospholipase A2 on chemotherapeutic-induced death and phospholipid profiles in renal cells, Biochemical pharmacology, 70 (2005) 1697-1706.
[18] B. Peterson, K. Stovall, P. Monian, J.L. Franklin, B.S. Cummings, Alterations in phospholipid and fatty acid lipid profiles in primary neocortical cells during oxidant-induced cell injury, Chemico-biological interactions, 174 (2008) 163-176.
[19] R. Taguchi, J. Hayakawa, Y. Takeuchi, M. Ishida, Two-dimensional analysis of phospholipids by capillary liquid chromatography/electrospray ionization mass spectrometry, J Mass Spectrom, 35 (2000) 953-966.
[20] J.D. Steketee, P.W. Kalivas, Drug wanting: behavioral sensitization and relapse to drug-seeking behavior, Pharmacological reviews, 63 (2011) 348-365.
[21] G.F. Koob, N.D. Volkow, Neurocircuitry of addiction, Neuropsychopharmacology : official publication of the American College of Neuropsychopharmacology, 35 (2010) 217-238.
[22] G. Buzsaki, E.I. Moser, Memory, navigation and theta rhythm in the hippocampal-entorhinal system, Nature neuroscience, 16 (2013) 130-138.
[23] W. Sun, G.V. Rebec, Lidocaine inactivation of ventral subiculum attenuates cocaine-seeking behavior in rats, The Journal of neuroscience : the official journal of the Society for Neuroscience, 23 (2003) 10258-10264.

[24] R.A. Fuchs, K.A. Evans, C.C. Ledford, M.P. Parker, J.M. Case, R.H. Mehta, R.E. See, The role of the dorsomedial prefrontal cortex, basolateral amygdala, and dorsal hippocampus in contextual reinstatement of cocaine seeking in rats, Neuropsychopharmacology : official publication of the American College of Neuropsychopharmacology, 30 (2005) 296-309.

[25] S.R. Vorel, X. Liu, R.J. Hayes, J.A. Spector, E.L. Gardner, Relapse to cocaine-seeking after hippocampal theta burst stimulation, Science, 292 (2001) 1175-1178.

[26] A.C. Bostan, R.P. Dum, P.L. Strick, The basal ganglia communicate with the cerebellum, Proceedings of the National Academy of Sciences of the United States of America, 107 (2010) 8452-8456.

[27] R.S. Snider, A. Maiti, S.R. Snider, Cerebellar pathways to ventral midbrain and nigra, Experimental neurology, 53 (1976) 714-728.

[28] Y. Ikai, M. Takada, Y. Shinonaga, N. Mizuno, Dopaminergic and non-dopaminergic neurons in the ventral tegmental area of the rat project, respectively, to the cerebellar cortex and deep cerebellar nuclei, Neuroscience, 51 (1992) 719-728.

[29] M. Carbo-Gas, D. Vazquez-Sanroman, L. Aguirre-Manzo, G.A. Coria-Avila, J. Manzo, C. Sanchis-Segura, M. Miquel, Involving the cerebellum in cocaine-induced memory: pattern of cFos expression in mice trained to acquire conditioned preference for cocaine, Addiction biology, 19 (2014) 61-76.

[30] M. Miquel, R. Toledo, L.I. Garcia, G.A. Coria-Avila, J. Manzo, Why should we keep the cerebellum in mind when thinking about addiction?, Current drug abuse reviews, 2 (2009) 26-40.

[31] S. MacKay, D.J. Meyerhoff, W.P. Dillon, M.W. Weiner, G. Fein, Alteration of brain phospholipid metabolites in cocaine-dependent polysubstance abusers, Biological psychiatry, 34 (1993) 261-264.

[32] J.D. Christensen, M.J. Kaufman, J.M. Levin, J.H. Mendelson, B.L. Holman, B.M. Cohen, P.F. Renshaw, Abnormal cerebral metabolism in polydrug abusers during early withdrawal: a 31P MR spectroscopy study, Magnetic resonance in medicine : official journal of the Society of Magnetic Resonance in Medicine / Society of Magnetic Resonance in Medicine, 35 (1996) 658-663.

[33] S. Akiba, T. Sato, Cellular function of calcium-independent phospholipase A2, Biol Pharm Bull, 27 (2004) 1174-1178.

[34] B.M. Ross, S.D. Turenne, Chronic cocaine administration reduces phospholipase A(2) activity in rat brain striatum, Prostaglandins, leukotrienes, and essential fatty acids, 66 (2002) 479-483.